F 1503/2

BULETINUL INSTITUTULUI POLITEHNIC DIN IAȘI

Tomul XXVI (XXX)

Fasc. 1—2

Secţia II

CHIMIE ŞI INGINERIE CHIMICĂ

1980

ORSZÁGOS MŰSZAKI KÖNYVTÁR ÉS DOKUMENTÁCIÓS KÖZPONT 1883

BULETINUL INSTITUTULUI POLITEHNIC DIN IAŞI

Tomul XXVI (XXX)

Fasc. 1—2

Secţia II

CHIMIE şi INGINERIE CHIMICĂ

1980

COLEGIUL DE REDACȚIE

Prof. dr. doc. **VAL. BLIDARU,**
Prof. dr. doc. **N.V. BOȚAN,**
Prof. dr. ing. **GH. CAȘLER,**
Prof. dr. ing. **M. GAFIȚANU** (președinte)
Prof. dr. **P. MÂLCOMETE,**
Prof. dr. doc. **D. MANGERON,**
Prof. dr. ing. **T. SILION,**
Acad. prof. dr. doc. **CR. SIMIONESCU,**
Prof. dr. ing. **I. VLAD.**

COMITETUL DE REDACȚIE AL SECȚIEI

II. CHIMIE și INGINERIE CHIMICĂ

Prof. dr. ing. **N. ASANDEI**
Prof. dr. doc. **MAGDA PETROVANU**
Prof. dr. doc. **RADU TUDOSE**

REDACȚIA

Prof. dr. doc. **D. MANGERON**
(redactor responsabil)
Prof. dr. ing. **HUGO ROSMAN**
(secretar)
ECATERINA IRIMIEA
(tehnoredactor)

BULETINUL INSTITUTULUI POLITEHNIC DIN IAŞI
BULLETIN OF THE POLYTECHNIC INSTITUTE OF JASSY
ИЗВЕСТИЯ ЯССКОГО ПОЛИТЕХНИЧЕСКОГО ИНСТИТУТА
Tom XXVI (XXX), fasc. 1–2 1980

Secţia II

CHIMIE şi INGINERIE CHIMICĂ

SUMAR

Pag.

S. W. FOX (S.U.A.), Cînd va fi posibilă obţinerea organismelor vii în laborator ? (engl., rez. rom.) · · · 9

G. OSTROGOVICH şi I. IORGA, Studii în domeniul 1, 3, 5-triazinelor (XIX) (franc., rez. rom.) · · · 11

E. COMANIŢĂ, M. TUTOVEANU şi E. AL BOUCHI AL DABBAGH (R.A.Siria), Reacţia hidrazidelor acizilor ciclopropan- şi 1-metil-ciclopropan-1,2-dicarboxilici (engl., rez. rom.) · · · 17

M. KRIŠTOFIČ, A. PIKLER şi J. BENISKA (R. S. Cehoslovacia), Studiul amestecurilor de poli-ε-caprolactamă—polieteruree (engl., rez. rom.) · · · 25

V. MANOVICIU, I. MANOVICIU, D. BANDUR şi G. BANDUR, Cercetări asupra unor plastifianţi inverşi (II) (germ., rez. rom.) · · · 31

E. TURSKA, S. BIADACZ şi H. JANECZEK (R. P. Polonă), Umflarea poliacrilonitrilului în amestecuri de DMF—apă şi DMSO—apă (engl., rez. rom.) 39

D. MUNTEANU, G. THORESZ şi I. NANU, Studiul stabilităţii termice a răşinelor ciclohexanon-formaldehidice obţinute prin policondensare perlată (engl., rez. rom.) · · · 47

N. ASANDEI, GH. ADAMESCU, M. RUSU, S. PETROVAN şi M. NICU, Amestecuri polietilenă—cauciuc (I) (engl., rez. rom.) · · · 53

I. MUREŞAN şi L. ZADOR, Conformaţiile poliacidului acrilic în amestecuri de solvent apă—etanol (engl., rez. rom.) · · · 59

I. DIACONU şi SV. DUMITRESCU, Studiul proprietăţilor electrice ale polimerilor (VII) (engl., rez. rom.) · · · 63

SP. OPREA şi E. DUMITRIU, Reactivitatea monomerilor acrilici (IV) (engl., rez. rom.) · · · 71

I. NEGULESCU, C. MIHĂILESCU, GH. DRĂGAN şi GH. RUSU, Tranziţii structurale în polienii conjugaţi. Poliacetilena (engl., rez. rom.) · · · 77

A. NATANSOHN, ST. MAXIM şi D. FELDMAN (Canada), Rezolvarea rezonanţei metoxi în spectrele ^{1}H-RMN ale copolimerilor acrilat de metil—stiren (engl., rez. rom.) · · · 83

Pag.

CL. VASILIU-OPREA, CL. NEGULIANU, M. POPA şi F. WEINER, Reacţii de homo- şi copolimerizare iniţiate mecanochimic prin măcinare vibratorie (germ.,rez. rom.) 87

R. BUTNARU, GH. ROZMARIN şi I. SABIE, Vopsirea fibrelor monoacrilice (franc., rez. rom.) 99

V. COCHECI şi GH. PETCA, Consideraţii referitoare la determinarea dozei de coagulare prin J a r r -test (germ., rez. rom.) 105

C. ZĂINESCU şi R. Z. TUDOSE, Grosimea minimă la curgerea lichidelor newtoniene în film subţire (I) (franc., rez. rom.) 115

I. CURIEVICI şi ŞT. UNGUREANU, Cu privire la stadiul actual al modelării matematice a reactorului de oxidare catalitică a amoniacului (engl., rez. rom.) 123

BULETINUL INSTITUTULUI POLITEHNIC DIN IAŞI
BULLETIN OF THE POLYTECHNIC INSTITUTE OF JASSY
ИЗВЕСТИЯ ЯССКОГО ПОЛИТЕХНИЧЕСКОГО ИНСТИТУТА
Tom XXVI (XXX), Fasc. 1–2 1980

Section II

CHEMISTRY and CHEMICAL ENGINEERING

CONTENTS

	Pp.
S. W. FOX (U.S.A.), When will a Living Organism be Produced in the Laboratory ? (English, Romanian summary)	9
G. OSTROGOVICH et I. IORGA, Études concernant le domaine des triazines-1, 3, 5 (XIX) (French, Romanian summary)	11
E. COMANIŢĂ, M. TUTOVEANU and E. AL BOUCHI AL DALBAGH (Syria) Reactions of the Hydrazides of Cyclopropane and 1-Methylcyclopropane -1, 2-Dicarboxylic Acids (English, Romanian summary)	17
M. KRIŠTOFIČ, A. PIKLER and J. BENISKA (Czechoslovakia), Study of Mixtures of Poly-ε-caprolactam and Polyetherureas (English, Romanian summary)	25
V. MANOVICIU, I. MANOVICIU, D. BANDUR und G. BANDUR, Untersuchungen einiger umgekeherter Weichmacher (II) (German, Romanian summary)	31
E. TURSKA, S. BIADACZ and H. JANECZEK (Poland), The Swelling of Polyacrilonitrile in DMF – Water and DMSO – Water Mixtures (English, Romanian summary)	39
D. MUNTEANU, G. THORESZ and I. NANU, Thermal Stability Study of the Cyclohexanone – Formaldehide Resins Obtained through Pearled Polycondensation (English, Romanian summary)	47
N. ASANDEI, GH. ADAMESCU, M. RUSU, S. PETROVAN and M. NICU, Polyethylene – Rubber Blends (I) (English, Romanian summary)	53
I. MUREŞAN and L. ZADOR, Conformations of Poly(acrylic Acid) in Water – Ethanol Solvent Mixtures (English, Romanian summary)	59
I. DIACONU and SV. DUMITRESCU, Investigations on Electric Properties of Polymers (VII) (English, Romanian summary)	63
SP. OPREA and E. DUMITRIU, Reactivity of Acrylic Monomers (IV) (English, Romanian summary)	71
I. NEGULESCU, C. MIHĂILESCU, GH. DRĂGAN and GH. RUSU, Structural Transitions in Conjugated Polyenes. Polyacetylene (English, Romanian summary)	77

Pp.

A. NATANSOHN, ST. MAXIM and D. FELDMAN (Canada), Methoxy Signal Resolution in the ^{1}H-NMR Spectra of Methyl Acrylate—Styrene Copolymers (English, Romanian summary) 83

CL. VASILIU-OPREA, CL. NEGULIANU, M. POPA und F. WEINER, Mechanochemisch durch Schwingmahlung initiierte Homo- und Kopolymerisationsreaktionen (German, Romanian summary) 87

R. BUTNARU, GH. ROZMARIN et I. SABIE, Teinture des fibres modacryliques (French, Romanian summary) 99

V. COCHECI und GH. PETCA, Betrachtungen über die Bestimmung der Koagulationsdosis durch den J a r r-Test (German, Romanian summary) . . 105

C. ZĂINESCU et R. Z. TUDOSE, Minimum d'épaisseur pour l'écoulement des liquides non-newtoniens en film mince (I) (French, Romanian summary) 115

I. CURIEVICI and ŞT. UNGUREANU, On the Present State of the Mathematical Modeling of the Ammonia Catalytic Oxidation Reactor (English, Romanian summary) 123

BULETINUL INSTITUTULUI POLITEHNIC DIN IAŞI
BULLETIN OF THE POLYTECHNIC INSTITUTE OF JASSY
ИЗВЕСТИЯ ЯССКОГО ПОЛИТЕХНИЧЕСКОГО ИНСТИТУТА
Том XXVI (XXX), Вып. 1—2 1980

Секция II

ХИМИЯ И ХИМНЧЕСКАЯ ПРОМЫШЛЕННОСТЬ

СОДЕРЖАНИЕ

Стр.

С. ФОКС (США), Когда будет возможно создать в лаборатории живый организм ? (англ., рез. рум.) 9

Г. ОСТРОГОВИЧ и И. ИОРГА, Исследования в области 1,3,5-триазинов (XIX) (франц., рез. рум.) 11

Е. КОМАНИЦЭ, М. ТУТОВЯНУ и Э. АЛ. БОУКИ АЛ ДАББАГ (А.Р. Сирия), Реакции гидразид циклопропан- и 1-метилциклопропан-1,2-двухкарбоксильных кислот (англ., рез. рум.) 17

М. КРИШТОФИЧ, А. ПИКЛЕР и Ж. БЕНИСКА (С. Р. Чехословакия), Исследование смесей поли-ε-капролактам-полиэфирмочевины (англ., рез. рум.) 25

В. МАНОВИЧЮ, И. МАНОВИЧЮ, Д. БАНДУР и Г. БАНДУР, Исследование некоторых обратных пластификаторов (II) (нем., рез. рум.) 31

Е. ТУРСКА, С. БЯДАЧ и Х. ЯНЕЧЕК (Н. Р. Польша), Набухание полиакрилонитрила в смеся ДМФ—вода и ДМСО—вода (англ. рез. рум.) 39

Д. МУНТЯНУ, Г. ТОРЕС и И. НАНУ, Исследование термостабильности циклогексанон-формальдегидных смол полученных путем поликонденсации в перлах (англ., рез. рум.) 47

Н. АСАНДЕЙ, Г. АДАМЕСКУ, М. РУСУ, С. ПЕТРОВАН и М. НИКУ, Бленд полиэтилен—каучук (I) (англ., рез. рум.) 53

Ю. МУРЕШАН и Л. ЗАДОР, Конформации полиакриловой кислоты в смесях растворителей вода—этиловый спирт (англ., рез. рум.). . 59

И. ДЯКОНУ и С. ДУМИТРЕСКУ, Исследование электрических свойств полимеров (VII) (англ., рез. рум.) 63

С. ОПРЯ и Э. ДУМИТРЙУ, Реактивность способность акрильных мономеров (IV) (англ., рез. рум.) 71

Стр.

И. НЕГУЛЕСКУ, К. МИХЭИЛЕСКУ, Г. ДРЭГАН и Г. РУСУ. Структурные транзиции в полиенах. Полиацетилены (англ., рез. рум.) 77

А. НАТАНЗОН, С. МАКСИМ и Д. ФЕЛЬДМАН (Канада), Определение резонанса группы метокси в спектрах ^{1}H-ЯМР сополимеров метил—акрилат стирол (англ., рез. рум.) 83

К. ВАСИЛИУ-ОПРЯ, К. НЕГУЛЯНУ, М. ПОПА и Ф. ВЕЙНЕР, Реакции гомо-сополимеризации инициированные механохимическим путем при виброразмоля (нем., рез. рум.) 87

Р. БУТНАРУ, Г. РОЗМАРИН и И. САБЬЕ, Крашение модакрильных волокон (франц., рез. рум.) 99

В. КОКЕЧ и Г. ПЕТКА, Некоторые соображения относительно определения дозы коагулирования при помощи Жаррр-теста (нем., рез. рум.) 105

К. ЗЭЙНЕСКУ и Р. ТУДОСЕ, Минимальная толщина в течении неньютоновских жидкостях в пленочных слоях (I) (франц., рез. рум.) 115

И. КУРЬЕВИЧ и ШТ. УНГУРЯНУ, О современном состоянии моделирования реактора каталитического окисления аммиака (англ., рез. рум.) 123

BULETINUL INSTITUTULUI POLITEHNIC DIN IAŞI
Tomul XXVI (XXX), fasc. 1—2, 1980
Secţia III
CHIMIE şi INGINERIE CHIMICĂ

D.C. 547.466:576.08

WHEN WILL A LIVING ORGANISM BE PRODUCED IN THE LABORATORY?

BY

SIDNEY W. FOX

Dedicated to Professor Dr. CRISTOFOR SIMIONESCU, member of the Academy, on his 60 th anniversary

Investigators in one subject matter area of concern to Professor Cr. Simionescu sometimes hear the question of when will a living organism be produced in the laboratory. In a similar vein, some otherwise thorough treatments of the origin of life (e. g.[1], [2]) include statements that a living organism has not yet been produced in the laboratory. This question and this statement are not in a scientific focus. The question, or the statement, has to be analyzed, and then rephrased.

The question, as asked, makes the same assumption as the story of Genesis — that life was an act of instant creation. The newer scientific view, on the other hand, is that life arose in successive chemical steps (Fig. 1). Instead of asking about, or declaring about the „synthesis of life in the laboratory", the meaningful question is: what stage has been attained in the laboratory ?

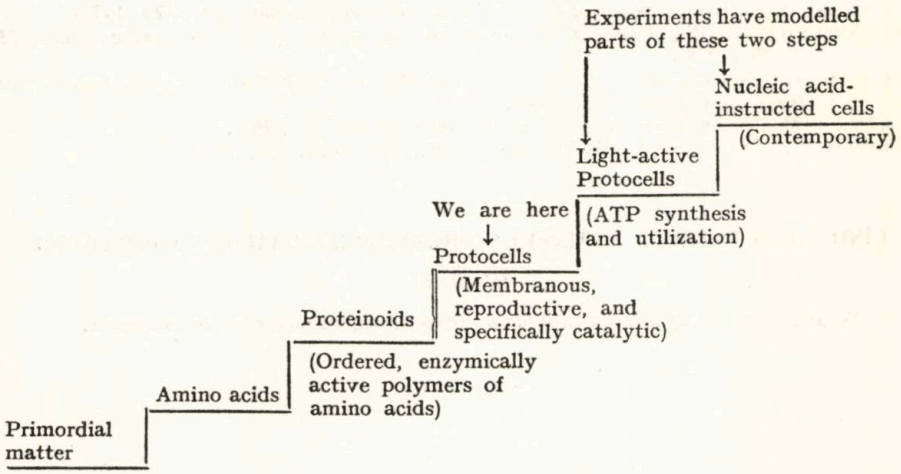

Fig. 1. — Stepwise emergence of living organisms, as modelled in the laboratory.

We can say that *contemporary* living organisms have not been demonstrated as produced in the laboratory. We can say at least, as did A s i m o v in 1967 [3], that the proteinoid microspheres produced in the laboratory [4], „while a long way from the completely alive side of the boundary zone, are at least a small way past the nonalive side". (S. also [5], [6]).

One, or the most, dramatic step demonstrated in model experiments is the conversion of amorphous matter (of the right kind) to organized, reproductive, membranous, cell-like units [4]. It has been learned that, intrinsically, *such a unit would already possess a number of biological properties* [7] ; this set of circumstances would have enabled evolution from protocells to cells having more total biological activity.

In the same line of reasoning, asking the question of whether life exists on Mars, or in some other solar system, is as laced with difficulty as the many attempted definitions of life in the past. C a l v i n, for example, has pointed out that the definition of life has „subjective arbitrariness" to it [8]. J a c o b [9] states that biologists no longer attempt to define life. We need instead to rephrase the question and ask what is the stage of molecular evolution in any given site.

A c k n o w l e d g m e n t. Background research for the views expressed here has been supported by Grant NGR-10-007-008 of the National Aeronautics and Space Administration. Contribution No. 336 of the Institute for Molecular and Cellular Evolution.

Received, December 21, 1979

University of Miami, Florida, U.S.A.
Institute for Molecular and Cellular Evolution

REFERENCES

1. S l e s n i c k I. L. et al., *Biology*. Scott, Foresman and Co., Glenview, Illinois, 1980, 34.
2. W i l s o n E. O. et al., *Life on Earth*. Sinauer Associates, Sunderland, Massachusetts, 1978, 616.
3. A s i m o v I., *Is Anyone There ?* Ace Books, New York, 1967, 86.
4. F o x S. W., *The Origin and Nature of Protolife*, in *The Nature of Life*, W. H. Heidcamp Ed., University Park Press, Baltimore, 1978, 23--92.
5. C h a i s s o n E., *The Scenario of Cosmic Evolution*. Harvard Mag., **80**, *2*, 29 (1977).
6. D i c k e r s o n R. E., *Chemical Evolution and the Origin of Life*. Scientific Amer., **239**, *3*, 70 (1978).
7. F o x S. W., N a k a s h i m a T., *The Assembly and Properties of Protobiological Structures*. BioSystems **12** (1980).
8. C a l v i n M., *From Molecules to Mars*. Bulletin AIBS, 29 (1962).
9. J a c o b F., *The Logic of Life*. Vintage Books, New York, 299, 1976.

CÎND VA FI POSIBILĂ OBŢINEREA ORGANISMELOR VII ÎN LABORAT OR ?

(Rezumat)

Se analizează şi se discută problema obţinerii organismelor vii în laborator.

BULETINUL INSTITUTULUI POLITEHNIC DIN IAȘI
Tomul XXVI (XXX), fasc. 1—2, 1980
Secția III
CHIMIE și INGINERIE CHIMICĂ

C.Z. 547.874

ÉTUDES CONCERNANT LE DOMAINE DES TRIAZINES-1,3,5

XIX*). RÉACTION HALOFORMIQUE (RÉ. HAL.) DU GROUPE DES C-MÉTHYLTRIAZINES 1, 3, 5 : REMARQUES D'ORDRE TERMINOLOGIQUE ET THÉORIQUE CONCERNANT LA NOTION DE RÉ. HAL. EN GÉNÉRAL, AINSI QUE LES ASPECTS CINÉTIQUES DE CE PROCESSUS EN FONCTION DES CONDITIONS DE SON DÉROULEMENT

PAR

G. OSTROGOVICH et I. IORGA

Dédié au professeur
Dr. CRISTOFOR SIMIONESCU,
membre de l'Académie,
à l'occasion de son 60-e anniversaire

1. À propos de la notion de Ré. hal. il y a lieu de remarquer dès le début que, de notre coté, nous lui attribuons exclusivement le sens complexe mais bien contouré avec lequel elle est apparue il y a déjà plus d'un siècle, grace justement a L i e b e n [2] et auquel le nom même est resté lié le plus souvent, malheureusement pas toujours dans ce même sens et par conséquent non dépourvu de tout équivoque.

Nous croyons que cette précision s'impose justement parce que sans cela, par la nature même des choses et à défaut d'une convention expresse, la signification des termes reste susceptible d'une certaine ambiguité.

En réalité il n'est point surprenant que cet aspect ait pu échapper à l'attention générale, tant et si bien que certains auteurs [3] ont été induits à faire appel exactement aux mêmes termes pour désigner également (par une restriction tacite de leur contenu notionnel primitif) la réaction finale de substitution d'un reste trihalogénométhylique $-CX_3$ par un groupe nucléophile hétérogène (de façon typique par un reste $-OH$) qui donne naissance ainsi à l'haloforme correspondant HCX_3, donc seulement la transformation individuelle par laquelle prend fin la succession de réactions comprise dans la notion globale et dont la signification constitue en vérité l'élément suggestif par excellence, en tant que facteur déterminant la dénomination de l'entier.

Dans cette situation il est incontestable que l'utilisation du nom attribué d'habitude à l'ensemble pour désigner également, en particulier, cette réaction finale, s'offre comme une posibilité absolument naturelle et extrêmement tentante, puisque cela ne présente à première vue rien qui puisse susciter quelque objection, bien que l'homonimie complète produise du même coup l'ambiguité que nous venons de remarquer. Mais il n'est pas moins évident que justement cette circonstance rend d'autant plus désirable d'établir d'une manière expresse une convention terminologique capable d'exclure l'équivoque.

Nous sommes d'avis que le contenu de cette convention s'impose de lui-même. En effet, puisque la transformation individuelle conclusive constitue effectivement une dégradation du squellette moléculaire et précisément une scission de celui-ce au niveau de la liaison entre le groupe $-CX_3$ et le reste de la molécule, nous n'avons que d'éviter pour elle le substantif générique „réaction" et la dénommer sans plus, d'une manière différenciée,

*) Note XVIII, v. Revue Roumaine Chim., 22 (1980), (sous presse).

dégradation ou *scission haloformique* (*Sci. hal.*) (l'adjectif étant évidemment irremplaçable). On peut réserver de la sorte, ainsi que nous l'avons fait dès le début, la dénomination *Ré. hal.* [4] (d'ailleurs la seule possible, puisqu'on ne voit aucune alternative meilleure) *pour toute la suite de transformations* qui implique d'abord, comme on le sait, sous l'action d'un hypohalogénite alcalin $M^{I}OX$ (ce qui signifie implicitement en présence d'ions HO^-) l'halogénation totale d'un groupe $-CH_3$ „actif", donc sa transformation en un groupe $-CX_3$ par trois réactions succesives SE (ou bien par deux ou par une seule, lorsqu'on part de l'un ou de l'autre des produits intermédiaires $-CH_2X$ et $-CHX_2$, aux atomes H de plus en plus mobiles en chacune des étapes successives (pour terminer immédiatement avec la *scission* en question, par une réaction normale SN_2(AE).

2. En abordant maintenant certaines questions de fond relatives à cette suite de transformations individuelles, il va de soi qu'elle peut se dérouler d'une manière complète seulement si l'on a soin de satisfaire la condition naturelle extrinsèque de mettre en jeu — avec 1 mol d'halogène élémentaire X_2 pour chaque atome-gramme de H susceptible de substitution — au moins 1 mol de HO^- *en plus* sur ce rapport équimoléculaire. Ainsi l'halogénation exhaustive peut avoir lieu intégralement, laissant disponible l'excès de HO^- nécessaire à la limite pour que la Sci. hal. finale puisse se derouler elle aussi de façon pratiquement complète, le tout étant représenté par les équations suivantes :

$$(1)\quad \left\{\begin{array}{l} \mathrm{Y{=}C{<}\,C{-}CH_3 + 3X_2 + 4HO^-} \\ \mathrm{Y{=}C{<}\,C{-}CH_2X + 2X_2 + 3HO^-} \\ \mathrm{Y{=}C{<}\,C{-}CHX_2 + X_2 + 2HO^-} \end{array}\right\} \rightarrow \mathrm{Y{=}C{<}\,C{-}O^-} + \mathrm{HCX_3} + \left\{\begin{array}{l} \mathrm{3X^- + 3H_2O} \\ \mathrm{2X^- + 2H_2O} \\ \mathrm{X^- + H_2O} \end{array}\right.$$

À défaut de cet excès formel, donc si le nombre de mols de HO^- présents initialement ne dépasse pas celui des atomes-grames de H méthylique actifs qui doivent être remplacés par des atomes d'halogène X, la transformation du méthyle ne va pas outre le composé trihalogénométhylique $-C(=Y)-CX_3$, conformément aux équations :

$$(2)\quad \left\{\begin{array}{l} \mathrm{Y{=}C{<}\,C{-}CH_3 + 3X_2 + 3HO^-} \\ \mathrm{Y{=}C{<}\,C{-}CH_2X + 2X_2 + 2HO^-} \\ \mathrm{Y{=}C{<}\,C{-}CHX_2 + X_2 + HO^-} \end{array}\right\} \rightarrow \mathrm{Y{=}C{<}\,C{-}CX_3} + \left\{\begin{array}{l} \mathrm{3X^- + 3H_2O} \\ \mathrm{2X^- + 2H_2O} \\ \mathrm{X^- + H_2O} \end{array}\right.$$

En d'autres termes, si le surplus initial de HO^- est compris entre 1 et 0 mol pour 1 mol du substratum, la Sci. hal. (et avec elle la Ré.hal.) ne peuvent avoir lieu que tout au plus dans la même proportion.

Mais cette circonstance, c'est-à-dire le fait qu'en présence d'un excès effectif de HO^- la Ré. hal. peut s'achever même rapidement, ne fournit aucune indication concernant *les aspects essentiels d'ordre cinétique* de cette succession de quatre (soit de trois ou de deux) transformations d'un groupe $-CH_3$, $-CH_2X$ ou $-CHX_2$.

À cet égard les traités de niveau universitaire ne négligent point de relever que — dans les conditions de la catalyse générale basique de l'halogénation exhaustive, y compris celles que les équations (1) définissent comme nécessaires à la limite pour qu'une Ré. hal. puisse avoir lieu intégralement, en un seul acte — la vitesse de formation du composé trihalogénométhylique $-C(=Y)-CX_3$ reste inévitablement limitée par celle de l'halogénation à l'échelon immédiatement précédent, donc normalement par celle du prémier échelon, qui dépend exclusivement de la concentration du catalyseur basique et, bien entendu, de celle du substratum.

On ne peut point en dire autant quant au rapport entre cette constante de vitesse initiale (connue dans un grand nombre de cas) et celle de la Sci. hal. finale, réaction que l'on n'a pas encore soumise à des mesures cinétiques, selon nos connaissances. Il s'agit en d'autres termes d'un dilemme encore irrésolu : si à toute température pratiquable la constante de vitesse de la Sci. hal. reste plus ou moins inférieure à celle de l'halogénation exhaustive — cas dans lequel elle serait déterminante pour la vitesse de la Ré. hal. — ou si elle peut assumer, au contraire, des valeurs plus grandes.

Dans ce dernier cas *une mesure directe* de l'„activite" (l'acidification) du groupe $-CH_3$ serait donnée uniquement par la vitesse d'halogénation en catalyse basique et précisément par sa vitesse au premier échelon, dont nous venons de dire qu'elle est limitative, car dans les conditions de ce genre de catalyse l'halogénation s'achève de plus en plus rapidement à chaque échelon, de sorte qu'à une concentration déficitaire de HO^- mais suffisante de X_2 il reste du substratum inaltéré dans la mesure du défaut et l'on obtient exclusivement le composé trihalogénométhylique $-C(=Y)-CX_3$ dans la même proportion que celle des ions HO^- présents au début.

Mais si la constante de vitesse de la Ré. hal. (dans les conditions d'un excès suffisant de HO^-, lorsqu'elle a lieu d'un trait, intégralement) était effectivement celle de la Sci. hal., alors— quoique la Ré. hal. soit conditionnée dans la phase d'halogénation par le caractère actif du groupe $-CH_3-$ sa vitesse globale ne constituerait qu'*une mesure indirecte* de cette activation, ne reflétant proprement que l'intensité du caractère électrophile du reste $-C(=Y)-$ dans la constellation $-C(=Y)-CX_3$.

D'autre part il y a lieu de rappeler le fait universellement connu lui aussi, que l'halogénation d'un groupe CH_3 ($\rangle CH_2$ ou $\rightarrow CH$) actif se laisse effectuer également en milieu acide (ou neutre au début), donc *en catalyse par les acides*, soit en *catalyse générale*, moins efficaces que celle basique et suivant un mécanisme différent. Dans ces conditions chacun des produits correspondants aux trois échelons peut être isolé assez nettement. Ensuite la Sci. hal. se laisse réalisée à son tour également de manière distincte, par l'action d'un nucléophile convenable, principalement en milieu plus ou moins *basique*.

À ce propos nous devons souligner un fait qu'aucun auteur n'a remarqué d'une manière expresse, à savoir que ce comportement (c'est-à-dire

la possiblité d'une Sci. hal. en milieu *basique*, qui caractérise de façon typique les composés trihalométhyl-carbonylés $-C(=O)-CX_3$ et qui est propre également aux triazines - 1, 3, 4 trihalométhylées) se retrouve uniquement chez celles-ci parmi tous les dérivés similaires de n'importe quelle autre hetéroarène azotée[1]). Bien plus il y a lieu de relever un aspect dont la signification est restée inaperçue aussi bien par ceux qui l'ont observé [6]... ...[9], que par les auteurs plus modernes. C'est que *certaines triazines C-trihalométhylées sont susceptibles d'une Sci. hal. hydrolitique en milieu acide*, qui est *sans analogie dans le domaine des* composés trihalométhyl-carbonylés[2]).

Il s'ensuit que, dans la classe des triazines 1,3,5, les composés C-méthylés doivent donner également la Ré. hal., qui n'a pas encore été observée expérimentalement ni même soupçonnée avant nous, comme un processus découlant d'un seul coup. Par surcroît, cette réaction doit être observable non seulement en milieu alcalin (donc dans les conditions classiques, généralement pratiquées pour sa réalisation) mais bien aussi en milieu acide, ce qui constitue une variante absolument nouvelle du processus global et un caractère spécifique de certaines C-méthyl-triazines-1,3,5[3]).

Il en résulte qu'au moins pour ce domaine on ne peut plus parler simplement de Sci. hal. (et par conséquant de Ré. hal..) en sousentendant l'alcalinité du milieu, mais qu'il s'impose de spécifier, selon le cas, le domaine de pH dans lequel ces transformations peuvent se dérouler et précisément qu'elles sont effectuées comme une Sci. hal. (respectivement comme une Ré. hal.) „basique" ou „acide". Précision à laquelle nous sommes d'avis — particulièrement dans le cas de la première — d'en ajouter encore une, concernant la nature de l'agent nucléophile responsable, ce qui était à vrai dire déjà connu au moins partiellement dans le domaine des composés trihalométhyl-carbonyles.

---

[1]) Il s'agit évidemment de la positivation très accentuée des atomes C du noyau triazinique-1, 3, 5 en comparaison avec ceux qui se trouvent en *alpha* et en *gamma* chez d'autres hétéroarènes azotées. En vérité — tout en remarquant que la bis (trichlorométhyl)-2,6 pyridine est totalement résistante à la Sci.hal. aminolytique, puisqu'elle se laisse récuperée intégralement après traitement à l'NH_3 gazeux sec, durant deux heures en milieu de $HCO-NMe_2$ a 165°C[4] — nous n'avons trouvé dans la littérature aucun indice que les pyrimidines trihalométhylées (parmi lesquelles la tribromométhyl-2 pyrimidine) que l'on a préparées par halogénation des groupes $-CH_3$ dans le CH_3-COOH en présence de CH_3COONa [5], seraient susceptibles de Sci. hal. Nous penchons fortement à croire que celle-ci n'est point réalisable dans leurs cas non plus.

[2]) Le facteur essentiel de telles Sci. hal. „acides", n'est pas tant la positivation du centre de réaction (qui est importante également dans le cas des composés trihalométhyl-carbonylés) que, en particulier, son appartenance à un système susceptible de stabilisation dans l'étape d'addition du nucléophile et d'élimination de l'anion : $CH_3^{\ominus}$, qui doit se passer a notre avis uniquement dans les espèces neutres (non protonées), existantes en équilibre avec les cationiques.

[3]) D'une façon absolument singulière on a observé [10] de telles Ré. hal. „acides" dans le cas de l'acide malonique — donc chez une combinaison atypique — qui donne du HCX_3 avec l'I_2 ou le Br_2 en chauffant légèrement (30°...40°C) en *milieu acide* (H_2SO_4 dil.) mais *seulement en présence d'oxydants* tels que H_2O_2, HIO_3, HIO_4, $FeNH_4(SO_4)_2$, $Na_2Cr_2O_7$ et $KMnO_4$ (toutefois pas $HClO_4$ et $HClO_3$!). Encore auparavant M. G. Brown [11] avait signalé des phénomènes semblables dans le cas de l'acide kojique (hydroxyméthyl-2 hydroxy-5 pyrone-4) seulement avec l'HIO_3 en milieu aqueux. D'après Hashmi [10], si l'on ajoute alternativement de l'acide malonique et de l'I_2 ou du Br_2 à la solution des oxydants mentionnés ci-dessus et si l'on chauffe légèrement, on obtient du HCI_3, respectivement du $HCBr_3$ identifiés comme tels. La chromatographie des produits sur papier a permis d'identifier les acides mono-, di- et trijodoacétiques et l'acide dibromomalonique, soit les acides bromés correspondants.

Tableau 1

Réaction haloformique

(notion complexe qui implique une succession de réactions individuelles découlant d'une manière ininterrompue ou en étapes séparables)

Dans le groupe des C-méthyltriazines-1, 3, 5

(que les citations bibliographiques de la colonne II concernent exclusivement)

A. *En solution basique*

I

a) *Halogénation exhaustive* du groupe $-CH_3$, $-CH_2X$ ou $-CHX_2$, *en catalyse générale basique*, ordinairement par HO^- dans les milieux aqueux (éventuellement par Alc_3C-O^- dans l'Alc_3C-OH + un solvent aprotique ?)

Découlant d'un seul trait et suivie immédiatement de II.

Mécanisme: SE2 (intermédiares réactifs *carbanioniques*, représentables par les schémas $-CH_2^-$, $-CHX^-$, $-CX^-$, dont la structure est en réalité mésomère, bidentée, grace à la conjugaison avec le groupe activateur $-C(=Y)-$ dans la constellation $-C(=Y)-CH_3$ ($-CH_2X$, $-CHX_2$).

II

a) *Scission halo* {iodo / bromo / chloro} *-formique du groupe* $-CX_3$, à la température ordinare.

Mécanisme: SN2 (AE). I (et donc II) peut être compromise pratiquement d'une manière intégrale, lorsque le substratum possède un groupe fonctionnel protolysable (plus acide que le groupe $-CH_3$, $-CH_2X$ ou $-CHX_2$ actif). Dans tels cas la voie B reste généralement possible.

a_1) *Comme cloture immédiate* du processus global en : a_{11}) milieu aqueux : hydrolytique (HO^-); a_{12}) milieu anhydre : alcoolytique (Alc_3C-O^-) ?

a_2) *Indépendante* : réalisable avec les composés $-CX_3$ isolés comme tels par d'autres voies (p. ex. par la trimérisation unitaire ou mixte du $N=C-CCl_3$ [12], ou bien également par halogénation exhaustive mais en catalyse générale acide (voir ci-dessous :I.B).

Hydrolytique [13] ···[15]

Alcoolytyique [16] { a_{21}) Spontanément / a_{21}) Spontanément

Aminolytique [14], [17] } a_{22}) Spontanément ou en catalyse basique par $NAlc_3$ [14], [18].

Agents

a) XO^- plus exactement XOH [19] (présent dans le système grace à l'hydrolyse du premier) et en réalité le cryptocation X^+, provenant du deuxième.

Nucléophiles { *anioniques* : HO^- [13] ···[15] ou $AlcCH_2O^-$ (Alc_3CO^- ?) dans les alcools respectifs [16]. / *neutres* : NH_3[13], [14], $AlcNH_2$ [13], [14], [17] (éventuellement en milieux anhydres non hydroxylés [14]) et même $Ar-NH_2$ (en milieu de C_6H_6 et dans les conditions a_{22}) [18].

Test analytique (iodoformique !) en milieu { aqueux: test de L i e b e n. / dioxanique (aquo-dioxanique) : test de F u s o n - T u l l o k [20].

B. *En solution acide*

(ou initialement neutre, quand le début est lent (homolitique ?) pour s'accélérer tout de suite catalytiquement, par le HX engendré du fait de la réaction).

b) *Halogénation* comme ci-dessus, en milieu aqueux et *en catalyse générale acide* (éventuellement + *une base tamponante*, par exemple dans $CH_3COOH+CH_3COO^-$ [5], [21], [22]). Réalisable normalement comme processus indépendant (dont les étapes sont séparables mais se laissent parcourues également d'un seul trait, suivi immédiatement de II) [6], [8], [9].

Mécanisme: SE2 (intermédiaires réactifs : les formes tautomères $-(C=CH_2)-YH$).

b) *Scission halo* { chloro [6], [7], / bromo [8], [9] / iodo } *- formique*, exclusivement *hydrolytique*, plus lente que A. II (impliquant une température rehaussée).

Mecanisme: SN2 (AE).

b_1) *Comme cloture immédiate* du processus global [6], [8], [9] (à température rehaussée !), concourée généralement par le clivage hydrolytique du noyau, donc ne pouvant pas découler intégralement.

b_2) *Indépendante* (tout comme b_1). Possible chez les triazines 1, 3, 5 grace au fait que l'intermédiaire d'addition est plus stable que chez les $-C(=O)-CX_3$ et subit une nouvelle stabilisation aussi bien en éliminant l'anion : CX_3^- qu'en souffrant en partie la scission hydrolytique du noyau.

Agents

b_1) X_2 *élémentaire* (en réalité le cryptocation X^+) + *un oxydant* lorsqu'on opère avec l'I_2 et même avec le Br_2.

b_2) $AuCl_4H$ aqueux dans le cas de l'acétoguanamide (1H, 3H oxo-2,4 méthyle-6 triazine 1, 3, 5) [23].

b_1) Le nucléophile neutre OH_2 [6] ···[9].

b_2) Mécanisme inéclairci : la Sci. hal. parait ne pas avoir lieu même partiellement, étant exclue par l'hydrolyse du noyau au niveau d'une étape d'halogénation moins avancée*).

*) Expériences inédites de A. O s t r o g o v i c h qui a pu saisir au cours des anées '40, la formation d'acide glyoxylique à partir du dérivé dichloro-méthylé.

On voit donc que, dans cette classe d'hétéroarenes, les notions de Ré. hal. et de Sci. hal. acquièrent effectivement un contenu plus large et multiforme, grace au fait qu'elles couvrent en principe non seulement un interval de pH > 7 mais également un interval < 7 et grace a la plus grande variété des agents nucléophiles qui peuvent produire une Sci. hal., puisqu'à ceux que l'on connaissait déjà on doit ajouter l'agent H_2O en milieu acide.

Nous avons dit qu'elles couvrent „en principe", parce qu'on peut se rendre compte assez facilement que des facteurs restrictifs peuvent intervenir dans un sens ou dans l'autre chez la plupart des C-méthyltriazines-1, 3, 5. Par exemple certains composés appartenants à cette classe (telles que la TMT et en général toute triazine C-alcoylée) sont sensibles aux acides en milieu aqueux, qui provoquent le clivage hydrolitique du noyau. Il va sans dire qu'elles peuvent se prêter uniquement à la Ré. hal. „basique". D'autres sont protolysables, possèdent donc un caractère acide, respectivement ampholytique. C'est le cas des C-oxo-N-hydrodérivés qui engendrent en milieu basique les espèces anioniques correspondantes. Chez celles-ci l'activité du méthyle est annulée par la charge négative du noyau, de sorte que l'halogénation même est empêchée. De telles triazines se prêteront exclusivement a la Ré. hal. „acide".

En tout cas, si le milieu est acide, on peut affirmer *a priori* que la constante de vitesse de la Sci. hal. doit être inférieure à celle de l'halogénation au *dernier* échelon, car celle-ci peut s'achever même à la température ordinaire, tandis que la Sci. hal. (et donc la Ré. hal.) „acides" prétendent pour pouvoir se dérouler une température minima d'au moins 30°...40° C.

Il nous semble opportun de clore les remarque de cette Note, en consignant systématiquement sous forme synoptique, dans un tableau final, un résumé des différents aspects et données qui précedent, y compris les faits fondamentaux plus ou moins généralement connus (Tableau 1).

Par quelques notes ultérieures nous rendrons compte de nos observations nouvelles à caractère semiqualitatif sur la Ré. hal. d'une série de C-méthyl-triazines-1, 3, 5, ainsi que des mesures cinétiques de ses phases en milieu basique ou en milieu acide.

Reçue le 11 février 1980

Institut Polytechnique „Traian Vuia", Timișoara

BIBLIOGRAPHIE

1. Ostrogovich G., Simionescu T., St. și Cerc. Șt. chim., Acad. R.P.R. (Baza de cercetări Timișoara), **7**, 69—97 (1960) ; C.A., **55**, 14477 (1961).
2. Lieben A., Ann. der Chem., Suppl., **7**, 218, 377 (1870).
3. Nenițescu C. D., *Chimie organică*. 7-ème éd., t. **II**, EDP, Buc., 1974, 5—7.
4. Grundmann Chr., Weisse G., Chem. Ber., **84**, 684 (1951).
5. Brown B. R., Hammick D. L., Thewlis B. H., J. Chem Soc., 1145 (1951).
6. Nencki M., Ber., **9**, 232 (1876).
7. Tscherven-Iwanow N., J. Prakt. Chem., (2), **46**, 145 (1892).
8. Ostrogovich A., Ann., **288**, 318 (1895).
9. Ostrogovich A., Bull. Soc. Șt. Buc., **14**, 49, 288 (1905).
10. Hashmi M. H. et al., Pakistan J. Sci. Res., **15**, *1*, 7—10 (1963).
11. Brown M. G., J. Chem. Soc., 2283—2286 (1956).
12. Smolin E., Rappoport L., *s-Triazines and Derivatives*. Intersc. Publ. Co. Inc., New York, London, 1954, 149—152.
13. Weddige A., J. prakt. Chem., (2), **28**, 76 (1886).

14. Kreutzberger A., J. Amer. Chem. Soc., **79**, 2629 (1957).
15. Ostrogovich G., Catalina E., Iorga I., Bul. Șt. și tehn. Inst. polit., Timișoara, **19** (**33**), 216 (1974).
16. Kober E., J. Org. Chem., **25**, 1728 (1960); U.S. Pat. 3 014 907, C.A., **56**, 8731 (1962).
17. Geigy J. R., A.G. Germ. Pat. 1 107 448 (Cl. 451) (auteurs F. Kunelsi, H. Gysin); C.A., **56**, 8731 (1962).
18. *** Jap. pat. 7 031 300 (1971); C.A., **74**, 53 054 et 125 137 (1971).
19. Morgan, Bardwell, Cullis, J. Chem. Soc., 3190 (1950).
20. Fuson R. C., Tullok Ch. W., J. Am. Chem. Soc., **56**, 1638 (1934).
21. Koenigs, Ber., **31**, 2364 (1898).
22. Schaefer F. C., Ross J. H., J. Org. Chem., **29**, 1522 (1964).
23. Ostrogovich A., Gazz. Chim. Ital., **44**, *II*, 575 (1914).

STUDII ÎN DOMENIUL 1, 3, 5-TRIAZINELOR

XIX. Reacția haloformică (Re. hal.) în domeniul 1, 3, 5-triazinelor: observații de ordin terminologic și teoretic privind noțiunea generică de Re. hal. și aspectele cinetice ale acestui proces în funcție de condițiile desfășurării sale

(Rezumat)

Se stabilește în primul rînd o convenție terminologică pentru procesul prin care o grupă $-CH_3$ „activă" se desprinde sub formă de haloform HCX_3, prin halogenare exhaustivă și substituție nucleofilă (SN) a grupei $-CX_3$, întrucît unii autori au denumit-o pe aceasta din urmă cu aceiași termeni de „reacție haloformă" cu care Lieben a denumit ansamblul tranformărilor individuale implicate. Numim „scindare haloformică" (Sci. hal.) această reacție finală, rezervînd denumirea de „reacție haloformică" (Re. hal.) pentru toată succesiunea de reacții decurgînd dintr-o dată în mediu bazic și cuprinzînd în primul rînd halogenarea exhaustivă prin trei reacții succesive SE. Apoi, cu cîteva remarci ce privesc mai ales caracterele cinetice ale fiecărei transformări individuale, se fac cunoscute unele fapte încă nesemnalate în literatură, referitoare la comportarea C-metil-1, 3, 5-triazinelor: ele sînt susceptibile de Re. hal. clasică, pe care noi o denumim „bazică" (formă previzibilă prin faptul că s-au constatat deja numeroase Sci. hal. bazice ale derivaților C-trihalometilici) ca și de Re. hal. (deci și de Sci. hal.) „acidă", variantă deja semnalată de mult timp, fără ca nimeni să fi remarcat caracterul său excepțional și care constituie un nou aspect al procesului global, absolut specific pentru unele dintre ele, adică fără analogie în domeniul compușilor trihalogeno-metil-carbonilici.

BULETINUL INSTITUTULUI POLITEHNIC DIN IAŞI
Tomul XXVI (XXX), fasc. 1—2, 1980
Secţia III
CHIMIE şi INGINERIE CHIMICĂ

D.C. 547.461

REACTIONS OF THE HYDRAZIDES OF CYCLOPROPANE AND 1-METHYLCYCLOPROPANE-1,2-DICARBOXYLIC ACIDS

BY

EUGENIA COMANIŢĂ, MARIA TUTOVEANU and ERFAN AL BOUCHI AL DABBAGH

Dedicated to Professor Dr. CRISTOFOR SIMIONESCU, member of the Academy, on his 60 th anniversary

1. Introduction

The hydrazides of dicarboxylic acids of the type of isophthalic, terephthalic and phenylendioxydiacetic acids can react with iso- and isothiocyanic esters leading to bifunctional compounds of the class of acylsemi- and thiosemicarbazides [1]...[3] and with diisocyanic esters giving polyacylsemicarbazide derivatives [4].

In the present paper the study of some acylthiosemicarbazides obtained through the hydrazides of cyclopropane and 1-methylcyclopropane-1, 2-dicarboxylic acid is reported. A new element is brought by the insertion between the thiosemicarbazide residues of a threemembered ring for which geometrical and optical isomers might be differentiated. The acylthiosemicarbazides were converted by cyclization reactions into heterocyclic compounds which show the above mentioned sterical characteristics due to the presence of the cyclopropane ring.

2. Results and Discussions

2.1. Synthesis of Intermediates

The 4-R-substituted 1, 2-cyclopropane-dicarboxythiosemicarbazides were obtained by applying the usual method of hydrazide addition to the C=N bond in isothiocyanates. It was necessary to prepare firstly the esters of the cyclopropane-1, 2-dicarboxylic acids in order to treat them with hydrazine hydrate in view to obtain the corresponding hydrazides.

The three-membered ring was formed by applying the method based on the reaction between ethyl acrylate or methacrylate and ethyl chloroacetate in the presence of sodium methoxide [5]. The two ethylic esters of the 1, 2-cyclopropanedicarboxylic acid (diastereoisomers *cis* and *trans*) are separated according to the literature indications, by the fractional distillation (methyl esters : *trans*, B.p.$_{16mm}$ 82°...84°C ; *cis*, B.p.$_{12mm}$102°C). This operation is rather difficult since the passing from one fraction to another is not distinct. Three fractions were collected under 10 mm Hg, namely at 60°...100°C, 100°...120°C and above 120°C, respectively.

The first fraction contains unreacted chloroacetic ester together with other byproducts contaminating the cyclopropane dicarboxylic ester. From

this reason this fraction cannot be employed for hydrazide preparation. The second fraction consists of a mixture of *cis—trans* isomers of esters which after the reaction with hydrazine hydrate lead to compounds with different melting points of 172° and 210°...212°C, respectively ; for the *cis* and *trans* isomers of dihydrazide, the melting points mentioned in literature are of 167°...178°C and 207°...211°C, respectively. The separation is based on

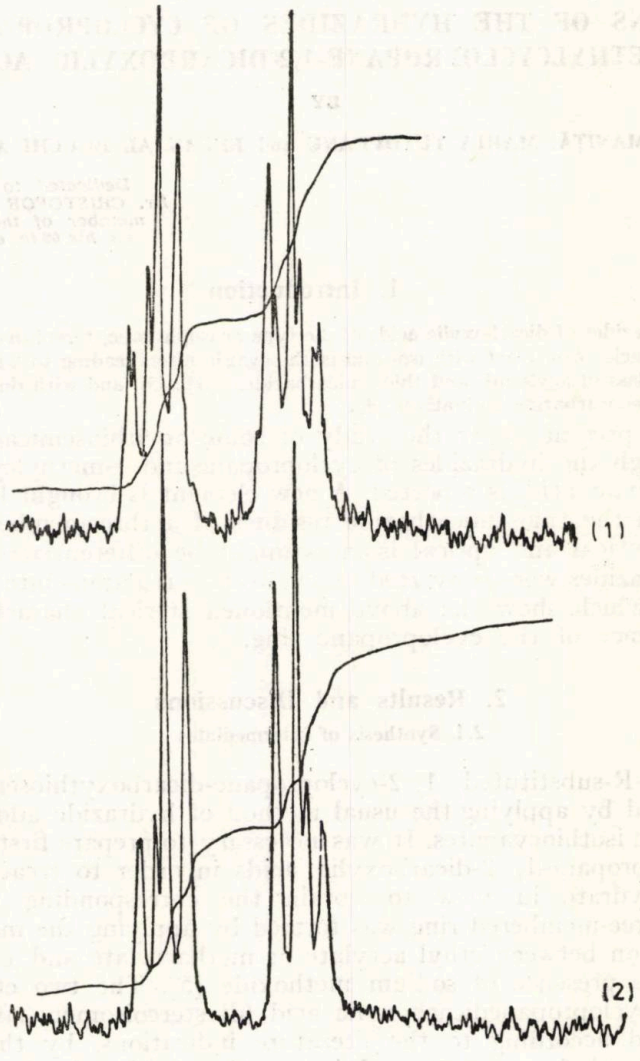

Fig. 1. — The NMR spectra for *cis* (*1*) and *trans* (*2*) isomers of 1,2-cyclopropanedicarboxyhydrazide.

the increased solubility of the low melting compound in hot ethylic alcohol. The nitrogen content as well as the NMR spectra recorded in deuterated water, confirm the hydrazide structure of these two substances. As

can be seen in Fig. 1, the isomeric hydrazides show two triplets corresponding to two methylenic protons and two protons CH. The shapes almost identical of the spectra do not indicate differences in configurations. This aspect would have been discussed in the case of a nonpolar solvent, but the substances under study are not soluble in it.

The third fraction, the less volatile one, leads exclusively to a low melting isomer (m.p. 172°C) by the reaction with hydrazine hydrate.

By a similar method the hydrazide of 1-methyl-1,2-cyclopropanedicarboxylic acid was synthesized.

2.2. Preparation of Acyl-thiosemicarbazides

The addition of hydrazides of cyclopropanedicarboxylic- and methylcyclopropanedicarboxylic acids to isothiocyanic esters takes place according to the following reaction scheme :

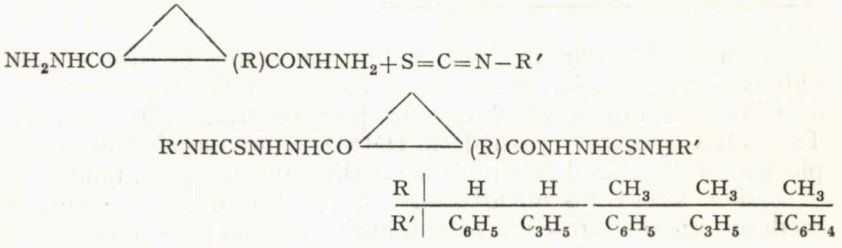

R	H	H	CH_3	CH_3	CH_3
R′	C_6H_5	C_3H_5	C_6H_5	C_3H_5	IC_6H_4

The ethylic alcohol is used as a solvent from which the acylthiosemicarbazides separate as white, crystalline substances, some of them even during refluxing. They are purified from either DMF—water mixture or ethanol. The thiosemicarbazides obtained from hydrazide of methylcyclopropanedicarboxylic acid are soluble in hot ethanol and show melting points as high as those of similar compounds without methyl group in the ring.

In the case of hydrazide of cyclopropanedicarboxylic acid, the both isomers (m.p. 172°C and 210°...212°C) were reacted with isothiocyanic esters which resulted in dithiosemicarbazides with rather closed melting points. However, the NMR spectra recorded in DMSO show some structural differences made also evident by the δ values presented in Table 1.

The ring protons are hidden by the DMSO signals.

2.3. Cyclization into Triazolthiones and R-amino-thiadiazoles

The 4-substituted 1-acyl-thiosemicarbazides are known to undergo cyclodehydration into 3,4-disubstituted triazol-5-thiones when treated with bases. With cyclopropane derivatives, bis (5-thiono-4-R-3-triazolyl) cyclopropanes are obtained according to the following reaction :

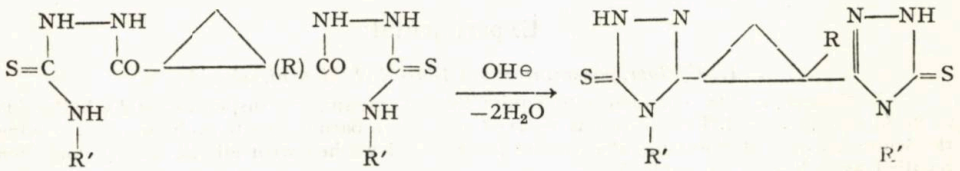

R, R′ are the same as for acyl-thiosemicarbazides

Table 1

Values of δ in the NMR Spectrum of 4-Allyl-substituted Cyclopropanedicarboxythiosemicarbazide

Protons	δ values, [ppm]	
	Hydrazide m.p., [°C]	
	210°...212°C	172°C
$=CH_2$	5	5
$=CH$	5.72	5.68
$HN-CH_2$	8.1	8.05
$HN-CS$	9.17	9.5
$HN-CS$	9.5	10.28
$HN-CO$	10.31	13.72

Table 2

Values in the NMR Spectra of 4-Phenyl (or allyl)-triazoles

Protons	δ values, [ppm]	
	4-phenyl	4-allyl
NH	13.7	13.7
C_6H_5	7.38	—
CH_2-N	—	4.65
$=CH_2$	—	5
$=CH$	—	5.75

The cyclization proceeds under the action of diluted sodium hydroxide when heated on steam bath. By acidulation the triazoles precipitate as white substances which may be purified from DMF—water or ethanol. The NMR spectra recorded in DMSO show clearly the presence of the phenyl (or allyl) and NH protons at the values, (ppm), indicated in Table 2.

The acyl-thiosemicarbazides may also undergo cyclization in acid medium. In the presence of sulphuric acid, at low temperature, a water molecule is eliminated as follows:

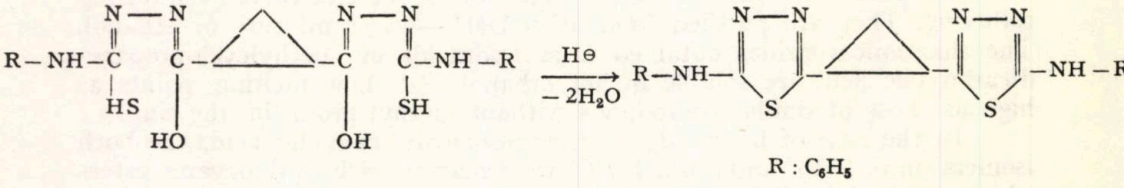

R : C_6H_5

When the reaction is over the thiadiazoles are precipitated by adding ammonia solution till a weakly alkaline pH.

The cyclization into triazolthiones and 5-R-amino-thiadiazoles were followed by the disappearance of the amide I band ($\nu_{C=O}$) 1 680 cm^{-1} in the IR spectra of acyl-thiosemicarbazides. In Fig. 2 the IR spectra of a thiosemicarbazide and of the corresponding triazole are shown comparatively.

The synthesized compounds and their characteristics are listed in Table 3.

3. Experimental

a) *1,2-Cyclopropanedicarboxy-1,1-bis-(4-R-thiosemicarbazide)*

Isothiocyanic ester is added in an equimolecular amount to a suspension of 2 g hydrazide in 50 ml ethylic alcohol. The mixture is refluxed on a steam bath for about an hour. After cooling the white crystals of thiosemicarbazide are filtered and washed with ethylic alcohol and then purified as indicated in Table 3.

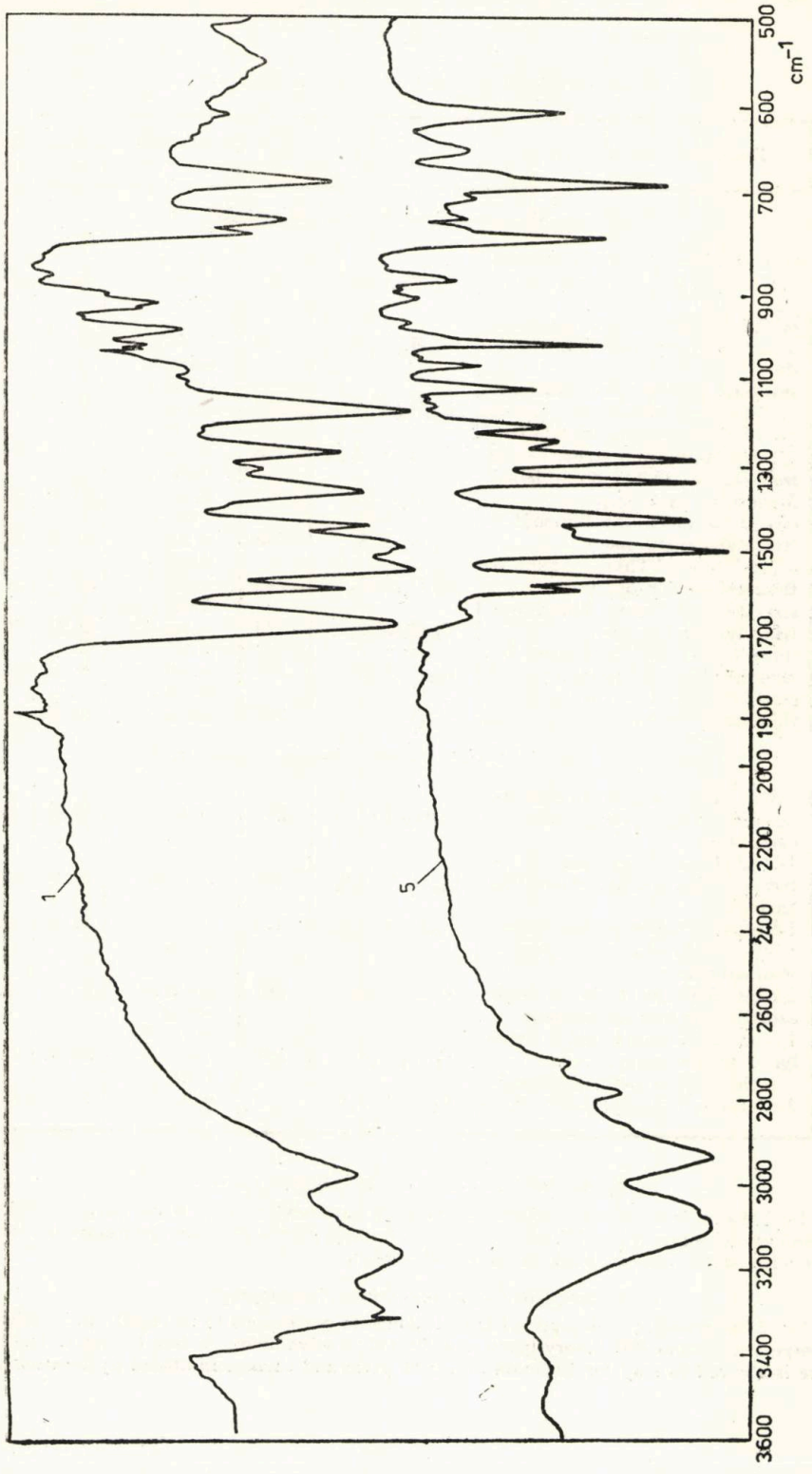

Fig. 2. — IR absorption spectra of some investigated compounds (1,5 — s. the Table 3).

Table 3

Thiosemicarbazides and their Cyclization Products

Nr.	Denomination of product	Molecular formula	M.p. °C	Recryst. solvent	N% calc.	N% found
	a) *1,2-Cyclopropanedicarboxylic derivatives*					
1	*trans*-1,2-Cyclopropanedicarboxy-1,1'-bis (4-phenylthiosemicarbazide)	$C_{19}H_{20}N_6O_2S_2$	205	DMF + water	19.62	19.79
2	*cis*-1,2-Cyclopropanedicarboxy-1,1'-bis (4-phenylthiosemicarbazide)	$C_{19}H_{20}N_6O_2S_2$	198	DMF + water	19.62	19.22
3	*trans*-1,2-Cyclopropanedicarboxy-1,1'-bis (4-allylthiosemicarbazide)	$C_{13}H_{20}N_6O_2S_2$	202	DMF + water	23.59	23.15
4	*cis*-1,2-Cyclopropane-dicarboxy-1,1'-bis (4-allylthiosemicarbazide)	$C_{13}H_{20}N_6O_2S_2$	198	DMF + water	23.59	23.07
5	*trans*-1,2-bis (5-Thiono-4-phenyl-3-triazolyl)-cyclopropane	$C_{19}H_{16}N_6S_2$	325	DMF + water	21.42	20.98
6	*cis*-1,2-bis (5-Thiono-4-phenyl-3-triazolyl)-cyclopropane	$C_{19}H_{16}N_6S_2$	318	DMF + water	21.42	21.10
7	*trans*-1,2-bis (5-Thiono-4-allyl-3-triazolyl)-cyclopropane	$C_{13}H_{16}N_6S_2$	243	DMF + water	26.25	26.00
8	*cis*-1,2-bis (5-Thiono-4-allyl-3-triazolyl)-cyclopropane	$C_{13}H_{16}N_6S_2$	251	DMF + water	26.25	26.42
9	*trans*-1,2-bis (2-phenylamino-5-thiadiazolyl)-cyclopropane	$C_{19}H_{16}N_6O_2$	266	DMF + water	21.42	21.66
10	*cis*-1,2-bis (2-phenylamino-5-thiadiazolyl)-cyclopropane	$C_{19}H_{16}N_6O_2$	262	DMF + water	21.42	21.75
	b) *1-Methyl-1,2-cyclopropanedicarboxylic derivatives*					
11	1-Methyl-1,2-cyclopropanedicarboxy-1,1'-bis) (4-phenyl-thiosemicarbazide)	$C_{20}H_{22}N_6O_2S_2$	242	DMF + water	19.00	19.16
12	1-Methyl-1,2-cyclopropanedicarboxy-1,1'-bis (4-allylthiosemicarbazide)	$C_{14}H_{22}N_6O_2S_2$	168	ethanol	22.70	22.23
13	1-Methyl-1,2-cyclopropanedicarboxy-1,1'-bis (4-iodophenylthiosemicarbazide)	$C_{20}H_{20}N_6O_2S_2I_2$	174	DMF + water	12.10	12.30
14	1,2-bis (5-Thiono-4-phenyl-3-triazolyl)-1-methylcyclopropane	$C_{20}H_{18}N_6S_2$	207	ethanol + water	20.68	20.50
15	1,2-bis (5-Thiono-4-allyl-3-triazolyl)-1-methylcyclopropane	$C_{14}H_{18}N_6S_2$	244	ethanol + water	25.14	25.00
16	1,2-bis (5-Thiono-4 iodophenyl-3-triazolyl)-1-methylcyclopropane	$C_{20}H_{16}N_6S_2I_2$	178	DMF + water	12.76	13.12

b) *1,2-bis-(5-Thiono-4-R-3-triazolyl)-cyclopropane*

1 g Thiosemicarbazide and 25 ml diluted NaOH are heated on a steam bath for an hour, After cooling the solution is acidified with diluted hydrogen chloride. The precipitate is filtered, washed with water and purified by recrystallization.

c) *1,2-bis-(2-R-Amino-5-thiadiazolyl)-cyclopropane*

1 g of fine powdered thiosemicarbazide is added in portions to 10 ml H_2SO_4 under stirring. at a temperature below 0°C. Every portion is allowed to solve before adding the next. The fluid mixture is allowed to stay for 10 hours in a cold place and then precipitated by treating with

ammonia solution under cooling till a weakly alkaline pH. The precipitated thiadiazole is filtered and purified from DMF—water.

Received, February 5, 1980

Polytechnic Institute, Jassy,
Department of Organic and
Macromolecular Chemistry

REFERENCES

1. Matei I., Comaniţă E., Bul. Inst. polit. Iaşi, **XIII (XVII)**, *1—2*, 269 (1967).
2. Tutoveanu M., Comaniţă E., C. r. Acad. Bulg. Sci., **26**, *3*, 375 (1973).
3. Tutoveanu M., Comaniţă E., C.r. Acad. Bulg. Sci., **28**, *6*, 763 (1975).
4. Comaniţă E., Tutoveanu M., Vâţă M., Savin A., Acta chim. Acad. Scie. hung., **83**, *2*, 217 (1974).
5. Baldwin J. E., Andrist A. M., Ford P. W., Chem Ind., *1*, 930 (1971).
6. Shono T., Morikawa T., Okayama R., Oda R., Die Makromol. Chem., **81**, 142 (1965).

REACŢIA HIDRAZIDELOR ACIZILOR CICLOPROPAN- ŞI 1-METIL-CICLOPROPAN-1,2-DICARBOXILICI

(Rezumat)

Din esterii acizilor 1,2-ciclopropan- şi 1-metil-1,2-ciclopropandicarboxilici s-au preparat hidrazidele corespunzătoare. In primul caz, fracţionarea esterului, efectuată în vederea separării izomerilor *cis—trans*, a permis ca în reacţia cu hidratul de hidrazină să se obţină hidrazide diastereoizomere (p.t. 210°...212°C şi 172°C). Reacţia ulterioară cu izotiocianaţii de fenil, alil şi *p*-I-fenil a condus la 1,2-ciclopropandicarboxi-1,1'-bis(4-R-tiosemicarbazide), care cercetate sub raportul izomeriei *cis—trans*, pun în evidenţă la produşii sintetizaţi din cele două hidrazide ale acidului 1,2-ciclopropandicarboxilic diferenţe între punctele de topire şi valori distincte pentru protonii NH—CO. Compuşii tiosemicarbazidici au fost supuşi ciclizării în cataliză bazică şi acidă, în scopul obţinerii unor derivaţi ai bis-(triazolil)-, respectiv bis-(tiadiazolil)-ciclopropanului. Spectrele IR şi RMN atestă structura compuşilor sintetizaţi.

BULETINUL INSTITUTULUI POLITEHNIC DIN IAŞI
Tomul XXVI (XXX), fasc. 1—2, 1980
Secţia III
CHIMIE şi INGINERIE CHIMICĂ

D.C. 547.473.2 ; 547.495.2

STUDY OF MIXTURES OF POLY-ε-CAPROLACTAM AND POLYETHERUREAS

BY

M. KRIŠTOFIČ, A. PIKLER and J. BENISKA

Dedicated to Professor Dr. CRISTOFOR SIMIONESCU, member of the Academy, on his 60 th anniversary

1. Introduction

Among the procedures for the preparation of new types of poly-ε-caprolactam fibres the physical modification still holds good. By means of preparation of heterogeneous polymer mixtures, as one of the technical ways, it is possible to modify the properties of polyamide fibres in a wide range. At the present time the aim of the modification of the mentioned fibres is to increase the electrical conductivity and the sorption ability and to improve dye adhesion, etc.

This work on physical modification deals with the study of polymer mixtures of poly-ε-caprolactam (PAD) with polyetherureas (PEU) and with some service properties of fibres prepared in this way.

2. Theoretical

Diphenylmethan-4,4′-diisocyanate (MDI) and α, ω-diaminodipropylene derivates of ethylene glycole were used for the synthesis of polyetherureas. The reaction proceeded according to the scheme:

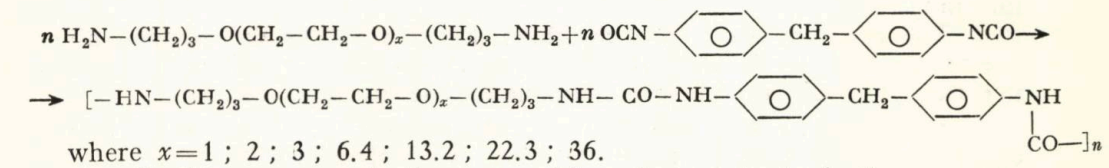

where $x = 1$; 2 ; 3 ; 6.4 ; 13.2 ; 22.3 ; 36.

In this manner polyetherureas with various content of ethoxy groups were prepared. They were marked as follows:

PEU_1 ($x=1$) ; PEU_2($x=2$) ; PEU_3 ($x=3$) ; PEU_4 ($x=6.4$) ;

PEU_5 ($x=13.2$) ; PEU_6 ($x=22.3$) ; PEU_7 ($x=36$).

Some physical properties of the prepared polyetherureas and of poly-ε-caprolactam are stated in Table 1.

Table 1

Some Physical Properties of Polyetherureas and Polycaprolactam

Component	$[\eta]$ 100 ml.g^{-1}	η_1 Pa.s	η_2 Pa.s	M.p. °C
PAD_6	0.84	5.0	0.86	224
PEU_1	0.05	1.98	0.34	228
PEU_2	0.1	2.01	0.33	246
PEU_3	0.1	2.19	0.34	235
PEU_4	0.24	2.39	0.36	220...225
PEU_5	0.49	3.27	0.43	238...242
PEU_6	0.59*)	3.68*)	0.70	225...230
PEU_7	0.63	3.82	0.73	232...240

$[\eta]$ — limitting viscosity number ; η_1, η_2 — dynamic viscosity ($p = 19.6$ kPa, 20°C), determined in methacresole (η_1) and in tetrachloroethane (1 : 3) (η_2) ; *) values derived from the relation $[\eta] = f(x)$ and $\eta_1 = f(x)$.

3. Experimental

We have studied the compatibility of components in the polymer mixture. For this reason the mutual miscibility of PAD_6 and PEU (80 : 20 wt.%) was studied viscosimetrically [1], [2]. The measurements were based on the dynamic viscosities of solutions of mixtures from both components and of pure components. The determination was carried out in phenol—tetrachloroethane 1 : 3 wt. %. The $\Delta_i/\Delta\eta$ deviation, or the so-called compatibility parameter, was evaluated with the relation :

$$\frac{\Delta i}{\Delta \eta} = \frac{(\eta_1 W_1 + \eta_2 W_2) - \eta_{mexp}}{\eta_2 - \eta_1},$$

where : η_1, η_2 — dynamic viscosity of components *1*, *2*, W_1, W_2 — weight fraction of components *1*, *2*, η_{mexp} — measured dynamic viscosity of the mixture.

The following cases are possible : a) $\Delta i/\Delta\eta < 0.1$ — the components are compatible ; b) $\Delta i/\Delta\eta = 0.1$ — the components are compatible in a limited range ; c) $\Delta i/\Delta\eta > 0.1$ — the components are incompatible.

The dependence of the compatibility parameter on the number of oxyethylene units in the basic polyetherurea unit is given in Table 2 and Fig. 1.

It is evident from the obtained results that the compatibility of the system depends on the type of polyetherurea. The heterogeneous system PAD_6—PEU with values $x = 1...6.4$ is incompatible. At $x = 13.2$ the components are compatible in a limited range. Only systems with PEU_6 and PEU_7 are compatible with polyamide. It can be seen that the mutual miscibility of polyamide and polyetherureas improves with the increasing number of ethyleneoxide units in PEU.

Table 2

The Dependence $\Delta_i/\Delta\eta$ *vs. the Number of Ethylene Oxide Elements* (x) *in the System* PAD_6—PEU (80:20) *at Various Loads*

x_i	Mixture	$\frac{\Delta_i}{\Delta\eta}$				
		p, [kPa]				
		4.90	7.84	11.77	15.69	19.61
1	PAD_6+PEU_1	0.125	0.128	0.133	0.139	0.142
2	PAD_6+PEU_2	0.113	0.116	0.125	0.130	0.140
3	PAD_6+PEU_3	0.108	0.113	0.120	0.127	0.136

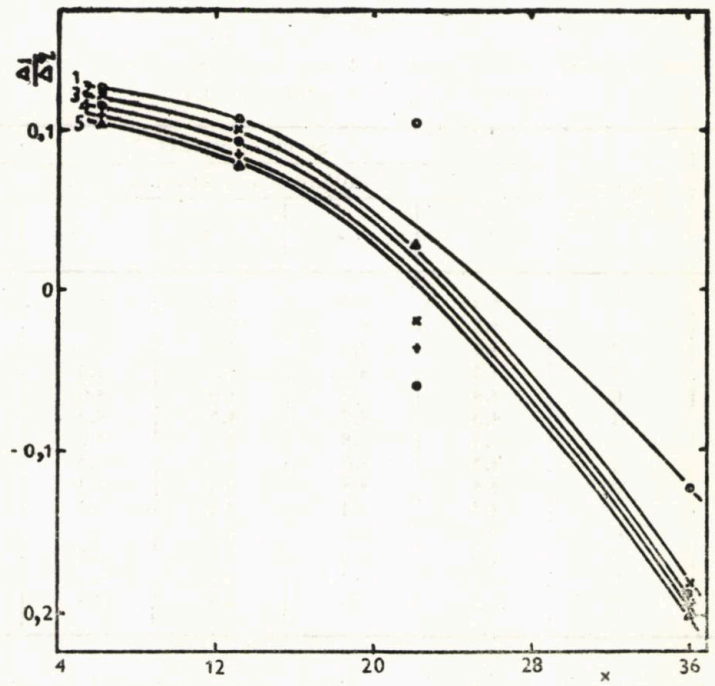

Fig. 1. — Dependence of the compatibility parameter ($\Delta_i/\Delta\eta$) vs. the number of ethylene oxide elements (x) in the basic unit of the polyetherureas; *1* — 19.61 kPa; *2*—15.69 kPa; *3* — 11.77 kPa; *4*—7.84 kPa; *5*—4.90 kPa.

The compatibility of the components in the studied system is also a function of the molecular weight of the polyetherureas. This functionality can be observed in the relations of the limiting viscosity number and the compatibility parameter. The mutual compatibility of PAD_6 and PEU

improves after the values of PEU, comparable with those of PAD_6, have been obtained.

It can also be assumed that the compatibility of components of the system will be influenced besides the interaction of amide and urea groups, also by the interaction of amide and ether groups of the components in the system [4].

Further fibres from heterogeneous polymer mixtures were prepared, where the sorption of steam, the electrostatic charge and the dyeability was studied.

The moisture uptake of the fibres was influenced only by the presence of high molecular polyetherureas (Table 3). PEU_6 and PEU_7 in the fiber affect the regularity of the forming structure, they cause the formation of defects, which contribute to the increasing of the diffusion of low molecular substances. The chemical character of the polyether component itself also influences the sorption properties of the fiber.

Table 3

Dependence of the Moisture Sorption on the Type and on the concentration of the Additive in the Fiber PEU_{1-6}, $\lambda=3$; PEU_7, $\lambda=3.4$

Additive	Number of washings	Sorption of H_2O,[%] Additive concentration, [%]				
		0	2	4	6	9
PEU_1	0	4.4	4.5	4.6	4.5	4.5
	1	4.5	4.6	4.6	4.5	4.4
PEU_2	0	4.4	4.7	4.6	4.4	4.4
	1	4.5	4.6	4.5	4.5	4.5
PEU_3	0	4.4	4.7	4.6	4.6	4.6
	1	4.5	4.7	4.5	4.5	4.5
PEU_4	0	4.4	4.8	4.6	4.6	4.4
	1	4.5	4.6	4.6	4.5	4.4
PEU_5	0	4.4	4.8	4.9	5.1	5.1
	5	4.5	5.1	5.1	5.1	5.1
PEU_6	0	4.4	4.8	5.5	6.1	—
	5	4.5	5.5	5.6	5.6	—
PEU_7	0	4.4	5.2	5.2	6.3	6.3
	5	4.5	5.9	5.8	5.8	5.9

The electrostatic charge of the fibres was decreased in consequence of the admixture of additives (Table 4). The concentration of additives in the fiber in which a substantial decrease of the static charge is observed, depends on the length of the polyether chain and on the molecular weight of PEU. With the increasing number of the ethylene oxide elements and with the increasing molecular weight of PEU, the decreasing of effective concentration of the additives takes place in view of a substantial decrease of the static charge.

The partial washing of polyetherureas from the fiber has a negative influence on the static charge.

Table 4

Dependence of the Electric Charge on the Type and on the Concentration of the Additive in the Fiber

Additive	Number of washings	Electrostatic change, [kV] Additive concentration, [%]				
		0	2	4	6	9
PEU_5	0	13.4	12.3	11.0	1.9	0.7
	5	13.5	11.7	10.0	3.3	1.6
PEU_6	0	13.4	8.6	2.2	1.3	—
	5	13.5	8.2	3.3	1.6	—
PEU_7	0	13.4	2.6	2.5	1.2	1.0
	5	13.5	6.1	6.1	3.1	2.5

The dyeability of the polyamide fibres containing polyetherureas was improved (Table 5). The surface dyeability improvement depends on the amount of the present urea groups, proved by the higher adsorption of the dye in the case of PEU_5 in comparison with PEU_7.

Table 5

Dyeability of Mixed Fibres

Value	Additive concentration, [%]					
	PEU_5			PEU_7		
	2	4	9	2	4	9
A	2.42	3.34	3.42	1.31	2.05	2.66

A—Ratio of absorbances for solutions of mixtures and for the basic polymer (indicates how many times more is the dye adsorbed on the studied sample).

4. Conclusions

From the obtained results for the compatibility of the system PAD_6—PEU as well as from the studied physical properties of the modified fibres is evident that PEU_7 is a convenient additive for the modification.

Received, December 27, 1979

Slovak Technical University, Bratislava, Czechoslovakia

REFERENCES

1. Zelinger I., Heidingsfeld V., *Směsi PVC s kaučuky* (I). Coll. of Papers of the Technical University for Chemical Technology, Prague, 1966, 63.
2. Marčincin A., *Katalog analyticko-fyzikálnych metód*. VÚCHV, Svit, 1975, 37.

3. Krištofič M., Pikler A., Chemické vlákna, 26, 54 (1976).
4. Krištofič M., *Štúdium prípravy a vlastností polymérnych vláknotvornych zmesi*. Ph.D. Diss., Slovak Technical University, Bratislava, 1978.

STUDIUL AMESTECURILOR DE POLI-ε-CAPROLACTAMĂ—POLIETERUREE

(Rezumat)

Se prezintă obținerea intermediarilor polieterureici și se studiază compatibilitatea lor cu poli-ε-caprolactama. Asupra fibrelor realizate din amestecuri cu un conținut de 2%, 4%, 6% și 9% polieteruree se efectuează măsurători de absorbție a vaporilor de apă, a încărcării electrostatice și a proprietăților tinctoriale.

BULETINUL INSTITUTULUI POLITEHNIC DIN IAŞI
Tomul XXVI (XXX), fasc. 1—2, 1980
Secţia III
CHIMIE şi INGINERIE CHIMICĂ

D.K. 66.063.72

UNTERSUCHUNGEN EINIGER UMGEKEHRTER WEICHMACHER (II)

VON

VIRGINIA MANOVICIU, I. MANOVICIU, DANIELA BANDUR und G. BANDUR

Herrn Professor
Dr. CRISTOFOR SIMIONESCU,
Mitglied der Akademie,
zum 60. Geburtstag gewidmet

1. Vorwort

In einer vorangehenden Arbeit [1], die die experimentellen Befunde bezüglich einer Reihe direkter und umgekehrter Weichmacher unten angegebener Structur analysiert [2] · · · [5] :

(A)

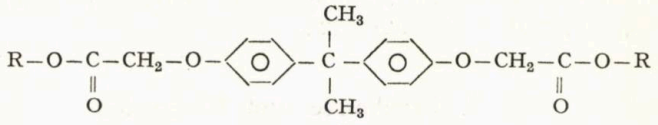

(B)

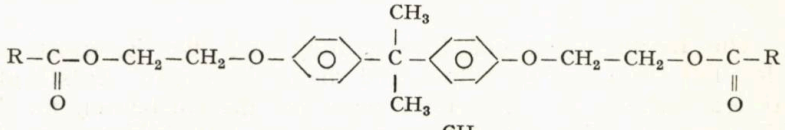

(C)

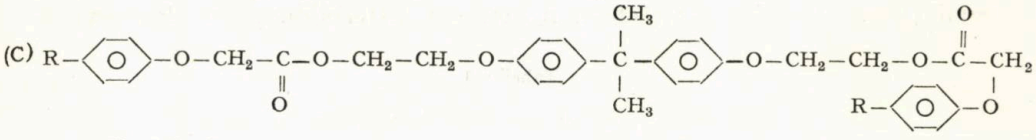

(R = Alkyl)

wurde gezeigt, daß bei der Bestimmung der Kompatibilität des Systems Weichmacher—PVC, ausser der Zahl der polaren, nichtpolaren und polarisierbaren Gruppen, die als Kriterium von G. van Veersen [6] · · · [10] bezeichnet wurde, auch der Platz den diese Gruppen im Molekül einnehmen, wie auch die Richtung der Polarisierung, eine wichtige Rolle spielt.

Für die in Betracht gezogenen Reihen wurde gezeigt, daß die Weichmacherkapazität in Bezug auf PVC umso größer ist, je näher sich die polaren Gruppen zum Molekülende befinden. Ausser dem, scheint es, daß die positive Polarisierung der Endgruppen dem Weichmacher bessere Eigenschaften verleiht als die Vergrößerung der Elektronendichte am Molekülende.

Die gegenwärtige Arbeit hat den Zweck zu untersuchen in welchem Masse die vorher gezeigten elektronischen Effeckte ihre Bedeutung auch im Falle folgender Strukturen beibehalten :

(D)

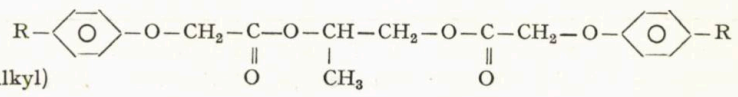

(R = Alkyl)

Diese Strukturen sind ähnlich deren aus (B) und (C), weil sie Ester eines Diols (1, 2-Propylenglykol) mit Monokarboxylsäuren sind, folglich der Klasse der „umgekehrten Weichmachern" angehören [3].

2. Experimentellen Teil

Im Falle der Synthese der phenolischen Ester—Äther der Reihe (4) wurden folgende Substanzen verwendet :

1. *p* - Kresoxyessigsäure ;
2. *o* - Kresoxyessigsäure ;
3. *o* - Sek-Butyl-Phenoxyessigsäure ;
4. *p* - Nonyl-Phenoxyessigsäure.

Diese Säuren wurden alle im Laboratorium nach bekannten Methoden [11], [12] synthetisiert und haben eine Reinheit, die dem verfolgten Zwecke entspricht (das Fehlen der fremden Banden im IR-Spektrum und der Schmelzpunkt entspricht den Literaturdaten).

5. 1, 2-Propylenglykol p. a. Austranal ;
6. *p*-Toluolsulfonsäure (Monohydrat) p. a. Merck.

Die säurekatalysierte Estersynthese wurde in einer gewöhnlichen Veresterungsapparatur durchgeführt.

3. Ergebnisse und Disskusion

Die Bedingungen der Esterbildung und die Esterausbeute werden in der Tabelle 1 widergegeben und die Abb. 1 gibt Aufschluß über den Reaktionsverlauf. Die Tabelle 1 zeigt daß die Ausbeuten an Ester hoch sind (>80%) und die Geschwindigkeit der Esterbildung aus Phenoxyes-

Tabelle 1

Bedingugen und Verhältnisse im Esterbildungsprozess

Ester*)	Ausganskomponenten		Katalysator p. Toluol-Sulfonsäure	Toluol ml	maximale Veresterungstemperatur °C	Wassermenge ml		Ausbeute	
	Säure g (Mol)	Diol g (Mol)	g (%)			Berechnet	Gefunden	g	%
1	200 (1,2)	42 (0,55)	2,42 (1)	150	120	19,7	20	168	82,4
2	123 (0,74)	25,6 (0,34)	1,49 (1)	150	118	12,1	12,8	108	86
3	121 (0,58)	20 (0,26)	1,40 (1)	150	123	9,52	10,1	101	92
4	226 (0,81)	28 (0,37)	2,54 (1)	150	126	13,3	14,3	190	86

*) Die Numerotierung der Ester in den Tabellen und Abbildungen entsprechen der Säurenumerotierung aus dem Text für die Synthese der phenolischen Äther—Ester.

sigsäuren mit 1,2-Propylenglykol groß ist und der höchste Umsetzungsgrad in weniger als zwei Stunden erreicht wird.

Aus den unternommenen Versuchen (s. Tabelle 2) geht hervor, daß die Reinheit der Ester zu ihrem charakterisieren Weichmacher genügend

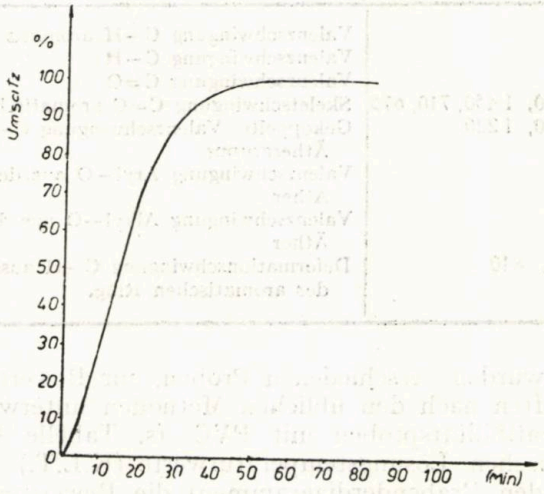

Abb. 1. — Ausbeuteveränderung im Verlauf der Zeit (Ester *4*).

hoch ist. Die Säurezahlen sind kleinen als 5 mg KOH/g (mit Aussnahme der Probe *4* deren Endbearbeitung besonders schwierig war) ; die Verseifungszahlen sind, in den Grenzen der experimentellen Fehler, den berechneten Werten nahe ; der Gehalt an flüchtigen Komponenten ist kleiner als 1%.

Die IR-Analyse eines Ester-Films, die mit einem SPECORD 71 R Apparat unternommen wurde, beweisst die Struktur der Ester. Die charakteristischen Banden sind in Tabelle 3 zusammengefasst.

Das Fehlen der fremden Banden weist auf die fortgeschrittene Reinheit der Estere hin.

Tabelle 2

Die wichtigsten Eigenschaften der Ester

Ester	M	Verseifungszahl mg KOH/g		Säurezahl mg KOH/g	n_D^{22}	Viskosität bei 20°C cP	Flüchtige Produkte %	Aussehen
		berechnete	gefunden					
1	372	301,6	298	4	1,5315	1 791	0,74	flüßig
2	372	301,6	304	2,5	1,5310	—	0,54	flüßig
3	456	246,1	243,1	2,35	1,5180	1 722	0,38	flüßig
4	611	183,6	178,5	14	1,5123	42 360	$9{,}6.10^{-4}$	flüßig—zäh

Tabelle 3

Charakteristische Banden im IR-Spektrum

Bande, [cm^{-1}]	Zuordnung
3 030	Valenzschwingung C—H aromatischer Ring
2 950	Valenzschwingung C—H
1 750	Valenzschwingung C=O
1 600, 1 580, 1 500, 1 450, 710, 675	Skeletschwingung C=C aromatischer Ring
1 300, 1 280, 1 240, 1 220	Gekoppelte Valenzschwingung C—C, O—C aus der Äthergruppe
1 180, 1 160	Valenzschwingung Aryl—O aus dem Aryl—Alkyl-Äther
1 080, 1 060	Valenzschwingung Alkyl—O aus dem Aryl—Alkyl-Äther
880, 860, 840, 810	Deformationschwingung C—H ausserhalb der Fläche der aromatischen Ring.

Die Ester wurden verschiedenen Proben, zur Bewertung der Weichmachereigenschaften nach den üblichen Methoden unterworfen.

Die Kompatibilitätsproben mit PVC (s. Tabelle 4) erlauben auf Grund der kritischen Lösungstemperaturwerte (K.L.T.) und des Drehmomentes (aus den Brabenderdiagrammen) die Bewertung der synthetisierten Äther — Ester als primäre Weichmacher (Probe *1*, *2*), als sekundärer Weichmacher (Probe *3*) und als Extender (Probe *4*).

Tabelle 4

Kompatibilitätsproben mit PVC

Ester	KLT °C	Drehmoment m kg	Gebbildungs-zeit, [Min.]	Anmerkung
1	120	3,7	momentan	primär
2	133	4,1	0,1	primär
3	165	2,57	9,5	secundär
4	165	—	—	Extender

Aus den experimentellen Daten geht hervor, daß sich die vorheringen Bewertungen [1], auf Grund der elektronischen Effekte in Bezug auf die Strukturen (A), (B) und (C), bei den Strukturen (D) nicht verifizieren. Es ist wahrscheinlicher, daß in der Reihe (D), die sterischen Effekte vorwiegend und deshalb das Fallen der Kompatibilität mit PVC in folgender Reihe :

$$\text{Ester } 1 \approx \text{Ester } 2 > \text{Ester } 3 > \text{Ester } 4.$$

Der Vergrösserung der sterischen Hinderungen der Substituenten R, entspricht :

$$p\text{-}CH_3 < O-CH_3 < \text{sec}-C_4H_9 \ll C_9H_{19}\ .$$

Für die primären Weichmacher wurde ein komplettes Bewertungsstudium unternommen, dessen Ergebnisse in Tabelle 5 widergegeben sind.

Die Bewertungsproben wurden mit folgendem Rezept durchgeführt: $PVC_{(s)}$ $(K=67)=100$ g, Weichmacher 50 g, Stabilisator 2 g, Walzen 140°... 145°C, Dauer 3 Min., Pressen 150°C, Dauer 3 Min.

Tabelle 5

Proben zur Bestimmung der Ester 1 und 2 als primäre Weichmacher

Probe	Bestimungstyp	Masseinheit	Ester *1*	Ester *2*	D.O.F.
a	KLT	°C	120	133	114
b	Drehmoment	m Kg	3,70	4,10	3,50
c	Gelbildungszeit	Min.	momentan	0,1	0,5
d	Shorehärte 3″	°Sh	90	91	80
e	Shorehärte 10″	°Sh	87,5	88	78
f	Modul 100%	Kgf/cm²	165	149	106
g	Bruchdehnung	%	220	233	200
h	Bruchfestigkeit	Kgf/cm²	251	257	147
i	Wasserverluste	%	0,03	0,045	0,06
j	Wasserabsorbtion	%	0,12	0,15	0,13
k	Extraktion in Mineralöl	%	0,23	0,24	1,24
l	Extraktion in Benzin	%	0,78	0,65	14,62
m	Migration in Bezug auf Kautschuk	%	1,06	0,68	1,89
n	Clash-Berg	°C	+7	+7	−27
o	Flüchtigkeit	%	3,45	3,80	1,57
p	Thermische Beständigkeit in Bezug auf Kongorot	Min.	60	30	32

Aus der Tabelle 5 geht hervor, daß die studierten primären Weichmacher einige bessere und einige schlechtere Eigenschaften als der Vergleichsweichmacher, Dioktylphtalat (DOF) aufweisen.

Die Kompatibilität mit PVC (Probe *a*, *b*, *c*) haben fast gleiche Werte mit denen der Vergleichsprobe (*a* und *b*), und bessere Werte als diese im Falle *c*. Diese Daten heben eine interesante Tatsache hervor und zwar, daß die Ester *1* und *2* ähnliche Eigenschaften mit den direkten Weichmachern und von diesen sogar mit den primären Weichmachern aufweisen, obwohl sie umgekehrte Weichmacher sind.

Die Versuche *d*, *e* und *f* zeigen eine schwächere Effizienz als die Vergleichsprobe, was auf eine schwächere Solvatierungskapazität des PVC hinweist.

Die Proben *g* und *h* haben bessere mechanische Eigenschaften als die Vergleichsprobe, was auf bessere Effizienz hinweist.

Die Beständigkeitseigenschaften der mit PVC kompoundierten Weichmacher (Proben *i*...*o*) sind besser als jene der Vergleichsprobe, was sehr wahrscheinlich auf die Unterschiede der Löslichkeiten in den verwendeten Extraktionsmitteln, zurückzuführen ist.

Die Proben *n* und *p* zeigen eine gute Beständigkeit der Weichmacher bei hohen Temperaturen, aber ein schwächeres Verhalten bei niedrigen Temperaturen an.

Um einige Aspekte des Verhaltens des studierten Weichmacher im System mit PVC, klarzustellen, wurden einige rheologischen Eigenschaften in einem Temperaturbereich zwischen $-15°$ und $+25°C$, studiert (s. Abb. 2).

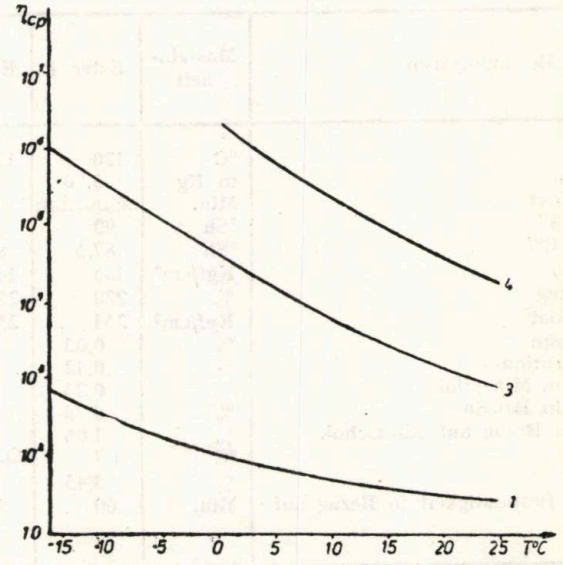

Abb. 2. — Viskositätsänderung mit der Temperatur (Ester *1, 3, 4*).

Man kann beobachten, daß die Viskosität des Esters *1* um einige Größeneinheiten kleiner ist als die der Ester *3* und *4*. Zur gleichen Zeit ist die Abhängigkeit der Viskosität der Probe *1* von der Temperatur kleiner. Diese Tatsache könnte noch ein Argument für die Behauptung sein, daß der Ester *1* ein primärer, der Ester *3* ein sekundärer Weichmacher und der Ester *4* ein Extender ist, nebst den vorheringen Bemerkungen in Bezug auf die Beziehung Kompatibilität—Effizienz.

Der Ester *4*, der schwache Weichmacheneigenschaften aufweist (K.L.T. $>165°C$), wurde als Extender bezeichnet. Dieses Verhalten wurde durch seinen Effekt im System mit primären Weichmachern DOF und DBF untersucht wobei man die Viskosität der PVC-Pasten im Verlauf der Zeit verfolgte (Abb. 3 und 4).

Es wurde beobachtet ein Zusatz von 5% Ester *4* den zwei vorhim erwähnten primären Weichmachern, die Beständigkeit der PVC-Pasten viel vergrößert, (also das Verkleinern des Wachsens der Viskosität der Pasten im Verlauf der Zeit), daß sehr wichtig in der Verarbeitung ist.

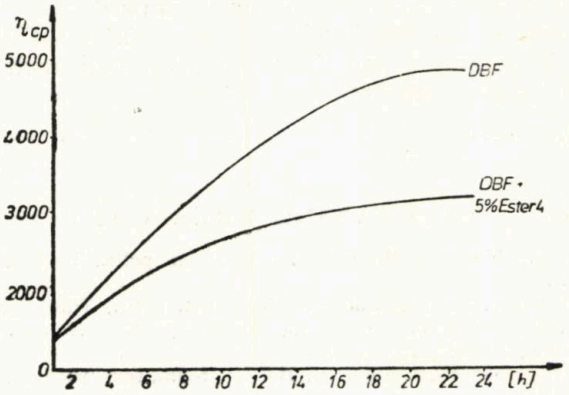

Abb. 3. — Viskositätsänderungen der PVC-Pasten im Verlauf der Zeit; DBF und DBF+5% Ester 4. Rheoviskosimeter „Rheotest R.V." ; Schergefälle=9 Min.$^{-1}$

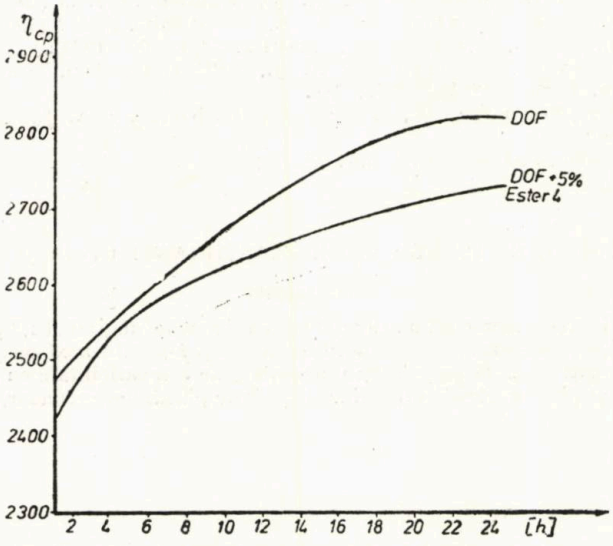

Abb. 4. — Viskositätsänderung der PVC-Pasten im Verlauf der Zeit; DOF und DOF + 5% Ester 4. Rheoviskosimeter „Rheotest R.V."; Schergefälle = 27 Min.$^{-1}$

4. Schlussfolgerungen

In der Klasse der umgekehrter Weichmacher wurden vier neue Substanzen dargestellt und charakterisiert, die Diester des 1,2-Propylenglykols mit *p*-Kresoxyessigsäure, *o*-Kresoxyessigsäure, *o*-Sek-Butyl-Phenoxyessigsäure und *p*-Nonyl Phenoxyessigsäure sind.

Die studierten Ester weisen verschiedene Eigenschaften in Bezug auf die Kompatibilität mit PVC auf und funktionieren als primäre Weichmacher (die ersten zwei), sekundärer Weichmacher (der dritte) und Extender (der letzte).

In der Interpretierungsmethode der Kompatibilität Weichmacher—PVC, wurden den sterischen Effekten eine größere Bedeutung als den elektronischen beigemessen und diese Tatsache wird auch von den Viskositätsunterschieden unterstützt.

Eingegangen am 22. Dezember 1979

Technische Hochschule „Tr. Vuia", Timișoara

LITERATURVERZEICHNIS

1. Manoviciu V., Nuțiu M., Bul ști. tehn., Inst. polit., Timișoara, s. Chimie (unter Druck).
2. Nanu I., Boboescu V., Bul. ști. tehn., Inst. polit., Timișoara, **8** (22), 51 (1963).
3. Nanu I., Boboescu V., Rus R., Simion Gh., Bul. ști. tehn. Inst., polit., Timișoara, **11** (25), *1*, 9 (1966).
4. Boboescu V., Rus R., Nanu I., Bul. ști. tehn., Inst. polit., Timișoara, **14** (28), *2*, 487 (1969).
5. Manoviciu V., Manoviciu I., Ciopor R., Secoșan E., Bul. ști. tehn., Inst. polit., Timișoara, s. Chimie (unter Druck).
6. van Veersen G., Brit. Plastics, *7*, 442 (1965).
7. van Veersen G., Menleberg A. J., Kunststoffe, *1*, 23 (1966).
8. van Veersen G., Menleberg A. J., Kunststoffe, *7*, 561 (1967).
9. van Veersen G., Dykers J., Plastica, *25/3*, 105 (1973).
10. van Veersen G., Menleberg A. J., SPE 30 th., Ann. Techn. Conf., Part 1, Tech. Papers, 18 Mai 1972, 314.
11. Alfrey, Wiederhorn M., Stein R., Tobolsky A. J., Colloid Sci., *4*, 211 (1949).
12. * * * Pat. Canada, *733 997* (C.A. 65-1361 6*g*).

CERCETĂRI ASUPRA UNOR PLASTIFIANTI INVERȘI (II)

(Rezumat)

S-au sintetizat și caracterizat patru produse noi și anume: diesteri ai 1,2-propilen-glicolului cu acizi *p*-crezoxi (*1*), *o*-crezoxi (*2*), *o*-sec-butil-fenoxi (*3*) și *p*-nonil-fenoxi-acetic (*4*).

Esterii studiați prezintă proprietăți diferențiate de compatibilitate cu P.V.C.

Esterii (*1*) și (*2*) sînt plastifianți primari, (*3*) este plastifiant secundar, iar (*4*) extender.

BULETINUL INSTITUTULUI POLITEHNIC DIN IAŞI
Tomul XXVI (XXX), fasc. 1—2, 1980
Secţia II
CHIMIE şi INGINERIE CHIMICĂ

D.C. 678.779

THE SWELLING OF POLYACRYLONITRILE IN DMF—WATER AND DMSO—WATER MIXTURES

BY

E. TURSKA, S. BIADACZ and H. JANECZEK

Dedicated to Professor Dr. CRISTOFOR SIMIONESCU, member of the Academy, on his 60 th anniversary

1. Introduction

The present work constitutes a part of extensive investigations on the possibilities of the liquid-induced crystallization of polyacrylonitrile. Results obtained when studying the swelling of polyacrylonitril films in the mixtures of N, N'-dimethylformamide — water and dimethylsulphoxide—water are herein reported.

Literature data concerning the structure of polyacrylonitrile are rather limited and very often contradictory. Some authors postulate a crystalline—amorphous structure of that polymer [1], while others suggest that it is paracrystalline [2], [3]. Chemical structure of polyacrylonitrile and the very strong interaction between the CN groups determine its possessing a number of uncommon properties, as confirmed by numerous works. Andrews et al.[4] investigated the swelling of polyacrylonitrile films in aqueous solutions of iodine and potassium iodide and found that process to proceed in three stages. The first and third stages involved the diffusion of the penetrant to two different amorphous phases, while in the second stage there takes place a change of the conformation of the amorphous phase chains to a helix conformation. According to these authors, the fact that the polymer does not dissolve upon reaching even a very high degree of swelling (up to about 300 per cent of weight increase) provides direct evidence for the existence of a crystalline phase. Basing on results of their investigations Andrews et al. proposed a three-phase structural model of the polyacrylonitrile in which two amorphous phases with different degrees of ordering and a crystalline phase are present.

Ganzyuk [5] studied the influence of various organic solvents on polyacrylonitrile fibres using the weighting method for the following swelling liquids : xylene, toluene, benzene, acetone, ethanol and methanol. He found the tendency to swell of that polymer to grow with the increase of the solvent dipole moment. Content of the penetrant was never found to exceed 13% by weight. Recently, Rigbi [6] determined the theoretical compositions of mixtures which should have proved good swelling agents for the polyacrylonitrile. These mixtures were however found by us to be impractical for swelling polyacrylonitrile films, and it was therefore decided to use for that purpose the aqueous solutions of DMF and DMSO. The latter swelling systems exhibit good swelling properties and are also readily accessible. The IMF—water system is widely used for the spinning of PAN fibres. The process of fibre forming is known to influence decisively the structure of resultant fibres, and hence their final properties.

That problem shall constitute the subject of our future investigations. However, in order to obtain a general characterization of properties of fibres it is essential to make a thorough study of the changes taking place on swelling and in the swollen state. The present work is a part of our studies devoted to that problem.

2. Experimental

Polyacrylonitrile films 60 and 100 μm thick were used in the present study. These were obtained by casting the DMF solution of polyacrylonitrile onto a glass plate. The films thus obtained were vacuum-dried for 24 hours.

X-ray studies and microscopic observations in polarized light did not show the presence of a crystalline phase in the PAN film samples. The polyacrylonitrile used was prepared by the radical polymerization of acrylonitrile (monomer supplied by Koch Light Laboratories Ltd.) in the presence of AIBN as initiator. As swelling agents the aqueous solutions of N, N-dimethylformamide (VEB Jenapharm Laborchemie, Apolda, GDR) and dimethylsulphoxide (Reachim, USSR) were used. The polyacryloamide film swelling process was investigated in the aqueous solutions of DMF and DMSO by the weighting (gravimetric) and calorimetric methods. A thermochemical method involving the use of a type BMR differential calorimeter [7] was used to determine the heat effect of the film swelling process.

Measurements were started on breaking a glass phial containing a known amount of polyacrylonitrile film, after the calorimeter had been adequately thermostated and the state of thermal equilibrium attained in both measuring cells. The PAN film-containing phial was placed inside the calorimetric cell filled with the swelling liquid. Film samples weighing from 0.4 to 1.0 g were used, while the volume of the swelling liquid was equal to 16 ml.

The thermoelectric force produced by the calorimeter thermopile was recorded on the E2 - 10 recorder (Laboratorni Pristroje, Prague). Changes of the thermoelectric force represented the heat effects taking place in the course of the swelling process studied.

The amount of heat evolved during the swelling process was calculated from the following relation:

$$Q(t)\Big|_{t_0}^{t_1} = k\ \theta(t)\Big|_{t_0}^{t_1} + \alpha \int_{t_0}^{t_1} \theta(t)\,dt,$$

where: $Q(t)\Big|_{t_0}^{t_1}$ — the amount of heat envolved in the calorimeter measuring cell in the time interval from t_0 till t_1; $\theta(t)\Big|_{t_0}^{t_1}$ — changes of the thermoelectric force in the same period, $\theta(t)$ — time dependence of the thermoelectric force changes, t — time, k — thermal capacity of the calorimeter, $\alpha = 0.4072$ cal/mV.min — coefficient of heat losses (determined experimentally).

The calorimeter thermal capacity was determined after each measurement.

The calorimeter may be treated as a single-body system during the thermal capacity and heat effect determinations, owing to the very small values assumed by the second and third time constants.

The value of the constant K was determined using the proceduer described by T u r s k a and J a n e c z e k [8].

3. Results and Discussions

The process of swelling polyacrylonitrile films in mixtures of DMF and DMSO with water (DMF and DMSO content 90...95 per cent by weight) was investigated over the temperature range of from 30°C to 70°C.

No swelling was observed at the lower temperatures, the films dissolving at higher temperatures.

Results of determinations of the degree of swelling by the weighting method are given in Table 1.

Table 1

Results Obtained by the Weighting Method for the Process of Swelling the Polyacrylonitrile Films

Mixture composition %		Temperature °C	Swelling period min	Equilibrium degree of swelling %
DMF	H_2O			
90	10	40	240	1···2
		50	21	8·5
		55	15	9·4
		60	12	12·5
		70	10	20
95	5	80	2...3	dissolution
		40	240	0
		50	25	7·8
		55	22	10.2
		60	10	25
DMSO	H_2O			
90	10	30	240	1···2
		50	26	6
		55	18	11·3
		60	5	13
		70	2	dissolution
95	5	30	240	12
		55	10	dissolution

The equilibrium degree of swelling of the film was found to depend on process temperature and on the concentration of DMF and DMSO in the mixtures studied. The highest equilibrium degree of swelling, attained for the DMF—water mixture at 60°C, was found to be equal to 25 per cent at a DMF concentration of 95 per cent by weight. In the case of the mixture DMSO—water, the equilibrium degree of swelling did not rise above 13 per cent at 60°C and a DMSO concentration of 95 per cent by weight.

For the swelling mixtures used in the present work the increase of temperature above 60°C was found to result initially in a partial and then complete dissolution of the polyacrylonitrile films investigated.

Table 2

Heat Effects Obtained by Microcalorimetric Measurements for the Polyacrylonitrile Film Swelling Process

Mixture composition %		Temperature °C	Swelling period min	Heat effect cal/g
DMF	H_2O			
90	10	30	24 hrs.	0.68
		50	21	0.68
		55	15	0.6
		60	12	0.4(10 min)
95	5	30	24 hrs.	0.5
		50	25	1.9
		55	22	1.1
		60	10	0.3
DMSO	H_2O			
90	10	30	24 hrs.	0.72
		55	26	1.3
95	5	30	24 hrs.	0.7
		55	10	0.2

Results of thermochemical measurements are listed in Table 2. Heat effects of the film swelling process were found to be small and fall into the range of from 0.4 to 1.9 cal/g. Besides the two cases described below, the available measuring techniques did not provide any evidence for the dissolution of films during the actual measurements. In the case of the DMF—water system studied at 60°C, partial dissolution of the film was observed along with a negative heat effect. When investigating at 55°C the DMSO—water system containing 95 per cent by weight of DMSO it was found, that the swelling of films was accompanied by a heat effect equal to 0.6 cal/g, with the films subsequently undergoing complete dissolution. Total heat effect was found to be equal to —15 cal/g. Thermokinetic curves were determined for all cases studied, typical examples of those curves being shown in Figs. 3 and 4.

The shapes of the thermokinetic curves depicting the course of the phenomena observed for the systems investigated may be seen to differ significantly from the thermokinetic curves obtained when studying the swelling and crystallization processes of other polymers. These differences may be observed very distinctly when comparing the thermokinetic curves shown in Fig. 3 and obtained for polyacrylonitrile with the thermokinetic curves obtained for polyoxyphenylene and polycarbonate (Figs. 1 and 2) [8], [9]. In both these cases the thermokinetic curves show not only the heat effects connected with the process of swelling, but also the superimposed crystallization process heat effects, the degrees of crystallinity being in both cases equal to about 40 per cent.

Thermokinetic curves obtained for the process of swelling of polyacrylonitrile in the mixtures of DMF and DMSO with water are fundamentally different from the polyacrylonitrile thermokinetic curves referred to above [3]...[5].

On the basis of these thermokinetic curves the process of swelling may be said to proceed rather rapidly. The maximum rate of heat evolution

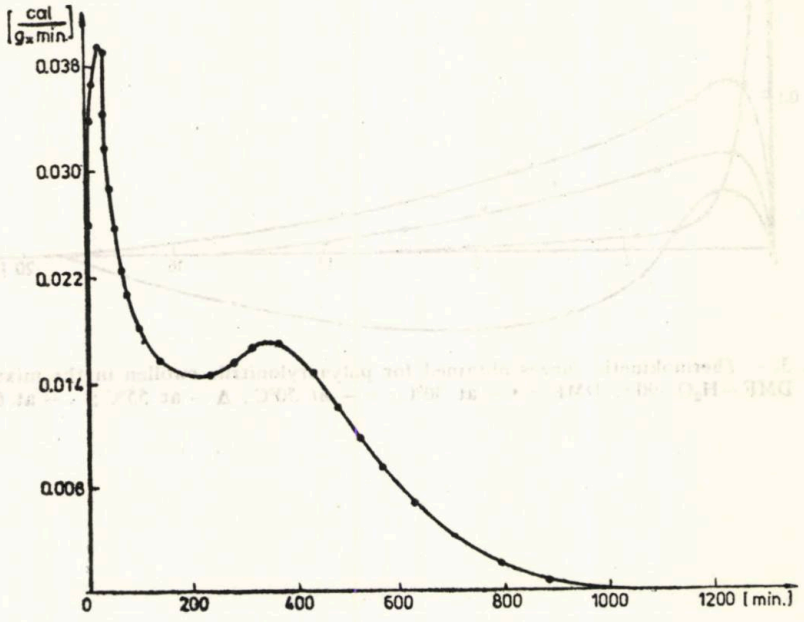

Fig. 1. — Thermokinetic curves obtained for polyoxyphenylene films swollen in decalin at 21°C.

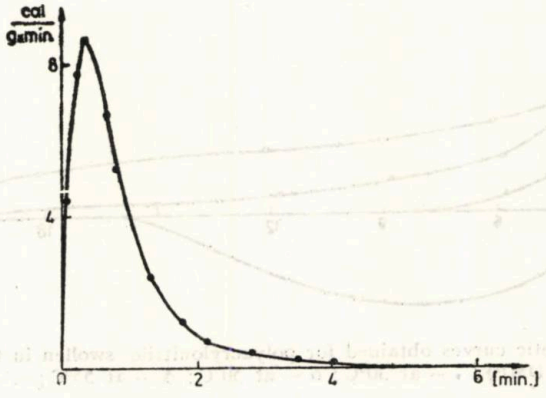

Fig. 2. — Thermokinetic curves obtained for a Bisphenol-A polycarbonate swollen in acetone at 20°C.

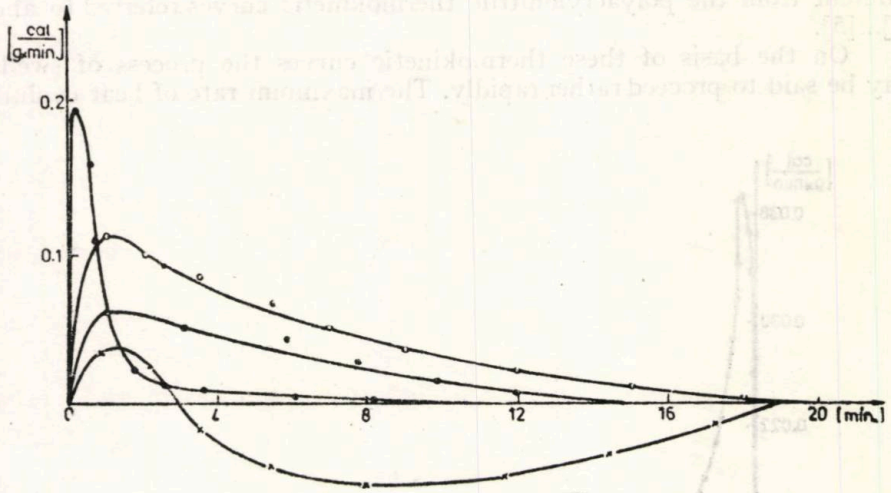

Fig. 3. — Thermokinetic curves obtained for polyacrylonitrile swollen in the mixture DMF—H_2O (90% DMF) : • — at 30°C ; o — at 50°C ; Δ — at 55°C ; × — at 60°C.

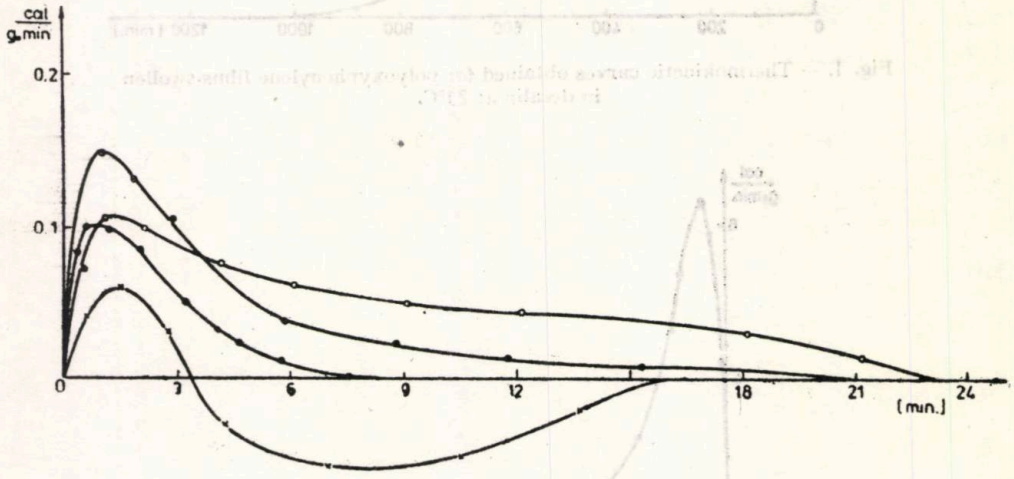

Fig. 4. — Thermokinetic curves obtained for polyacrylonitrile swollen in the mixture DMF — H_2O (95% DMF) : • — at 30°C ; o — at 50°C ; Δ — at 55°C ; × — at 60°C.

was to be observed after about 2 min. the whole process coming to an end generally after a period of some 10...12 min, No further changes were found to occur on the thermograms after an extra period of 24 hours. No morphological changes were found to take place in the swollen films studied by X-ray and calorimetric techniques and by microscopic observations carried out in polarized light. It may be therefore stated that, for polyacrylonitrile films swollen in the systems studied, the swelling process proceeds in a way that is different from that generally encountered. On the basis of results obtained so far in our studies of the influence of the swelling process on the changes in the structure of polyacrylonitrile it may be said, that the only morphological changes to be observed in that polymer upon swelling are those connected with non-crystalline (amorphous) areas characterized by a low degree of structural ordering. This result suggests that other techniques of instrumental analysis, and particularly that of wide-line NMR, should be used in further investigations of swelling processes studied in the present work.

Received, February 2, 1980

Institute of Polymer Chemistry,
Polish Academy of Sciences,
Zabrze, Poland

REFERENCES

1. Hinrichsen G., J. Polym. Sci., Part C, *38*, 303 (1972).
2. Bohn C. R., J. Polym. Sci., *55*, 531 (1961).
3. Chiong R., J. Polym. Sci., *1*, 2765 (1963).
4. Andrews R. D., J. of Macr. Sci., *2*, 281 (1974).
5. Ганаюк, Хим. Волокна, *2*, 59 (1976).
6. Rigbi Z., Polymer, **19**, 1229 (1978).
7. Zielenkiewicz A., Bull. Acad. Pol. Sci. Ser. Sci. Chem., **21**, 333 (1973).
8. Turska E., Janeczek H., Polymer, **19**, 81 (1978).
9. Turska E., Janeczek H., Polymer, **20**, 855 (1979).

UMFLAREA POLIACRILONITRILULUI ÎN AMESTECURI DE DMF—APĂ ȘI DMSO—APĂ

(Rezumat)

Se studiază comportarea la umflare a poliacrilonitrilului în sisteme selectate de solvent cu scopul de a determina modificările morfologice ale polimerului.

Ca agenți de umflare s-au utilizat amestecuri de MDSO—apă și DMF—apă.

Măsurătorile s-au efectuat pe cale gravimetrică și termochimică.

BULETINUL INSTITUTULUI POLITEHNIC DIN IAŞI
Tomul XXVI (XXX), fasc. 1—2, 1980
Secţia III
CHIMIE şi INGINERIE CHIMICĂ

D. C. 668.44

THERMAL STABILITY STUDY OF THE CYCLOHEXANONE-FORMALDEHYDE RESINS OBTAINED THROUGH PEARLED POLYCONDENSATION

BY

DAN MUNTEANU, G. THORESZ and I. NANU

Dedicated to Professor Dr. CRISTOFOR SIMIONESCU, member of the Academy, on his 60 th anniversary

1. Introduction

The obtaining of the macromolecular compounds in the heterogeneous systems, especially in the aqueous ones, is very attractive due to many technological advantages. Of a special interest is the particular case in which the macromolecular compounds are obtained during the synthesis, in a uniform geometrical shape, controllable and reproductible, that of microsphere, called pearls. This technique is often utilized in the case of polymerisation, but much more seldom by polycondensation, and then only in organic medium.

The fact that the pearled polycondensation in aqueous medium was not studied in detail (informations about this being contained only in a few patents [1]...[9]) has encouraged the idea of carrying out a systematic research [10]. For the study of this method, the choice of a proper polycondensation was necessary. The resin has to correspond to the proposed scientific purpose but it must also find practical utilizations. These conditions are fulfilled by the cyclohexanone-formaldehyde (CF) resins. As the reaction between cyclohexanone (C) and formaldehyde (F) is exothermic and irreversible, the polycondensation may be conducted in aqueous medium [11]...[14].

The initial study of the thermal stability of the CF resins obtained through pearled polycondensation is the aim of this paper.

2. Experimental

The polycondensation was carried out in aqueous medium and basic catalysis, varying the F : C molar ratio between 0.8 : 1 and 4.0 : 1, maintaining constant the other parameters. An aqueous solution of 0.05% carboxymethylcellulose (suspension stabilizer) was charged at room temperature into the polycondensation vessel. After charging of C and F (37% aqueous solution stabilized with 10% methanol) the mixture was stirred (500 RPM) adding dropwise (during 5...10 min.) 0.3 moles catalyser (30% KOH aqueous solution). The ratio between water and organic phase was 4 :1. Because the reaction is exothermic, the temperature increases to 40°...45°C,

after that the mixture being heated up to 80°C and maintained one hour (slight reflux because of methanol). After cooling to 40°C the obtained pearls, having an average diameter between 500 and 1 500 μm, were filtered, washed with warm water and dried at 40° ... 50°C up to a constant weight. The same series of CF resins was obtained through precipitating polycondensation, using identical conditions, except the addition of the suspension stabilizer.

To study the thermal stability of the synthesized resins, the thermogravimetric analysis was used. The thermal decomposition of the CF resins was carried out in an inert medium (N_2, 8 l/h) using a thermobalance MOM (Budapest) type F. Paulik, J. Paulik, L. Erdely, with a constant heating rate (6°C/min.), in the temperature range 20°...500°C, the sample weight being 100 mg.

3. Results and Discussions

According to the literature, the CF resins have the following structure:

(I)

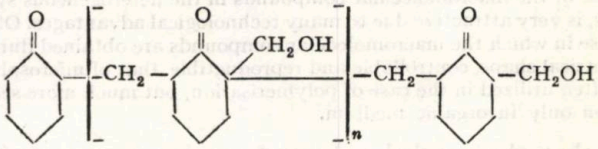

(II)

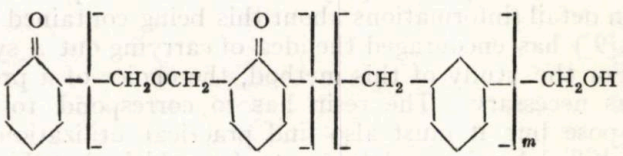

(III)

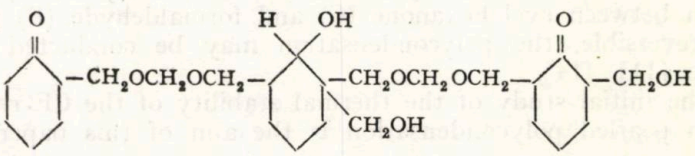

Tiliczenko [14] ... [16] has proposed the structure (I), but later Abo [17] has proposed the structure (II) and (III). The exact structure of the CF resins is still not established. The methylol groups (end- or intrachain groups) and the methylene- and methylenether bridges represent preferential positions for the thermal splitting of the resins.

Fig. 1 represents the dynamic thermograms of the CF resins obtained with F : C molar ratio between 0.8 : 1 and 4.0 : 1. At all the analyzed samples, the first weight losses occur at about 60°C, but they are small until they reach the proper initial decomposition temperature (T_i). They appear because of the para-formaldehyde traces from the resins. T_i varies, depending on F : C molar ratio, in the range 120°...190°C.

Investigating the dynamic thermograms of the CF resins with different composition, a similar behaviour may be noticed. Two decomposition intervals have been distinguished. In the first one, between T_i and about 350°C, the decomposition is relatively slow. The weight losses grow up to 250°...260°C, temperature at which an inflexion point occurs, so that in the next range, up to 350°C, the decomposition is much more slow. The DTG curves show that in the first decomposition interval, the decomposition rate reach a maximum at 240°C.

In the second interval, after 350°C, a fast decomposition of the samples was observed, so that up to 440°...450° C the variation of weight losses as a function of temperature is almost linear. Beyond this temperature, the decomposition is again more slow, being actually finished at 490°C (80...90% weight loss). The DTG curves show a maximum decomposition rate at about 420°C.

The previously described shape of the thermogravimetric curves becomes much more distinct by the resins synthesized at F : C molar ratio larger then 1. 7 : 1.

Altough the characteristical decomposition intervals are similar by all the resins, as a function of their composition, great differences have been found. The weight losses decrease by increasing the F : C molar ratio from 0.8 : 1 up to 1.9 : 1. By further increasing of the F : C molar ratio, the dependency is inverted, respectively the weight losses increase.

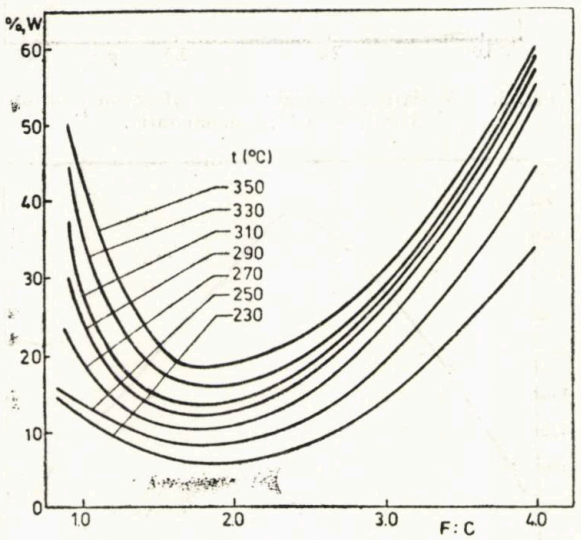

Fig. 2. — Variation of weight losses (in the range 230° ··· 350°C) with F : C molar ratio.

Fig. 2 shows more clear this behaviour. The variation of weight losses with F : C molar ratio was plotted for various temperatures between 230°C and 350°C, i.e. in the first thermal decomposition interval. All the curves have the same shape, so that for any temperature inside this in-

terval, the weight losses have a minimum, placed at a F : C molar ratio of about 2 : 1.

The same behaviour may be observed from Fig. 3, which is a plot of weight losses obtained from the isothermal thermograms, after one hour heating at 315°C, against F : C molar ratio.

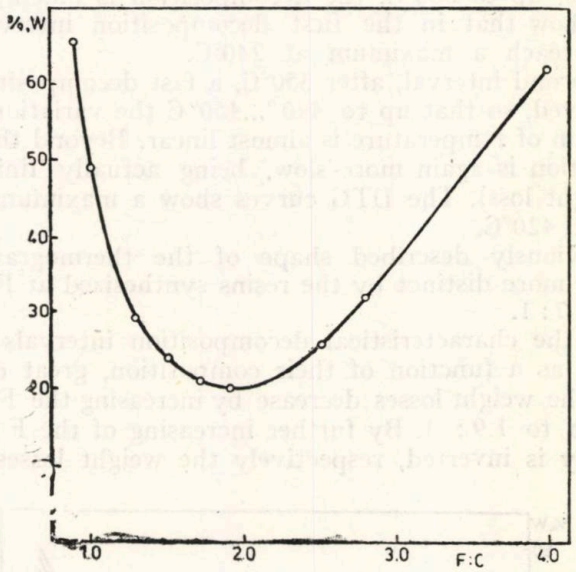

Fig. 3. — Variation of weight losses (after one hour at 315°C) with F : C molar ratio.

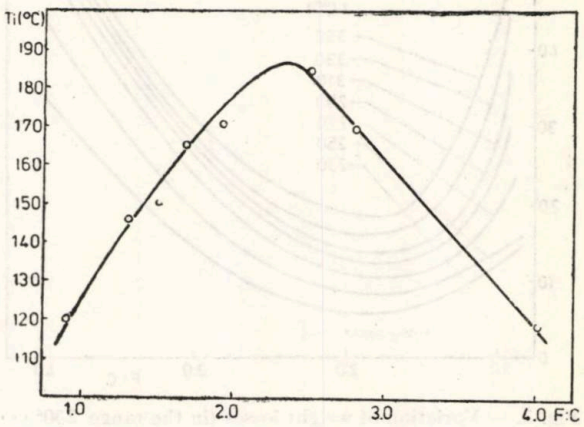

Fig. 4. — Initial decomposition temperature (T_i) vs. F : C molar ratio.

Fig. 4 illustrates the pronounced variation of T_i with the F : C molar ratio. By its increasing up to 2.5 : 1, T_i grows from 120°C to 190°C decreasing then again at 120°C for a F : C molar ratio of 4 : 1.

Differences between the thermal stability of the resins obtained through pearled and precipitant polycondensation have not been found. This is a supplementary proof for the structural identity of the CF resins synthesized by these two methods.

The obtained results show that the thermal stability of the CF resins depends, to a great extent, on the F : C molar ratio. The dependence on this ratio, both of T_i and the weight losses from the first decomposition interval, shows that a maximum thermal stability of the CF resins may be obtained with a F : C molar ratio of about 2 : 1. The same optimum value of the F : C molar ratio was also found from the study of their influence upon the other properties of the CF resins : softening point, solubility, pearls granulometry.

The results obtained from the initial study of the CF resins thermal stability justifies the continuation of this work. The determination of the thermal decomposition reactions mechanism may contribute to the structure elucidation of the CF resins obtained through pearled polycondensation, this being the topics of future investigations.

4. Conclusions

1. The thermal stability of a series of CF resins, obtained through pearled polycondensation in aqueous medium, using F : C molar ratios between 0.8 : 1 and 4.0 : 1, was studied by means of thermogravimetric analysis.

2. The thermal decomposition occurs in two intervals : between T_i and 350°C (with a maximum rate at 240°C) and between 350°C and 500°C (with a maximum rate at 420°C).

3. The thermal stability of the CF resins depends, to a great extent, on their composition. The variation of T_i (between 120°C and 190°C), and of the weight losses determined both from the dynamic thermograms (in the first decomposition interval between 230°C and 350°C) and from the isothermal thermograms (after one hour at 315°C) show that a maximum thermal stability was obtained with a F : C molar ratio of about 2 : 1. The same optimum ratio has been also found from the study of their influence on the other properties of the resins.

Received, January 28, 1980

Research Laboratory „Solventul", Timişoara,
Research Laboratory „Azur", Timişoara,
and
Polytechnic Institute, „Traian Vuia", Timişoara

REFERENCES

1. Rosenkranz H. G., Germ. (East) Pat., *10 908* (1955).
2. Rosenkranz H. G., Germ. Pat., *1 099 734* (1961).
3. Rosenkranz H. G., Jodl P., Germ. Pat., *1 167 528* (1964).
4. Rosenkranz H. G., Barthel D., Winter H., Germ. (East) Pat., *46 836* (1966).
5. Rosenkranz H. G., Barthel D., Winter H., Germ. (East) Pat., *50 232* (1966).
6. Rosenkranz H. G., Barthel D., Winter H., Germ. Pat., *1 262 600* (1968).
7. Rosenkranz H. G., Barthel D., Winter H., Germ. Pat., *1 265 415* (1968).
8. Rosenkranz H. G., Barthel D., Winter H., USSR Pat., *205 292* (1968).
9. Debowski Z., Nowak Z., Pol. Pat., *58 126* (1969).

10. Thoresz G., *The Study of Pearled Polycondensation on the Model of a Cyclohexanone-formaldehyde Resin*, (in Romanian). Ph. D. Diss., Polyt. Inst., Timișoara, 1979.
11. Scheiber J., *Chemie und Technologie der künstlichen Harze*. Wiss. Verlagsgesellschaft m.b.H., Stuttgart, 1943, 303.
12. * * * *Encyclopaedya of Polymer Science and Technology*. Vol. 11, John Willey & Sons, New York, 273.
13. Imoto M., Saito M., J. Chem. Soc. Japan, Ind. Chem. Sect., **68**, 2416 (1965).
14. Тиличенко М.Н., Жикова Л.В., ЖПХ, **25**, 64 (1952).
15. Тиличенко М. Н., ЖПХ, **36**, 192 (1963).
16. Тиличенко М.Н., СССР пат., 143 796 (1962).
17. Abo M., J. Chem. Soc. Japan., Ind. Chem. Sect., **72**, 1366 (1969).

STUDIUL STABILITĂȚII TERMICE A RĂȘINILOR CICLOHEXANON-FORMALDEHIDICE OBȚINUTE PRIN POLICONDENSARE PERLATĂ

(Rezumat)

Se studiază prin analiză termogravimetrică termostabilitatea unei serii de rășini ciclohexanon-formaldehidice (CF) obținute prin policondensare perlată, în mediu apos, utilizîndu-se rapoarte molare formaldehidă (F) : ciclohexanonă (C) de 0,8 : 1 și 4,0 : 1. ATG pune în evidență faptul că descompunerea termică se produce în două intervale : pînă la 350°C (cu o viteză maximă la 240°C) și între 350°C și 500°C (cu o viteză maximă la 420°C). Termostabilitatea rășinilor CF este puternic influențată de compoziția lor. Temperatura inițială de descompunere crește de la 120°C la 190°C (pentru raportul molar F : C = 2,5 : 1) scăzînd apoi la 120°C (pentru raportul molar F : C = 4,0 : 1). Pierderile în greutate determinate din termogramele dinamice (în primul interval de descompunere, între 230°C și 350°C) și din termogramele izoterme (315°C, 60 min) arată o dependență similară, termostabilitatea maximă avînd-o rășinile cu raportul molar F : C de circa 2 : 1, același raport optim obținîndu-se și la studiul influenței sale asupra altor proprietăți ale rășinilor.

BULETINUL INSTITUTULUI POLITEHNIC DIN IAŞI
Tomul XXVI (XXX), fasc. 1—2, 1980
Secţia III
CHIMIE şi INGINERIE CHIMICĂ

D. C. 678.76: 678.4

POLYETHYLENE—RUBBER BLENDS

I. PHYSICO-MECHANICAL PROPERTIES

BY

N. ASANDEI, GH. ADAMESCU, M. RUSU, SIMION PETROVAN and M. NICU

Dedicated to Professor Dr. CRISTOFOR SIMIONESCU, member of the Academy, on his 60 th anniversary

1. Introduction

The compounds of thermoplastic polymers and rubbers were intensely studied in the last years [1], [2]. From these compounds, those of polyethylene and different rubbers play a particular role [3].

In the researches concerning polyethylene—rubber blends, some of them were carried out aiming the degree of compatibility of the components from the system [4] ··· [9] and others searched the variation of physico-mechanical properties and processing parameters against the composition [10] ··· [18]. These researches established that the compounds in which polyethylene is the major component, behave close to this and can be processed as plastic materials and those with rubbers as vulcanized compounds [3], [10] ··· [20]. The compatibility of the polymers from a compound is determined by the structure of the polymers and their concentration [4] ··· [9].

The aim of this paper is to study the influence of the addition of different elastomers on the main physico-mechanical properties of the high pressure polymerization polyethylene.

2. Experimental

In order to carry out this study, the following materials were used:

a) High pressure polyethylene (PE), type A22FMA/002, MFI 0.2 g/10 min and a density of 930 kg/m^3 produced by Piteşti Petrochemical Plant.

b) Polyisoprene rubber (PI), type CAROM 2 200, containing 96% 1,4-*cis* units and Mooney viscosity (1 +4) 100°C 77, produced by Borzeşti Petrochemical Plant.

c) Copolymer butadiene-α-methylstyrene (BAMS), type CAROM 1 502, containing 22.6% bonded α-methylstyrene and a Mooney viscosity (1 +4) 100°C 50, produced by Borzeşti Petrochemical Plant.

d) Copolymer butadiene-acrylonitrile (BAN), type ELAPRIM S, containing 39% bonded acrylonitrile and Mooney viscosity (1 +4) 100°C 50, produced by MONTEDISON (Italy).

Compounds containing 2.5, 5, 7.5, and 10% (by weight) elastomer were prepared as following: mixing at 150°C for 10 min. and cutting the resulted sheets on a knife cutting machine; cut sheets were transformed

in granules using an extruder with a screw of 120 mm diameter and $L/D=24$. For a better mixing, the blends were again granulated using a laboratory granulator, type Ko-Buss, at a temperature of 140°C. From the obtained granules, tubular sheets were extruded using a K i e f f e l extruder (screw diameter 25 mm and $L/D=12$). From the sheets, samples were prepared for testing the physico-mechanical properties (tensile strength, elongation at break, tear resistance, impact resistance and sliding coeficient).

3. Results and Discussions

In the Fig. 1 tensile strength is plotted against elastomer content from the blend. As is seen from this figure, one can find that, in all cases, the increase in elastomer content from the compound determines a decrease of tensile strength. This decrease is lower for the compounds with PI and BAMS and greater for the system with BAN. The shape of the curves is the same for both machine and cross-section directions.

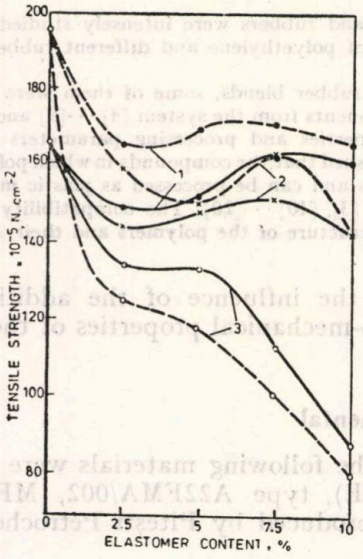

Fig. 1. — Tensile strength variation vs. the elastomer content; — machine direction;---cross direction; *1* — PE—PI blends; *2* — PE—BAMS blends; *3* — PE—BAN blends.

Regardless of testing direction, in the case of PE—PI and PE—BAMS blends, a minimum of tensile strength is recorded at 2.5% elastomer and a maximum at 7.5% rubber, respectively.

Elongation at break from the compounds with PI and BAMS increases as the elastomer content increases (Fig. 2), for both machine and cross-section directions. In the case of PE—BAN compounds elongation curves show a maximum. For the machine direction this maximum is recorded at 2.5% elastomer but for the cross direction at 5% rubber content.

Tear resistance for the two directions of the sheets, decreases as the elastomer content increases (Fig. 3). As in case of tensile strength, the decrease of tear resistance is much more important for the compounds with

BAN and much lower for the other types of compounds. The curves for the PE—PI and PE—BAMS blends show a maximum at 5% elastomer content for machine direction, and at 7.5% rubber content for cross direction, respectively. Also, tear resistance of the PE—BAN sheets tested on cross direction records a maximum at 7.5% elastomer in the compound.

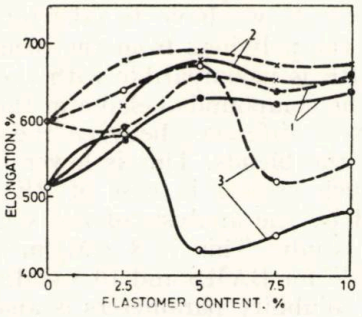

Fig. 2. — Elongation at break variation vs. the elastomer content (s. Fig. 1 for notations).

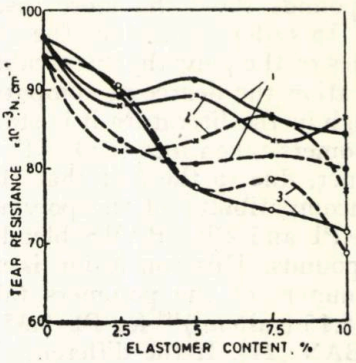

Fig. 3. — Variation of tear resistance vs. the elastomer content in the blends (s. Fig. 1 for the notations).

If the impact resistance is analysed against elastomer content in the compound, it is found that in case of PE—PI and PE—BAMS systems, this characteristic is larger than that of PE, and in case of PE—BAN compound the change is rather unsignificant (Fig. 4).

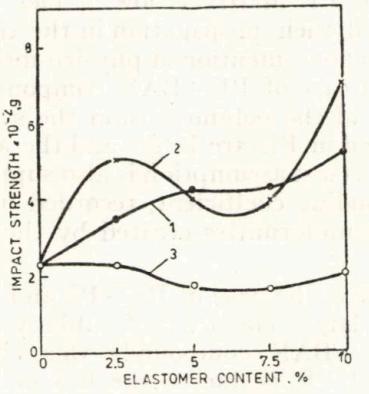

Fig. 4. — Impact strength vs. the elastomer content from the blends (s. Fig. 1 for the notations).

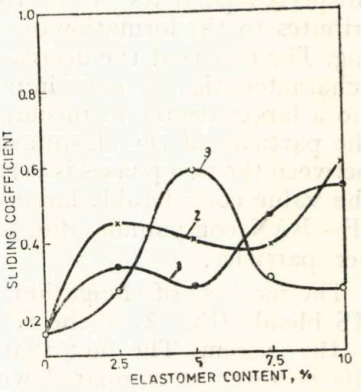

Fig. 5.—Sliding coefficient variation vs. the elastomer content from the blends (s. Fig. 1 for the notations).

Sliding coefficient of the samples from the blends containing different percentages of elastomer is larger than that of PE (Fig. 5). In the case of PE—BAN compound this properties shows a maximum at 5% elastomer in the compound.

Analysing the influence of PI, BAMS or BAN addition on the main physico-mechanical properties of the high pressure polymerization PE, it is found that as the elastomer content in the compounds increases, a decrease in tensile strength and tear resistance and an increase of elongation, impact resistance and sliding coefficient are recorded. The trend of modifications is not the same for all the compounds. The PE—BAN compounds show the more intense changes of the characteristics.

In order to explain the change of different physico-mechanical properties of the polyethylene—rubber compounds, we have to take into consideration the degree of compatibility of the polymers from the blends. Although in the literature it is stated that PE is incompatible with the three elastomers taken into study [1], not all the compounds behave in the same manner, due to the fact that there exists a difference between the degree of incompatibility of the polymers from the blends. This is lower for the PE—PI and PE—BAMS blends and much greater in case of PE—BAN compounds. This conclusion is supported by the analysis of the solubility parameters of the polymers taken into study. This is 8 $(cal/cm^3)^{1/2}$ for PE, 8.15 $(cal/cm^3)^{1/2}$ for PI, 8.35 $(cal/cm^3)^{1/2}$ for BAMS and 10.3 $(cal/cm^3)^{1/2}$ for BAN [21]. If the difference between solubility parameters is analysed, this is 0.15 for PE—PI compounds, 0.35 in case of PE—BAMS and 2.3 for the PE—BAN system. It is well known that the larger the difference between solubility parameters is, the larger the degree of incompatibility of the polymers from a compound [22]. Based on this finding, it may be stated that the decrease of tensile strength and tear as the elastomer content increases in the compound (Figs. 1 and 3) is determined not by the difference between the values of these characteristics for the two polymers, but by their incompatibility.

The studied compounds are heterogeneous and the adhesion between the dispersed particles of the rubber and PE matrix is low, a fact which contributes to the formation of cracks and their propagation in the time of testing. The fact that the decrease of the above mentioned physico-mechanical characteristics is more important in case of PE—BAN compounds is due to a larger degree of incompatibility of the polymers from the system. So the particles of the elastomer dispersed in PE are larger and the adhesion between the two phases is very low. This last assumption is also supported by the value considerably larger of the sliding coefficient, recorded in case of PE—BAN compounds, due to the nonuniformities created by the large rubber particles.

The increase of elongation, recorded in the case of PE—PI and PE—BAMS blends (Fig. 2) is the result of a larger elasticity of rubbery phase from the system. The fact that, for PE—BAN compounds this characteristic is lower as compared with that of PE, is due to the loss of phase adhesivity. The same explanation may be given for the impact resistance variation (Fig. 4).

The general trend of main physico-mechanical characteristics variation against rubber content in the compounds with PE, may be explained on the base of the difference on dispersion degree of the rubber phase at various contents in the compound. For the blends of which components are characterized by a lower degree of incompatibility (PE—PE and PE—

BAMS), the dispersion of the elastomer is better at a content between 5...7.5%. At this composition, maxima in physico-mechanical properties are recorded, except sliding coefficient, which shows a minimum. This minimum is an additional proof for the large dimensions of the rubber particles from the compound at this composition.

It seems that, for PE—BAN compounds, the best dispersion of rubber phase in PE is obtained at 2.5% elastomer.

The difference between the degree of dispersion of the elastomers, at different rubber contents, is not determined by the mixing process but by the polymer characteristics.

4. Conclusions

The addition of 2.5...10% PI, BAMS or BAN in high pressure polymerization PE determines a decrease of tensile strength and tear resistance and an increase of elongation at break, impact resistance and sliding coefficient. These modifications are larger in the case of PE—BAN compounds due to a larger degree of incompatibility of the polymers from the system.

Although heterogeneous, these compounds may find practical utilizations, because the sheets obtained from them have a larger sliding coefficient as compared to that of PE (giving better conditions for storage in piles) and a better impact resistance.

The PE—PI and PE—BAMS compounds containing 5...7.5% elastomer are remarkable, their sliding coefficient and impact resistance being superior, without important changes of tensile strength and tear resistance.

By the addition of low amounts of elastomer in the high pressure polymerization PE, an improve of the resistance anisotropy of the sheets may be obtained.

Received, January 5, 1980

Polytechnic Institute, Jassy,
Department of Organic and
Macromolecular Chemistry

REFERENCES

1. Paul D. R., Newman S., *Polymer Blends.* Vol. 2, Academic Press, N.Y., 1978.
2. Dunn J. R., Rubber Chem. Tech., **49**, 976 (1971).
3. Feldman D., Rusu M., Materiale plastice, **7**, *3*, 106 (1970).
4. Виноградов Е. Л., Марынов А. М., Сибирякова Н. А., Курбатова И. В., Высокомол. соедин., **14**, *7*, 1952 (1972).
5. Игрон Б., Васильева Н., Голуб Е., Каучук и резина, **10**, 23 (1973).
6. Deanin R. D., Raymond O. N., Kennankeril C. P., Am. Chem. Soc., Dir. Org. Coat. Plast., Chem. Pap., **35**, *1*, 259 (1975).
7. Павлии В. Г., Гусев В. И., Ягфаров М. Ш., Хим. высокомол. соедин. нефтехим., 115 (1973).
8. Голдман А. Я., Поляков Ю. С., Курбатова И. В., Сибирякова Н. А., Пласт. массы, *7*, 17 (1972).
9. Виноградов Е. Л., Курбатова И. В., Марынов А. М., Сибирякова И. А., Пласт. массы, *7*, 24 (1972).
10. Уткина И. С., Андреева Е. С., Пласт. массы, *9*, 53 (1976).

11. Вдовин М. Т., Торнер Р. В., Панадий О. М., Сапкина Л. Н., Пласт. массы, *10*, 28 (1976).
12. Казанцева В. В., Аскадский А. А., Слонимский Г. Л., Высокомол. соедин., **B15**, *2*, 137 (1973).
13. Муджири Б. Г., Акутин М. С., Соголова Т. И., Кебер М. Л., Котомин В. С., Пласт. массы, *1*, 36 (1976).
14. Лифшиц А. Д., Заёнчиковский А. Д., Остряков И. А., Казх. Обур. Пром., **16**, *6*, 54 (1974).
15. Pielikhowski J., Wierzbikova K., Pr. Nauk. Inst. Technol. Org. Tworzyn. Sztucznych Polytech. Wroklaw, **16**, 265 (1975).
16. Динзбург Б. Н., Иванов Ю. В., Казх. Обур. Пром., **15**, *2*, 52 (1973).
17. Качинов И. М., Агув А. Д., Пласт. массы, *4*, 36 (1976).
18. Falender J. R., Lindsey S. E., Sam J. C., Polym. Eng. Sci., **16**, *1*, 54 (1976).
19. Volintiru T., Mehr B., Materiale plastice, **10**, *1*, 10 (1973).
20. Mehr B., Volintiru T., Materiale plastice, **10**, *11*, 604 (1973).
21. Brandrup J., Immergut E. H., *Polymer Handbook*. John Wiley, N.Y., 1975.
22. Bohn L., Rubber Chem. Tech., **41**, 495 (1968).

AMESTECURI POLIETILENĂ—CAUCIUC

I. Proprietăţile fizico-mecanice

(Rezumat)

Se prezintă caracteristicile principale ale amestecurilor pe bază de polietilenă şi 2,5...10 cauciuc poliizoprenic, copolimer butadien-α-metilstirenic sau copolimer butadien-acrilonitrilic.

Se discută influenţa tipului şi a conţinutului de elastomer asupra proprietăţilor fizico-mecanice (tracţiune, alungire, rezistenţa la impact, rezistenţa la sfîşiere şi coeficientul de alunecare).

Deşi creşterea conţinutului de elastomer determină o reducere a unor caracteristici, amestecurile studiate pot să-şi găsească utilizări datorită creşterii rezistenţei la impact şi a coeficientului de alunecare.

Tomul XXVI (XXX), fasc. 1–2, 1980
Secția II
CHIMIE și INGINERIE CHIMICĂ
BULETINUL INSTITUTULUI POLITEHNIC DIN IAȘI

D.C. 547.391.1

CONFORMATIONS OF POLY(ACRYLIC ACID) IN WATER–ETHANOL SOLVENT MIXTURES

BY

IUDITA MUREȘAN and LUCIA ZADOR

Dedicated to Professor Dr. CRISTOFOR SIMIONESCU, member of the Academy, on his 60 th anniversary

1. Introduction

It is known that poly(acrylic acid) and its copolymers change their conformation by neutralization in aqueous media from a tight to a loose coil [1]...[4]. Even if for poly(acrylic acid) a similar transition has not been established, we managed to bring about in this case also a transformation of its conformation by changing the dielectric constant of the medium. To this aim water–ethanol mixtures of different compositions were used as solvent.

The results of potentiometric [5], viscometric [6], conductometric [7], rheological [8] and optical measurements (unpublished yet) show that by neutralization in aqueous media containing more than 40% EtOH, (w/w), the poly(acrylic acid) changes its conformation from a swollen coil to a compact globule, according to the schematic representation of Fig. 1.

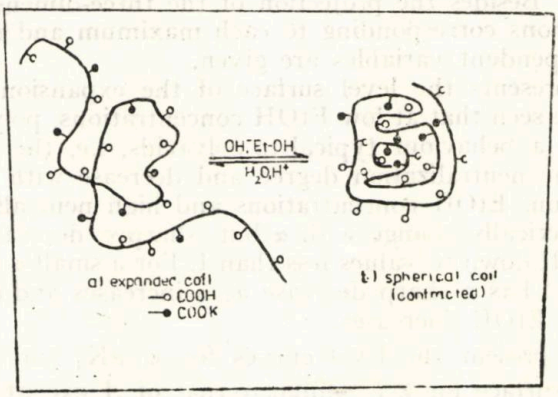

Fig. 1. — Swollen coil — compact globule conformational transition at polyacrylic acid.

2. The Building of Level Surfaces

The aim of the present paper is to establish a synthetic tabel regarding the structural modifications of the solution of poly(acrylic acid) which occur at the neutralization in a mixted solvent water–ethanol. With these

purpose we have built level surfaces illustrating the simultaneous influence of the neutralization degree (α) and of the composition of the solvent mixture (% EtOH) upon the investigated properties (X), where X means the specific conductivity, λ—the optical density (measured at a wave length of $5 \cdot 10^{-7}$m), D—the exponent of the acidity constant pK_a, (calculated with Eq. (1))

$$pK_a = pH + \log \frac{1-\alpha}{\alpha} + c_{H_2O}, \tag{1}$$

and A, an expansion coefficient. The last one was defined by the ratio between the cubic root of the viscosity index in the respective solvent and that in 0.2 N HCl solution, at $c = 7.92 \times 10^{-4}$ g/l (1.11×10^{-2} monomer mol/l)

$$A = \left(\frac{\eta_{sp}}{c}\right)^{1/3} / \left(\frac{\eta_{sp}}{c}\right)^{1/3}_{0.2\,N\,HCl}$$

The acidic medium was used in order to have as reference state that of the non-ionized polymer.

The level diagrams were built using the plots of experimental data in the following co-ordinates:

$$X = X(\alpha)_{\%EtOH} \quad \text{and} \quad X = X(\%\ EtOH)_{\alpha}.$$

Each curve on the level surface represents the locus of points in which X has a constant value specified on the diagram. Intervals of equal characteristics were chosen so that the density of the level line gives the measure of X variation. Besides the projection of the three-dimensional representation, two sections corresponding to each maximum and minimum value of the two independent variables are given.

Fig. 2 represents the level surface of the expansion coefficient.

It could be seen that at low EtOH concentrations, poly (acrylic acid), (PAA), exhibits a behaviour typical to polyacids, i.e. the coil dimensions increase with the neutralization degree and decrease with the content of EtOH. At medium EtOH concentrations and high neutralization degrees, A, does not practically change with α but sharply decreases in a narrow range of % EtOH down to values less than 1. For a small α and a high content of alcohol A has a sharp decrease as α increases and registers a slow decrease as % EtOH increases.

Figs. 3...5 present the level curves for λ, pK_a and D.

The level surface for λ is similar to that of A except the domain of low values of both parameters.

The interesting variation of pK_a with the investigated parameters, especially that pK_a registers a maximum as % EtOH increases, could be explained also by the conformational transformation to a compact globule.

Optical density has a sudden increase with α and the content of EtOH in the domain where A is less than 1.

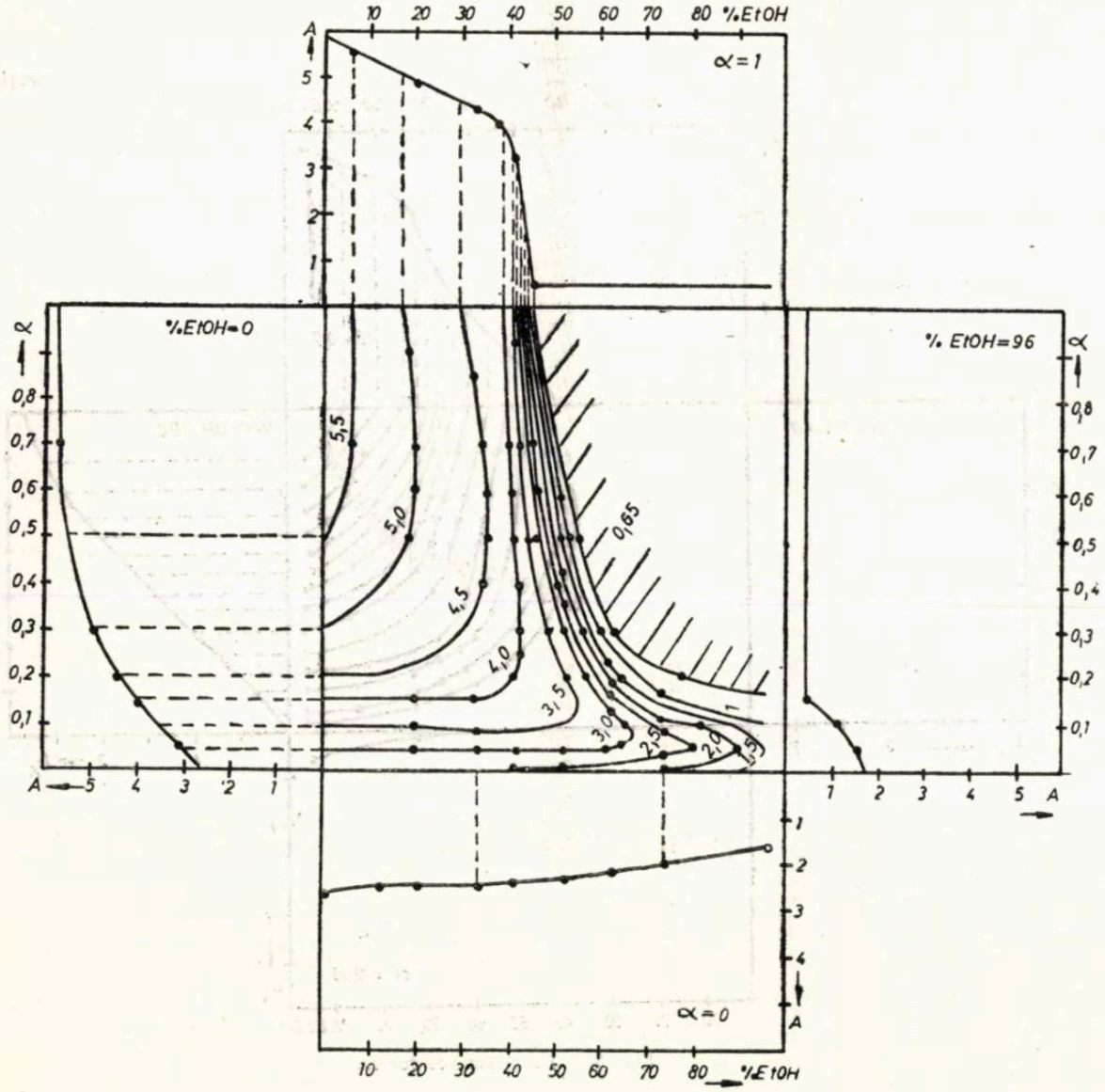

Fig. 2. — Level surface for A.

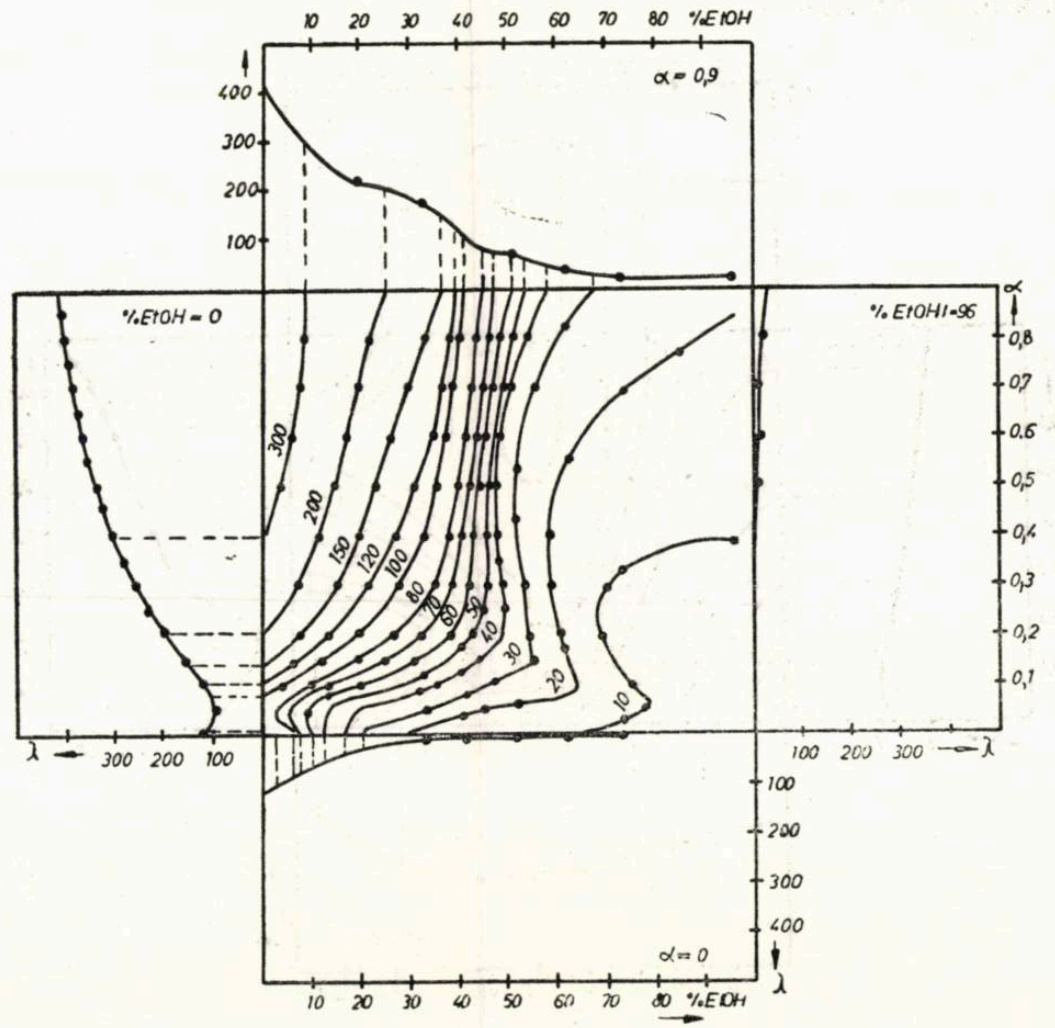

Fig. 3. — Level surface for λ

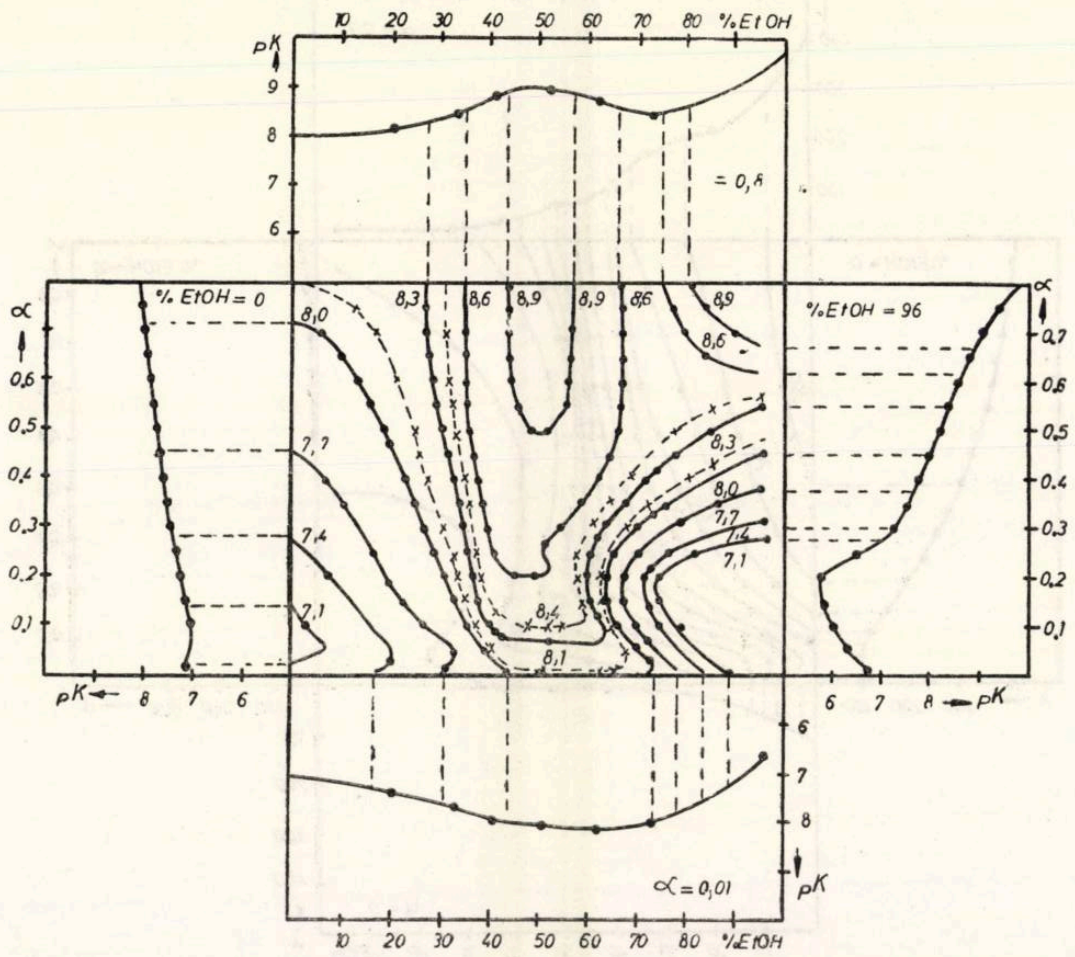

Fig. 4. — Level curves for pK_a.

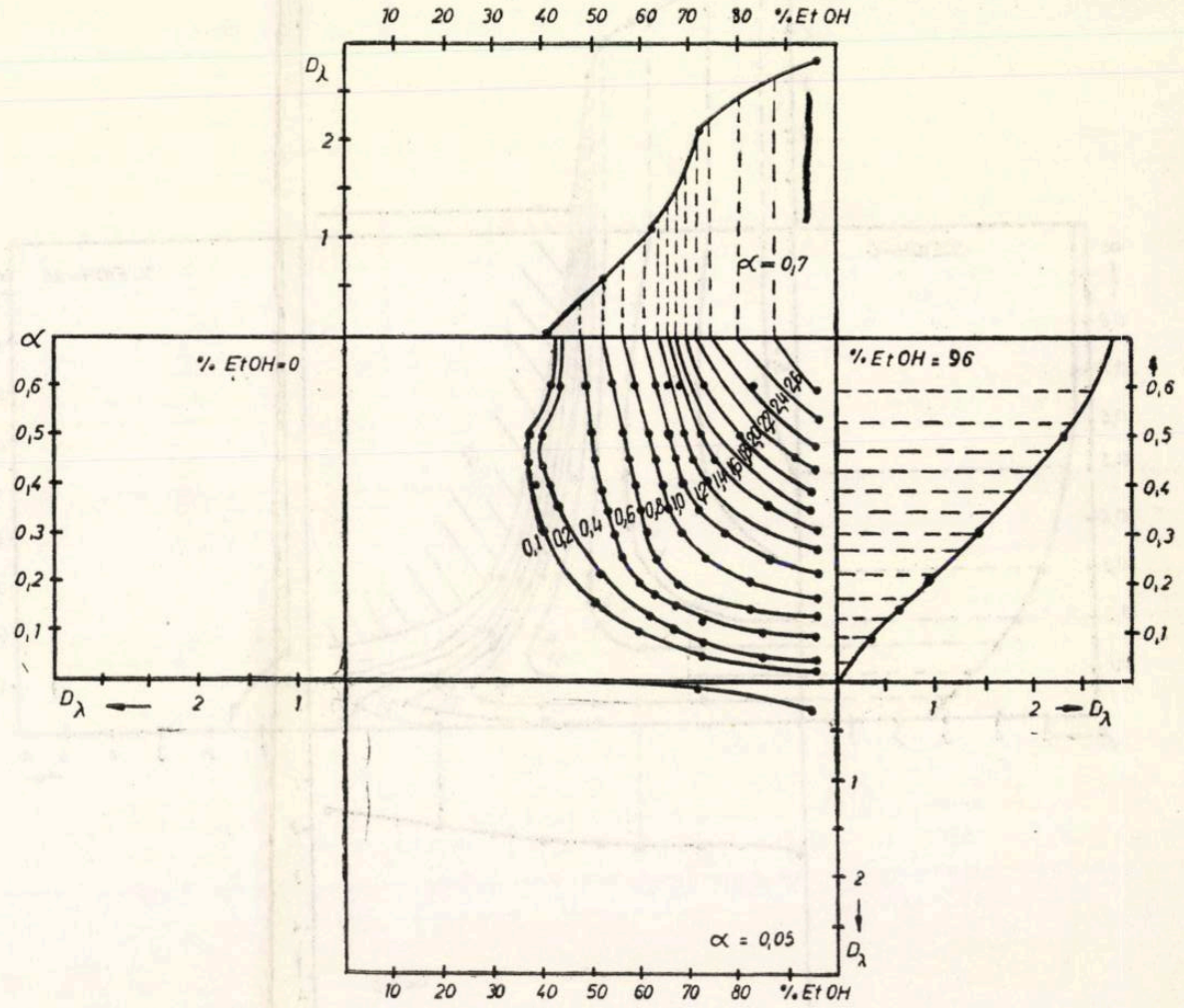

Fig. 5. — Level surface for D.

3. Interpretation of the Results

The superposition of diagrams represented in Figs. 2...5 suggests that the surface α vs. % EtOH could be divided in the structural domains shown in fig. 6.

The first domain, *I*, corresponds to the usual behaviour of polyacid solutions. The change of different characteristics inside the domains *I* and *II* is given in the Fig. 6. In the domain *I* the shape of the chains changes from a swollen coil to an extended helix as a function of their change. This domain will be called the coil domain. The *a* zone is the most tipical part of it. In the *b* zone the characteristics changes very little with α because as a result of counter-ions binding the charge of the chains changes unsignificantly with the neutralization degree.

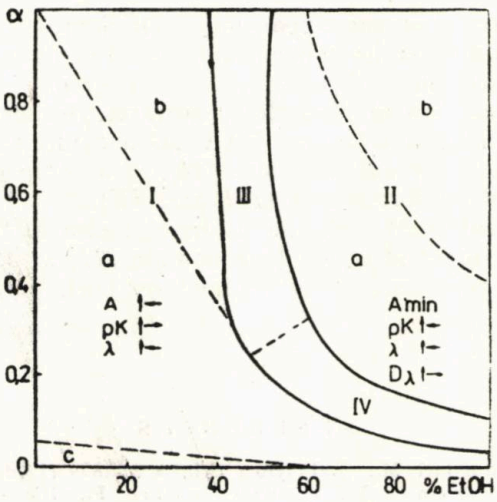

Fig. 6. — Delimitation of structural zones at PAA of concentration 1.11×10^{-2} monomer mol/l.

The domain *II* is characterized by opalescence and a sub-unitar expansion coefficient. Here the chains achieve a tighter packing than in a noncharged state in water. For this reason this domain will be denominated as *globular domain*. It could be seen that *A* has low values, around 0.65, which are not practically influenced by any parameter. The difference against the domains *I* lies not only in the compact form of the macromolecules (A minimum value) and the appearance of the opalescence but also in the inverse variation of pK_a with % EtOH. The *b* zone of the domain *II* corresponds to some systems in which the macromolecules start to aggregate.

The third domain, *III*, is that of conformational transition from the coil to globule at somewhat high neutralization degrees. It is characterized by an almost total independence of the characteristic against α and a sudden variation of the characteristics with the increase of % EtOH.

Thus, between 39% and 45% EtOH the dimensions of coils decreases more than four times and simultaneously the transparent solutions start to opalesce.

The domain *IV* corresponds to the transition between *I* and *II* at low neutralization degrees and is the most interesting regarding the influence of α upon different characteristics. The effect of this parameter is opposite as compared with that from the domains *I* and *II*, or in other words instead to increase, the expansion coefficient, the conductivity and pK_a decrease with the increasing charge of the chain. The coil dimensions register a gradual decrease with the decrease of the dielectric constant of the medium (as in the domain *I*).

4. Conclusions

1. Level surfaces of the expansion coefficient, specific conductivity, acidity and optical density have been built based on their dependence upon the solvent composition and neutralization degree.

2. By superposition of these level surfaces, the surface α vs. %EtOH could be divided in domains where PAA has a conformation of a swollen coil (*Ia*) or of a partially extended coil (*Ib*), of a compact globule (*II*), as well as transitional conformations (*III* and *IV*).

3. For high values of α, the determinant factor of the conformational transition is the content of EtOH (the domain *III*) while at low neutralization degrees the transition is determined by both parameters.

Received, December 28, 1979

Babeş—Bolyai University, Cluj-Napoca

REFERENCES

1. Leyte J. C., Mandel M., J. Polymer Sci., A 2, 1879 (1964).
2. Barone G., Crescenzi V., Quadrifoglio F., Ricerca sci., **35** (II-A), 393 (1965).
3. Barone G., Crescenzi V., Quadrifoglio F., Ricerca sci., **35** (II-A), 1069 (1965).
4. Barone G., Crescenzi V., Vitagliano V., Quadrifoglio F., Ricerca sci., **36**, 477 (1966).
5. Mureşan I., Zador L., Stud. Univ. Babeş-Bolyai, Chem., **18**, 89 (1973).
6. Zador L., Mureşan I., Rev. Roumaine Chim., **19**, 353 (1974).
7. Zador L., Mureşan I., Stud. Univ. Babeş-Bolyai, Chem., **24**, 48 (1979).
8. Mureşan I., Zador L., Informare Documentară Selectivă, **3**, 33 (1978).
9. Zador L., Mureşan I., Stud. Univ. Babeş-Bolyai, Chem., (in print).

CONFORMAŢIILE POLIACIDULUI ACRILIC ÎN AMESTECURI DE SOLVENT APĂ—ETANOL

(Rezumat)

Se prezintă sub forma unor suprafeţe de nivel rezultatele studiului potenţiometric, conductometric, viscozimetric şi optic. Corelarea acestora permite împărţirea suprafeţei α—% EtOH în domenii caracterizate prin forma de ghem (umflat sau îndreptat), respectiv de sferă compactă a catenelor de poliacid acrilic, precum şi un domeniu de tranziţie conformaţională între aceste forme.

BULETINUL INSTITUTULUI POLITEHNIC DIN IAŞI
Tomul XXVI (XXX), fasc. 1—2, 1980
Secţia III
CHIMIE şi INGINERIE CHIMICĂ

D. C. 678.769; 537.211

INVESTIGATIONS ON ELECTRIC PROPERTIES OF POLYMERS
VII. ON THE A. C. ELECTRIC CONDUCTIVITY OF POLY(2-ETHYNYLNAPHTALENE)

BY

I. DIACONU and SVETLANA DUMITRESCU

Dedicated to Professor Dr. CRISTOFOR SIMIONESCU, member of the Academy, on his 60 th anniversary

1. Introduction

Some aspects regarding the d.c. conductivity of poly (2-ethynylnaphtalene) (P2EN) such as structure—conductivity corelation, origin, nature and sign of charge carriers are already investigated [1], [2].

A progress in understanding the conduction process in disordered materials, including polymers, can not be achieved unless the a.c. conductivity measurements are perfor med. These measurements can establish the role of localized states (regularly found in these materials) in the electric conduction process [3] · · ·[5].

In the present paper, the a.c. conductivity results on $P2EN_{c-c}$ and $P2EN_{t-c}$ are analysed.

2. Experimental

The synthesis and the structural analysis of the polymer were elsewhere presented [6].

Investigated polymers had the *cis*-cisoidal (60% crystallinity) and *trans*-cisoidal (amorphous) structures.

The conductivity measurements were performed on disc-shaped samples with 13 mm in diameter prepared by compressing the polymer powder in a evacuated mould (10^{-2} Torr) under a pressure of 10^5 N/cm^2. The discs were provided with vacuum evaporated gold electrodes of circular form. In order to remove current leakages on surface, the electrodes had a diameter of only 10 mm and were centrally placed on both sides of the disc.

Measurements were carried out in dry nitrogen at normal pressure, using the chamber already described [7]. Before starting the measurements, the samples were stored in the evacuated chamber (10^{-6} Torr) for two days. A.c. conductivity was measured with a General Radio 1 616 bridge. For d.c. conductivity measurements, the TR—2 201 Orion teraohmmeter was used.

3. Results and Discussion

The curves representing the frequency dependence of the measured conductivity of $P2EN_{c-c}$ in the range $10 \ldots 10^5$ Hz, at various temperatures, are presented in Fig. 1. On a separate axis, the d.c. conductivity values

at the same selected temperatures are also indicated. Over the temperature range considered, the isomeric and physical structures of polymer do not alter [2].

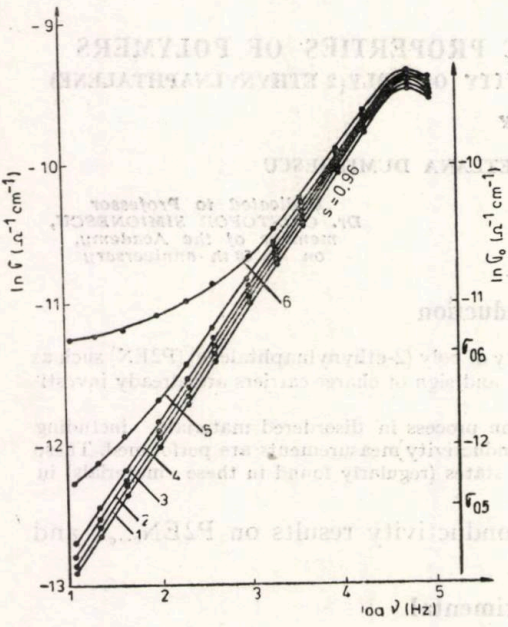

Fig. 1. — The frequency dependence of measured conductivity of P2EN$_{ee}$: *1* — 190°K; *2* — 236°K; *3* — 278°K; *4* — 297°K; *5* — 338°K; *6* — 373°KH; d.c. conductivities at the last two temperatures are also indicated.

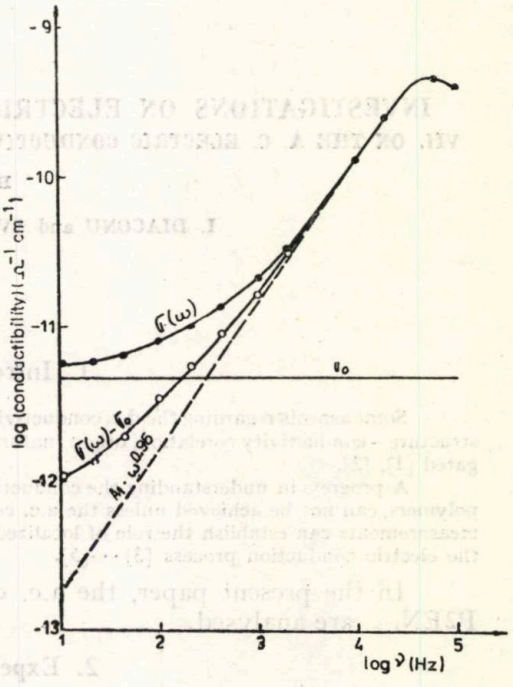

Fig. 2. — Substruction of the frequency independent conductivity from the measured conductivity for the curve *6* (Fig. 1).

At temperatures lower than 300°K, in the range $10...2\cdot10^4$ Hz, the measured conductivity $\sigma(\omega)$ is much higher than d.c. value σ_0 and obeys the relation

$$\sigma(\omega)=A_1\,\omega^s, \tag{1}$$

where A_1 is a constant, ω — angular frequency and $s=0.96$.

Above 300° K, a critical frequency which is temperature dependent, limits the frequency range over that $\sigma(\omega)\approx\omega^{0.96}$. Out of these ranges, $\sigma(\omega)$ falls smoothly to a frequency independent value, close to σ_0, as frequency decreases. The conductivity $\sigma(\omega)$ can be expressed as the sum of two terms:

$$\sigma(\omega)=\sigma_0+\sigma_1(\omega), \tag{2}$$

where σ_0 is frequency independent conductivity and $\sigma(\omega)-\sigma_0$ the frequency dependent one. Such an example is graphically shown in Fig. 2.

If frequency is taken as a parameter and the conductivity $\sigma(\omega)$ is plotted as a function of $1/T$, the curves presented in Fig. 3 are obtained.

It is clear that activation energy is frequency and temperature dependent. Its value is very small at low temperatures, over the whole frequency range, but rapidly increases above a critical temperature which is frequency dependent. For low frequencies it is evidenced that the limit of the activation energy is just the value determined from d.c. conductivity measurements.

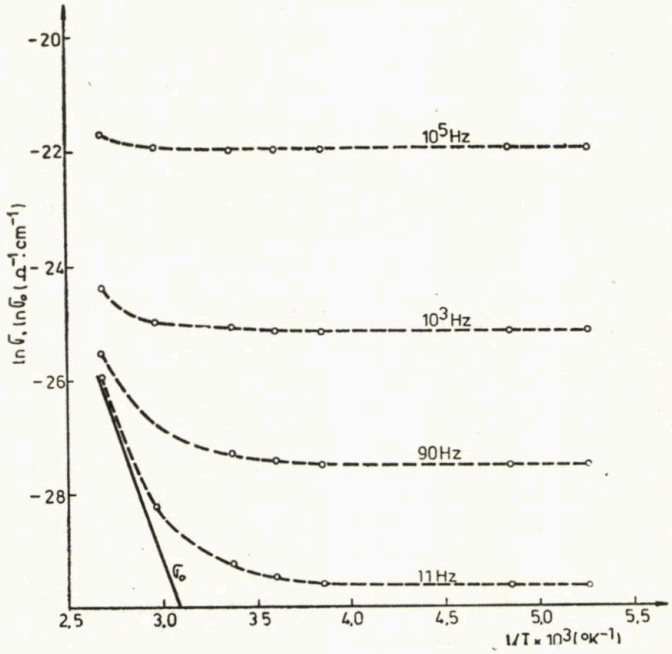

Fig. 3. — The temperature dependence of the measured a.c. conductivity (for various frequency) and d.c. conductivity of $P2EN_{c-c}$.

Over the frequency and temperature range where $\sigma(\omega)\approx\sigma_1(\omega)\approx\omega^{0,96}$ the frequency dependent conductivity depends sublinearly on temperature, whereas out of this range, the dependence is supralinear.

Analysing the a.c. conductivity results obtained on a variety of disordered materials, P o l l a k [8]...[10] found that for hopping of charge carriers between isolated pairs of randomly distributed localized states, a.c. conductivity obeys the relation (1), where s decreases from unity (for single hops) to 0.5 for multiple hops. At higher temperatures multiple hops frequently occur, while at low temperatures single hops predominate. According to this model, the transfer of charge between localized states is single phonon assisted (quantum hopping model). As a result, the a.c. conductivity depends linearly or sublinearly on temperature and the charge transport between localized states is mainly by tunneling through the potential barrier separating the sites.

Later, P i k e [11] showed that as the a.c. conductivity depends supralinearly on temperature the hopping model of charge carriers between

localized states over potential barriers (classical hopping model) is better for explainig the results.

Comparing our data to the predictions of the quantum and classical hopping models, it may be concluded that over the frequency and temperature range where $\sigma(\omega) \approx \omega^{0.96}$, the electric conduction in $P2EN_{c-c}$ is almost entirely by single quantum hops.

Intrinsec band conduction should be frequency independent [12]. Therefore in the frequency and temperature range where values of σ_0 are significant (relation (2) is valid), it may be considered that conduction process takes place by two parallel mechanisms: band mechanism and hopping mechanism. As temperature increases and frequency decreases the contribution of the former increases as compared to the later. This fact is clearly ilustrated in Fig. 2. One can be also seen that the frequency dependence of the substraction of σ_0 from $\sigma(\omega)$ does not follow the law valid for high frequencies ($\sigma_1(\omega) \approx \omega^{0.96}$). The values of s decreases with frequency decreasing. This provides evidence that in $P2VN_{c-c}$, at temperatures higher than 300° K, the hopping mechanism depends on frequency; by frequency decreasing a gradual passing from conduction by single quantum hops to one by multiple hops takes place. Since the frequency dependent component depends supralinearly on temperature, the classical hops are prevalent.

At all temperatures considered, as frequency increases above about $2 \cdot 10^4$ Hz, the conductivity rises less and less, rapidly reachs a maximum at $6 \cdot 10^4$ Hz and then decreases. The position of the maximum is independent on temperature. This evidence that the polarization process which generates the electric conduction is not dipolar or Maxwell—Wagner in nature. The maximum could be assigned to a preferential distribution of the pairs of localized states characterized by a relaxation time τ obeying the relation $6 \cdot 10^4 \tau \approx 1$. However the straight line portions of the frequency dependent conductivity curves are due to a broad distribution of relaxation times with no predominant pair of sites with a certain relaxation time.

When the real part of the complex conductivity $\sigma_1(\omega)$ varies as ω^s, with s invariable on a frequency range, the Kramers—Kronig relation predicts for the imaginary part $\sigma_2(\omega)$ a similar frequency law [13]:

$$\sigma_2(\omega) = A_2 \omega^s \tag{3}$$

where the constant A_2 is related to A_1 as

$$\frac{A_2}{A_1} = \operatorname{tg} \frac{1}{2\pi s}. \tag{4}$$

The relation (3) can be written as

$$C - C_\infty = A_2 \omega^{s-1}, \tag{5}$$

where C is measured capacitance and C_∞ —capacitance at optical frequencies.

In fig. 4 is plotted the frequency dependence of the values $(C - C_\infty)d : \varepsilon_0 S = (\varepsilon_1 - \varepsilon_\infty) : \varepsilon_0$, for $P2EN_{c-c}$, where d is thickness of the sample, S— area of the electrodes, ε_0—permitivity of free space, ε_1 and ε_∞—dielectric constants at ω and infinite frequency respectively. It was assumed that C_∞ is roughly equal to the value of C at 10^5 Hz.

It is clear that at temperatures lower than 300° K, the Kramers-Kronig relation is obeyed; the values of s for conductivity (Fig. 1) and capacitance (Fig. 4) obtained by using the Eqs. (1) and (5) respectively

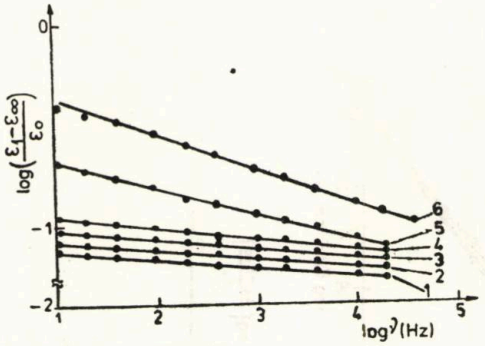

Fig. 4. — The frequency dependence of dielectric constant of P2EN$_{c-c}$: *1* — 190°K, s=0.95; *2* — 236°K, s=0.95; *3* — 278°K, s=0.95; *4* — 297°K, s=0.94; *5* — 338°K, s=0.87; *6* — 373 °K, s=0.82.

are in a fair agreement. This agreement proves that the hopping mechanism is involved for at least another decade in frequency on either side of the measuring range [3],[11].

At T>300°C K the Kramers—Kronig relation is not longer obeyed even though the capacitance keeps the same power-law relation over the whole frequency range. This fact can be attributed to the presence

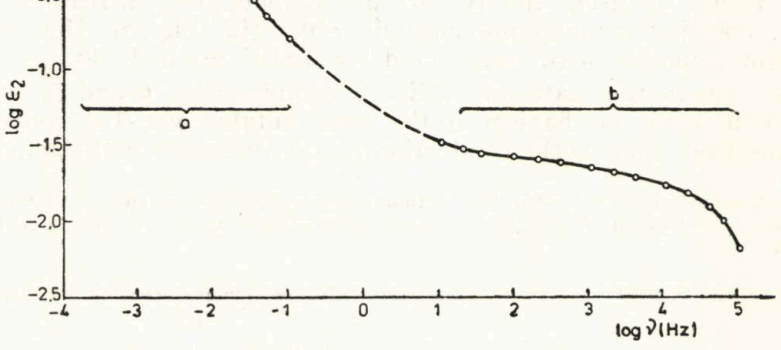

Fig. 5. — The frequency dependence of the dielectric loss of P2EN$_{c-c}$ at 297°K: a — from transient current measurements; b — from curve *4* (Fig. 1).

of the predominant multiple hops made obvious by measurements of the real part of the conductivity. These multiple hops can generate a space charge accumulated at phase boundaries (Maxwell–Wagner polarization.

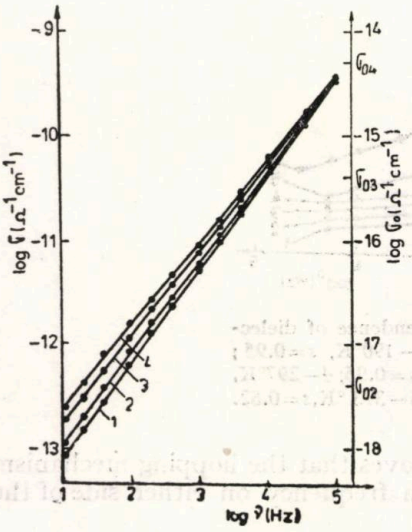

Fig. 6. — The frequency dependence of the measured conductivity of $P2EN_{t-c}$: *1* — 190°K, $s=0.9$; *2* — 300°K, $s=0.86$; *3* — 347°K, $s=0.83$; *4* — 373°K, $s=0.8$: d. c. conductivities, at the last three temperatures, are also indicated.

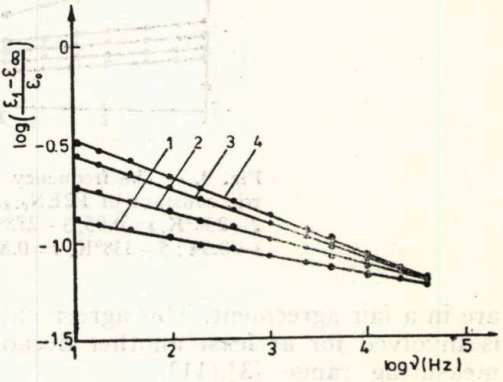

Fig. 7. — The frequency dependence of the dielectric constant of $P2EN_{t-c}$: *1* — 190°K, $s=0.905$; *2* — 300°K, $s=0.85$; *3* — 347°K, $s=0.825$; *4* — 373°K, $s=0.8$.

It is expected that the Maxwell-Wagner polarization to increase at frequencies lower than 10 Hz.

Indeed, the dielectric losses, evaluated from the transient current measurements by using the Hamon's method [14], increase with frequency, reaching a maximum around $3 \cdot 10^{-3}$ Hz (Fig. 5). However this maximum coincides with that found by TSDC method [15].

A.c. conduction data on $P2EN_{t-c}$ samples (Fig. 6 and 7) show the quantum hopping mechanism as the most suitable one. The contribution of the multiple hops to the conduction process increases with temperature.

Acknowledgements. The authors express their sincere thanks to Prof. D. D. Eley from Nottingham University, England, for assistance with a.c. conductivity measurements.

Received, January 9, 1980

Institute of Macromolecular Chemistry „P. Poni", Jassy
and
Polytechnic Institute, Jassy,
Department of Organic and Macromolecular Chemistry

REFERENCES

1. Simionescu Cr. Dumitrescu Sv., Percec V., Ioanid G., Plast. u. Kautsch., **25**, 222 (1978).
2. Diaconu I., Dumitrescu Sv., Simionescu Cr., Materiale plastice, **16**, 159 (1979).
3. Pollak M., Geballe T. H., Phys. Rev., **122**, 1742 (1961).
4. Mott N. H., Davis E. A., *Electronic Processes in Non-crystalline Materials.* Clarendon Press, Oxford, 1971.
5. Lewis J. E., Edris M., Phys. Rev., **B 11**, 4033 ((1975).
6. Simionescu Cr., Dumitrescu Sv., Percec V., Polym. J., **8**, 139 (1976).
7. Diaconu I., Dumitrescu Sv., Europ. Polym. J., **14**, 971 (1978).
8. Pollak M., Phys. Rev., **133 A**, 564 (1964).
9. Pollak M., Phys. Rev., **138 A**, 1822 (1965).
10. Pollak M., Phil. Mag., **23**, 519 (1971).
11. Pike G. E., Phys. Rev., **B 6**, 1572 (1972).
12. Rockstand H. K., Solid State Com., **7**, 1507 (1969).
13. Rockstand H. K., J. Non-crystalline Solids, **2**, 192 (1970).
14. Hamon B. V., Proc., IEE, Pt. IV, **99**, 151 (1952).
15. Dumitrescu Sv., Diaconu I., National Chem. Symp., Bucharest, Romania, 1978, Part II, Preprints, 106.

STUDIUL PROPRIETĂŢILOR ELECTRICE ALE POLIMERILOR

VII. Asupra conductibilităţii electrice în curent alternativ a poli(2-etinilnaftalenului)

(Rezumat)

S-a studiat dependenţa conductibilităţii electrice în curent alternativ a poli(2-etinilnaftalenului) funcţie de temperatură (190°... 250°K) şi frecvenţă (10...10^5Hz) stabilindu-se că mecanismul de conducţie în acest polimer depinde în primul rînd de structura sterică a polimerului: un mecanism de salt combinat cu unul de bandă (la temperaturi ridicate) în cazul polimerului *cis-cisoidal* şi un mecanism de salt singular în cazul polimerului *cis-transoidal.*

BULETINUL INSTITUTULUI POLITEHNIC DIN IAŞI
Tomul XXVI (XXX), fasc. 1—2, 1980
Secţia II
CHIMIE şi INGINERIE CHIMICĂ

D. C. 578.13

REACTIVITY OF ACRYLIC MONOMERS

IV. COPOLYMERIZATION OF N-PROPYLACRYLAMIDE WITH METHYL ACRYLATE AND *n*-BUTYL ACRYLATE

BY

SPIRIDON OPREA and EMIL DUMITRIU

Dedicated to Professor Dr. CRISTOFOR SIMIONESCU, member of the Academy, on his 60 th anniversary

1. Introduction

In a previous paper [1] were presented the results of the investigation of N-*n*-butylacrylamide copolymerization with *n*-butyl acrylate when it was stated that though both macroradicals show some afinity for the opposite monomers, the butyl acrylate ended macroradical shows a higher reactivity. In the broad scheme of investigation of the reactivity of acrylic monomers also included the copolymerization of other acrylamides with acrylic esters. Thus, in the present paper one can study the behaviour in the copolymerization of the systems *n*-propylacrylamide—methyl acrylate and *n*-propylacrylamide—butyl acrylate, respectively.

The knowledge of rules controlling the copolymerization of N-substituted acrylamides with acrylic esters allows a greater variability of properties of the resulting copolymers to be achieved. As it was pointed out in the previous paper [1] the acrylamides know large applications in the fields of coatings, acrylic rubbers, synthetic lather, etc. Therefore, major properties of these products (distribution of comonomers along the polymer chain, which is important for the introducing functional groups, mechanical properties, hydrophilicity, reactivity, etc.) can be influenced if it were known the laws governing the copolymerization of the monomers used in the synthesis of such macromolecular products.

2. Experimental

2.1. Monomers

N-*n*-Propylacrylamide (PrAm) was prepared by reacting 1 mol of acryloylchloride with 2.2 mols of propylamine in benzene solution at 0°C. Propylamine hydrochloride was removed by filtration. The benzene solution of the monomer was concentrated in vacuum, the crude monomer was first redistilled under vacuum and nitrogen, then rectified on a packed column, b.p. = 108°C/10 mm Hg. The purity of monomer was checked by IR and NMR.

Methyl acrylate (MeA), Merck reagent, was distilled at normal pressure to remove the inhibitor.

Butyl acrylate (BuA) was commercial-grade material which was carefully distilled before use.

2.2. Initiator

α,α′ - Azobis (izobutironitrile) (AIBN), was recrystallized three times from ethanol.

2.3. Solvents

Benzene, dioxane and light petroleum were dried and purified by the usual methods.

2.4. Copolymerization

Copolymerization of the two binary systems was initiated by AIBN (0.2% mole from monomers) and carried out in sealed glass tubes in dioxane solution (5 M) at 60°±0.1°C. All experiments were carried out at low conversions, below 10%. The copolymers were precipitated by an excess of methanol and purified by repeated dissolution and precipitation from solution in dioxane. The samples were dried under vacuum at 60°C. The composition of the copolymers was determined by analysis for nitrogen content (micro K j e l d a h l method). The reaction conditions and results are summarized in Tables 1 and 2.

The reactivity ratios were determined from the differential form of the general copolymerization equation by the K e l e n-T ü d ö s method [2].

Table 1

Copolymerization of N-Propylacrylamide (PrAm) with Methyl Acrylate (MeA) in Dioxane Solution at 60°C

No.	Mole fraction of PrAm in monomer feed	Time min	Conversion %	Nitrogen %	Mole fraction of PrAm in copolymer
1	0.1	20	1.79	1.23	0.076
2	0.2	20	1.99	2.51	0.162
3	0.3	20	2.18	3.45	0.226
4	0.4	20	2.39	4.39	0.294
5	0.5	20	3.79	5.46	0.374
6	0.6	20	4.36	6.34	0.444
7	0.7	20	5.90	7.24	0.517
8	0.8	20	6.75	8.22	0.600
9	0.9	20	9.23	9.85	0.747

Table 2

Copolymerization of N-Propylacrylamide (PrAm) with Butyl Acrylate (BuA) in Dioxane Solution at 60°C

No.	Mole fraction of PrAm in monomer feed	Time min	Conversion %	Nitrogen %	Mole fraction of PrAm in copolymer
1	0.1	20	1.07	1.28	0.115
2	0.2	20	1.28	2.35	0.209
3	0.3	20	1.50	3.23	0.286
4	0.4	20	1.82	4.14	0.363
5	0.5	20	2.26	5.01	0.434
6	0.6	20	3.06	5.98	0.513
7	0.7	20	4.19	7.02	0.597
8	0.8	20	5.02	8.23	0.691
9	0.9	20	5.95	9.68	0.802

3. Results and Discussion

If one follows the conversion variation against the monomer feed for a given time one can observe (Fig. 1) that between the two systems appears a certain difference which mentained over all concentration range of propylacrylamide. Moreover, it can be stated that the reaction rate increases with the increasing of propylamine concentration. This fact would indicate that the reactivity of the system is determined by the presence and the amount of substituted acrylamide.

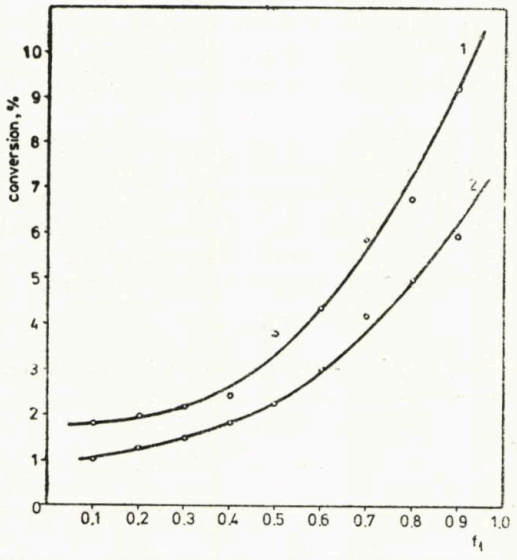

Fig. 1. — Copolymer conversion against the monomer feed : *1*—propylacrylamide—methyl acrylate system ; *2*—propylacrylamide—butyl acrylate system.

As it is known the study of the behaviour of monomers in the copolymerization process can offer important information on the reactivity of these. Though the above mentioned results show an increase of the reactivity of system with the increasing of propylacrylamide concentration, it was stated that the copolymers of propylacrylamide with methyl acrylate

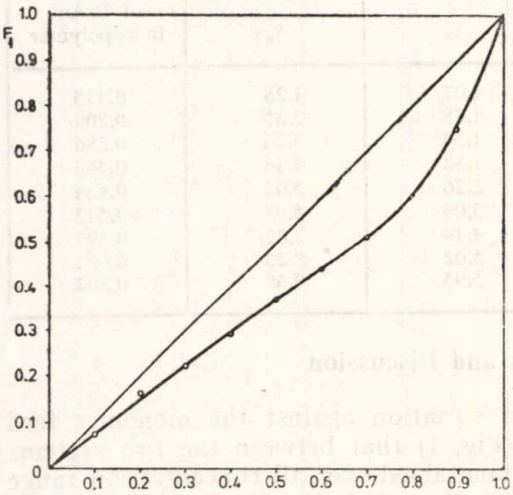

Fig. 2. — Copolymerization diagram of the system N-propylacrylamide—methyl acrylate; polymerized in dioxane solution at 60°C.

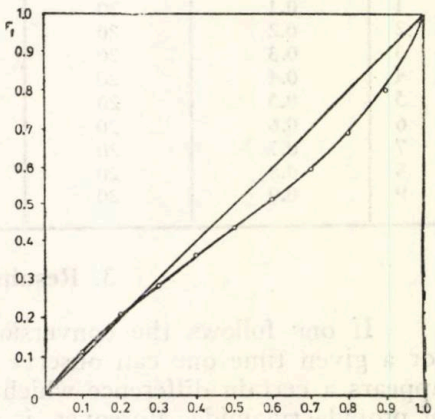

Fig. 3. — Copolymerization diagram of the system N-propylacrylamide—butyl acrylate; polymerized in dioxane solution at 60°C.

and those with butyl acrylate contain smaller amounts of propylacrylamide than the charge. The copolymerization results are presented in Figs. 2 and 3 where both the experimental points and calculated copolymerization curves were plotted.

In both cases the composition of the monomer f_1 and of the copolymer F_1 is related to propylacrylamide. Figs. 2 and 3 show the copolymerization of propylacrylamide with methyl acrylate and *n*-butyl acrylate, respectively. The results indicate that a change in the alkyl group within the C_1-C_4 range influences the reactivity to certain extent. This can also be observed from the relatively lower r_1 and higher r_2 values.

Table 3

Copolymerization Parameters of N-Propylacrylamide with Methyl Acrylate and n-Butyl Acrylate

Monomer M_2	Kelen-Tüdös method		Fineman-Ross method	
	r_1	r_2	r_1	r_2
Methyl acrylate	0.263	1.197	0.258	1.193
n-Butyl acrylate	0.401	0.797	0.381	0.747

Methyl acrylate shows a higher reactivity than the butyl acrylate of which radical is more bulkly. In the case of methyl acrylate the values $r_1=k_{11}/k_{12}=0.263$ and $r_2=k_{22}/k_{21}=1.197$ indicate the fact that both macroradicals show a greater afinity for this monomer. In the case of butyl acrylate the values $r_1=k_{11}/k_{12}=0.401$ and $r_2=k_{22}/k_{21}=0.797$ indicate that both

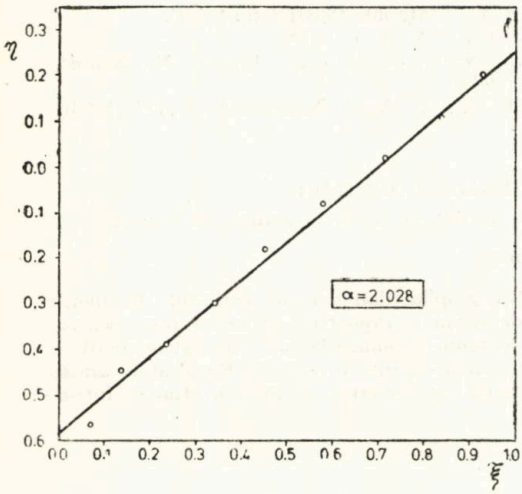

Fig. 4. — K e l e n - T ü d ö s plot for copolymerization of N-propyl-acrylamide and methyl acrylate in dioxane at 60°C.

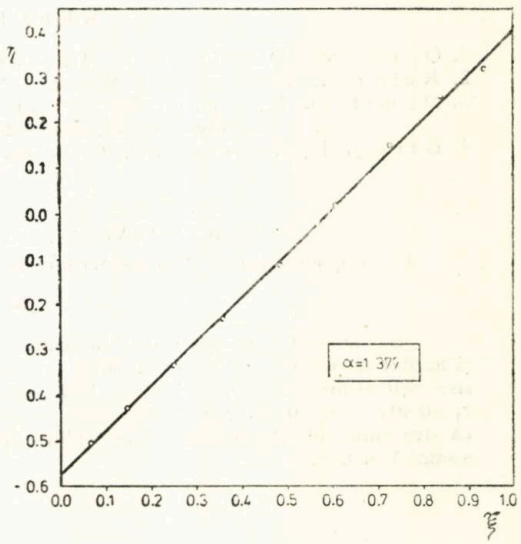

Fig. 5. — K e l e n - T ü d ö s plot for copolymerization of N-propylacrylamide and *n*-butyl acrylate in dioxane at 60°C.

macroradicals show afinity for the opposite monomers but $k_{21}<k_{12}$. Moreover, the composition diagram (Fig. 3) shows the existence of an azeotropic point at small propylacrylamide concentrations. It can also be shown that the behaviour of propylacrylamide—butyl acrylate system resembles very much with those of *n*-butylacrylamide — butyl acrylate system ($r_1=0.310$ and $r_2=0.905$ [1]). Therefore the influence of the substituent of acrylamide in the range C_3-C_4 can be considered as being unsignificant.

The behaviour of acrylamides appears more interesting if one compares the behaviour of a monosubstituted acrylamide with those of a disubstituted acrylamide in the case of the copolymerization with methyl acrylate. Thus, comparing the N-propylacrylamide with N, N-diethylacrylamide, ($r_1=0.41$ and $r_2=0.52$ [3]), one can stabilise some important differences, the last system shown a strong tendency to alternate. We can say that in the case of acrylamides, firstly the extent of substitution has importance. In the same class the differences are very small as B o r k *et al.* [4] confirmed. Therefore, the obtained results for the studied systems show that the copolymerization process of a substituted acrylamide with acrylic esters, the nature of ester influences the process in some extent. Moreover the

above mentioned results offer information on the way it can be realised in practice the copolymerization of such monomers so as to obtain a certain macromolecular product.

Received, January 19, 1980

Polytechnic Institute, Jassy,
Department of Organic and
Macromolecular Chemistry

REFERENCES

1. Oprea Sp., Dumitriu E., Iordache V., Materiale Plastice (in print).
2. Kelen F., Tüdös F., J. Macromol. Sci. Chem., **A—9**, 1 (1975).
3. Dumitriu E., Oprea Sp., Maxim S., Nathanson A., Dima M., Kolloid Z. — Z. Polymere, 11, 257, 1203 (1979).
4. Bark J. F., Wyman D. P., Coleman L. E., J. Appl. Polym. Sci., **7**, 451 (1963).

REACTIVITATEA MONOMERILOR ACRILICI

IV. Copolimerizarea N-propilacrilamidei cu acrilat de metil şi acrilat de *n*-butil

(Rezumat)

S-a studiat copolimerizarea radicalică a N-*n*-propilacrilamidei cu acrilatul de metil şi acrilat de *n*-butil în dioxan la 60°C. Au fost determinate rapoartele de reactivitate pentru sistemele studiate : $r_1 = 0{,}263$ şi $r_2 = 1{,}197$ pentru sistemul propilacrilamidă—acrilat de metil şi $r_1 = 0{,}401$ şi $r_2 = 0{,}797$ pentru sistemul propilacrilamidă—acrilat de *n*-butil. Rezultatele arată că structura radicalului alchil al esterului influenţează reactivitatea compuşilor studiaţi într-o anumită măsură.

BULETINUL INSTITUTULUI POLITEHNIC DIN IAŞI
Tomul XXVI (XXX), fasc. 1—2, 1980
Secţia III
CHIMIE şi INGINERIE CHIMICĂ

D. C. 662.766

STRUCTURAL TRANSITIONS IN CONJUGATED POLYENES
POLYACETYLENE

BY

I. NEGULESCU, C. MIHĂILESCU, CH. DRĂGAN and GH. RUSU

Dedicated to Professor
Dr. CRISTOFOR SIMIONESCU,
member of the Academy,
on his 60 th anniversary

1. Introduction

The fully conjugated hydrocarbon polymer, polyacetylene, $(CH)_x$, has been known for many years, i.e. as early as 1929 [1]. Later on, N a t t a *et al.* [2] synthesized and characterized *trans*-$(CH)_x$ by use of a Z i e g l e r catalyst but the chemistry of polyacetylene isomers has been thouroughly studied in sixties and seventies [3] ··· [9]. However, the electrical properties of isomeric acetylene polymers have been only recently studied intensively [10]. The conductivities of *cis* and *trans* isomers were reported to be 1.7×10^{-9} and 4.4×10^{-5} $ohm^{-1}\,cm^{-1}$ respectively [11]. It has been also shown that when flexible, crystalline and silvery films of semiconducting *cis*-$(CH)_x$ (A) or *trans*-$(CH)_x$ (B) polymer were doped with controlled amounts of electron-attracting species such as halogens or AsF_5, their electrical conductivity could be

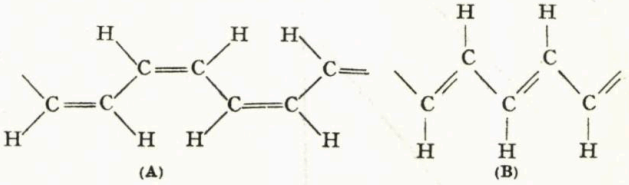

(A) (B)

systematically controlled up to 10^{11} overall increase in conductivity [12]. Formation of n-type and p-type semiconductors by doping $(CH)_x$ with NH_3 or alkali metals, and halogens or AsF_5, respectively, has led to the preparation of covalent organic polymer semiconductor junctions by C h a n g *et al.* [13]. The electrical properties of both crystalline and amorphous $(CH)_x$ were long ago found to be very sensitive to oxygen sorption [14] which causes a marked decreases in the conductivity. However, no parallel kinetics of thermal oxidation and isomerization of polyacetylene has been reported yet.

In the present work, some aspects of the isomerization and thermal oxidation of acetylene polymers are reported in view of the topological thermodynamics principles [15].

2. Experimental

Acetylene was purified by passing through dry-ice trap, H_2SO_4 trap and silicagel—P_2O_5 mixture packed column and then through columns packed with KOH, $CaCl_2$, and silicagel, respectively. Tetrabutoxytitanium was synthesized from sodium butoxide and $TiCl_4$ in toluene and purified

by fractional distillation under reduced pressure. Triethyl aluminium was used as purchased (Fluka). Solvents were dehydrated, distilled and stored under inerte atmosphere. Silvery films of *cis*-rich $(CH)_x$ were synthesized according to the method reported by I t o *et al.* [8]. Polyacetylene was doped by treatment of polymer films with iodine vapor at room temperature in vacuum for different periods of time.

Infrared spectra were recorded on a Perkin Elmer 577 spectrometer.

Thermal data were obtained using a Du Pont DS Calorimeter (990).

Electrical contacts were assured to films of *cis*-$(CH)_x$ by means of Degussa colloidal silver after removing the superficial layer of the sample. The conductivity was measured by the usual d.c. technique.

3. Results and Discussion

Though similar results were obtained by different authors regarding the synthesis of polyacetylene isomers, [5]...[9], [16], some specification should be made on the lowest temperature at which *cis* to *trans* isomerization can occurs. Recently W e t m o r e *et al.* [17] have shown that the first excited state of acetylene is the *cis* $^3B_2$ state, predicted to lie 3.43 eV above the ground state while the lowest trans triplet state is ^3B_u (3.78 eV). Consequently polyacetylene should always be obtained as *cis*-$(CH)_x$ unless different forms of energy determine the appearance of the thermodynamically more stable *trans* isomer. The change of the isomeric composition at

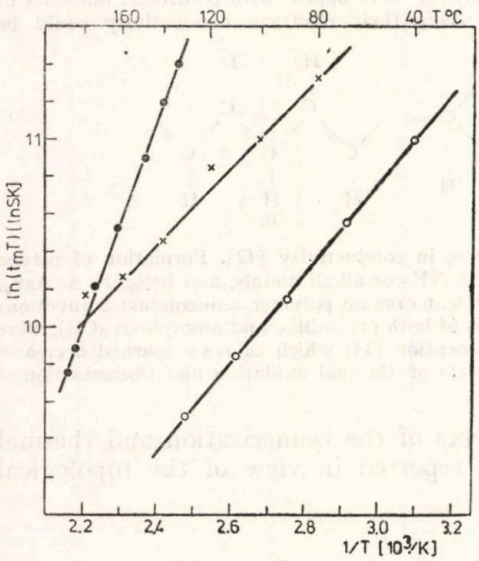

Fig. 1. — The kinetic of the exothermic flux associated with the isomerization of 75% *cis*-$(CH)_x$ (o), and to thermal oxidation of 91.5% *trans*-$(CH)_x$(•), obtained by isomerization of the *cis*-rich polymer in vacuum at 118°C, 3 hours, and by isomerization in silicon oil at 100°C, 0.5 hours (×).

different synthesis temperatures [8], i.e. 98% *cis* at −78°C, 95% *cis* at −18°C, 79% *cis* at 0°C, 59% *cis* at 18°C, and 7.5% *cis* at 100°C, suggests the existence of a barrier temperature at which the *trans* isomer could not arise, unless other energetic factors are present, e.g. the light.

To this aim the exothermic flux associated to isomerization of the *cis*-$(CH)_x$ was isothermally followed by DSC (Fig. 1) based on the kinetic model given by equation [18]:

$$\ln (t_m T) = -\frac{E}{RT} + K, \quad (1)$$

where: t_m represents the periods of times associated to the maximum of the exothermic flux, K is a constant proportional to the amount of the component inert to the investigated process, e.g. the amount of the already isomerized units or of the *cis* units hindered to isomerize due to steric circumstances, and E, R and T have the well known meanings.

Two kinds of samples were considered for this study with 75...85% *cis* units and 90...95% *trans* units, respectively, the last ones being obtained by heating the *cis*-rich polymer in vacuum at 118°C, 3 hours, or in silicon oil to avoid the penetration of the oxygen. The isomeric content of polymers was determined from procedure of I t o *et al.* [8] considering the IR absorptions from 740 cm^{-1} (*cis*) and 1 015 cm^{-1} (*trans*) shown in Fig. 2.

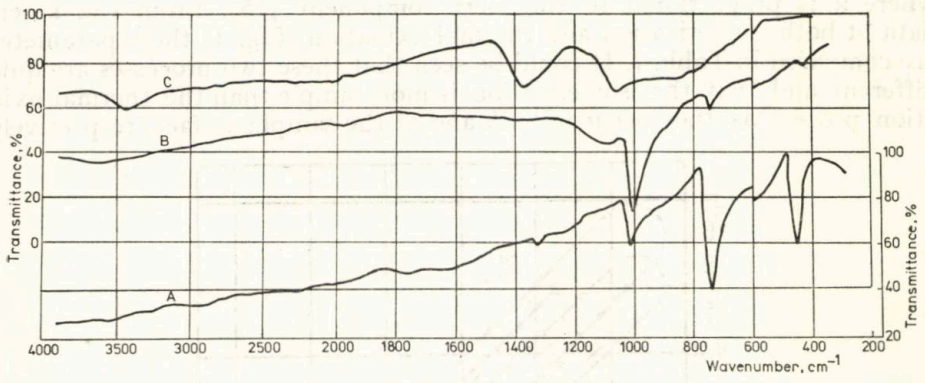

Fig. 2. — IR Spectra of: (A) — *cis*-rich polyacetylene film, 83.5% *cis*, (B) — *trans*-rich polyacetylene film obtained by isomerization of the *cis*-rich polymer in vacuum at 118°C, 3 hours, 8.5% *cis*, and (C) — iodine doped cis sample $((CH)\ I_{0.105})_x$.

By linear regression the activation energy for isomerization of the 75% *cis*-$(CH)_x$ was calculated as 19.9 kJ/mol (Table 1). The temperature at which this process could start was found as $T_0^i = 236° \pm 2°K$ in very good agreement with the reported experimental results [5], [8].

E and K parameters define univocally the behaviour of the system so that on one hand the nature of the transformation process could be identified as

$$R_{id} = \frac{E/K}{E_{st}/K_{st}}, \quad (2)$$

Table 1

Kinetic Parameters for the Thermal Isomerization and Thermal Oxidation of Polyacetylene according to Eq. (1)

Process	$-E$ kJ/mol	K ln (sK)	R_{ta}	$\varkappa$ ln (s Kmol/kJ)	Observations
Isomerization*)	19.9	3.6	1.00	0.61	Sample, 10 mg
Thermal oxidation	12.3	5.6	0.40	3.09	Sample, 10 mg pre-isomerized in silicon oil at 100°C 0.5 hours
Thermal oxidation	49.0	−2.9	—	—	Sample, 2 mg pre-isomerized in vacuum at 118°C, 3 hours

*) Initial *cis* content, 75%.

where E_{st} and K_{st} refer to a standard process and on the other hand the amplitude of the transformation could be expressed as

$$\varkappa = K - \ln E, \tag{3}$$

where $\varkappa$ is proportional to the inert component [15]. From the kinetic data of both isomerization and thermal oxidation (Fig. 1) these parameters are compared in Table 1. It could be seen that these two processes are quite different and that the isomerization is more ample than the thermal oxidation process as they occur in bulk and at the sample surface, respectively.

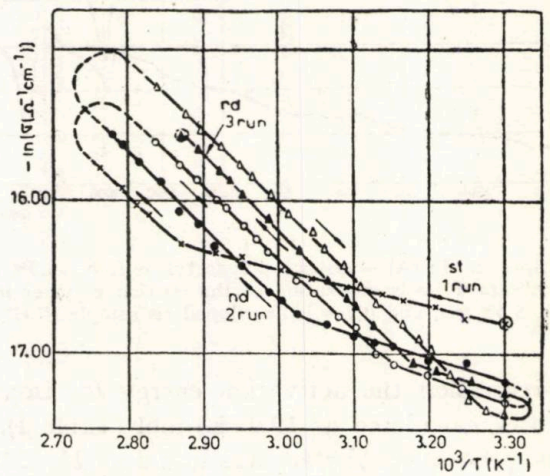

Fig. 3. — Change of the electrical conductivity of a *cis*-rich $(CH)_x$ sample with temperature during the isomerization process : initial *cis* content 83.5% (×) and final *cis* content 55% (▲).

The *cis* to *trans* isomerization is also reflected by the change of the electrical parameters in a three consecutive heating up — cooling down cycles between 303°...363° K(Fig. 3), the electrical conductivity increasing

Table 2

Kinetic Parameters for the Thermal Oxidation and Iodine Elimination of Iodine Doped Polyacetylene, $((CH)I_n)_x$, *according to Eq. (1)* (samples of 2 mg)

n	$-E$ kJ/mol	$-K$ ln(sK)	R_{id}	$\varkappa$ ln(s Kmol/kJ)
0.000	49	2.90	1.00	0.99
0.105	31	0.66	0.36	2.77
0.202	26	2.49	0.62	0.77
0.239	56	6.20	0.54	−2.18

as the sample isomerized, i.e. the *cis* content decreased from an initial content of 83.5% to 55% after the third run. The activation energy of the conductivity, E_a, given by

$$\sigma = \sigma_0 \exp(-E_a/RT), \tag{4}$$

was comprised between 0.3...0.4 eV and decreased to the lower limit with the increase of the *trans* units into the polymer as shown by the slope of the third run in comparison with that of the precedent two runs.

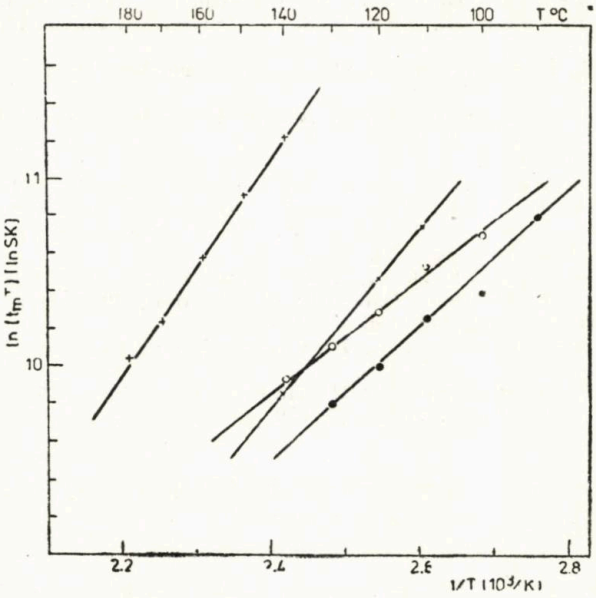

Fig. 4. — The kinetics of the exothermic flux associated with thermal oxidation and iodine elimination of $((CH)I_n)_x$: + — $n=0.000$, *trans*; • — $n=0.105$; o — $n=0.202$; × — $n=0.234$.

In the case of $(CH)_x$ samples doped with iodine, the thermal oxidation occurs simultaneously with an exothermic elimination of the halogen. The kinetics of these two overlaped processes is different from that of the

autooxidation of *trans* $(CH)_x$, as illustrated in Fig. 4. It could be seen from comparison of $\varkappa$ values (Table 2) that the higher the iodine content into the polymer the higher the content of the active component, i.e. initially a content up to 10% iodine has an antioxidant effect but higher values determine the acceleration of these two processes.

Received, January 26, 1980

„P. Poni" Institute of Macromolecular Chemistry, Jassy,
ICECHIM, Center of Physical Chemistry, Bucharest
and
University „Al. I. Cuza", Jassy

REFERENCES

1. Job A., Champetier G., C. R. Acad. Sci., **189**, 1089 (1929).
2. Natta G., Mazzanti G., Corradini P., Atti. Accad. Naz. Lincei, Cl. Sci. Fis., Mat. Nat. Rend., **25**, *3* (1958).
3. Watson W. H. Jr., McMordie W. C. Jr., Lands L. G., J. Polym. Sci., **55**, 137 (1961).
4. Hatano M., Shimamura K., Ikeda S., Kambara S., Repts. Progr. Polym. Phys. Japan, **11**, 123 (1968).
5. Kleist F. D., Byrd N. R., J. Polym. Sci., **A-1**, *7*, 3419 (1969).
6. Shirakawa H., Ikeda S., Polym. J., **2**, 231 (1971).
7. Shirakawa H., Ito T., Ikeda S., Polym. J., **4**, 460 (1973).
8. Ito T., Shirakawa H., Ikeda S., J. Polym. Sci. Polym. Chem. Ed., **12**, 11 (1974)
9. Ito T. Shirakawa H., Ikeda S., J. Polym. Sci. Polym. Chem. Ed., **13**, 1943 (1975).
10. Labes M. M., Love P., Nichols L. F. Chem. Rev. **79**, 1 (1979) and references herein.
11. Chiang C. K., Fincher C. R. Jr., Park Y. W., Heeger A. J., Shirakawa H., Louis E. J., Gau S. C., MacDiarmid A. G., Phys. Rev. Lett., **39**, 1098 (1977).
12. Chiang C. K., Fincher C. R. Jr., Heeger A. J., Shirakawa H., Louis E. J., MacDiarmid A. G., J. Am. Chem. Soc., **100**, 1013 (1978).
13. Chiang C. K., Gau S. C., Park Y. W., Heeger A. J., MacDiarmid A. G., Bull. Am. Phys. Soc., **23**, 304 (1978).
14. Berets D. J., Smith D. S., Trans. Faraday Soc., **64**, 823 (1968).
15. Drăgan G., Ph. D. Diss., University of Bucharest, 1979; Rev. Roum. Chim., **24**, 627 (1979); Acta Polymerica (in press).
16. Hsu S. L., Signorelli A. J., Pez G. P., Baugham R. H., J. Chem. Phys., **69**, 106 (1978).
17. Wetmore R. W., Schaeffer III, H. F., J. Chem. Phys., **69**, 1648 (1978).
18. Drăgan G., Rev. Roum. Chim., **23**, 629 (1978).

TRANZIȚII STRUCTURALE ÎN POLIENI CONJUGAȚI
Poliacetilena

(Rezumat)

S-au preparat filme argintii de poliacetilenă înalt cristalină și s-a determinat cea mai joasă temperatură la care apare izomerizarea *cis/trans*, 236°±2°K. Atît cinetica izomerizării cît și cea a auto-oxidării termice au fost descrise pe baza principiilor termodinamicii topologice. Au fost de asemenea preparate probe de poliacetilenă dopate cu iod și s-a urmărit cinetica eliminării halogenului și auto-oxidarea probelor.

BULETINUL INSTITUTULUI POLITEHNIC DIN IAŞI
Tomul XXVI (XXX), fasc. 1—2, 1980
Secţia III
CHIMIE şi INGINERIE CHIMICĂ

D. C. 678-13

METHOXY SIGNAL RESOLUTION IN THE ^{1}H-NMR SPECTRA OF METHYL ACRYLATE—STYRENE COPOLYMERS

BY

ALMERIA NATANSOHN, STELIANA MAXIM and DOREL FELDMAN

Dedicated to Professor Dr. CRISTOFOR SIMIONESCU, member of the Academy, on his 60 th anniversary

1. Introduction

The ^{1}H-NMR spectra of acrylic—aromatic copolymers present a splitting of the OCH_3 (or OCH_2R) signal due to the sequence distribution and configuration[1]. The spacing between the three parts of methoxy signal is bigger or smaller, depending on comonomer structure. In order to calculate the sequence distribution and configuration parameters it is necessary to have a well-resolved spectrum. In this paper we obtained a better resolution of the OCH_3 signal in methyl acrylate—styrene copolymers by adding the shift reagent $Eu(fod)_3$.

2. Theoretical

Analysing the splitting of the methoxy signal in the ^{1}H-NMR spectra of methyl acrylate—styrene copolymers, it results that :

a) The OCH_3 signal is split in three parts (Fig. 1) having 0.15 ppm between them. The resolution at 60 MHz is not sufficient for a precise quantitative analysis.

b) Assignment of OCH_3 signal can be made as in Table 1 [1]. f_i... is the molar fraction of i... sequence (assignment for triad sequences) and σ is the probability of a coisotactic alternant diad. For the methyl acrylate—styrene system ($r_1=0.18$, $r_2=0.75$[2]),$\sigma=0.8$ [2]. Sequence fractions can be calculated according to H a r w o o d [4]. Knowing the monomer feed ratio and keeping the low conversion rule, one can calculate the A, B and C parts of the OCH_3 signal.

c) The σ-value indicates a great tandency to coisotacticity, which can be explained by a substituent association on the same part of the macromolecular chain :

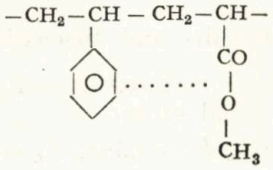

Table 1

Assignment of the Methoxy Signal

Part of the signal \ Fraction	f_{111}	f_{211}	f_{212}
A	1	$1-\sigma$	$(1-\sigma)^2$
B		σ	$2\sigma(1-\sigma)$
C			σ^2

The rare earth paramagnetic complexes act as L e w i s acids in the presence of basic groups (C=O, for example) (5). The effect of adding such a complex in the NMR spectrum is an induced shift of signals corresponding to the groups neighbouring the basic function. The shift is to higher fields (complexes of Pr) or to lower fields (complexes of Eu). However, the shift is accompanied by a broadening of signals, due to the paramagnetism. There is an optimum concentration of the complex, the shift being sufficiently high and the broadening sufficiently low.

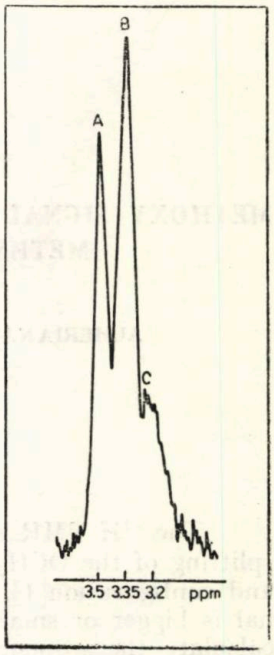

Fig. 1.—OCH_3 signal from the ^{1}H-NMR spectrum of sample AMS 1.

3. Experimental

Tris (1, 1, 1, 2, 2, 3, 3 heptafluoro 7,7 dimethyl octanedionato) europium III, Eu $(fod)_3$, was used as shift reagent and was synthetised by complexing $Eu(NO_3)_3$ with heptafluoro dimethyl octanedione.

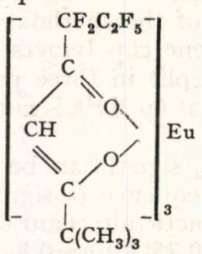

The copolymer was synthetised in bulk at 60°C using AIBN as initiator. The conversion was kept low for AMS1 (methyl acrylate : styrene = =6.143) and high for the aseotropic feed ratio AMS2 (methyl acrylate : styrene=0.305). The methyl acrylate was radical polymerized in bulk.

The ^{1}H-NMR spectra were run on a JEOL C-60HL spectrometer in $CDCl_3$ solutions at 60°C and room temperature.

4. Results and Discussion

In Fig. 2 one can see the methoxy signal of the AMS 2 sample. The theoretic calculus for this signal gives :

$$F_A=0.076,\ F_B=0.348,\ F_C=0.576.$$

As is obvious in the Fig. 2 the *A*, *B* and *C* parts are overlapped and a measure of the fractions can be made only by curve decomposition. The error is very big.

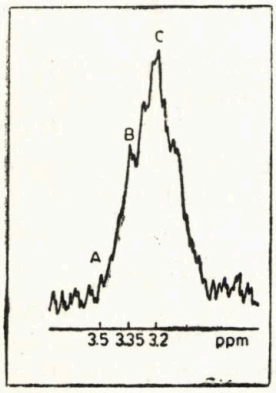

Fig. 2. — OCH_3 signal from the ^1H-NMR spectrum of sample AMS2.

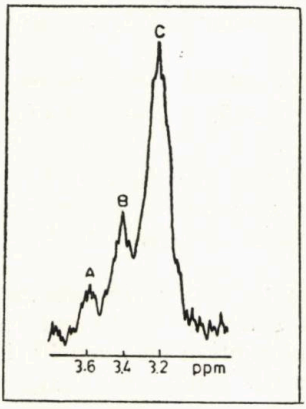

Fig. 3. — ^1H-NMR spectrum of sample AMS 2 with 0.02% $Eu(fod)_3$ — the OCH_3 signal.

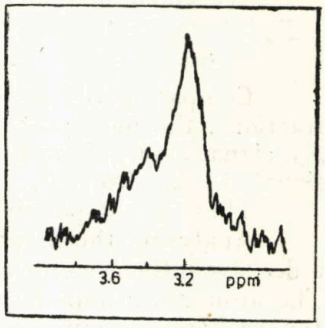

Fig. 4. — OCH_3 signal from the ^1H-NMR spectrum of sample AMS2 with 0.04% $Eu(fod)_3$.

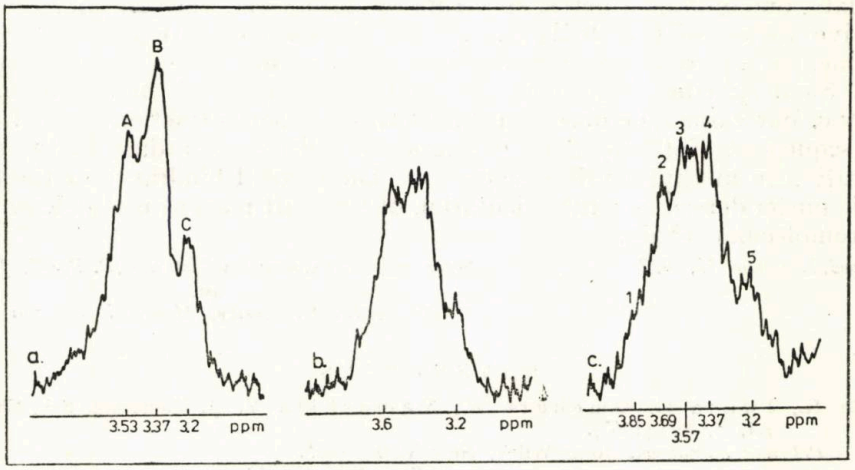

Fig. 5. — OCH_3 signal from the ^1H-NMR spectrum of sample AMS1 with different $Eu(fod)_3$ concentrations: *a* — 0.01%, *b* — 0.02%, *c* — 0.03%.

Adding $Eu(fod)_3$ the greatest induced shift is experienced by *A* fraction, followed by *B* and *C*. The result is a signal separation (Fig. 3···5). The spacing between signals is now 0.20 ppm. At higher concentration in $Eu(fod)_3$ the signals broaden and the spectrum becomes unresolved (Fig. 4).

Adding $Eu(fod)_3$ at AMS1 sample has a more complicated effect. In the Fig. 5 the effect is presented for three $Eu(fod)_3$ concentrations.

In all cases the spectra are less resolved than the initial one (Fig. 1), but a multiplicity can be seen appearing in Fig. 5 *b* and *c*.

An attempt to assign these signals must consider the sequence and configuration influence. In order to know the configuration influence we added $Eu(fod)_3$ at polymethylacrylate solution. There is no splitting in OCH_3 signal, unlike polymethylmethacrylate [6], only a signal broadening. Therefore, the multiplicity appearing in AMS1 sample is due only to sequence distribution effects.

We calculated methoxy signal composition in triad sequences:

$$F_A = \underset{f_{111}}{0.276} + \underset{f_{211}}{0.100} + \underset{f_{212}}{0.009} = 0.385, \quad F_B = \underset{f_{211}}{0.399} + \underset{f_{212}}{0.072} = 0.471, \quad F_C = \underset{f_{212}}{0.144}.$$

Comparing the signal intensities in Fig. 5 *c* with the triad sequence fractions, the most probable assignment seems to be: signal $1-f_{211}$ from F_A, signal $2-f_{111}$ from F_A, signal $3-f_{211}$ from F_B, signal $4-f_{212}$ from F_B, signal $5-f_{212}$ from F_C.

There is no possibility to verify this assignment at 60 MHz.

Analysing the induced shifts, it is obvious that the steric factor has a decisive influence on the interaction between $Eu(fod)_3$ and the C=O group. The aromatic groups hinder the bulky $Eu(fod)_3$ molecule to approach to the carbonyl group.

5. Conclusions

Adding $Eu(fod)_3$ to the copolymer samples with low content of methyl acrylate, one obtains a better spectrum resolution and one can calculate the relative ratios of the OCH_3 signal. For the samples with low content of styrene, the spectrum becomes more complicated due to the sequence splitting. Such splitting is present also in the samples with high content of styrene, but cannot be observed due to the very small fractions of 111 and 211 sequences. $Eu(fod)_3$ does not produce splitting according to the configuration in methyl acrylate sequences. The sterical hindrance of the aromatic nuclei determines the orientation of the shift reagent molecule on the macromolecular chain.

Received, November 15, 1977

Macromolecular Chemistry Institute „P. Poni", Jassy
and
Concordia University, Montreal, Canada

REFERENCES

1. Ito K., Iwase S., Umehara K., Yamashita Y. J. Macromol. Sci., Chem., A1, *5*, 891 (1967).
2. * * * *Polymer Handbook*. John Wiley, New York, 1975.
3. Ito K., Yamashita Y., J. Polym. Sci., **B 3**, 637 (1965).
4. Harwood H. J., Ritchey W. M., J. Polym. Sci., **B 2**, 601 (1964).
5. von Ammon R., Fischer R. D., Angew. Chem., **84**, *16*, 737 (1972).
6. Katritzky A. R., Smith A., Tetrahedron Lett., 1765 (1971).

REZOLVAREA REZONANȚEI METOXI ÎN SPECTRELE ^{1}H-RMN ALE COPOLIMERILOR ACRILAT DE METIL – STIREN

(Rezumat)

Adăugînd $Eu(fod)_3$ la soluțiile copolimerilor acrilat de metil — stiren în $CDCl_3$ se obține o rezolvare mai bună a semnalului metoxi și o scindare în plus datorată secvențelor. În acest mod devine posibilă măsurarea fracțiunilor semnalului OCH_3 la copolimerii cu conținut mic de acrilat de metil. Rezolvarea spectrelor se datorește împiedicării complexării carbonilului cu $Eu(fod)_3$ provocată de efectele sterice ale nucleului aromatic al stirenului.

BULETINUL INSTITUTULUI POLITEHNIC DIN IAŞI
Tomul XXVI (XXX), fasc. 1—2, 1980
Secţia II
CHIMIE şi INGINERIE CHIMICĂ

D.K. 678-13

MECHANOCHEMISCH DURCH SCHWINGMAHLUNG INITIIERTE HOMO- UND KOPOLYMERISATIONSREAKTIONEN

VON

CLEOPATRA VASILIU-OPREA, CLAUDIA NEGULIANU, MARCEL POPA
und FELICIA WEINER

Herrn Professor
Dr. CRISTOFOR SIMIONESCU,
Mitglied der Akademie,
zum 60. Geburtstag gewidmet

1. Einführung

Die mechanochemische Homo- und Kopolymerisation ist in der mechanochemischen Synthese in geringem Maße vertreten. V. A. K a r g i n hat die ersten Versuche durchgeführt, wobei er ein kristallines Monomeres mit ionischer Gitterstruktur, uzw. das Natriumakrylat, durch Schwingmahlung und in Anwesenheit eines organischen Lösungsmittels (in geringen Mengen) polymerisierte [1].

Andere Forschungsrichtungen, die von der Feststellung ausgingen, daß die mechanische Energie die Fähigkeit besitze äußerst rasche Prozeße in der Struktur kondensierter chemischer Stoffe auszulösen, haben die Initiierung der Polymerisation einiger kristalliner Monomeren (Akrylamid, Natriumakrylat, Trioxan, Salizylaldehyd) aufgrund der Einwirkung einer Stoßwelle getestet, deren Frontdruck bei 1,5 ... 3.10^4 At.lag. Die Temperatur beträgt, unter den explosiven Bedingungen dieser Reaktionen, maximal +50°C [2], [3].

Die Tatsache, daß die Dispergierung anorganischer Salze, in Anwesenheit von Vinylmonomeren, die Homo- und Kopolymerisation derselben begünstigt, u. zw. ohne Anwendung der üblichen Initiatoren oder Katalysatoren, darf gegenwärtig als nachgewiesen betrachtet werden [4] ... [8].

Die mechanochemisch durch Schwingmahlung initiierten Polymerisationsreaktionen, die im vorliegenden Beitrag untersucht werden, verwenden die Monomeren nicht in kondensiertem (festem, kristallinem), sondern in flüssigem Zustand, mit Ausnahme des ε-Kaprolaktams. Die Reaktionen finden ohne Anwendung von Initiatoren, Katalysatoren oder anorganischen Salzen statt.

Die eingesetzte Apparatur und die Bedingungen, unter denen man die Schwingmahlung durchführte, sind in den vorherigen Beiträgen ausführlich beschrieben worden [9]...[11]. Kurz vor dem Ansatz der Synthesen wurden die flüssigen Monomeren durch Vakuumdestillation und das ε-Kaprolaktam durch wiederholte Neukristallisationen aus Azeton und Benzol gereinigt.

2. Ergebnisse und Diskussion

Tabelle 1 vermittelt die Kenndaten hinsichtlich der unter identischen Bedingungen durchgeführten Homopolymerisation von Monomeren mit unterschiedlicher Struktur, sowie einige Charakteristika derselben Mono-

meren. Es wird festgestellt, daß das Akrylnitril die maximale Reaktionsfähigkeit (94,4%) unter den untersuchten Monomeren aufweist, gefolgt von Styrol (42,8%), ε-Kaprolaktam (37,7%), Isopren (28,7%), während die restlichen Monomeren variable Konversionsgrade erreichen, die den Prozentsatz 17...10% decken.

Tabelle 1

Die Bedingungen unter denen die mechanochemische Synthese, (durch Schwingmahlung), einiger Homopolymeren durchgeführt wurde und einige Charakteristika der letzteren. (Unverändert blieben: das Füllungsverhältnis, $\eta=0,5\%$; die Mahldauer, $t=96$ Stunden; die Temperatur, $T=18°\pm2°C$; die Atmosphäre in den Reaktionsgefäßen = inert = gereinigter Stickstoff).

Nr.	Das Monomere		Konversion	Löslichkeit	Rückstand bei Kalzination
	Benennung	Chemische Formel	%	%	%
1	Akrylnitril	$CH_2=CH$ | $C\equiv N$	94,4	55 (in DMF)	8,2
2	Styrol	$CH_2=CH$ | C_6H_5	42,8	19,7 (in DMF)	
3	ε-Kaprolaktam*)	$(CH_2)_5-NH$ $\diagdown CO \diagup$	37,7	45 (in *m*-Kresol)	90,3
4	Isopren	$CH_2=C-CH=CH_2$ $\diagdown CH_3$	28,7	6,4 (in Methanol)	—
5	α-Methyl Styrol	$CH_2=C$ $\diagup CH_3$ $\diagdown C_6H_5$	17,2	unlöslich	50
6	Benzonitril	$C_6H_5-C\equiv N$	15,5	—	—
7	Methylmetakrylat	$CH_2=C-CH_3$ $\diagdown COOCH_3$	12,7	—	—
8	Vinylazetat	$CH_2=CH$ | $OCOCH_3$	12,13	—	—
9	Azetonitril	$CH_3-C\equiv N$	10,8	unlöslich	—
			6,7*)	unlöslich	—

*) $\eta=0,4\%$; Reaktionsmedium: Luft

Die Analyse der Absorptionsspektra im IR(infrarot)-Bereich läßt, im allgemeinen, die Anwesenheit der für die respektiven Homopolymeren spezifischen Spektralbänden erkennen, mit Ausnahme des Poly(Akrylnitrils), das außer dem für die Gruppe $-C\equiv N$ spezifischen Spektralband ab

2 250 cm^{-1} auch andere Maxima aufweist, die den Bindungen $>C=N-$ bei 1 606 und $>C=C<$ 1 600...1 700 cm^{-1} entsprechen, Bindungen die im Koordinationssystem angeordnet sind. Dieses Ergebnis wurde auf die Mitbeteiligung an der Reaktion auch der Gruppe $>C=N-$ zurückgeführt. Zur Bestätigung dieser Hypothese hat man die Homopolymerisation von Nitrilen durchgeführt, bei denen die vinylische Doppelbindung fehlt : Azetonitril, Benzonitril.

Es wurde festgestellt, daß beide Substanzen polymerisieren, wobei spezifische durch die Struktur dieser Substanzen bedingte Konversionsgrade registriert worden sind. Der höhere Konversionsgrad des Benzonitrils kann aufgrund des Verbindungseffektes der Elektronen aus dem aromatischen Kern mit denen aus der Gruppe $-C\equiv N$ erklärt werden, wodurch die dreifache Bindung labil wird.

Als erstes Charakteristikum der erhaltenen Polymeren darf ihre besondere Stabilität gegenüber den Lösungsmitteln Erwähnung finden. Die Kenndaten in Tabelle 1 bestätigen die Eigenschaften dieser Polymeren als schwer lösliche und unlösliche Substanzen. Unter Wärmeeinwirkung (20°...700°C) schmilzt und erweicht keine der erhaltenen Verbindungen.

Die Kenndaten in Tabelle 2 beweisen, daß die chemische Zusammensetzung des Substrats einen entscheidenden Einfluß auf die Polymerisation ausübt. Der maximale Konversionsgrad wird bei der Mischung Akrylnitril—Vinylazetat registriert (Verhältnis 5 : 1/92,58%). Handelt es sich um Systeme von Komonomeren, in denen eine der Komponenten das Akrylnitril ist, so stellt man fest, daß maximale Konversionsgrade dann erreicht werden, wenn das Akrylnitril quantitativ vorherrscht ; dies bestätigt die Fähigkeit dieses Monomeren leicht zu polymersieren, u.zw. unter Einwirkung der mechanischen Energie, im Prozeß der Schwingmahlung.

Ein anderer Faktor, der die Kopolymerisation beeinflußt, ist der Abnutzungsgrad der Apparatur, insbesondere derjenige der Mahlkörper. Aufschlußreiche Unterschiede hinsichtlich der Konversionsgrade können dann festgestellt werden, wenn man Kugeln mit einem Durchmesser von 9 mm verwendet, die eine lange Nutzungsdauer haben (cca. 10 Jahre) und dieselben, aber nicht abgenutzten Mahlkörper. So z.B. beträgt der Konversionsgrad 48% (im System Akrylnitril—α Methyl Styrol/Verhältnis der Komonomeren 1 : 1), wenn alte Kugeln und nur 36,1%, wenn neue Mahlkörper eingesetzt werden.

Die Daten der Elementaranalyse heben den geringen Kohlenstoffgehalt hervor, der je nach der Art des Monomeren zwischen 73,5% und 13,48% schwankt. Im System Akrylnitril—Vinylazetat erreicht der infolge des Brennprozeßes entstandene Rückstand sehr hohe Werte : 50,5%, wenn das Verhältnis zwischen diesen Komonomeren 1 : 2, und 56%, wenn jenes Verhältnis 1 : 5 beträgt.

In Abb. 1 wird die Einwirkung der Dauer auf die Homopolymerisationsreaktionen dargestellt. Dieser Faktor ist aufgrund von Synthesen untersucht worden, die in einem Zeitraum 24...120 Stunden durchgeführt wurden. Das erste Charakteristikum der erhaltenen Kurven ist es, daß diese ein Maximum erreichen, dessen Lage von der Art des untersuchten Systems abhängt. Die Ergebnisse der Polymerisation von ε-Kaprolaktam (Kurven *4*, *5*) und von Azetonitril (Kurve *6*) sind neuesten Daten und es

wurden. diesbezüglich, noch keine Synthesen durchgeführt, die eine Dauer von 96 Stunden überschreiten, so daß die Abzweigung der Kurven fehlt.

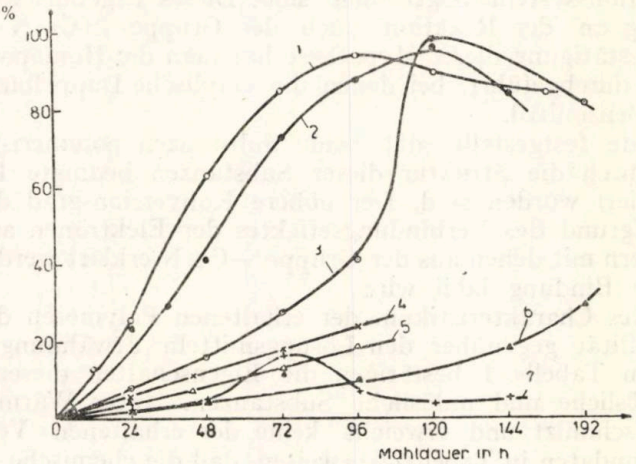

Abb. 1. — Die Abhängigkeit des Konversionsgrades verschiedener Monomeren, in den entsprechenden Homopolymeren, von der Dauer der Schwingmahlung: *1*—Polyacrylnitril (PAN) in inertem Medium (gereinigter Stickstoff); *2*—Idem in Gegenwart von atmosphärischer Luft; *3*—Polystyrol (PS); *4*—Poly-ε-Kaprolaktam, in Gegenwart von $MnCl_2.4H_2O$ (10 g : 2 g); *5*—Idem (Monomere 10 g : 0,2 g Salz); *6*—Polyazetonitril; *7*—Polyazetonitril.

Über die kleinen Zeiträume (24...96 Stunden) darf gesagt werden, daß das Konversionsmaximum des Akrylnitrils, das im reaktionsinertem Medium seine größte Polymerisationsfähigkeit aufweist, bei 96 Stunden liegt; darüber hinaus verlangsamt sich die Polymerisation (Kurve *1*). Fungiert die Luft als Gasatmosphäre im Reaktionsgefäß, so resultiert eine formähnliche Kurve, doch wird das Konversionsmaximum erst nach 120 Stunden erreicht (Kurve *2*). Das Styrol ist ein weiteres Monomeres, das eine gute Reaktionsfähigkeit hat. In einem Zeitraum von 24...96 Stunden reaktioniert es langsamer, nachher aber findet eine Selbstbeschleunigung des Prozeßes statt. Das Maximum liegt bei 120 Stunden, darüber hinaus fällt der Konversionsgrad ab.

Abb. 2 stellt die typischen Kurven dar, die die Variation der Konversionsgrade in Bezug zur Zeitdauer verfolgen. Aufgrund ihrer Reaktionsfähigkeit, die an den maximalen Konversionsgraden bewertet wird, sind die untersuchten Kopolymerensysteme in folgende Reihe eingeordnet worden:

Akrylnitril—Styrol > Akrylnitril—α Methyl Styrol >
> Akrylnitril—Vinylazetat > Akrylnitril—Vinylazetat—α Methyl Styrol.

Um die mechanochemisch synthetisierten Polymeren charakterisieren zu können, hat man einige ihrer Grundeigenschaften determiniert. So z.B. wurde die Löslichkeit unter allen gegebenen Umständen untersucht. Eine Schlußfolgerung, die aufgrund der registrierten Kenndaten gezogen werden kann, ist die, daß die neuentstandenen Homo- und Kopolymeren stets aus zwei Fraktionen bestehen: einer löslichen und einer unlöslichen,

u.zw. im Hinblick auf die spezifischen Lösungsmittel. Die lösliche Fraktion wächst, in der Regel, quantitativ an, u.zw. in dem Maße in dem der Konversionsgrad durch die Verlängerung der Synthesedauer waschst.

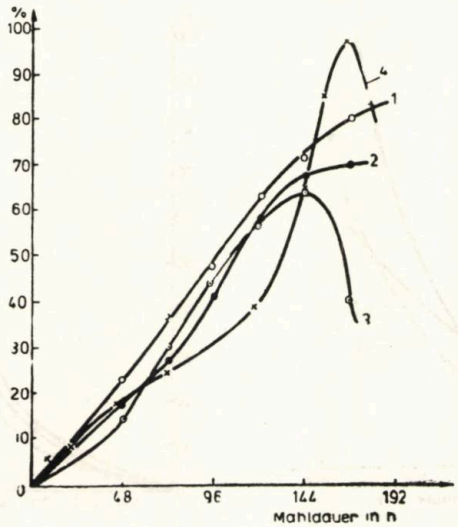

Abb. 2. — Die Abhängigkeit des Konversionsgrades verschiedener Komonomeren-Systeme, in den entsprechenden Kopolymeren, von der Dauer der Schwingmahlung: *1*—Akrylnitril—α Methyl Styrol (AN—α MS); *2*—Akrylnitril — Vinylazetat (AN—AcV); *3*—Akrylnitril—Vinylazetat—α Methyl Styrol (AN—AcV—αMS); *4*—Akrylnitril —Styrol (AN—S).

Abb. 3 veranschaulicht die Variation des prozentuellen Inhalts in der löslichen Fraktion im Verhältnis zur Synthesedauer einiger Kopolymeren. Untersucht wurden die aus Akrylnitril—α Methyl Styrol (5 : 1), Akrylnitril—Vinylazetat (5 : 1) und dem ternären Kopolymeren Akrylnitril—Vinylazetat—α Methyl Styrol (10 : 1 : 1) gebildeten Systemen. Die Kopolymeren, die infolge der Synthetisierung der beiden ersten Systeme entstanden, weisen annähernd gleiche, begrenztere Auflösungsfähigkeiten auf, während das ternäre Kopolymere eine größere Auflösungsfähigkeit hat (Kurven *1*, *2*/Kurve *3*).

An denselben Kopolymeren wurde auch die Thermostabilität untersucht, indem die als Kriterium betrachteten Gewichtverluste durch thermogravimetrische und thermodifferentielle Analyse (Apparat vom Typ P a u l i k-P a u l i k-E r d e l y) determiniert worden sind (Abb 4). Bis zu Temperaturen von fast 400°C verhalten sich alle Verbindungen annähernd identisch, wobei man Gewichtverluste von cca. 50% registrierte. Im Bereich höherer Temperaturen (400°...700°C) ist das Verhalten der Verbindungen derart unterschiedlich, daß man sie, im Hinblick auf ihre Thermostabilität, in folgende Reihe gliedern kann:

Akrylnitril — Vinylazetat (5 : 1) > Akrylnitril — Vinylazetat — α Methyl Styrol (10 : 1 : 1) > Akrylnitril—α Methyl Styrol (5 : 1).

Die Polymeren, die durch mechanochemische Synthese, durch Schwingmahlung und unter Anwendung von metallischer Apparatur (V_2A—Stahl)

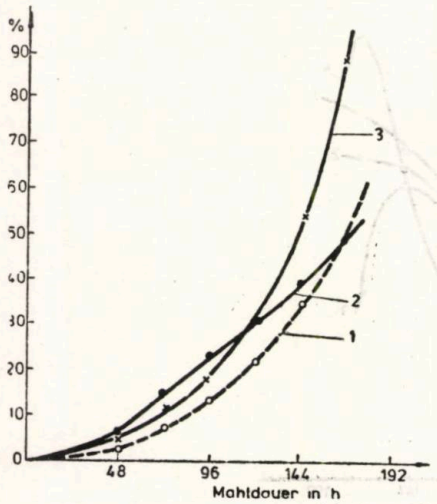

Abb. 3. — Die Abhängigkeit der Löslichkeit (in Dimethylformamid—DMF) einiger Kopolymeren, von der Dauer der Schwingmahlung: *1*—AN—αMS (5 : 1); *2*—AN—AcV(5 : 1); *3*—AN—AcV—α MS (10 : 1: 1). Die Bedingungen, unter denen die Testsubstanzen synthetisierten: $\eta = 0{,}5\%$, in inerter Atmosphäre $T = 18° \pm 2°C$.

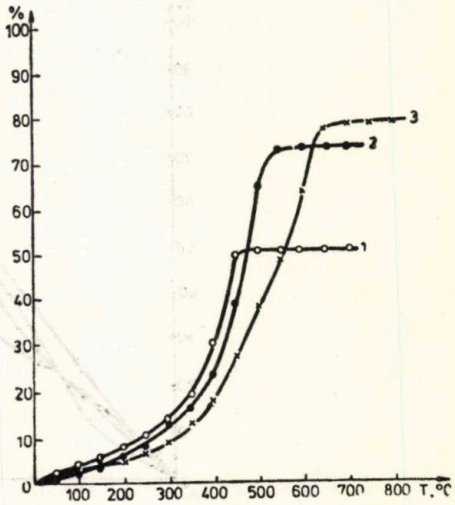

Abb. 4.—Die Abhängigkeit der durch thermogravimetrische Analyse determinierten Gewichtsverluste, von der Zersetzungstemperatur einiger Kopolymeren: *1*—AN—AcV (5 : 1); *2*—AN—AcV—αMS (10 : 1 : 1); *3* — AN—α MS (5 : 1).

erhalten wurden, beinhalten chemisch gebundenes Eisen, besonders in den löslichen Fraktionen. Die Analyse dieser Fraktionen registriert die Anwesenheit des chemisch gebundenen Eisens, sogar nach der Durchführung von Reinigungen, Auflösungen und Neufällungen. In unlöslichen Fraktionen verbleibt, im allgemeinen, das Eisen in fein zerteiltem Zustand und man kann es durch gegenwärtig bekannte physikalische Methoden nicht absondern. Die Analyse dieser Eisenrestteile zeigt ein modifiziertes Gitter, an dessen Oberfläche Fraktionen des organischen Teils der Reaktionsmasse durch Koordination zurückbehalten werden. Die Elementaranalyse dieser unlöslichen Fraktionen zeigt, daß sie Kohlenstoff in kleinen Mengen enthalten (zuweilen 5...6%) und daß die Pyrolyse große Mengen von Rückstand hinterläßt (50...56% in Tabelle 2, manchmal sogar 90%); diese Residuen können durch die gegenwärtig bekannten physikalischen und chemischen Methoden nicht zersetzt werden, u.zw. zum Zwecke der Freisetzung des Metalls (z.B. als Oxyd, infolge des Brennprozeßes). Die Absorptionsspektralanalyse dieser Verbindung läßt die Anwesenheit von Banden erkennen, die für jenes Polymere spezifisch sind gegenüber dem sich die Verbindung als reaktionsfähig gezeight hat (Spektralanalyse im IR-Bereich).

Die Einsetzung des Eisens in die chemische Struktur dieser Substanzen verleiht ihnen magnetische Eigenschaften, die mit Hilfe der M ö ß b a u e r-und ESR-Spektroskopie (elektrischer Spin-Resonanz) dargelegt werden können.

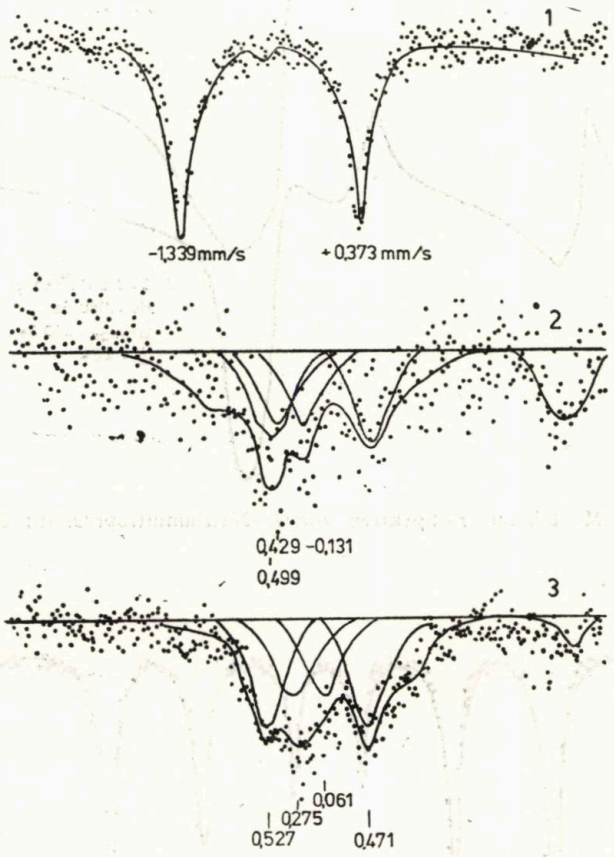

Abb. 5 — ESR—Spektren für die löslichen Fraktionen von: *1*—PAN; *2*—AN—S(Kopolymere).

Abb. 5 stellt die ESR-Spektren dar, die für das Poly(Akrylnitril), u.zw. für die in DMF (Dimethylformamid) lösliche Fraktion (Kurve *1*) und für das Kopolymeren AN—S (Akrylnitril—Styrol) spezifisch sind (Kurve 2).

Die M ö ß b a u e r-Spektroskopie ermöglicht die Scheidung zwischen dem chemisch gebundenen und dem als separate Phase eingeführten Eisen. Abb. 6 und 7 veranschaulichen die M ö ß b a u e r-Spektren, die für zwei Homopolymeren: Poly(Akrylnitril) (Abb. 5, Kurve *2*) und Polystyrol (Abb. 5, Kurve *3*) spezifisch sind, im Vergleich zu den Spektren einer Testsubstanz (Natriumnitroprussiat (Abb. 6 und 7, Kurve *1*)); Abb. 6 (Kurve *2*) stellt das M ö ß b a u e r-Spektrum des Kopolymeren AN—S dar. Die Aufnahmen zeigen, daß die von scharf umrissenen Peaks dargeleg-

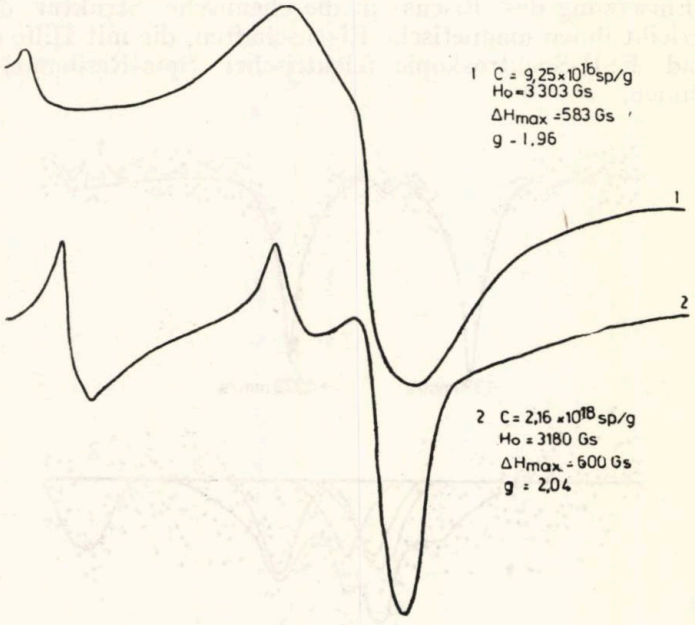

Abb. 6. — M ö ß b a u e r - Spektren von: *1*—Natriumnitroprussiat; *2*—PAN; *3*—PS.

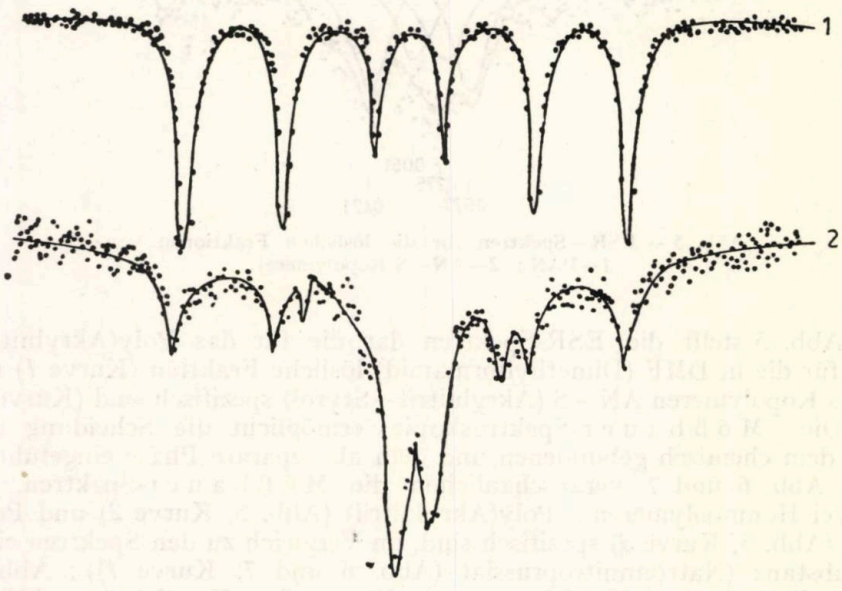

Abb. 7. — M ö ß b a u e r - Spektren von: *1*—Natriumnitroprussiat; *2*—AN—S (Kopolymer).

Tabelle 2

Die Bedingungen unter denen die mechanochemische Synthese, (durch Schwingmahlung), einiger Kopolymeren durchgeführt wurde und einige Charakteristika der letzteren. (Unverändert blieben das Füllungsverhältnis, $\eta = 0{,}5\%$; die Mahldauer, $t = 96$ Stunden; die Temperatur, $T = 18° \pm 2°C$; die Atmosphäre in den Reaktionsgefäßen = inert = gereinigter Stickstoff)

Nr.	Komonomeren gemenge	Komonomerenverhältnis	Konversion %	Rückstand bei Kalzination %	Löslichkeit in DMF %	Elementaranalyse C	H	N
1	Akrylnitril + + Styrol	1 : 1	45*) ***)	6,5	73,5	73,5	6,3	12,9
2	Akrylnitril + + Methyl Styrol	1 : 3	34,9	—	—	—	—	—
		1 : 1	36*) ***)	7,8	4	66,86	6,14	13,03
		3 : 1	48,0			—	—	—
			89,5					
3	Akrylnitril + + Vinylazetat	1 : 1	47,0**) ***	7,5	33,2	54,12	5,91	14,77
		1 : 2	33,99**) ***)	50,5	20,14	29,2	3,27	9,78
		1 : 5	20,21**) ***)	56,0	—	13,48	3,48	3,16
		2 : 1	56,05**) ***)	4,5	2,08	61,68	5,68	20,01
		5 : 1	92,58**) ***)	5,1	10,0	56,62	6,01	19,91
		3 : 1	87,16	—	unlöslich			
		1 : 3	6,1	—	unlöslich			
4	Isopren + + Styrol	1 : 1	20,50	—	—	—	—	—
5	Methylmetaakrylat + Styrol	1 : 1	11,57	—	—	—	—	—
6	Akrylnitril + + Vinylazetat + + Styrol	1 : 1 : 2	19,25	—	55****)			
		2 : 1 : 1	47,6	—	—			

*) $\eta = 0{,}4\%$; **) Mahlkörper mit geringen Abnutzungsgrad ; ***) lösliche Fraktion ; ****) Löslichkeit in Zyklohexanon.

ten maximalen Absorptionen, auf das Vorhandensein des chemisch gebundenen Eisenszurückgeführt werden dürfen, während das eingeschlossene Metall nur in Form von Spuren auftritt. Die ausführliche Auslegung der Mößbauer-Spektren ist unter [9] zu finden.

Auf Grund der experimentellen Daten darf der Gedanke vertreten werden, daß die kinetische Stoßenergie, infolge des Zussammenstoßes der Mahlkörper untereinander und mit den Apparaturwandungen, sich wenigstens teilweise verbraucht, u.zw. bei der Zerstörung der Metallpartikeln und bei der Anregung der Elektronen an den Oberflächenschichten der Metallatome.

Die Zerstörung des Metallgitters befolgt die bekannten Gesetze über die Bildung und Fortpflanzung der Mikroriße, und deren Endergebnis die

Bildung einer neuen Fläche ist. Dieser Effekt wird durch die Korrosionswirkung der dem Polymerisationsprozeß unterworfenen flüssigen Monomeren beschleunigt.

Beim gegenwärtigen Stand der von uns durchgeführten Forschungen dürfen folgende Hypothesen aufgestellt werden, die die Initiierung der Homo- und Kopolymerisation unter den Bedingungen einer Schwingmahlung betreffen:

1. Das flüssige Monomere wird durch Sorption an der Oberfläche des angeregten Metalls zurückbehalten, so daß es die unter der Einwirkung der Stoßenergie labil gewordenen Elektronen leicht übernehmen kann:

$$Me \xrightarrow{M.E.} Me^+ + e^- \qquad CH_2=\underset{\displaystyle R}{\underset{|}{CH}} + e^- \longrightarrow \ddot{C}H_2-\underset{\displaystyle R}{\underset{|}{\dot{C}H}} \quad (I)$$

2. Das Monomere koordiniert an der Oberfläche des fein zerteilten Metalls und bildet einen aktiven Mittelpunkt, der folgende Form aufweist:

$$Me + CH_2=\underset{\displaystyle R}{\underset{|}{CH}} \xrightarrow{M.E.} Me^+\ddot{C}H_2-\underset{\displaystyle R}{\underset{|}{\dot{C}H}} \quad (II)$$

Die Erweiterung der Kette kann an beiden Enden des aktiven Mittelpunktes vorsichgehen, da die Art des Reaktionsmediums den anionischen oder radikalischen Mechanismus anregt:

$$\ddot{C}H_2-\underset{\displaystyle R}{\underset{|}{\dot{C}H}} + CH_2=\underset{\displaystyle R}{\underset{|}{CH}} \longrightarrow \ddot{C}H_2-\underset{\displaystyle R}{\underset{|}{CH}}-CH_2-\underset{\displaystyle R}{\underset{|}{\dot{C}H}} \quad (I)$$

und beziehungsweise

$$Me^+\ddot{C}H_2-\underset{\displaystyle R}{\underset{|}{\dot{C}H}} + CH_2=\underset{\displaystyle R}{\underset{|}{CH}} \rightarrow Me^+\ddot{C}H_2-\underset{\displaystyle R}{\underset{|}{\dot{C}H}} \longrightarrow Me^+\ddot{C}H_2-\underset{\displaystyle R}{\underset{|}{CH}}-CH_2\dot{C}H \quad (II)$$

Der zweite Mechanismus erklärt die chemische Bindung des Metalls in der Polymerestruktur, eine Tatsache, die durch ESR- und M ö ß b a u e r-Spektroskopie bewiesen wurde.

3. Schlußfolgerungen

1. Die mechanische Stoßenergie, die im Verlauf der Schwingmahlung abgegeben wird, kann die Homo- und Kopolymerisation von vinylischen, dienischen und zyklischen Monomeren initiieren.

2. Die Grundfaktoren, die die mechanochemische Homo- und Kopolymerisation bei Raumtemperatur beeinflussen, sind folgende: die mechanischen Umstände (Füllverhältnis, Herstellungsmaterial der Apparatur, Abnutzungsgrad der Reaktionsgefäße und der Mahlkörper u.a.), das Reaktionsmedium (inerte oder aktive Art der Gasatmosphäre, Anwesenheit von Radikalakzeptoren, von Polaragenzien usw.), die chemische Art der an der Reaktion beteiligten Monomeren, die chemische Zusammenstzung des Substrats, wenn Kopolymerisation stattfindet.

3. Die Homo- und Kopolymerisationsreaktionen werden an den Wandungen der Reaktionsgefäße und an der Oberfläche der Mahlkörper katalysiert.

4. Die Aktivierung der Homo- und Kopolymerisation durch Schwingmahlung in einer V_2A-Stahl-Apparatur läßt die chemische Bindung des Eisens in der Struktur der synthetisierten Verbindungen als miteinbegriffen gelten; dieser Sachverhalt, der durch ESR- und Mößbauer-Spektroskopie nachgewiesen wurde, führt eigentlich zur Entstehung von Metallpolymeren.

5. Unter den untersuchten Monomeren hat das Akrylnitril, das an der Polymerisation nicht nur mit der Vinylgruppe, sondern auch mit der dreifachen Bindung —CN teilnimmt, und andererseits das Styrol eine ganz besondere Reaktionsfähigkeit.

Eingegangen am 21. Januar 1980

Technische Hochschule, Jassy,
Lehrstuhl für organische und
makromolekulare Chemie

LITERATURVERZEICHNIS

1. Каргин В. А., Кабанов В. А., Высокомол. соедин., 3, 787 (1961).
2. Баркалов И. М., ДАН СССР, 147, 395 (1962)
3. Barkalov, I. M., J. Polym. Sci, C 16, 2597—2600 (1967).
4. Плате Н. А., Каргин В. А., Прокопенко В. В., Высокомол.соедин., 1, 1714 (1959).
5. Kargin V. A., Kabanov V. A., J. Polym. Sci., 52, 151 (1961).
6. Plate N. A. Kargin V. A., J. Polym. Sci., C, 4 (1963).
7. * * * *Механоэмисся и механохимия твердых тел.* Изд. ИЛИН, Фрунзе, 1974.
8. Плате Н. А., Строганов Л. Б., Высокомол. соедин., А 14, 2 (1972).
9. Vasiliu-Oprea Cl., Avram I., Avram R., Die Angew. Makromol. Chemie, 68, 1 (1978).
10. Simionescu Cr., Vasiliu-Oprea Cl., Negulianu Cl., Europ. Polymer J., 15, 1037 (1979).
11. Vasiliu-Oprea Cl., Popa M., Die Angew. Makromol. Chemie (im Druck).
12. Vasiliu-Oprea Cl., Popa M., Unveröffentliche Daten.

REACŢII DE HOMO- ŞI COPOLIMERIZARE INIŢIATE MECANOCHIMIC PRIN MĂCINARE VIBRATORIE

(Rezumat)

Se studiază sinteza mecanochimică, prin măcinare vibratorie, la temperatura mediului ambiant, a unor homo- şi copolimeri folosind o serie de monomeri vinilici, dienici şi ciclici. Se constată că procesul studiat este influenţat de regimul mecanic aplicat, de natura monomerului, de compoziţia chimică a substratului în cazul copolimerizării, de prezenţa unor acceptori radicalici sau ale unor medii polare.

Polimerii astfel obţinuţi posedă o structură şi proprietăţi particulare ce-i diferenţiază de variantele corespunzătoare sintetizate prin fabricaţia curentă. Unii dintre ei sînt termostabili paramagnetici, prezintă stabilitate chimică avansată şi caracter de semiconductori.

BULETINUL INSTITUTULUI POLITEHNIC DIN IAŞI
Tomul XXVI (XXX), fasc. 1—2, 1980
Secţia III
CHIMIE şi INGINERIE CHIMICĂ

C.D. 677.474:667.64

TEINTURE DES FIBRES MODACRYLIQUES

PAR

ROMEN BUTNARU, GH. ROZMARIN et I. SABIE

Dédié au professeur
Dr. CRISTOFOR SIMIONESCU,
membre de l'Académie,
à l'occasion de son 60-e anniversaire

1. Introduction

Dans la gamme des fibres synthétiques celles polyacryliques ont des capacités mondiales qui atteignent plusieurs centaines de milliers de tonnes, ce qu'on peut attribuer aux qualités supérieures des textiles obtenues, ainsi qu'à l'accessibilité des ressources existantes (méthane, éthylène, acéthylène). Ayant une structure très compacte les fibres polyacryliques opposent une résistance remarquable à la diffusion des colorants. Pour mieux faire face à cet incovenient et favoriser l'affinité tinctoriale des pareilles fibres on fait appel habituellement aux procédés d'incorporation de deux types de produits à caractère d'acide ou de base, en fonction de la nature des colorants cationiques ou anioniques utilisés ultérieurement. Mais l'addition des substances pareilles affaiblit d'une manière plus ou moins efficace l'organisation surmoléculaire des fibres en provoquant, par conséquence, une meilleure accessibilité aux colorants.

C'est ainsi que sont apparues sur le marché mondial les fibres dites *modacryles* ayant un taux de 50 à 85 pour cent d'acrylonitrile [1] et qui gagnent des nouvelles propriétés, à savoir : stabilité dimensionnelle, élasticité accrue, caractéristiques antistatisantes et ignifugeantes, toucher meilleur etc.

Dans ce qui suit on essaye à établir les conditions de teinture des fibres modacryles avec des colorants cationiques.

2. Partie expérimentale

On a utilisé des fibres modacryliques fabriquées à Săvineşti ayant une composition de 72% acrylonitrile et 28% de chlorure de vinylydène (insolubilité totale en acétone). On a considéré les variables ci-dessous: temps de teinture, concentration en colorant, rapport de bain et température. La recette de teinture utilisée était la suivante: X (%) colorant cationique (Jaune mélacryle G4) ; 2% Magycryle (égalisateur cationique) ; 2% acétate de sodium ; 15% sulfate de sodium, 0,5% acide acétique (pH = =4,5). La qualité de la teinture était contrôlée par dosage du rendement de fixage du colorant par les fibres, en déterminant les concentrations dans le bain de teinture et, ensuite, dans le bain épuisé.

Les conditions de teinture ont été fixées conformément à un plan expérimental, en utilisant la méthode de la régression multiple. Puisqu'on ne connaît rien quant au comportement des fibres modacryliques pendant la teinture aux colorants cations, on a choisi les conditions proches connues pour les polyacrylonitriles. La méthode du planning expérimental [2] a

indiqué, pour les quatre variables considérées, un nombre de 31 expériences, codifiées conformément au tableau 1 et détaillées dans le tableau 2.

Tableau 1

Codification des paramètres

Paramètres \ Code	−2	−1	0	+1	+2
x_1 — temps de teinture, [min.]	30	45	60	75	90
x_2 — concentration du colorant par rapport aux fibres, [%]	1	2	3	4	5
x_3 — rapport de bain	1 : 20	1 : 35	1 : 50	1 : 65	1 : 80
x_4 — température, [°C]	86	89	92	95	98

Tableau 2

Le planning des expériences et les résultats obtenus

No. des expériences	x_1	x_2	x_3	x_4	Rendement de fixage %
1	−1	−1	−1	−1	50
2	+1	−1	−1	−1	27
3	−1	+1	−1	−1	30
4	+1	+1	−1	−1	80
5	−1	−1	+1	−1	59
6	+1	−1	+1	−1	19
7	−1	+1	+1	−1	28
8	+1	+1	+1	−1	25
9	−1	−1	−1	+1	55
10	+1	−1	−1	+1	60,4
11	−1	+1	−1	+1	24
12	+1	+1	−1	+1	45
13	−1	−1	+1	+1	56
14	+1	−1	+1	+1	60
15	−1	+1	+1	+1	42,5
16	+1	+1	+1	+1	83
17	−2	0	0	0	9
18	+2	0	0	0	48
19	0	−2	0	0	31
20	0	+2	0	0	34
21	0	0	−2	0	38
22	0	0	+2	0	50
23	0	0	0	−2	36
24	0	0	0	+2	43
25	0	0	0	0	41
26	0	0	0	0	64
27	0	0	0	0	48
28	0	0	0	0	63
29	0	0	0	0	64
30	0	0	0	0	63
31	0	0	0	0	63

On a calculé les coefficients de régression, on les a testé et on a éliminé les cofficients non significatifs, ce qui a fourni une équation qui représente le modèle mathématique du processus de la teinture du modacryle avec des colorants cations (η—rendement de fixage du colorant):

$$\eta = 58 + 2{,}27\, x_1 + 4{,}47\, x_4 - 5{,}37\, x_1^2 - 4{,}36\, x_2^2 - 2{,}62\, x_4^2 + 10{,}15\, x_1 x_2 - \\ - 3{,}21\, x_1 x_3 + 5{,}4\, x_1 x_4 - 2{,}78\, x_2 x_4 + 7{,}09\, x_3 x_4.$$

Dans la fig. 1 on a représenté la variation du rendement par rapport à chacun des paramètres étudiés, les autres étant maintenus constants dans le centre du domaine expérimental.

Il s'avère que le rendement est une fonction directe de x_1, x_2 et x_4, mais n'en dépend d'aucun façon du rapport de bain choisi. Pour les autres trois paramètres variables le rendement augmente, passe par un maximum, après quoi il est en baisse. C'est ainsi que les valeurs maxima du rendement se situent à proximité du centre même du domaine expérimental choisi, c'est-à-dire à 63 min. (temps), 3% (colorant) et 94,5°C (température). Un

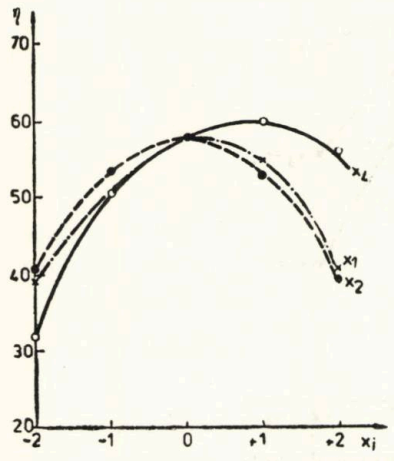

Fig. 1. — Variation du rendement de fixage du colorant avec les paramètres étudiés.

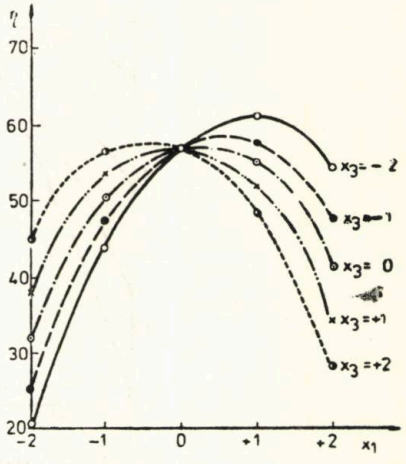

Fig. 2. — Variation du rendement de fixation du colorant avec le temps de teinture et le rapport de bain.

comportement pareil des fibres modacryles pendant la teinture peut être expliqué soit par une saturation en colorant, soit par une décomposition thermique des groupements $-NaSO_3$ intervennant pour une durée qui dépasse 60 min. Il faut y ajouter encore que, pour des concentrations plus fortes en colorant, les cations du celui-ci peuvent s'associer grâce aux mouvements cinétiques et provoquer par cette voie une diminution de la diffusion des particules dans la structure des fibres.

On peut observer que le rendement n'en dépend pas du rapport de bain adopté, mais, en même temps, ont lieu des interactions entre les paramètres x_1 et x_3 ou entre x_4 et x_3. Par conséquent on a étudié la variation

du rendement par rapport à x_1 et x_4 en imposant pour x_3 des diverses valeurs (v. les fig. 2 et 3).

L'allure des courbes n'en change guère, c'est-à-dire qu'elles accusent aussi des maxima. Pour un temps de teinture de 60 min. le rendement devient maximum après quoi il diminue d'autant plus que la décomposition des groupes $-NaSO_3$ est plus intense [3]. Le rendement est en baisse encore quand les rapports de bains sont petits, alors que pour des valeurs plus grandes du rapport de bain le rendement augmente avec la température. Ceci est expliquable compte tenu que pour des petits rapports la concentration du colorant dans le bain est d'autant plus grande, ce qui favorise l'associa-

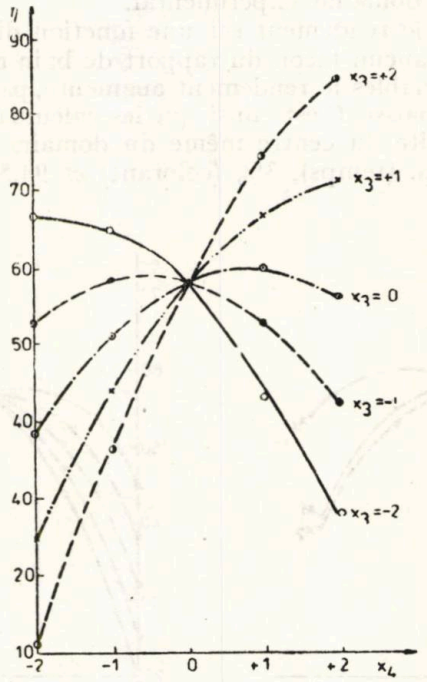

Fig. 3. — Variation du fixage du colorant avec la température et le rapport de bain.

tion des cations et affaiblit la vitesse de diffusion des particules dans les fibres. Par contre, pour des rapports de bain élevés la concentration du colorant diminue tout aussi que les possibilités d'association des particules, ce qui rend très probable une pénétration plus accrue des cations du colorant dans la structure des fibres teintées.

3. Conclusions

1. On a étudié la variation du rendement de fixage du colorant pendant la teinture des fibres modacryliques en utilisant la méthode de la régression multiple.

2. Le fixage du colorant n'en dépend pas directement des valeurs du rapport de bain, mais seulement de la durée, de la concentration du colorant et de la température du processus.

3. Le rapport de bain influence indirectement le fixage en corrélation avec le temps et la température.

4. Les valeurs maxima du rendement de fixage se situent à 63 min. pour le temps, 3% pour la concentration du colorant et à la temperature de 945°C.

5. Le comportement des fibres modacryles à la teinture avec des colorants cationiques est analogue à celui des fibres polyacrylonitriles à l'exception de la température qui est un peu moindre (94,5° contre 98°C).

Reçue le 7 février 1980

Institut Polytechnique, Jassy,
Chaire de Chimie Organique
et Macromoléculaire

BIBLIOGRAPHIE

1. Nistor A., Ind. text. 22, *1*, 15—18 (1971).
2. Cox W., *Experimental Design.* J. Wiley, New York, London, 1968.
3. Grindea M., *Tehnologia vopsirii şi imprimării textilelor.* EDP, Buc., 1968.

VOPSIREA FIBRELOR MODACRILICE

(Rezumat)

S-a studiat variaţia randamentului la vopsirea fibrelor modacrilice cu coloranţi cationici utilizînd metoda regresiei multiple. S-a ajuns la concluzia că randamentul nu depinde în mod direct de hidromodul, ci numai de durată, concentraţia colorantului şi temperatură. Hidromodulul influenţează în mod indirect randamentul prin interacţiunea cu durata şi temperatura.

Randamentul de vopsire prezintă maxime pentru durata de 63 min, 3% colorant şi la o temperatură de 94,5°C. Comportarea fibrelor modacrilice la vopsire cu coloranţi cationici este asemănătoare în ansamblu cu cea a fibrelor poliacrilonitrilice cu excepţia temperaturii care este mai scăzută la cele modacrilice (94,5° faţă de 98°C).

BULETINUL INSTITUTULUI POLITEHNIC DIN IAŞI
Tomul XXVI (XXX), fasc. 1—2, 1980
Secţia II
CHIMIE şi INGINERIE CHIMICĂ

D.K. 541.18.048

BETRACHTUNGEN ÜBER DIE BESTIMMUNG DER KOAGULATIONS-DOSIS DURCH DEN JARR-TEST

VON

V. COCHECI und GH. PETCA

Herrn Professor
Dr. CRISTOFOR SIMIONESCU,
Mitglied der Akademie,
zum 60. Geburtstag gewidmet

1. Die Koagulierung bei Wasserreinigungen ist heute ein unumgänglicher und wichtiger Prozeß. Bei ihrer Anwendung spielt die optimale Dosierung des Koagulierungsmittels eine äusserst wichtige Rolle. Für diese Dosierung wurden Labormethoden ausgearbeitet und auch mathematische Gleichungen bestimmt die es erlaubten auf Grund von charakterischen Kenngrößen des Wassers die optimale Dosierung zu berechnen [1]. Zur Zeit ist der Jarr-Test jedoch die dafür am meisten verwendete Methode. Grundsätzlicher beruht diese Methode auf Koagulationsversuche mit unterschiedlicher Dosierung des Koagulationsmittels. Die Wasserproben werden dabei einheitlich behandelt, wobei, für die Verteilung des Koagulanten, ein schnelles Rühren von einigen Minuten und darauf ein langsames, von einigen zehn Minuten vorangeht. Aus der verbliebenen Wassertrübung der Proben, wird darauf die entsprechende Dosierung, für die vorausgesetzte remanente Trübung, bestimmt.

Zu den, für Industriewasserbehandlungen, am meist verwendeten Koagulationsmittel zählt in erster Reihe das Fe (II)-Sulfat. Meistens wird es zusammen mit Kalk als Alkalisationsmittel verwendet, wobei der optimale pH-Wert bei der Verwendung von Eisensulfat als Koagulationsmittel bei 8,5 · · ·9 liegt und bei einer gleichzeitigen Dekarbonatierung den Wert von 10,5 erreichen kann.

Bei diesen pH-Bedingungen kann mit der Koagulierung ein gleichzeitiges Ausscheiden des Kalziumkarbonats, stattfinden. Findet das Ausscheiden des Kalziumkarbonats während des Abklärungsprozeßes statt, kann, durch die kleine Absetzungsgeschwindigkeit des fein verteilten Kalziumkarbonats, die dadurch entstehende Trübung des Wassers die Wirksamkeit des eigentlichen Koagulationsprozeßes, denaturieren.

In der von uns ausgeführten Arbeit, verfolgten wir die Bestimmung der optimalen Bedingungen für die Durchführung des Jarr- Testes für Eisensulfat als Koagulierungs- und Kalk als Alkalisationsmittel, wobei der Niederschlag des Kalziumkarbonats entweder vermieden wird oder während der langsamen Rührung stattfindet.

2. Das gleichzeitige Vorhandensein von CO_2 und CaO im Wasser ist nur in einem bestimmten Konzentrationsbereich möglich der von den Kenngrößen, die das Gleichgewicht des $CaO-CO_2-H_2O$ Systems bestimmen, begrenzt ist [2]...[4]. Die Debikarbonatierung des Wassers mit Kalziumhydroxid finden in zwei Phasen statt:

1. Die Beifügung von $Ca(OH)_2$ die eine Verschiebung des Systems in einem unbeständigem Zustand zur Folge hat und sich durch eine Übersättigung an $CaCO_3$ kennzeichnet.

2. Das Übergehen des mit $CaCO_3$ übersättigtem Systems aus dem unbeständigen in einem beständigem Gleichgewichtzustand, durch die Fällung des $CaCO_3$.

Praktisch setzt die erste Phase einerseits, die Bestimmung des optimalen Kalkgehaltes, der dem System zugefügt wird, voraus, anderseits die Bestimmung des Parameters der eindeutig festlegt ob die zugefügte $Ca(OH)_2$-Menge die optimale ist.

Für die Kennzeichnung des Debikarbonatierungsprozeßes werden folgende Größen verwendet: die mit Methylorange bestimmte Alkalinität (m), die mit Phenolphthalein bestimmte Alkalinität (p), der pH-Wert und die ($2p-m$)-Größe.

Findet die Debikarbonatierung des Wassers gleichzeitig mit dem Koagulierungsprozeß statt, so ist der pH-Wert von größter Bedeutung. Im Falle des theoretischen Systems $CaO-CO_2-H_2O$, kann man den optimalen pH-Wert durch die Gleichungen (1)...(5) bestimmen, die das Gleichgewicht im $CaO-CO_2-H_2O$ System definieren:

$$(1) \qquad H^+ + OH^- \rightleftharpoons H_2O, \quad K_w = [H^+]\,[OH^-] = 10^{-14};$$

$$(1') \qquad CO_{2aq} + H_2O \rightleftharpoons H_2CO_3, \quad K = [CO_{2aq}]/[H_2CO_3] = 600;$$

$$(1'') \qquad H_2CO_3 \rightleftharpoons H^+ + HCO_3^-, \quad K_a = [H^+]\,[HCO_3^-]/[H_2CO_3] = 2{,}5.10^{-4};$$

$$(2) \qquad HCO_3^- \rightleftharpoons H^+ + CO_3^{2-}, \quad K_2 = [H^+]\,[CO_3^{2-}]/[HCO_3^-] = 4{,}7.10^{-11}.$$

Zur Vereinfachung geht aus (1') und (1'') hervor:

$$K_1 = [H^+][HCO_3^-]/[H_2CO_3] + [CO_{2aq}] \text{ weil } [CO_{aq}] \gg [H_2CO_3]$$

haben wir:

$$(3) \qquad K_1 = [H^+]\,[HCO_3^-]/[CO_{2aq}] = 4{,}45.10^{-7}.$$

Für das theoretische System gilt die Elektroneutralitätsgleichung:

$$(4) \qquad 2[Ca^{2+}] + [H^+] = [HCO_3^-] + 2[CO_3^{2-}] + [OH^-].$$

Das Löslichkeitsprodukt des $CaCO_3$, bei 25°C, ist:

$$(5) \qquad L = [Ca^{2+}][CO_3^{2-}] = 0{,}9.10^{-8}.$$

Der optimale Debicarbonatierungs-pH-Wert des theoretischen Systems, der auf Grund der Gleichungen (1)...(5) berechnet wurde, hat den Wert 10.

Die natürlichen Gewässer enthalten ausser Ca^{2+} auch andere Kationen und ausser Bikarbonaten auch Anionen von starken Säuren. Aus diesem Grund wird zur Berechnung des optimalen pH-Wertes Ca^{2+} mit $[Ca^{2+}] - [Ca_n^{2+}]$ in der Gleichung (4) ersetzt, wobei $[Ca_n^{2+}]$ die molare Konzentration der Kalziumionen darstellt, die an Anionen der starken Säuren gebunden sind. $[Ca_n^{2+}]$ wird von folgender Gleichung bestimmt:

$$(6) \qquad [Ca_n^{2+}] = [Ca^{2+}] - \frac{1}{2}.10^{-3}m.$$

Unter diesen Bedingungen nimmt die Gleichung (4) das Form:

$$(7) \qquad 2([Ca^{2+}] - [Ca_n^{2+}]) = 2[CO_3^{2-}] + [HCO_3^-] + [OH^-] - [H^+].$$

Durch die Anwendung der Gleichung (7) an Stelle von Gleichung (4), kann man der pH-Wert für eine optimale Debikarbonatierung in Abhängigkeit von $[Ca_n^{2+}]$ berechnen. Diese Abhängigkeit wird in Abb. 1 dargestellt

Aus Abb. 1 ist ersichtlich daß, wenn $[Ca_n^{2+}]<0$, dann ist der optimale pH-Wert >10, und wenn $[Ca_n^{2+}]>0$ fällt der optimale pH-Wert unter 10. Daraus folgt das der pH-Wert des Wassers nicht eindeutig die optimale Menge von $Ca(OH)_2$ bestimmen kann. Aus den Gleichungen (1)...(7) folgt, daß die einzige Größe die eindeutig die optimale Menge von $Ca(OH)_2$ bestimmt, $2p-m$ ist. Die vorhandene Hydroxydmenge ist optimal, wenn $2p-m=0$.

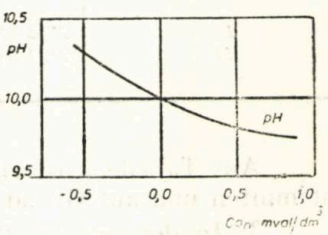

Abb. 1. — Die Veränderlichkeit des optimalen Debikarbonatierung-pH-Wertes in Abhängigkeit von $[Ca_n^{2-}]$.

Die zur Debikarbonatierung nötige $Ca(OH)_2$-Menge hängt von dem Bikarbonatgehalt, von CO_2, von der Eisensulfatdosis (d_{Fe}), sowie von dem $(d_{Ca}+d_{Fe})/d_{tp}$ Verhältnis ab, wobei d_{Ca} die vom Kalziumion bestimmte Härte des Wassers dargestellt und d_{tp} die zeitliche Härte ist.

Die CaO-Menge kann auch auf Grund folgender empirischer Gleichungen berechnet werden:

a) wenn $d_{tp}>d_{Ca}+d_{Fe}$, dann:

$$M_{CaO}=28\,(d_{tp}+d_{Fe}+C)\,; \tag{8}$$

b) im Falle $d_{tp}=d_{Ca}+d_{Fe}$,

$$M_{CaO}=28(d_{Ca}+d_{Fe}+C)+19{,}2\,; \tag{9}$$

c) wenn $d_{tp}<d_{Ca}+d_{Fe}$,

$$M_{CaO}=28(d_{tp}+d_{Fe}+d_{Mg}-d_p+C)+19{,}2, \tag{10}$$

worin: M_{CaO} — nötige CaO-Menge, [g/m³ Wasser); d_{tp} — zeitliche Härte [mval/dm³], C — CO_2-Konzentration, [mval/dm³], d_p — dauernde Härte [mval/dm³], d_{Fe} — Koagulierungsdosis, [mval/dm³]; d_{Mg} — Magnesiumgehalt im Wasser, [mval/dm³].

Für die Überprüfung der Gleichungen wurde die Kalkdosis, für zwei Wasserproben deren Kenngrößen in der Tabelle 1 wiedergegeben sind, experimentell bestimmt. Die berechneten und experimentell bestimmten Mengen der Kalkdosis sind in Tabelle 2 wiedergegeben.

Tabelle 1

Probe	m	Ca^{2+}	CO_2	Fe^{2+}
	mval/dm³			
1	2,65	2,6	0,2	0,25
2	1,38	1,2	0,35	0,25

Tabelle 2

Probe	Berechnete Dosis	experim. berechnete CaO-Dosis
	g CaO/m³	
I	28(2,65+0,25+0,2)=86,8	85
II	28(1,28+0,25+0,35)=54,5	56,5

Aus Tabelle 2 ist eine gute übereinstimmung der experimentell bestimmten und auf Grund der Gleichung (8) berechneten Werte, zu ersehen.

3. In der zweiten Phase des Debikarbonatierungsprozeßes wird das $CaCO_3$ ausgefällt. Dieser Prozeß stellt formell eine Reaktion II. Grades dar [5]. Die durchgeführten Unternehmungen zur Bestimmung der Geschwindigkeitskonstanten haben, da beim Ausfällen von $CaCO_3$ eine Induktionszeit vorhanden ist, zu großen Abweichungen bei kurzen Reaktionszeiten geführt. Die Keimbildungs- und die Wachstumsgeschwindigkeit ist bestimmend in diesem Prozeß [5].

Als bestimmende Zustandsgrößen für die Ausfällungsgeschwindigkeit wird die Differenz zwischen der Konzentration des $[\Delta Ca^{2+}]$ in der übersättigten Lösung und seiner Gleichgewichtskonzentration angesehen:

$$\frac{dc}{dt} = K[\Delta Ca^{2+}]^n \quad (11)$$

Wie Dieter und Heinrich zeigen [5], erklärt die Gleichung (11) nicht alle bei der Ausfällung von $CaCO_3$ bemerkten Erscheinungen. Sie haben eine neue Gleichung zur Bestimmung der Kristallisierungsgeschwindigkeit von $CaCO_3$ festgelegt und zwar;

$$\frac{dc}{dt} = K\Omega^q[\Delta Ca^{2+}]^n, \quad (12)$$

wobei: Ω — die zur Ausfällung zur Verfügung stehende Oberfläche der $CaCO_3$-Kristalle; n — von dem Zustand des Prozeßes abhängiger Kennwert.

Zur Bestätigung des vorher gezeigten, wurde experimentell die Abhängigkeit der Endtrübung in Abhängigkeit vom pH-Wert verfolgt. Der pH-Wert hängt von der zugefügten CaO-Menge ab. Die Versuche wurden an einem Wasser mit folgendem Hauptkennwerten durchgeführt: $m=2,7$ mval/dm³; $d_{Ca}=2,65$ mval/dm³; $d_{Mg}=0,6$; $T°=120°SiO_2$.

Die zugeführte Koagulierungsdosis war 20 mg Fe^{2+}/dm³. Für die Erhaltung eines bestimmten pH-Wertes wurde $Ca(OH)_2$ beigefügt, wobei die Konzentration vom Ca^{2+} im Wasser verändert wurde. Die Bedingungen des Jarr-Testes waren folgende: 2 Min. rasches Rühren, 10 Min. langsames Rühren und 30 Min. Zeit zum Absetzen. Es wurden konische 500 ml Behälter benützt. Die Veränderung der Trübung in Abhängigkeit vom pH-Wert ist in der Abb. 2 wiedergegeben.

Tabelle 3

Probe	Kalkdosis mval/dm³	pH	$T°$ restlich °SiO_2	P	m mval/dm³	$2p-m$
1	—	8,28	9,80	—	—	—
2	—	8,53	7,40	—	—	—
3	—	9,10	4,35	—	—	—
4	1,2	9,34	4,25	0,38	2,44	−1,68
5	1,6	9,42	6,25	0,42	2,04	−1,22
6	2,0	9,45	11,00	0,44	1,58	−0,70
7	2,5	9,55	13,50	0,49	1,44	−0,16
8	3,0	10,50	11,00	0,96	1,43	0,55

Aus Abb. 2 geht hervor dass im pH-Bereich von 8,25...9 und von 9,6...10,5 die Trübung des Wassers abfällt, während sie im pH-Bereich 9...9,6 ansteigt.

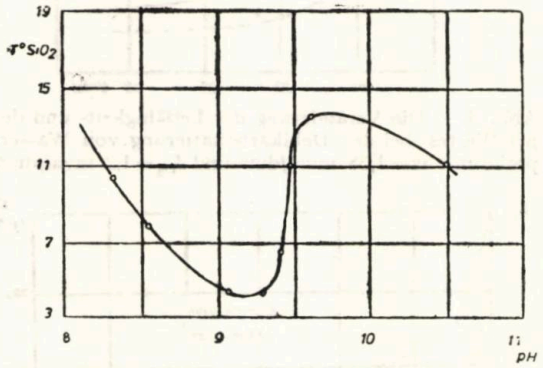

Abb. 2.—Die Veränderung der Trübung in Abhängigkeit von pH-Wert.

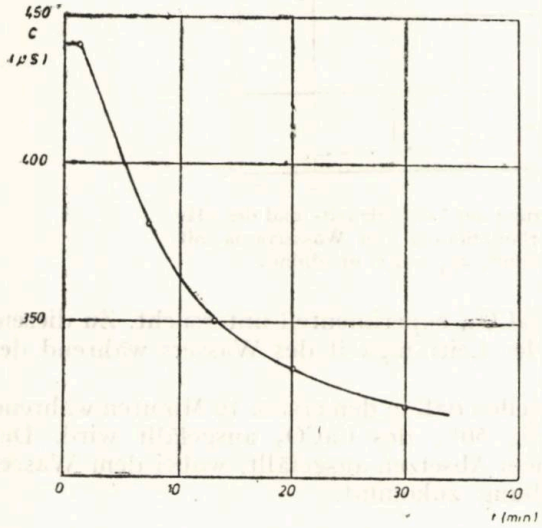

Abb. 3. — Die Veränderung der Leitfähigkeit mit der Zeit bei der optimalen CaO-Dosis.

Aus Tabelle 3 geht hervor, daß die optimale Dosis von CaO 2,65 mval/ /dm³ ist. Bei dieser Dosis ist die Trübung ausgeprägt. Das gleichzeitige Ansteigen der Trübung mit dem pH-Wert wird vom Ausfällen des $CaCO_3$, während der Absetzung bewirkt. Um diese Tatsache zu bestätigen wurde

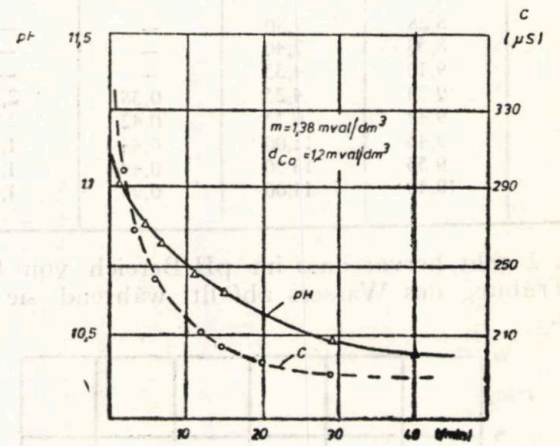

Abb. 4. — Die Veränderung der Leifähigkeit- und des pH-Wertes bei der Debikarbonatierung von Wasserprobe mit $m = 1{,}38$ mval/dm³ und $d_{Ca} = 1{,}2$ mval/dm³.

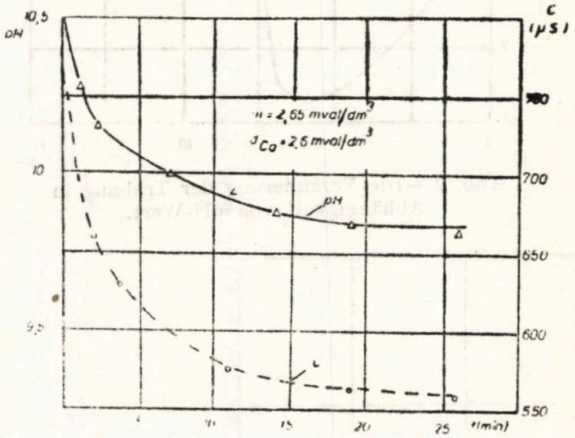

Abb. 5. — Die Veränderung der Leitfähigkeit- und des pH-Wertes bei der Debikarbonatierung von Wasserprobe mit $m = 2{,}65$ mval/dm³, $d_{Ca} = 2{,}6$ mval/dm³.

die Kinetik des Ausfällens von $CaCO_3$, experimentell untersucht. Zu diesem Zweck wurde die Veränderung der Leitfähigkeit des Wassers während des Koagulierungsprozeßes verfolgt.

Aus Abb. 3 kann man feststellen daß in den ersten 10 Minuten während dem langsamen Rühren beiläufig 50% des $CaCO_3$ ausgefällt wird. Der Rest des $CaCO_3$ wird während dem Absetzen ausgefällt, wobei dem Wasser eine größere rückständige Trübung zukommt.

Aus der Gleichung geht hervor, daß die Ausfällungsgeschwindigkeit des $CaCO_3$ von der Anfangskonzentration der Ca^{2+} im Wasser abhängig ist. In den Abb. 4 und 5 ist die Veränderung der Leitfähigkeit- und des pH-Wertes bei der Debikarbonatierung von zwei Wasserproben wiedergegeben, deren Kennwerte in Tabelle 1 angegeben wurde.

Es wurde mit optimalen CaO-Mengen, die in der Tabelle 2 angegeben sind, gearbeitet. Die Probe *1* entspricht einem Wasser mit einem großen Ca^{2+}-Gehalt, während Probe *2* einem kleinen Ca^{2+}-Gehalt entspricht. In beiden Fällen war, die zur Debikarbonatierung nötige Zeit, 20 Min.

Wie zu erwarten war, ist, im Einklang mit der Gleichung (12), die Debikarbonatierungszeit für Wasser mit einem kleinen Ca^{2+}-Gehalt, größer.

Diese Feststellungen suggerieren die Notwendigkeit bei der Ausführung des J a r r-Testes in unserem Fall, die Rührzeit zu verlängern.

Die experimentelle Festlegung der Rührzeit, welche von den Kennwerten des Wassers abhängt, benötigt eine stete Bestimmung des pH-Wertes und der Leitfähigkeit. Diese Tatsache würde jedoch die Schnelligkeit des J a r r-Testes für die Bestimmung der Koagulantdosis beeinträchtigen.

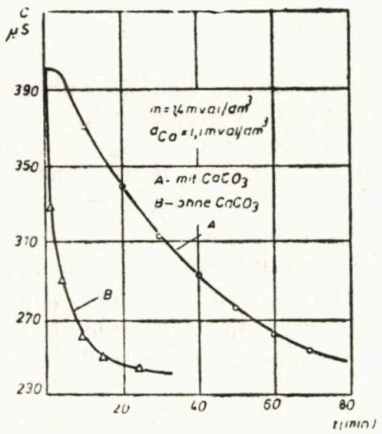

Abb. 6. — Die Veränderung der Leitfähigkeit in der Zeit, ohne (Kurve *A*) und mit Beifügung von (Kurve *B*) $CaCO_3$.

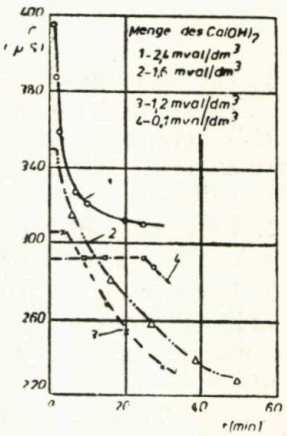

Abb. 7. — Die Veränderungskurven der Leitfähigkeit in der Zeit.

4. Aus der Gl. (12) geht hervor daß die Ausfällungsgeschwindigkeit des $CaCO_3$, auch von seiner aktiven Kristallisierungsoberfläche abhängig ist. Davon ausgehend, wurde experimentell der Einfluß kleiner $CaCO_3$-Mengen (20 mg $CaCO_3/dm^3$) bestimmt.

Aus Abb. 6 geht hervor, daß kleine Mengen von $CaCO_3$ die Ausfällungszeit viel verringern, wobei die Schnelligkeit des J a r r-Testes vergrößert wird.

Entsprechend der Gl. (6) kann man dieselbe Wirkung auch durch einen Überschuß des Reaktionsmittels erziellen. Wie aus der Abb. 7 hervor-

geht (Kurve *1*) erzielt man bei der Steigerung der CCO-Dosis um 50%, im Vergleich zur optimalen, eine Verringerung der Fällungszeit von 30 Min. auf 10 Min. Diese Arbeitsweise ist jedoch nicht angebracht, da der hohe pH-Wert die Koagulierungsbedingungen beeinträchtigt.

Auch in Abb. 7 sind die Veränderungskurven der Leitfähigkeit bei einem kleineren CaO-Gehalt als der optimale, gezeigt (Kurven *3*, *4*). Man stellt fest, daß die Induktionszeit, die dem waagerechten Abschnitt auf der Verlängerungskurve der Leitfähigkeit in der Zeit entspricht, mit dem Fallen der CaO-Dosis steigt. Die Induktionszeiten sind jedoch nicht nur von der beigefügten CaO-Menge (gleichzeitig vom pH) sondern auch vom Ca^{2+}-Gehalt im nichtbehandelten Wasser, abhängig. Dem in Abb. 7 beschriebenen Fall entspricht eine Induktionszeit von 25 Min. wobei das Wasser folgende Merkmale hat : $m=1{,}2$ mval/dm^3 ; $d_{Ca}=1{,}15$ mval/dm^3. Es wurde bei einem pH=9,2 gearbeitet.

Wenn der Koagulierungsprozeß ohne eine Debikarbonierung durchgeführt wird, kann der J a r r-Test, auf Grund der Induktionszeiten, ohne das Ausfällen des $CaCO_3$, nur an einem pH-Wert $<8{,}5$ durchgeführt werden.

Schlußfolgerungen

1. Bei der Bestimmung der Fe(II)-Sulfat-Dosis, anhand des J a r r-Testes, stellt man, wenn der Koagulationsprozeß gleichzeitig mit der Debikarbonatierung stattfindet, ein Ausfällen des $CaCO_3$ während der Absetzung, fest. Das so ausgefällte $CaCO_3$ versetzt dem Wasser eine Trübung, die die richtigen Ergebnisse der Koagulierung beeinträchtigen.

2. Es wurden die Arbeitsbedingungen des J a r r-Testes festgelegt, die das Ausfällen von $CaCO_3$ umgehen oder beim langsamen Rühren sichern.

3. Der optimale pH-Wert der Dikarbonatierung ist von dem Ca^{2+}-Wert abhängig und kann somit nicht eindeutig die optimale CaO-Dosis bestimmen. Die einzige Zustandsgröße, die eindeutig die richtige Dosierung des CaO nachprüft, ist die Größe $2p-m$.

4. Um die Verfälschung der Koagulierungsergebnisse, gegeben von der Resttrübung, welche von der Ausfällung des $CaCO_3$ verursacht ist, zu umgehen, ist eine Verlängerung der langsamen Rührungszeit, die sich experimentell durch Verfolgen der Änderung der Leitfähigkeit oder des pH-Wertes, bestimmen läßt.

5. Die Schnelligkeit des Verfahrens kann erhöht werden, indem die Rührungszeit durch Beifügen einer kleinen Menge ausgefälltem $CaCO_3$ verkleinert wird.

6. Findet der Koagulierungsprozeß ohne die Debikarbonatierung des Wassers statt, so darf der pH-Wert nicht über 8,5 erhöht werden, ansonsten besteht die Gefahr daß das $CaCO_3$ ausfällt, besonders im Falle eines Wassers mit einem hohen Gehalt an Ca-Ionen.

Eingegangen, am 8. Januar 1980

Technische Hochschule „Tr. Vuia", Timișoara

LITERATURVERZEICHNIS

1. Cocheci V., Rev. de Chimie, *1* (1972).
2. Grolster H., Chem. Ing. Tehn., **32**, 667 (1960).
3. Thomas J. F., Trussell R. R., Jawwa, **62**, *4*, 245 (1970).
4. Stumm W., Morgan J.J., *Aquatic Chemistry*. Willey-Interscience, 1970.
5. Dieter H., Wasser-Abwasser, **38**, *110*, 1057 (1969).
6. Held H. D., *Kühlwasser*. Vulcan-Verlag, Dr. W. Calsen, Essen, *1970*.

CONSIDERAŢII REFERITOARE LA DETERMINAREA DOZEI DE COAGULARE PRIN JARR-TEST

(Rezumat)

La determinarea dozei de sulfat feros prin Jarr-Test, în cazul cînd coagularea are loc concomitent cu debicarbonatarea apei, se constată precipitarea carbonatului de calciu în timpul decantării. Carbonatul de calciu astfel precipitat conferă apei o anumită turbiditate reziduală, care denaturează rezultatele coagulării. Se stabilesc condiţiile de desfăşurare a Jarr-Testului astfel încît fie că se evită precipitarea $CaCO_3$, fie că se realizează precipitarea $CaCO_3$ în timpul agitării lente.

BULETINUL INSTITUTULUI POLITEHNIC DIN IAŞI
Tomul XXVI (XXX), fasc. 1—2, 1980
Secţia II
CHIMIE şi INGINERIE CHIMICĂ

C.D. 66.069

MINIMUM D'EPAISSEUR POUR L'ÉCOULEMENT DES LIQUIDES NON-NEWTONIENS EN FILM MINCE

I. THÉORIE

PAR

CRISTIAN ZĂINESCU et RADU Z. TUDOSE

Dédié au professeur
Dr. CRISTOFOR SIMIONESCU,
membre de l'Académie,
a l'occasion de son 60-e anniversaire

1. Introduction

Un film liquide mince peut être maintenu continu sur une surface seulement si son épaisseur dépasse une certaine valeur critique. Au dessous de cette valeur se produit une division du film en ruisselets, l'écoulement offrant ensuite une image assez chaotique. La formation des ruisselets dans l'équipement de l'industrie chimique étant d'habitude un phénomène indésirable, ce qui intéresse c'est la déduction des conditions et des limites de la division des films continus. La question de l'écoulement minimal, restreinte à l'écoulement se déroulant au long des surfaces nonachuffées, a été abordée théoriquement de deux manières.

Un premier groupe d'études a fait usage de la théorie classique de la stabilité linéaire. Le travail de Anshus et Ruckenstein en est exemple [1]. Analysant les conditions d'amplification ou d'amortissement de la perturbation, la théorie linéaire ne peut pas offrir d'informations sur le mécanisme du ruissellement ou sur la géométrie des ruisselets issus. Aussi, un paramètre très important du phénomène — l'angle de mouillage — n'intervient pas dans cette théorie.

La méthode basée sur l'équilibre énergétique forme l'objet du deuxième groupe d'études dont le passage en revue a été fait par Mikielewicz et Moszynski [2]. Les auteurs présentent aussi une analyse de l'écoulement minimal des films minces newtoniens. L'analyse se base sur le développement de deux idées essentiellles à savoir, la première, assumée par Hobler [3], considère que le ruissellement se produit si l'énergie du film, en configuration divisée, présente un minimum local. La deuxième, formulée pour la première fois par Bankoff [4], considère qu'un film vertical se divise initialement en ruisselets à section en forme de segment de cercle, correspondant à une tension superficielle constante.

Dans ce qui suit on propose une extension de l'analyse de Mikielewicz et Moszynski pour le cas des films non-newtoniens pseudoplastiques.

2. Analyse

On considère l'écoulement minimal, mais totalement développé, isotherme et purement gravité d'un film liquide pseudoplastique obéissant à la loi de l'énergie ;

$$\tau = K\dot{\gamma}^n,$$

où K représente la consistance du liquide et n l'indice d'écoulement. Le mouvement se produit au long d'un plan vertical et lisse, auquel on associe

un système d'axes de coordonnées rectangulaires (Fig. 1). L'écoulement est stable, laminaire et les vagues superficielles sont absentes de sorte que le film a une épaisseur constante δ_0 et le profil de vitesse s'exprime par [5] :

$$w_f = w(y) = -\left(\frac{\rho g}{k}\right)^{\frac{1}{n}}\left(\frac{n}{n+1}\, y^{\frac{n+1}{n}} - \delta_0 y^{\frac{1}{n}}\right), \tag{1}$$

où ρ est la densité du liquide et g—l'accélération gravitationnelle.

On considère ensuite le même écoulement, mais en ruisselets. La forme d'un ruisselet est obtenue à l'aide de la formule de Laplace:

$$p_L - p_G = \frac{\sigma_{LG}}{R}.$$

Ici p_L et p_G représentent les pressions dans la phase liquide et celle gazeuse, R—le rayon de courbure de la surface de séparation entre les deux phases et $\sigma_{LG} = \sigma$—la tension superficielle du liquide. L'écoulement étant isotherme, la tension superficielle est constante. La pression de la phase gazeuse est aussi constante et celle de la phase liquide ne diffère, elle non plus, dans la section du ruisselet. Il en résulte que le rayon de courbure doit être lui aussi constant, c'est-à-dire le ruisselet aura la forme d'un segment de cercle ayant l'angle de mouillage $2\theta_0$, θ_0 étant l'angle de mouillage de la surface-support.

En ce qui concerne le profil de vitesse, on suppose la section du ruisselet divisée en bandes longitudinales étroites de sorte que chaque bande ait une largeur constante dx et une hauteur variable $\delta(x)$(Fig. 2). On admet que le profil de vitesse en chaque bande est le même que celui d'un film continu d'épaisseur $\delta(x)$. Donc, pour un ruisselet il en résulte :

$$w_s = w(x, y) = -\left(\frac{\rho g}{k}\right)^{\frac{1}{n}}\left(\frac{n}{n+1}\, y^{\frac{n+1}{n}} - \delta(x) y^{\frac{1}{n}}\right). \tag{2}$$

Il est avantageux à écrire $x = R\sin\theta$, où $0 \leqslant \theta \leqslant \theta_0$. Alors la hauteur des bandes est :

$$\delta(x) = R(\cos\theta - \cos\theta_0). \tag{3}$$

Pour chacune de ces deux configurations d'écoulement (en film continu et en ruisselets) on détermine le débit massique et l'énergie.

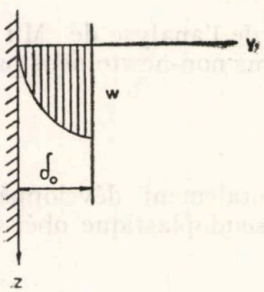

Fig. 1. — Schéma de l'écoulement.

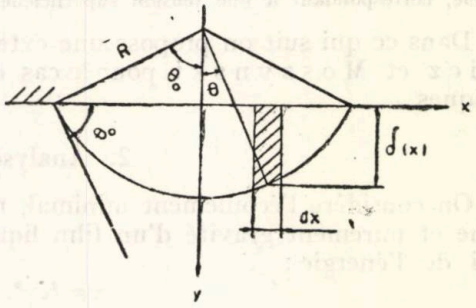

Figl. 2. — Configuration du ruisselet.

Pour une largeur de référence B du plan d'écoulement, le débit massique du film continu peut être écrit sous la forme :

$$Q_f = B \int_0^{\sigma_0} \rho w(y)\, dy. \tag{4}$$

En substituant l'expression de la vitesse (1) et intégrant, on obtient le débit par unité de largeur du film continu :

$$q_f = \frac{Q_f}{B} = \frac{n}{2n+1} \rho \left(\frac{\rho g}{k}\right)^{\frac{1}{n}} \delta_0^{\frac{2n+1}{n}}. \tag{5}$$

Pour le ruisselet, le débit massique par la même largeur de référence est :

$$Q_s = 2 \int_0^{R \sin\theta_0} \int_0^{\delta(x)} \rho\, w(x, y) dx\, dy. \tag{6}$$

Il en résulte :

$$Q_s = \frac{n}{2n+1} \rho \left(\frac{\rho g}{k}\right)^{\frac{1}{n}} R^{\frac{2(n+1)}{n}} \int_0^{\theta_0} (\cos\theta - \cos\theta_0)^{\frac{2n+1}{n}} \cos\theta\, d\theta. \tag{7}$$

En notant

$$F_1(n, \theta_0) = \int_0^{\theta_0} (\cos\theta - \cos\theta_0)^{\frac{2n+1}{n}} \cos\theta\, d\theta \tag{8}$$

et en introduisant le rapport λ entre la largeur mouillée par le ruisselet et la largeur de référence, c'est-à-dire

$$\lambda = \frac{2R \sin\theta_0}{B}. \tag{9}$$

on obtient pour le débit massique des ruisselets par unité de largeur l'expression suivante :

$$q_s = \frac{Q_s}{B} = \frac{n}{2n+1} \rho \left(\frac{\rho g}{k}\right)^{\frac{1}{n}} \lambda\, R^{\frac{2n+1}{n}} \frac{F_1(n_1 \theta_0)}{\sin\theta_0}. \tag{10}$$

Pour chaque configuration d'écoulement les débits doivent être égaux :

$$q_f = q_s. \tag{11}$$

L'égalité entre les expressions (5) et (10) conduit à la condition importante:

$$\left(\frac{\delta_0}{R}\right)^{\frac{2n+1}{n}} = \lambda \frac{F_1(n, \theta_0)}{\sin\theta_0}. \tag{12}$$

On exprimera les énergies en se rapportant toujours à la largeur de référence et, en plus, à l'unité de longueur du plan d'écoulement. L'énergie

totale peut être considérée comme la somme de l'énergie cinetique et de celle interfacique.

Pour le film continu on peut écrire :

$$E_f = B\left[\int_0^{\delta_0} \frac{\rho}{2} w^2(y)\, dy + \sigma_{LG} + \sigma_{SL}\right]. \tag{13}$$

Dans cette relation $\sigma_{LG}=\sigma$ et σ_{SL} représentent les tensions à l'interface liquide—gaz et à l'interface solide—liquide. En intégrant on obtient l'expression suivante de l'énergie du film continu par unité de largeur :

$$e_f = \frac{E_f}{B} = \left[\frac{n}{2(n+2)} - \frac{n^2}{(n+1)(3n+2)}\right]\left(\frac{\rho g}{k}\right)^{\frac{2}{n}} \rho \delta_0^{\frac{3n+2}{n}} + \sigma_{LG} + \sigma_{SL}. \tag{14}$$

L'énergie d'un ruisselet avec la surface séchée ci-jointe est :

$$E_s = 2\int_0^{R\sin\theta_0}\int_0^{\delta(x)} \frac{\rho}{2} w^2(x, y)\, dx\, dy + \sigma_{SL}\cdot 2R\sin\theta_0 + \sigma_{LG}\,\theta_0 + \sigma_{SG}(B - 2R\sin\theta_0), \tag{15}$$

où σ_{SG} est la tension à l'interface solide—gaz. Sur la ligne de contact des trois phases entre les tensions interfacielles il y a la relation :

$$\sigma_{SG} = \sigma_{SL} + \sigma_{LG}\cos\theta_0.$$

L'équation (15) devient donc :

$$E_s = 2\left[\frac{n}{2(n+2)} - \frac{n^2}{(n+1)(3n+2)}\right]\left(\frac{\rho g}{k}\right)^{\frac{2}{n}} \rho R^{\frac{3(n+1)}{n}} \int_0^{\theta_0} (\cos\theta - \cos\theta_0)^{\frac{3n+2}{n}} \cos\theta\, d\theta + \sigma_{LG}(2R\theta_0 + B\cos\theta_0 - 2R\sin\theta_0\cos\theta_0) + B\sigma_{SL}. \tag{16}$$

Si l'on introduit la notation

$$F_2(n, \theta_0) = \int_0^{\theta_0} (\cos\theta - \cos\theta_0)^{\frac{3n+2}{n}} \cos\theta\, d\theta \tag{17}$$

et on utilisè le rapport λ (v. (9)), l'équation de l'énergie du ruisselet par unité de largeur devient :

$$e_s = \frac{E_s}{B} = \left[\frac{n}{2(n+2)} - \frac{n^2}{(n+1)(3n+2)}\right]\left(\frac{\rho g}{k}\right)^{\frac{2}{n}} \rho\,\lambda\, R^{\frac{3n+2}{n}} \frac{F_2(n, \theta_0)}{\sin\theta_0} + \lambda\sigma_{LG}\left(\frac{\theta_0}{\sin\theta_0} - \cos\theta_0\right) + \sigma_{LG}\cos\theta_0 + \sigma_{SL}. \tag{18}$$

En substituant la condition (12), l'équation (18) prend la forme :

$$e_s = \left[\frac{n}{2(n+2)} - \frac{n^2}{(n+1)(3n+2)}\right]\left(\frac{\rho g}{k}\right)^{\frac{2}{n}} \rho\lambda^{-\frac{2n}{2n+1}}\left[\frac{\sin\theta_0}{F_1(n,\theta_0)}\right]^{\frac{3n+2}{2n+1}} \times$$
$$\times \delta^{\frac{3n+2}{n}} \frac{F_2(n,\theta_0)}{\sin\theta_0} + \lambda\sigma_{LG}\left(\frac{\theta_0}{\sin\theta_0} - \cos\theta_0\right) + \sigma_{LG}\cos\theta_0 + \sigma_{SL}. \tag{19}$$

La configuration d'écoulement en ruisselets sera stable si son énergie admet un minimum pour une valeur $\lambda=\lambda_0<1$. Donc :

$$\frac{\partial e_s}{\partial\lambda} = 0 \tag{20}$$

et, par surcroit :

$$\frac{\partial^2 e_s}{\partial\lambda^2} > 0. \tag{21}$$

En différentiant l'équation (19) par rapport à λ, égalant avec zero et mettant en évidence $\lambda=\lambda_0$, il en résulte :

$$\lambda = \left(\frac{2n}{2n+1}\right)^{\frac{2n+1}{3n+2}}\left[\frac{n}{2(n+2)} - \frac{n^2}{(n+1)(3n+2)}\right]^{\frac{2n+1}{3n+2}} \rho^{\frac{2n+1}{3n+2}}\left(\frac{\rho g}{k}\right)^{\frac{2}{n}\cdot\frac{2n+1}{3n+2}} \times$$
$$\times \left(\frac{1}{\sigma}\right)^{\frac{2n+1}{3n+2}}\left[\frac{F_2(n,\theta_0)}{\sin\theta_0}\right]^{\frac{2n+1}{3n+2}}\left[\left(\frac{\theta_0}{\sin\theta_0} - \cos\theta\right)^{-1}\right]^{\frac{2n+1}{3n+2}} \frac{\sin\theta_0}{F_1(n,\theta_0)} \delta_0^{\frac{2n+1}{n}}. \tag{22}$$

Ensuite on définit l'épaisseur critique adimensionelle du film :

$$\delta_{cr} = \delta_0\left\{\left[\frac{n}{2(n+2)} - \frac{n^2}{(n+1)(3n+2)}\right]\left(\frac{\rho g}{k}\right)^{\frac{2}{n}}\frac{\rho}{\sigma}\right\}^{\frac{n}{3n+2}}. \tag{23}$$

L'équation (22) peut être donc écrite sous la forme :

$$\lambda = \left[\frac{2n}{2n+1}\cdot\frac{F_2(n,\theta_0)}{\sin\theta_0}\left(\frac{\theta_0}{\sin\theta_0} - \cos\theta_0\right)^{-1}\right]^{\frac{2n+1}{3n+2}} \frac{\sin\theta_0}{F_1(n,\theta_0)} \delta_{cr}^{\frac{2n+1}{n}}. \tag{24}$$

L'écoulement pelliculaire minimal peut être considéré de deux manières.

Conformément à la théorie de H o b l e r [3], élaborée sans tenir compte de la forme des ruisselets issus, on détermine l'épaisseur critique du film en imposant la condition d'égalité géométrique :

$$\lambda = 1. \tag{25}$$

De (24) résulte :

$$\delta_{cr} = \left[\frac{2n+1}{2n}\cdot\frac{\sin\theta_0}{F_2(n,\theta_0)}\left(\frac{\theta_0}{\sin\theta_0} - \cos\theta_0\right)\right]^{\frac{n}{3n+2}}\left[\frac{F_1(n,\theta_0)}{\sin\theta_0}\right]^{\frac{n}{2n+1}}. \tag{26}$$

Le deuxième mode de considérer l'écoulement minimal revient à la condition que les énergies correspondantes aux deux configurations d'écoulement soient égales :

$$e_f = e_s. \tag{27}$$

De (14), (19) et (22) on obtient :

$$\left[\frac{n}{2(n+2)}-\frac{n^2}{(n+1)(3n+2)}\right]\left(\frac{\rho g}{k}\right)^{\frac{2}{n}}\frac{\rho}{\sigma}\,\delta_0^{\frac{3n+2}{n}}+(1-\cos\theta_0)=$$

$$(28)\quad =\left\{\left[\frac{n}{2(n+2)}-\frac{n^2}{(n+1)(3n+2)}\right]\left(\frac{\rho g}{k}\right)^{\frac{2}{n}}\frac{\rho}{\sigma}\right\}^{\frac{2n+1}{3n+2}}\delta_0^{\frac{2n+1}{n}}\left(\frac{2n}{2n+1}\right)^{\frac{2n+1}{3n+2}}\times$$

$$\times\frac{3n+2}{2n}\cdot\frac{\sin\theta_0}{F_1(n,\,\theta_0)}\left[\frac{F_2(n,\,\theta_0)}{\sin\theta_0}\right]^{\frac{2n+1}{3n+2}}\left(\frac{\theta_0}{\sin\theta_0}-\cos\theta_0\right)^{\frac{2n}{3n+2}},$$

qu'on peut écrire sous la forme équivalente simple

$$(29)\qquad \delta_{or}^{\frac{3n+2}{n}}+\Phi(n,\theta_0)\,\delta_{cr}^{\frac{2n+1}{n}}+(1-\cos\theta_0)=0.$$

La fonction Φ a l'expression :

$$(30)\quad \Phi(n,\theta_0)=\frac{3n+2}{2n}\cdot\frac{\sin\theta_0}{F_1(n,\,\theta_0)}\left[\frac{2n}{2n+1}\cdot\frac{F_2(n,\,\theta_0)}{\sin\theta_0}\right]^{\frac{2n+1}{3n+2}}\left(\frac{\theta_0}{\sin\theta_0}-\cos\theta_0\right)^{\frac{2n}{3n+2}}.$$

Pour le cas particulier des films minces newtoniens ($n=1$), les relations finales (26) et (29) conduisent aux résultats de M i k i e l e w i c z et M o s z y n s k i [2] :

$$(31)\qquad \delta_{cr}=\left[\frac{3}{2}\cdot\frac{\sin\theta_0}{F_2(\theta_0)}\left(\frac{\theta_0}{\sin\theta_0}-\cos\theta_0\right)\right]^{\frac{1}{5}}\left[\frac{F_1(\theta_0)}{\sin\theta_0}\right]^{\frac{1}{3}},$$

$$(32)\qquad \delta_{cr}^5-\Phi(\theta_0)\,\delta_{cr}^3+(1-\cos\theta_0)=0.$$

3. Discussions

Le mode de variation de l'épaisseur critique adimensionelle avec l'angle de mouillage et avec l'indice d'écoulement est présenté dans les Fig. 3 et 4. En raison de la complexité des relations, les courbes ont été tracées à l'aide d'un calculateur FELIX C-256.

On remarque dès le début que l'équation (29) conduit à de moindres épaisseurs critiques adimensionelles, mais les deux relations mises en discussion prévoient l'augmentation de l'épaisseur minimale avec l'angle de mouillage. On a mis aussi en évidence ces aspects au cas newtonien, tant du point de vue théorique qu'expérimental [2].

En ce qui concerne l'influence de l'indice d'écoulement, on distingue certaines particularités. Ainsi, pour tout le domaine des valeurs raisonnables de l'angle de mouillage ($\theta_0=15°...60°$) la relation (26) prévoit l'augmentation de l'épaisseur minimale avec la diminution de l'indice d'écoulement. Pour les angles de mouillage hypothétiquement grands, à partir d'une valeur d'environ 75°, l'effet est contraire. Mais l'équation (29) reflète un autre comportement, à savoir, on constate tout d'abord une diminution des valeurs de δ_{Cr} avec la diminution de n. Ensuite, quand le comportement non-newtonien s'accentue ($n<0{,}6$), l'épaisseur critique ira considérablement d'une manière croissante.

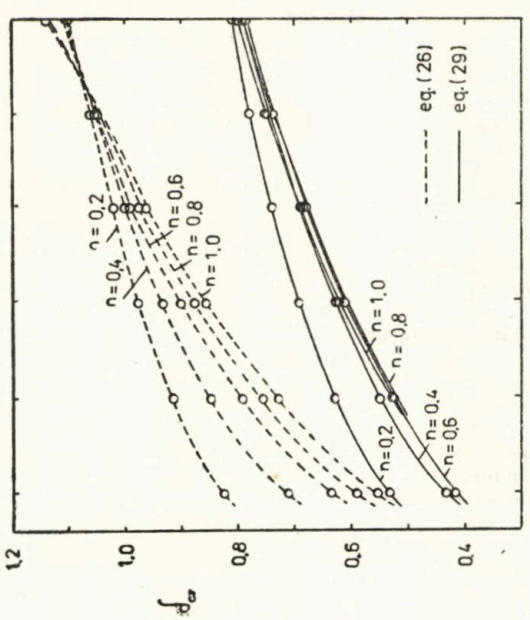

Fig. 3. — Variation de l'épaisseur critique adimensionelle avec l'angle de mouillage.

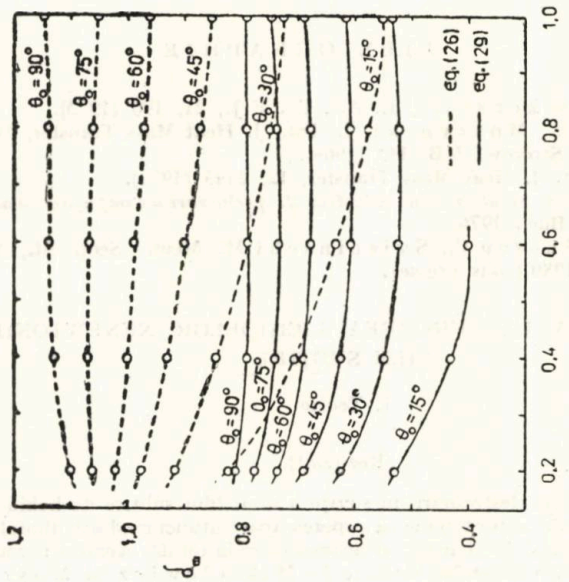

Fig. 4. — Variation de l'épaisseur critique adimensionelle avec l'indice d'écoulement.

Notations

B —largeur de référence ;
E — énergie ;
e — énergie par unité de largeur ;
F_1 — fonction définie par (8) .;
F_2 — fonction définie par (17) ;
g — accélération de la gravité ;
K — consistance du liquide ;
n — indice d'écoulement ;
p_G — pression dans la phase gazeuse ;
p_L — pression dans la phase liquide ;
Q — débit massique ;
q — débit massique par unité de largeur ;
R — rayon du ruisselet ;
w — vitesse ;
x,y,z — coordonnées ;
$\dot{\gamma}$ — taux de cisaillement ;
δ — épaisseur du film (ruisselet) ;
δ_0 — épaisseur minimale du film ;
δ_{cr} — épaisseur critique adimensionelle ;
θ — coordonnée angulaire ;
θ_0 — angle de mouillage ;
λ — rapport défini par (9) ;
ρ — densité du liquide ;
σ — tension superficielle ;
τ — effort de cisaillement ;
Φ — fonction définie par (30).

Reçue le 12 décembre 1979

Institut de Chimie macromoléculaire „P. Poni", Jassy
et
Institut Polytechnique, Jassy, Chaire de Génie chimique

BIBLIOGRAPHIE

1. Anshus B. E., Ruckenstein, E. A.I. Ch. E.J., 21, 190 (1975).
2. Mikielewicz J. R. Moszynski J., Int. J. Heat Mass Transfer, 19, 771 (1976).
3. Hobler T., Chem. Strosow, 2 B, 145 (1964).
4. Bankoff S. G., Int. J. Heat Mass Transfer, 12, 2143 (1971).
5. Tudose R. Z., *Procese şi utilaje în industria de prelucrare a compuşilor macromoleculari*, Ed. Tehn., Buc., 1976.
6. Tudose R. Z., Zăinescu C., Sviecinschi M., Mem. Secţ. Şt., Acad. R.S.R., III (1979—1980)(sous presse).

GROSIMEA MINIMĂ LA CURGEREA LICHIDELOR NENEWTONIENE IN FILM SUBŢIRE

I. Teorie

(Rezumat)

Se consideră problema destrămării în şuviţe a unui film subţire de lichid nenewtonian ce curge pe un plan vertical. Se presupune că ruperea apare atunci cînd atît filmul continuu cît şi suviţele rezultate au acelaşi debit masic şi aceeaşi energie totală. Analiza permite regăsirea, drept cazuri particulare, a rezultatelor obţinute de Mikielewicz şi Moszynski [2].

BULETINUL INSTITUTULUI POLITEHNIC DIN IAŞI
Tomul XXVI (XXX), fasc. 1—2, 1980
Secţia III
CHIMIE şi INGINERIE CHIMICĂ

D.C. 66 1.53

ON THE PRESENT STATE OF THE MATHEMATICAL MODELING OF THE AMMONIA CATALYTIC OXIDATION REACTOR

BY

I. CURIEVICI and ŞT. UNGUREANU

Dedicated to Professor Dr. CRISTOFOR SIMIONESCU, member of the Academy, on his 60 th anniversary

1. The design of the ammonia catalytic oxidation reactor has been long effected on an empirical basis, since no kinetic equation of the oxidation process existed, but the known empirical equations, as those proposed by L. E. Apelbaum and M. I. Temkin [1], V. I. Atroshenko and others [2], contain as variables but few of the parameters characteristic of the process, being thus limited in their application to certain working conditions. A new mathematical model has been established by us in 1968 [3] to overcome these difficulties.

Our model is based on the fact, known from earlier experimental works, that the diffussion of the ammonia to the catalyst surface is the rate determining factor. The original aspect of this model is:

$$\ln (1-x) = -\frac{M\alpha Pfn}{G}. \tag{1}$$

A semiempirical relation, published in 1950 by A.P. Oele [4], for the mass transfer coefficient, α, containing all the parameters influencing the process as variables, was used:

$$\alpha = 0.924 \frac{\lambda \mathcal{R}_e^{0,33}}{PC_p d}. \tag{2}$$

Having in mind the range of temperature and ammonia concentration under which the oxidation process is usually taking place and working up the data provided by literature about the parameters used in the matehmatical model (1) as well as the thermal effect of the oxidation reaction, the following relations were obtained:

$$\begin{cases} C_p = 6.45 + (1.52 + 4.08\, m_0) T_m \times 10^{-3}, \quad \lambda = (3.21 + 12.77 \times 10^{-3} T_m) \times 10^{-6}, \\ \mu = (12.5 + 29.2 \times 10^{-3} T_m) \times 10^{-6}, \quad M = 28.96 - 11.93\, m_0, \\ T_m = 3.2 \times 10^3\, m_0 + 0.94\, T_0 + 38, \end{cases} \tag{3}$$

all valid in the range $T_m \in [600°K, 1\,100°K]$ and $m_0 \in [0.09, 0.12]$, where T_m is the arithmetical mean between inlet gas temperature, T_0, and sieve exit temperature, T_f.

From relations (1)...(3) we obtain the mathematical model (4), not significantly different from the one published in 1968:

$$\ln (1-x) = \frac{10^{-3}\, T_0\, (141\, m_0 - 344) + 482\, m_0^2 - 1\,126\, m_0 - 106}{10^{-3}\, T_0\, (1.43 + 3.84\, m_0) + 13.06\, m_0^2 + 5.02\, m_0 + 6.51} \times$$

$$\times \frac{nf}{(27.45 \times 10^{-3}\, T_0 + 93.44\, m_0 + 13.61)^{1/3}} \times \frac{1}{(10^6\, d)^{2/3}\, G^{2/3}}. \tag{4}$$

In order to obtain the agreement with known experimental data, we have introduced the factor 2/3 into the second member of eq. (4); now, the final aspect of the mathematical model is:

$$\ln(1-x) = \frac{10^{-3}T_0(94\,m_0 - 229) + 321\,m_0^2 - 751\,m_0 - 70.67}{10^{-3}T_0(1.43 + 3.84\,m_0) + 13.06\,m_0^2 + 5.02\,m_0 + 6.51} \times$$

(5)

$$\times \frac{nf}{(27.45 \times 10^{-3}\,T_0 + 93.44\,m_0 + 13.61)^{1/3}} \cdot \frac{1}{(10^6 d)^{2/3}\,G^{2/3}}.$$

2. The Finnish researchers P. Uronen and E. Kiukanniemi [5] adopted our mathematical model (5) and, having experimentally established that during one operation period of the ammonia oxidation reactor representing the life-time of the catalytic sieves (about 3...5 months), the conversion of ammonia decreases continuously, they proposed adequate corrections.

Thus, the numerical coefficients in Eq. (5) were replaced by parameters, notated x_i, $(i=1, 2,...,13)$, the magnitudes of which were expressed on an experimental basis, as a second degree functions of the time variables (Table 1). At the same time, in order to point out the dependence of the original values of the parameters x_i at the moment $t=0$, on the operating temperature, a factor $(1+k\,\Delta T)$ was added to the model.

The final shape of this model is:

$$x = 1 - \exp \frac{(1+k\,\Delta T)[10^{-3}\,T_0\,(x_1\,m_0 - x_2) + x_3\,m_0^2 - x_4\,m_0 - x_5]\,nf}{[10^{-3}T_0(x_6 + x_7 m_0) + x_8 m_0^2 + x_9 m_0 + x_{10}](10^{-3}x_{11}T_0 + x_{12}m_0 + x_{13})^{0.33}10^6 d)^{2/3}G^{2/3}} \quad (6)$$

Table 1

Parameters	Numerical coefficients used by us in Eq. (5)	Values of parameters as functions of time, used by) P. Uronen and E. Kiukanniemi in Eq. (6
x_1	94	$2\,244.56 + 7.86669t - 6.55432t^2$
x_2	229	$228.779 - 0.349924t + 0.291447t^2$
x_3	321	$2\,474.41 + 19\,122.7t - 15\,935.6t^2$
x_4	751	$748.135 + 176.992t - 16.4017t^2$
x_5	70.67	$70.6699 + 14.7616t - 16.4017t^2$
x_6	1.43	$4.38364 - 12.6416t + 10.5346t^2$
x_7	3.84	$3.84067 + 4.7353t - 4.8574t^2$
x_8	13.06	$13.0603 - 0.54813t + 1.82361t^2$
x_9	5.02	$5.03001 - 0.17412t + 0.17848t^2$
x_{10}	6.5	$6.18196 + 1.43844t - 1.1949t^2$
x_{11}	27.45	$27.45 + 0.176865t - 0.181689t^2$
x_{12}	93.44	$93.44 + 0.004474t - 0.31397t^2$
x_{13}	13.61	$13.5005 + 0.48719t - 0.406132t^2$
k	—	$7.27 \times 10^{-4} + 5.34971 \times 10^{-4}t + 12.0557 \times 10^{-4}t^2$

We notice that most parameters calculated on the relations from Table 1 basis, at time $t=0$, have very close values to the numerical coefficients used by us in Eq. (5). This certifies the validity of our model.

3. Howard F. Rase, probably unacquainted with P. Uronen and E. Kiukanniemi's paper, resume in the wellknown handbook *Chemical Reactor Design for Process Plants* (1977), the problem of the ammonia catalytic oxidation reactor modeling, starting, essentially, from the model proposed by us and to which he refers six times ([6], pp. 116, 117, 118, 119).

The innovation introduced by H. F. Rase consists in the change of the mass transfer coefficient relation. Based on the last works in this field [7], H.F. Rase infers the equation [8], [6]:

$$\alpha = \frac{0.865\, Re^{-0.648}\, G}{P\, Se^{2/3} M \varepsilon} . \tag{7}$$

Using the Eq. (7) for α value in the mathematical model (1), obtained on a different basis than the one we used, H.F. Rase gives to this model the form.

$$\ln (1-x) = -\frac{5.81761 \times 10^{-5}\, n f\, T_m^{0.333}\, M^{0.667}}{\varepsilon^{0.352}\, d^{0.648}\, G^{0.648}\, \mu^{0.019}} , \tag{8}$$

in which the units utilized by the author are: d, [cm], G, [g/cm^2·sec], M, [g/mol], μ, [g/cm·sec], while the mean film temperature is taken as

$$T_m = T_f - 50. \tag{9}$$

In spite of the fact that the model (8) in its developed form is affected by a sign error in the calculus of M, the final result is not gravely influenced by this error, the computed data being in agreement with the known experimental ones.

It is important to notice that the correction factor 2/3 introduced by us into the relation (5) in order to obtain the agreement of the computation results with the experimental data, is substantiated by G. R. Gillespie's and R. E. Kenson's recent experimental works [9]. These researchers have shown that in reactors with up to 50 gauze pads only the upper 2/3's of the bed appears to be active as a catalyst ; the lower 1/3 of the bed operates as a gas distributor only and may be replaced by such a device.

4. Regarding the results presented above, we may conclude that the mathematical model (5) proposed by us in 1968 is still completely valid, but taking into account the new data concerning the mass transfer coefficient computation, used by H. F. Rase, this model gets the new form :

$$\ln (1-x) = -\frac{33.87 \times 10^{-6} (6.40 \times 10^3 m_0 + 0.88\, T_0 + 26)^{1/3} (28.96 - 11.93\, m_0)^{2/3}\, n f c_d}{186.9\, m_0 + 25.70 \times 10^{-3}\, T_0 + 13.26)^{0.019}\, d^{0.648}\, G^{0.648}\, (8-f)^{0.352}} , \tag{10}$$

where c_d, called by us „distributor factor", may have one of the magnituded : $c_d = 1$, for plants with a gas distributor ; $c_d = 2/3$, for plants without gas distributor.

The conversion values, computed by using Eq. (10), are closer to the experimental ones than the data obtained from Eq. (5), but the differences are insignificant, as may be seen in Table 2.

Table 2

Number of sieves n	Gas charge G	Conversion level, x		
		Experimental data [3]	Data obtained with Eq. (5)	Data obtained with Eq. (10)
1	0.285	0.854	0.8578	0.8404
2	0.285	0.985	0.9798	0.9745
2	0.694	0.870	0.8842	0.8727
3	0.285	0.999	0.9971	0.9959
3	0.694	0.956	0.9605	0.9546
3	1.116	0.890	0.9052	0.8970
The constant data of process:		$m_0 = 0.11$		$d = 9 \times 10^{-5}$ m
		$T_c = 390°K$		$f = 1.87$
		$T_f = 1\ 123°K$		$c_d = 2/3$

Although the correction proposed by P. Uronen and E. Kiukanniemi for taking into account the effect of catalytic properties changes during the operation is theoretically justified, the computed results using model (6) are not in agreement with those obtained with our model and with H. F. Rase's model, due probably to erroneous relations for time dependence of certain characteristic factors in the process (x_1, x_3, x_6). This problem needs, of course, further investigation.

In conclusion, the mathematical model represented by Eq. (10) containing as variables all the characteristic magnitudes of the reactor (x, T_0, G, d, n, f), is particularly useful in design. The verification of this model, for both cases, $c_d=1$ and $c_d=2/3$, gave satisfactory results.

Notations

C_p — molar specific heat at mean temperature, [Kcal/Kmol. grd],
c_d — distributor factor,
d — wire diameter, [m],
f — characteristic factor of sieves, representing the wire area-sieve area ratio,
G — gas charge on sieve square meter, representing nf m² active area for n sieves, [Kg/m²·sec],
M — molecular weight, [Kmol/Kg],
m_0 — molar fraction (volumetric) of NH_3 in initial mixture,
n — number of sieves,
P — initial overall pressure, [ata],
T_f — gas temperature beyond sieves, [°K],
T_m — mean temperature of gases, [°K],
T_0 — inlet gas temperature, [°K],
x — conversion level,
α — mass transfer coefficient, [Kmol/m². sec. ata],
ε — void fraction or screen porosity,
λ — thermal conductivity of gas mixture at mean temperature, [Kcal/m. sec. grd],
μ — dynamic viscosity of gas mixture at mean temperature, [Kg/m.sec].

Received, February 11, 1980

Polytechnic Institute, Jassy,
Department of Chemical Engineering

REFERENCES

1. Апелбаум Л. Е., Темкин М. И., ЖФХ, 22, 2, 179 (1948).
2. Атрощенко В. И., Каргин С. И., *Технология азотной кислоты*. Москва, 1962.
3. Curievici I., Ungureanu Şt., Bul. Inst. polit. Iaşi, **XIV (XVIII)**, *1—2*, 227 (1968).
4. Oele A. P., Chem. Eng. Sci., **III**, *1—2*, 146 (1958).
5. Uronen P., Kiukanniemi E., BCE & Process Techn., **17**, *4*, 323 (1972).
6. Rase H. F., *Chemical Reactor Design for Process Plants*. Vol. **II**, *Case Studies & Design Data*. John Wiley & Sons, N. Y., London, Sydney, Toronto, 1977, 115—122.
7. Satterfield C. N., Cortez D., H., Ind. Eng. Chem. Fundam., **9**, 613 (1970).
8. Rase H. F., *Chemical Reactor Design for Process Plants*. Vol. **I**, *Principles & Techniques*. John Wiley & Sons, N. Y., London, Sydney, Toronto, 1977, 532.
9. Gillespie G. R., Kenson R. E., Chem. Tech., 627 (1971).

CU PRIVIRE LA STADIUL ACTUAL AL MODELĂRII MATEMATICE A REACTORULUI DE OXIDARE CATALITICĂ A AMONIACULUI

(Rezumat)

Se analizează modelul matematic al reactorului de oxidare catalitică a amoniacului (5), publicat de autori în 1968 [3], ţinînd cont de cele mai recente cercetări în acest domeniu [5], [6] şi se ajunge la concluzia validităţii acestuia. Introducînd date noi referitoare la coeficientul de transfer de masă, propuse de H. F. Rase [6] şi alţii [7], se deduce un nou model (10), uşor modificat faţă de modelul (5), ale cărui rezultate concordă mai bine cu datele experimentale cunoscute.

Coli tipar 8

Tiparul executat sub cd. 98
la Întreprinderea poligrafică Iaşi
str. 7 Noiembrie nr. 49

40822

F 1503/2

BULETINUL INSTITUTULUI POLITEHNIC DIN IAȘI

Tomul XXVI (XXX)

Fasc. 3—4

Secția II

CHIMIE ȘI INGINERIE CHIMICĂ

1980

BIBLIOTECA CENTRALĂ UNIVERSITARĂ "MIHAIL KOGĂLNICEANU" IAȘI

BULETINUL INSTITUTULUI POLITEHNIC DIN IAȘI

Tomul XXVI (XXX)

Fasc. 3–4

Secția II

CHIMIE ȘI INGINERIE CHIMICĂ

1980

COLEGIUL DE REDACȚIE

Prof. dr. doc. **VAL. BLIDARU**
Prof. dr. doc. **N.V. BOȚAN**
Prof. dr. ing. **GH. CAȘLER**
Prof. dr. ing. **M. GAFIȚANU** (președinte)
Prof. dr. **P. MĂLCOMETE**
Prof. dr. doc. **D. MANGERON**
Prof. dr. ing. **T. SILION**
Acad. prof. dr. doc. **CR. SIMIONESCU**
Prof. dr. ing. **I. VIAD**

COMITETUL DE REDACȚIE AL SECȚIEI II. CHIMIE și INGINERIE CHIMICĂ

Prof. dr. ing. **N. ASANDEI**
Prof. dr. doc. **MAGDA PETROVANU**
Prof. dr. doc. **RADU TUDOSE**

REDACȚIA

Prof. dr. doc. **D. MANGERON** (redactor responsabil)
Prof. dr. ing. **HUGO ROSMAN** (secretar)
ECATERINA IRIMIEA (tehnoredactor)

BULETINUL INSTITUTULUI POLITEHNIC DIN IAŞI
BULLETIN OF THE POLYTECHNIC INSTITUTE OF JASSY
ИЗВЕСТИЯ ЯССКОГО ПОЛИТЕХНИЧЕСКОГО ИНСТИТУТА
Tomul XXVI (XXX), fasc. 3–4 1980

Secţia II

CHIMIE şi INGINERIE CHIMICĂ

SUMAR

Pag.

M. APOSTOLESCU, T. GOLGOŢIU şi V. ŞUNEL, Compuşi noi cu seleniu în moleculă (IV) (engl., rez. rom.) 9

ŞT. GAVRILIU şi N. CALU, Studiul oxidării în aer a carburii de wolfram în condiţii izoterme-izobare (rom., rez. franc.) 15

I. BERDAN, Combinaţii complexe ale Tl (III) cu liganzi de tipul heterociclurilor organice (I) (franc., rez. rom) 21

V. DULMAN, C. BURCOVEANU şi S. FIŞEL, Concentrarea Co (II) şi Ni (II) cu colectori microbiologici (levură din genul *Candida*) (rom., rez. engl.) . . 27

I. HÎNCU, E. ŞTEFANCU şi D. ŞTEFANCU, Contribuţie la studiul fizico-chimic al transformărilor în fază solidă, sub influenţa temperaturii, ale unor amestecuri binare de sulfuri şi azotat de amoniu (II) (franc., rez. rom.) . . 33

O. VICOL şi ŞT. REPEDE, Spectrele electronice ale unor chelaţi micşti ai Pd (II) cu α-aminoacizi (engl., rez. rom.) 37

N. CALU, I. BERDAN şi AL. CAŞCAVAL, Dipolmomentele electrice ale unor combinaţii complexe ale Tl (III) (germ., rez. rom.) 41

M. FURNICĂ, Determinarea spectrofotometrică a vanadiului (V) (rom., rez. franc.) 45

V. ABABI, N. BÎLBĂ, P. ONU, GH. MIHĂILĂ, N. NAUM şi C. LUCA, Caracterizarea structural-adsorptivă a tufurilor vulcanice activate (engl., rez. rom.) 51

N. NAUM, V. ABABI, GH. MIHĂILĂ şi E. POPOVICI, Alchilarea toluenului cu metanol pe zeoliţi sintetici (III) (engl., rez. rom.) 61

E. POPOVICI, M. CRUCEANU, A. POPA, GH. MIHĂILĂ, A. BOLD şi M. ALEXANDROAIE, Adsorbanţi zeolitici din catalizatori oxidici uzaţi (engl., rez. rom.) 67

AL. STANCU şi I. IBĂNESCU, Contribuţii la îmbunătăţirea procesului de concentrare şi condiţionare a molibdatului de sodiu (rom., rez. engl.) . . . 75

C. HAGIU şi C. CALISTRU, Proprietăţile soluţiilor în sistemele $NH_4H_2PO_4 - H_2O$ şi $(NH_4)_2HPO_4 - H_2O$ (rom., rez. engl.) 79

Pag.

C. CALISTRU, C. LEONTE și I. SIMINICEANU, Metodă pentru evidența și reducerea continuă a coeficienților de consum în industria amoniacului (rom., rez. engl.) 87

GH. SURPĂȚEANU, CR. LUCHIAN, M. CONSTANTINESCU, V. BĂRBOIU și M. PETROVANU, Triazoliu-ilide (IV) (engl., rez. rom.) 97

AL. CAȘCAVAL, Combinații organice ale sulfului (XII) (germ., rez. rom.) . . 105

I. CIOCOIU, V. DULMAN și S. FIȘEL, Complecși metalici ai unor anili cu nucleu benztiazolic (rom., rez. franc.) 109

B. ARVENTIEV și T. NICOLAESCU, Reacția dintre *o*-aminotiofenol și acid izotiocianic (engl., rez. rom.) 117

CR. SIMIONESCU și M. DUMITRIU, Contribuții la sinteza și studiul unor derivați de benzimidazol (engl. rez. rom.) 119

V. ȘUNEL, M. RUSU și I. MAZILU, Sinteza și studiul proprietăților electrice ale unor noi săruri de argint derivate de la N-(*p*-aminobenzoil)-L-asparagină (engl., rez. rom.) 123

BULETINUL INSTITUTULUI POLITEHNIC DIN IAŞI
BULLETIN OF THE POLYTECHNIC INSTITUTE OF JASSY
ИЗВЕСТИЯ ЯССКОГО ПОЛИТЕХНИЧЕСКОГО ИНСТИТУТА
Tom XXVI (XXX), Fasc. 3—4 1980

Section II

CHEMISTRY and CHEMICAL ENGINEERING

CONTENTS

Pp.

M. APOSTOLESCU, T. GOLGOŢIU and V. ŞUNEL, New Compounds Containing Selenium (IV) (English, Romanian summary) 9

ŞT. GAVRILIU et N. CALU, Étude de l'oxydation dans l'air de la carbure de tungstène dans des conditions isothermes-isobares (Romanian, French summary) 15

I. BERDAN, Combinaisons complexes du Tl (III) avec des ligands du type hétérocycles organiques (I) (French, Romanian summary) 21

V. DULMAN, C. BURCOVEANU and S. FIŞEL, Co (II) and Ni (II) Concentration with Microbiological Collectors (Yeast *Candida*) (Romanian, English summary) 27

I. HÎNCU, E. ŞTEFANCU et D. ŞTEFANCU, Contributions à l'étude physique et chimique des transformations en phase solide, sous l'influence de la température, dans un mélange binaire de sulfure et d'azotate d'ammonium (II) (French, Romanian summary) 33

O. VICOL and ŞT. REPEDE, Electronic Spectra of Some Mixed Chelates of Pd (II) with α-Amino Acids (II) (English, Romanian summary) 37

N. CALU, I. BERDAN und AL. CAŞCAVAI, Elektrische Dipolmomenten einiger Tl (III)-Komplexverbindungen (German, Romanian summary) 41

M. FURNICĂ, Détermination spectrophotométrique du vanadium (V) (Romanian, French summary) 45

V. ABABI, N. BÎLBĂ, P. ONU, GH. MIHĂILĂ, N. NAUM and C. LUCA, Structural-Adsorptive Characterization of the Activated Vulcanic Tuffs (English, Romanian summary) 51

N. NAUM, V. ABABI, GH. MIHĂILĂ and E. POPOVICI, Alkylation of Toluene with Methanol over Synthetic Zeolites (III) (English, Romanian summary) 61

E. POPOVICI, M. CRUCEANU, A. POPA, GH. MIHĂILĂ, A. BOLD and M. ALEXANDROAIE, Zeolitic Adsorbents from Waste Oxidic Catalysts (English, Romanian summary) 67

Pp.

AL. STANCU and I. IBĂNESCU, Contributions to the Improvement of the Processes of Sodium Molybdate Concentration and Conditionning (Romanian, English summary) 75

C. HAGIU and C. CALISTRU, Solution Properties in $NH_4H_2PO_4 - H_2O$ and $(NH_4)_2HPO_4 - H_2O$ systems (Romanian, English summary) 79

C. CALISTRU, C. LEONTE and I. SIMINICEANU, A Method for the Continuous Decreasing of the Specific Consumptions in the Ammonia Industry (Romanian, English summary) 87

GH. SURPĂŢEANU, C. LUCHIAN, M. CONSTANTINESCU, V. BĂRBOIU and M. PETROVANU, Triazolium-Ylide (IV) (English, Romanian summary) 97

AL. CAŞCAVAL, Organische Schwefelverbindungen (XII) (German, Romanian summary) 105

I. CIOCOIU, V. DULMAN et S. FIŞEL, Complexes métalliques de certains salicylidène-anils à noyau benzothiazolique (Romanian, French summary) 109

B. ARVENTIEV and T. NICOLAESCU, Reaction between *o*-Aminothiophenol and Isothiocyanic Acid (English, Romanian summary) 117

CR. SIMIONESCU and M. DUMITRIU, Contribution to the Synthesis and Study of some Benzimidazole Derivatives (English, Romanian summary) . . . 119

V. ŞUNEL, M. RUSU, G. I. RUSU and I. MAZILU, Synthesis and Electrical Properties of some New Silver Salts Derivatives of N-(*p*-aminobenzoyl)-L-Asparagine (English, Romanian summary) 123

BULETINUL INSTITUTULUI POLITEHNIC DIN IAŞI
BULLETIN OF THE POLYTECHNIC INSTITUTE OF JASSY
ИЗВЕСТИЯ ЯССКОГО ПОЛИТЕХНИЧЕСКОГО ИНСТИТУТА
Том XXVI(XXX), Вып. 3—4 1980

Секция II

ХИМИЯ и ХИМИЧЕСКАЯ ТЕХНОЛОГИЯ

СОДЕРЖАНИЕ

Стр.

М. АПОСТОЛЕСКУ, Т. ГОЛГОЦИУ и В. ШУНЕЛ, Новые соединение с селеным в молекуле (IV) (англ., рез. рум.) 9

Ш. ГАВРИЛИУ и Н. КАЛУ, Исследование окисления в воздухе карбида вольфрама в изотермических-изобарских условях (рум., рез. франц.) 15

И. БЕРДАН, Комплексные соединения таллия (III) с лигандами типа органических гетероциклов (I) (франц., рез. рум.) 21

В. ДУЛМАН, К. БУКОВЯНУ и С. ФИШЕЛ, Концентрирование Co (II) и Ni (II) микробиологическими коллекторами (дрожди рода) (рум., рез. англ.) 27

И. ХЫНКУ, Е. ШТЕФАНКУ и Д. ШТЕФАНКУ, Исследование изменения в твердой фазе под влиянием температуры двойных смесей из сулфидов и азотнокислой аммония (II) (англ., рез. рум.) 33

О. ВИКОЛ и ШТ. РЕПЕДЕ, Электронные спектры смешанных комплексных соединении Pd(II) с аминокислотами (англ., рез. рум.). . . 37

Н. КАЛУ, И. БЕРДАН и АЛ. КАШКАВАЛ, Электрические диполмоменты некоторых Tl(III) комплексные соединении (нем., рез. рум.) . . . 41

М. ФУРНИКЭ, Спектрофотометрическое определение ванадия (V) *о*-фенилендиамином (рум., рез. франц.) 45

В. АБАБИ, Н. БЫЛБЭ, П. ОНУ, Г. МИХЭИЛЭ Н. НАУМ и К. ЛУКА, Структурно-адсорбционное характеризирование активированых вулканических туфов (англ., рез. рум.) 51

Н. НАУМ, В. АБАБИ, Г.МИХЭИЛЭ и Е. ПОПОВИЧ, Алкилирование толуена метанолом на синтетических цеолитах (III) (англ., рез. рум.) 61

Е. ПОПОВИЧ, М. КРУЧЯНУ, А. ПОПА, Г. МИХЭИЛЭ, А. БОЛД и М. АЛЕКСОАЙЕ, Цеолитные адсорбенты из окисных употребляющих катализаторов (англ., рез. рум.) 67

АЛ. СТАНКУ и И. ИБЭНЕСКУ, Изучение процесса концентрации и кондиционирования молибдата натрия (рум., рез. англ.) 75

Стр.

К. ХАДЖЙУ и К. КАЛИСТРУ, Свойств растворых в системах $NH_4HP_2O_4$—H_2O и $(NH_4)_2HPO_4$—H_2O (рум., рез. англ.) 79

К. КАЛИСТРУ, К. ЛЕОНТЕ и И. СИМИНИЧЯНУ, Методы снежения коэффициентов в производстве аммиака (рум., рез. англ.). . . . 87

Г. СУРПЭЦЯНУ, К. ЛУКИАН, М. КОНСТАНТИНЕСКУ, В. БЭРБОЮ и М. ПЕТРОВАНУ, Триазолиевые илиды (IV) (англ., рез. рум.) 97

АЛ. КАШКАВАЛ, Органические серусодержащие соединения (XII) (нем., рез. рум.) 105

И. ЧОКОЮ, В. ДУЛМАН, С. ФИШЕЛ, Металлические комплексы некоторых анилов с бензотриазоловым ядром (рум., рез. франц.) . 109

Б. АРВЕНТЬЕВ и Т. НИКОЛАЕСКУ, Реакция *о*-аминотиофенола с изороданистоводородной кислотой (англ., рез. рум.) 117

КР. СИМИОНЕСКУ и М. ДУМИТРЙУ, Исследование структуры некоторых производных бензимидазола (англ., рез. рум.) 119

В. ШУНЕЛ, М. РУСУ, Г. И. РУСУ и И. МАЗИЛУ, Синтез и исследование электрических свойств некоторых серебрянных солей, полученных от N-(*p*-аминобензоил)-L-аспарагина (англ., рез. рум.) . 123

BULETINUL INSTITUTULUI POLITEHNIC DIN IAŞI
Tomul XXVI (XXX), fasc. 3—4, 1980
Secţia II
CHIMIE şi INGINERIE CHIMICĂ

D.K. 661.719.3

NEW COMPOUNDS CONTAINING SELENIUM

IV. DITHIOOXAMIDE DERIVATIVES

BY

MARIA APOSTOLESCU, TIBERIU GOLGOŢIU and VALERIU ŞUNEL

1. Introduction

The dithiooxamide has two structural forms, *cis* and *trans* :

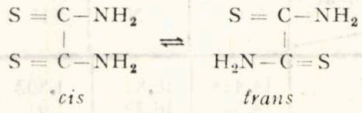

cis *trans*

In the present paper, based on the chemical analysis data and IR spectral measurements [1] as well as on the analogy with the oxamide structural form [2], the assumption was made that the thiooxamide reacts in *trans* form.

The selenious acid is used in synthesis of selenium compounds since it reacts with a great variety of compounds such as alcohols [3], butadiene [4], ethylenediamine [5], pyridine [6].

Selenium monochloride is particularly reactive in selenating reactions leading to compounds containing either one or several selenium atoms (linked by Se—Se bond) depending on the reagent nature [7] ... [11].

In the present paper the synthesis of two selenium dithiooxamide derivatives is reported: N, N′-bis (dithiooxamidyl)-selenoxide (denoted as BDSO) and N, N′-bis(dithiooxamidyl)-selenium (denoted as BDS).

Reagents used. Selenium monochloride was taken from „Schuchardt", München, original phials (d_4^{20}=2.90 g/cm³). Due to the reagent instability the phial was opened in chloroform. The concentration of the obtained solution was determined gravimetrically [12].

The dithiooxamide and the selenious acid were of analytical grade (Reidel, Berlin).

2. Results and Discussion

2.1. N, N′-bis(dithiooxamidyl)-selenoxide (BDSO)

To an alcoholic solution of dithiooxamide an aqueous selenious acid solution was added dropwise under stirring, in 30% exces to the theoretical amount. After about 15 min. a solid occurs and growths slowly. After stirring

one hour the reaction mixture is allowed to stay for 7 ... 8 hours and then filtered. The precipitate is washed with water then with ethylic alcohol and dried under vacuum.

The dried compound is a dark brick-red coloured crystalline powder insoluble in water and common organic solvents and sparingly soluble in dimethylformamide and benzene. The product is decomposed by the hot mineral acids.

The results of the elemental analysis are given in Table 1 and correspond to the general formula $C_4N_4S_4H_6Se$. The molecular weight determined cryoscopically in benzene was of 324 (the calculated molecular weight is 334).

The reaction takes probably place according to the following equation :

$$2C_2S_2N_2H_4+H_2SeO_3 \rightarrow C_4N_4S_4H_6SeO+2H_2O.$$

Table 1

Elemental Analysis Data

Compound \ Element		C	N	H	Se	S	O
BDSO	theoretical, [%]	14.414	16.817	1.802	23.724	38.438	4.805
	experimental, [%]	14.54	16.72	1.91	24.15	37.81*)	4.87
BDS	theoretical, [%]	16.509	9.688	2.076	27.337	44.290	—
	experimental, [%]	16.74	9.73	2.09	28.02	43.42*)	—

*) Calculated by difference.

2.2. N, N'-bis-(dithiooxamidyl)-selenium (BDS)

The reagents Se_2Cl_2 and dithiooxamide were used as solutions in chloroform at the temperature of 0° ... 3°C and 1 : 1 mole ratio.

Small amounts of Se_2Cl_2 solutions were added under good stirring and dried nitrogen atmosphere to the dithiooxamide solutions. A red solid phase separates after some minutes. The compound is then purified by solving in water. After evaporating the water the compound hydrochloride remains as an yellow-brown residue. The product is then obtained from its hydrochloride as a dark-yellow powder.

The elemental analysis data summarized in Table 1 correspond to the general formula $C_4N_4S_4H_6Se$. The reaction is assumed to take place according to the following equation :

$$2C_2S_2N_2H_4+Se_2Cl_2 \rightarrow C_4S_4N_4H_6Se+\frac{1}{8}Se_8+2HCl.$$

The separation of the elemental selenium may be accounted for by the existence of certain structural equilibria of Se_2Cl_2 [8].

The diselenic compound is also probably to occur as a reaction intermediate but its presence in the reaction product could not be detected.

The compound is hardly soluble in dimethilformamide, dichloroethane, cyclorhexanole, cyclohexanone, insoluble in water, ethylic alcohol, chloroform and acetone ; is decomposed by the mineral acids. The molecular weight determined cryoscopically in cyclohexanol was found to be 306 (the calculated molecular weight is 317).

3. IR Spectral Measurements

In a previous paper [1] the IR spectra of the selenious acid, dithiooxamide and BDSO are decribed. The IR spectrum of BDS is similar to that of BDSO excepting some differences occuring within the 14 ... 25 μ range as shown in Table 2.

Table 2

The Absorbtion Bands in the IR Spectrum

Dithiooxamid	BDSO	BDS
832 — v.str. 697 — m. $\nu_{C-S,\ o.p.}$ 620 — wk. 467 — wk 405 — sk.	875 — v.wk.sk. 797 — m. $\nu_{Se=O}$ $\nu_{Se=O}$ 677 — str. 665 — sh.wd. 640 — v.str. ν_{Se-N} 472 — m. sk. 418 — v.wk.	875 — m. 680 — m. $\nu_{C-S,\ o.p.}$ 655 — sh. 570 — str. ν_{Se-N} 550 — str. 440 sk. 400

v.str. = very strong ; str. = strong ; m. = medium ; wd. = wide ; wk. = weak ; sh. = shoulder ; sk = skeleton.

Based on the IR spectral measurements, the sterical considerations as well as on the physico-chemical analysis data the following structural formulas might be advanced for the described compounds :

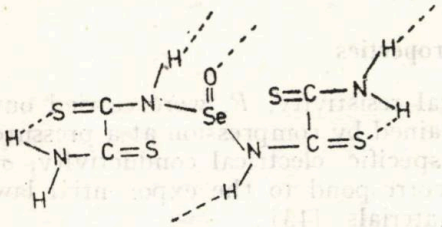

N, N′-bis-(dithioox amidyl)-selenoxide
(BDSO)

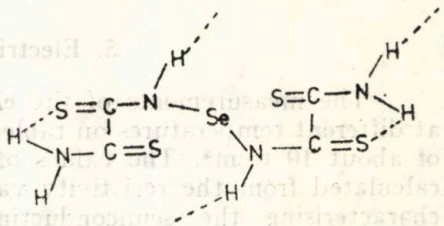

N, N′-bis-(dithiooxamidyl - 1 um
(BDS)

Assuming the coplanarity of the thiooxamidic group and taking into account the spatial orientation and the lengths of the chemical bonds as well as the sterical considerations the two N—Se—N bonds (both in BDSO and in BDS) are expected to form an obtuse angle [15]. In this case the selenium atom and Se=O, respectively, lies above the plane of the thiamidic groups.

The proposed structures promote the linkages through hydrogen bridges as seen in the IR spectrum [1].

4. Thermal Behaviour

In Fig. 1 the thermal behaviour is represented of dithiooxamide (curve *a*), BDSO (curve *b*) and BDS (curve *c*) within the 150° ... 270°C temperature range. The endothermal decomposing peaks indicating the breakage of Se—N and Se—C bonds are clearly evidenced [11].

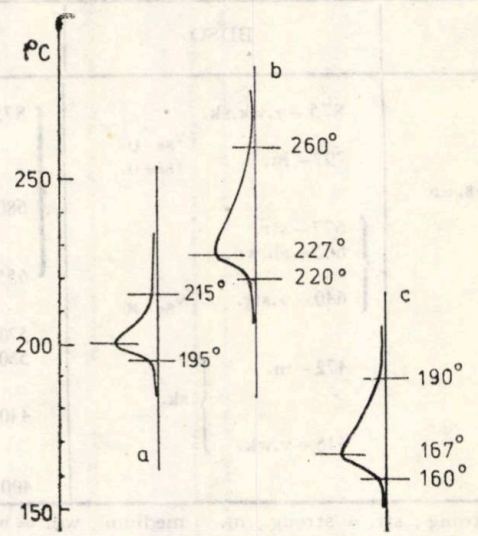

Fig. 1. — Thermal behaviour of dithiooxamide (*a*), BDSO (*b*) BDS (*c*).

The BDS shows a thermal stability lower than that of dithiooxamide while BDSO begins to decompose at a higher temperature due probably to the intermolecular bonds of the Se=O type.

5. Electrical Properties

The measurements of the electrical resistivity, R, were carried out at different temperatures on tablets obtained by compression at a pressure of about 10 t/cm^2. The values of the specific electrical conductivity, σ, calculated from the resistivity values correspond to the exponential law characterising the semiconducting materials [13]:

$$\sigma = \sigma_0 \exp [-Ea/(2kT)] ,$$

from which the value of the activation energy, E_a, can be calculated. The experimental results, plotted in log σ —$1/T$ coordinates (Fig. 2), allow the activation energy to be calculated by means of the relation $E_a = 2k$ tg α.

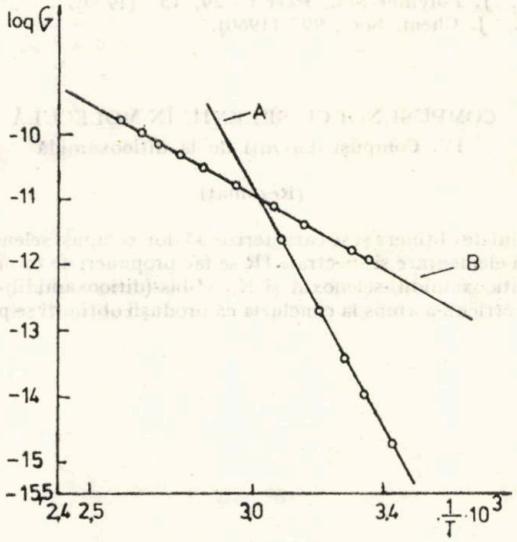

Fig. 2. — Dependence of log σ as function of $1/T$ for BDSO (A) and BDS (B).

The energies of activation were found to be 1.72 eV for BDSO and of 0.42 eV for BDS, respectively.

Since for the compounds showing semiconducting properties values of about 2.2 eV are given in literature [14], the obtained values for the compounds under study allow their placing among the semiconducting materials.

Received, July 14, 1978

Polytechnic Institute, Jassy,
Department of Inorganic and Analytical Chemistry
and
Department of Organic and Macromolecular Chemistry

REFERENCES

1. Golgoțiu T., Apostolescu M., Macovei V., Bul. Inst. polit., Iași, **XXIV (XXVIII)**, *3—4*, s. II, 15 (1978).
2. Scoott T. Jr., Wagner E. L., J. Chem. Phys., **30**, 465 (1959).
3. Гасанов В. И., Аверб. Хим. Ж., 2, 31 (1963).
4. William L., Mock Jones H., McCaushand, Tetrahedron Lett., **4**, 391(1968).
5. Bertini V., Angew. Chem. Dtsch., **79**, 530 (1967).
6. Ellis S., Hand, Pandler W. W., J. Org. Chem., **40**, 20, 2732 (1975).
7. Lautenschlaeger F., J. Org. Chem., **34**, *12*, 4002 (1969).
8. Brintzinger H. R., Pfannstiel-Vogel H., Z. Anorg. Chem., *256*, 75(1948).
9. Bertini V., Gazz. Chim. Ital., **97**, *12*, 1870 (1967).

10. Weinstock L. M., Danis P., Malvey D. M., Schaeffer J. C., Angew. Chem. Dtsch., **79**, 7, 315 (1967).
11. Grand D., Wazer J. R., J. Amer. Chem. Soc., **86**, 3012 (1964).
12. **Буклев М. Н., Зав. лаб., 4, 393 (1963).**
13. Katon J. E., *Organic Semiconducting Polymers*. Marcel Dekker, N. Y. 1968, 221.
14. Rembaun A., J. Polymer Sci., Part C, **29**, 157 (1970).
15. Tinter M. R., J. Chem. Soc., 997 (1960).

COMPUȘI NOI CU SELENIU ÎN MOLECULĂ

IV. Compuși derivați de la ditiooxamidă

(Rezumat)

Se prezintă modul de obținere și se caracterizează doi compuși selenici derivați ai ditiooxamidei. În baza analizei elementare și spectrale IR se fac propuneri de formule structurale pentru compușii N, N'-bis-(ditiooxamidil)-selenoxid și N, N'-bis-(ditiooxamidil)-seleniu. În urma studierii proprietăților electrice s-a ajuns la concluzia că produșii obținuți se pot încadra în categoria semiconductorilor.

BULETINUL INSTITUTULUI POLITEHNIC DIN IAŞI
Tomul XXVI (XXX), fasc. 3—4, 1980
Secţia II
CHIMIE şi INGINERIE CHIMICĂ

C.Z. 669.27

STUDIUL OXIDĂRII IN AER A CARBURII DE WOLFRAM ÎN CONDIŢII IZOTERME-IZOBARE

DE

ŞTEFANIA GAVRILIU şi N. CALU

1. Introducere

În tehnica modernă materialele dure, pe bază de carbură de wolfram, au căpătat o importanţă din ce în ce mai mare. Sfera lor de utilizare s-a extins foarte mult, de la prelucrarea prin aşchiere a metalelor, la trefilări, forarea sondelor, obţinerea matriţelor etc.

În literatura de specialitate există puţine informaţii privind comportarea la oxidare atît a carburii de wolfram în stare pură cît şi a pseudoaliajelor pe bază de carbură de wolfram. Un număr restrîns de lucrări tratează oxidarea în aer [1], [2], sub presiuni scăzute de oxigen [3] sau coroziunea chimică şi electrochimică [4], [5] a carburii de wolfram.

Cunoaşterea mecanismului cinetic al oxidării carburii de wolfram, în fază pură sau pseudoaliată, prezintă un interes deosebit atît în utilizările industriale ale acesteia cît şi în cadrul unor metode de recuperare a unor deşeuri de aliaje dure [6], [7].

În lucrările ale căror rezultate fac obiectul cercetărilor de faţă, studiul termogravimetric privind oxidarea în aer a carburii de wolfram compacte s-a efectuat în condiţii izoterme-izobare. Produşii de reacţie, în diferite trepte ale oxidării, au fost analizaţi chimic, cu raze X şi microscopic.

2. Rezultate şi discuţii

Oxidarea în aer a carburii unui metal presupune formarea oxizilor acestui metal, a carbonului liber, a oxizilor de carbon şi a nitrurilor, conform următoarelor tipuri de reacţii :

(1) $xMC+\frac{1}{2}yO_2=M_xO_y+xC$, (2) $xMC+\frac{1}{2}(x+y)\,O_2=M_xO_y+xCO$,

(3) $M_xC_{max}+\frac{1}{2}\,O_2=M_xC_{min}+CO$,

(4) $xMC+(\frac{1}{2}y+x)\,O_2=M_xO_y+xCO_2$, (5) $MC+\frac{1}{2}N_2=MN+C$.

Din punct de vedere termodinamic aceste reacţii sînt posibile pe un interval foarte larg de temperatură.

Calculele termodinamice, pentru condiţiile existenţei unei cantităţi de aer satisfăcătoare stoechiometriei reacţiei totale, arată că într-un interval larg de temperatură oxidarea carburii de wolfram conduce la trioxid de wolfram, aşa cum de fapt se observă şi din fig. 1.

L. D. M. Graw şi colaboratorii [8] au măsurat căldura de combustie a carburii de wolfram şi au calculat apoi căldura de formare cu ajutorul legii lui Hess, conform ecuaţiilor :

$WC + \frac{5}{2}O_2 = WO_3 + CO_2$	$\Delta H = -285\,800 \pm 80$ cal/mol
$C + O_2 = CO_2$	$\Delta H = -94\,050 \pm 11$ cal/mol
$W + \frac{3}{2}O_2 = WO_3$	$\Delta H = -195\,700 \pm 90$ cal/mol
$W + C = WC$	$\Delta H = -3\,950 \pm 100$ cal/mol

Puţinele informaţii furnizate în privinţa oxidării carburii de wolfram sînt uneori contradictorii [9]...[11], datorită probabil studierii unor materiale cu compoziţii chimice şi porozităţi diferite, în condiţii diferite.

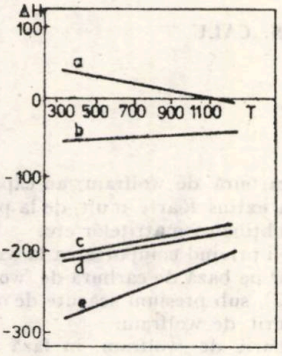

Fig. 1. — Dependenţa potenţialului izoterm-izobar la oxidare, funcţie de temperatură, pentru reacţiile : a — $WC + 4CO_2 = WO_3 + 5CO$; b — $WO_2 + 0{,}5O_2 = WO_3$; c — $WC + 2O_2 = WO_3 + CO$; d — $WC + 2O_2 = WO_2 + CO_2$; e — $WC + 2{,}5O_2 = WO_3 + CO_2$.

În lucrarea de faţă procesul oxidării în aer a carburii de wolfram, în intervalul de temperatură 500° ... 900°C, s-a studiat pe eşantioane paralelipipedice, obţinute prin tehnicile metalurgiei pulberilor. Caracteristicile probelor studiate sînt prezentate în tabelul 1.

Tabelul 1

Caracteristicile carburii de wolfram studiate

Compoziţia chimică, [%]			Densitatea	Porozitatea	Dimensiunile
W	C legat	C liber	g/cm³	%	mm
93,6	6,10	0,11	15,5	1,27	10 × 8 × 6

Înregistrările termogravimetrice au fost conduse cu o precizie de ±0,01 g, în aer, la presiune atmosferică şi în condiţii izoterme.

În urma unor experimentări preliminare s-a stabilit că în condiţiile unui curent foarte slab de aer, cu o viteză de 30 cm/sec, se obţin date reproductibile ale cineticii reacţiei de oxidare.

Curbele creşterii în greutate, funcţie de temperatură şi timp, sînt date în fig. 2 şi 3.

La menţinerea în aer a materialelor cu o porozitate de 1,27%, pînă la 500°C, pe suprafaţa lor apare o coloraţie violet-maronie, caracteristică oxizilor inferiori ai wolframului. O oxidare vizibilă a probelor de carbură de wolfram se sesizează de la 500°C iar la 650°C viteza de oxidare creşte considerabil. Din analiza curbelor cinetice se constată apariţia unui salt al oxidării rapide în intervalul de temperatură 700° ... 800°C.

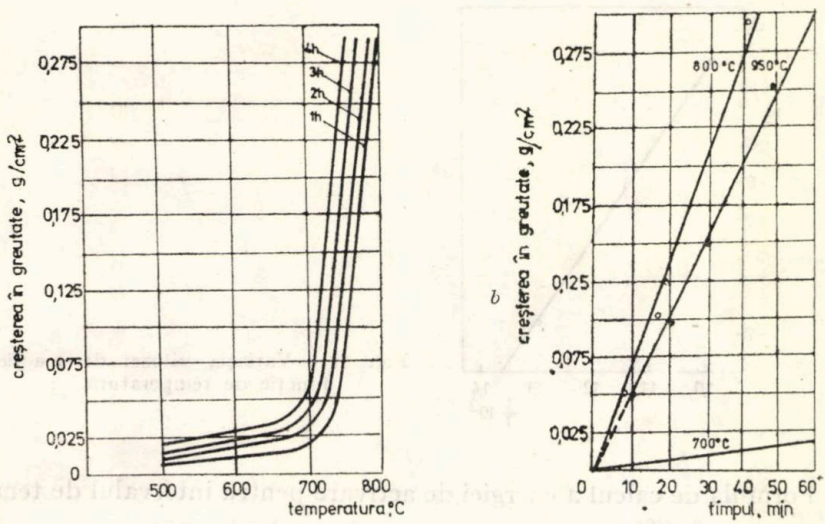

Fig. 2. — Curbele cineticii oxidării carburii de wolfram în aer, la presiune atmosferică: *a* — creşterea în greutate funcţie de temperatură; *b* — creşterea în greutate funcţie de timp.

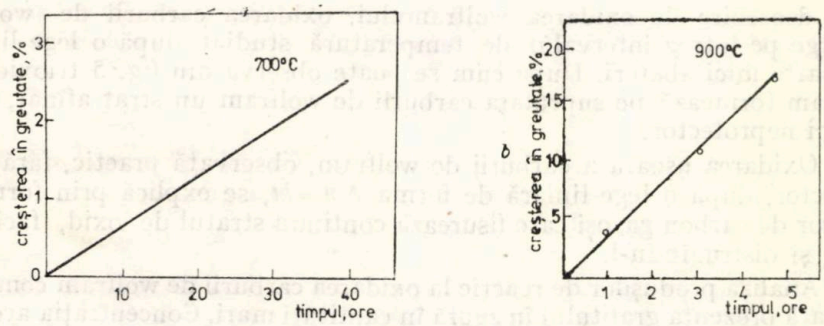

Fig. 3. — Creşterea procentuală în greutate, funcţie de timp, la oxidarea în aer a carburii de wolfram compacte: *a* — la 700°C; *b* — la 900°C.

La 700°C, carbura de wolfram se oxidează după o lege liniară, cu o constantă a vitezei de reacţie $k = 4 \cdot 10^{-6}$ g/cm² sec, iar la 800°C, după o lege aproape liniară, cu o constantă $k = 1{,}2 \cdot 10^{-4}$ g/cm² sec.

Pe baza legii lui Arrhenius

$$k = Ae^{-E/RT},$$

unde : k este constanta vitezei de reacţie ; E— energia de activare ; A — o constantă de integrare (constanta de acţiune sau factor de frecvenţă) şi R — constanta universală a gazelor, din panta transformărilor izotermeizobare, prezentate în fig. 4, s-a calculat energia de activare, găsindu-se pentru aceste condiţii valoarea de 28,73 kcal/mol.

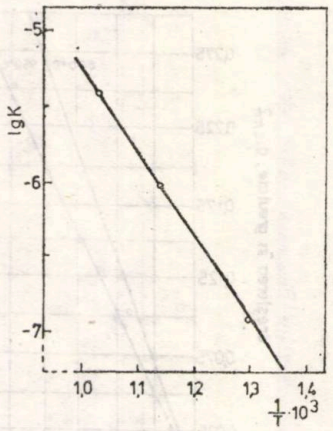

Fig. 4. — Variaţia vitezei de reacţie funcţie de temperatură.

Formula de calcul a energiei de activare pentru intervalul de temperatură $[T_1, T_2]$, a fost :

$$E = \frac{R \ln(k_1/k_2)}{1/T_2 - 1/T_1}.$$

Spre deosebire de oxidarea wolframului, oxidarea carburii de wolfram decurge pe întreg intervalul de temperatură studiat după o lege liniară, cu foarte mici abateri. După cum se poate observa din fig. 5 trioxidul de wolfram formează pe suprafaţa carburii de wolfram un strat afînat, poros şi deci neprotector.

Oxidarea uşoară a carburii de wolfram, observată practic, fără strat protector, după o lege liniară de forma $\Delta m = kt$, se explică prin formarea oxizilor de carbon gazoşi care fisurează continuu stratul de oxid, făcîndu-l poros şi distrugîndu-l.

Analiza produşilor de reacţie la oxidarea carburii de wolfram compacte nu arată prezenţa grafitului în zgură în cantităţi mari. Concentraţia acestuia scade pe măsură ce temperatura creşte : de la 0,5% la temperatura de 600°C, la 0,3% la cea de 800°C, iar la temperaturi mai ridicate grafitul nu se mai identifică. Carbonul se pierde la limita de faze iar oxizii de carbon se formează foarte repede şi simultan cu trioxidul de wolfram. Determinările concomitente ale creşterii în greutate a materialului de studiat, $\Delta m/q$ şi a cantităţii de bioxid de carbon degajat, $\Delta m_{CO_2}/q$, verifică ecuaţia [12] :

$$\frac{\Delta m_{CO}/q}{\Delta m/q} = \frac{44x}{16(1-x)\,y - 12x},$$

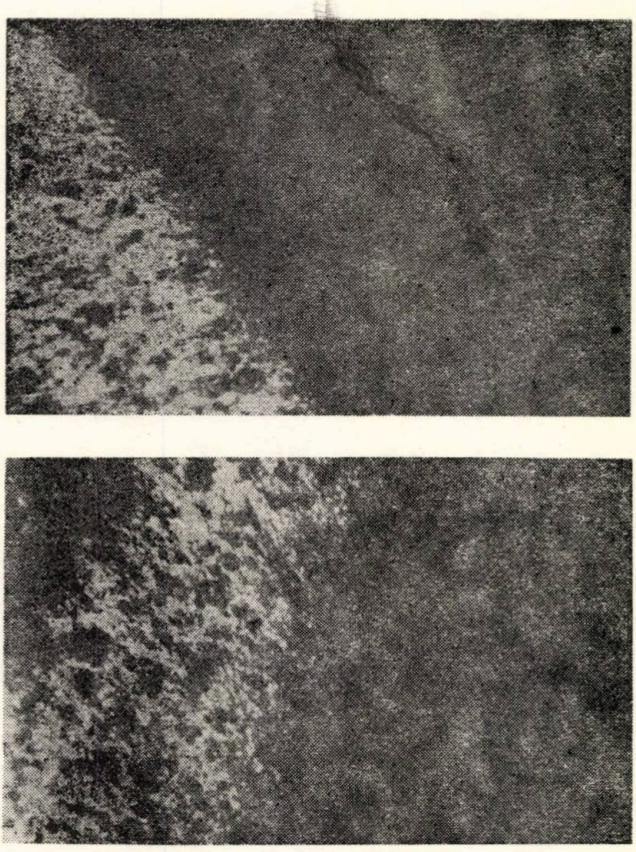

a

b

Fig. 5. — Structura stratului de oxid format pe suprafața carburii de wolfram, la oxidarea în aer, 2 ore la 600°C] × 100.

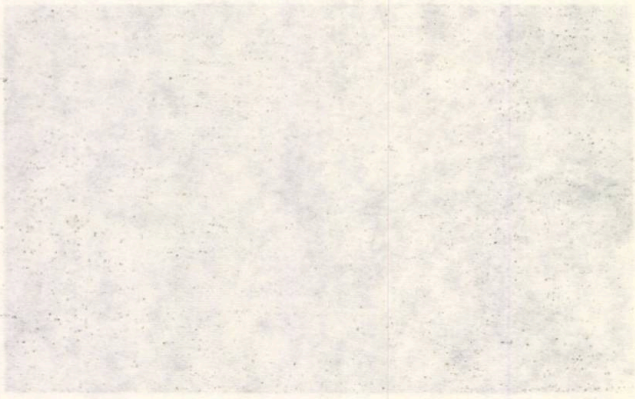

unde x este fracția molară a carbonului din carbură și y este numărul mediu al atomilor de oxigen pe fiecare atom de metal din stratul de oxid. Acest fapt exclude posibilitatea unei oxidări net preferențiale.

Roentgenograma și spectrele IR ale produșilor oxidării finale, prezentate în fig. 6 și 7, identifică prezența în cantitate preponderentă a trioxidului de wolfram.

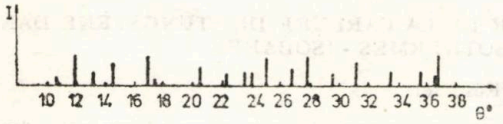

Fig. 6. — Roentgenograma produșilor oxidării carburii de wolfram în aer, la 700°C.

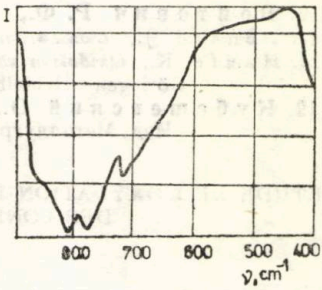

Fig. 7. — Spectrul IR al produșilor oxidării carburii de wolfram în aer, la 900°C.

Studiile termogravimetrice ale oxidării unor probe de carbură de wolfram, cu porozități diferite, arată că acest proces asta decurge cu viteze diferite. Vitezele de reacție cresc cu creșterea porozității. La temperaturi depășind 600°C oxidarea probelor cu porozități mai mari de 20% are loc cu sfărîmarea lor. Acest fapt se datorește tensiunilor interne apărute odată cu formarea trioxidului de wolfram și a oxizilor de carbon în interiorul probei, care conduce la o creștere în volum, ceea ce îngreuiază considerabil determinarea parametrilor cinetici ai reacției de oxidare.

3. Concluzii

1. S-a efectuat un studiu termogravimetric al oxidării fazei de carbură de wolfram compactă în condiții izoterme-izobare.

2. S-au adus precizări cu privire la mecanismul cinetic al reacției de oxidare.

3. S-au calculat vitezele de oxidare la temperaturi diferite, de exemplu la 700°C, $K=4 \cdot 10^{-6}$ g/cm² sec, iar din panta transformărilor izoterme-izobare s-a calculat energia de activare a procesului, $E=28{,}73$ kcal/mol.

4. A fost subliniată importanța influenței porozității asupra vitezei de reacție.

Primită la 5 iunie 1978

Institutul politehnic, Iași,
Catedra de chimie anorganică
și analitică

BIBLIOGRAFIE

1. Newkirk A. E., J. of the Amer. Chem. Soc., **77**, 4521 (1955).
2 Гимелфарб Ф. А., Зеликман А. Н., Изв. ВУЗ, Цветная метал., 3, 63 (1967).
3. Dufour L. C., Simon J., Bull. Soc. Chim. France, 9, 3643 (1968).

4. Woorhies J. D., J. Electrochem. Soc., 119 (2), 219 (1972).
5. Стрегнухина Л. В., Яковлева Е. Ф., Зимина Л. Н., Куяжева В. М., Завод. лаб., 3, 260 (1973).
6. Hynek I., Patent RSC nr. *143 587* (Cl C 22 C), 1971.
7. Roman P., Rogalschi S., Lucr. celei de a III-a Conf. a electr. Secţia a V-a Materiale Electrot., Bucureşti, iunie 1973.
8. Kubaschewski O., Evans E., *La Thermochimie en métallurgie*. GauthierVillars, Paris, 1964, 84.
9. Войтович Р. Ф., Пугач Е. А., Пороск. метал., 4, 124, 59 (1973).
10. Bénard J., *L'oxydation des métaux*. Gauthier Villars, Paris, 1962.
11. Hauffe K., *Oxidation von Metallen und Metallegierungen*. Springer Verlag, Berlin—Götingen—Heidelberg, 1965, 332.
12. Кубашевский О., Гопкинс Б. Е., *Окисление металлов и сплавов*. Изд. Металлургия, М,. 1965.

ÉTUDE DE L'OXYDATION DANS L'AIR DE LA CARBURE DE TUNGSTÈNE DANS DES CONDITIONS ISOTHERMES - ISOBARES

(Résumé)

On présente les résultats de l'étude thermogravimétrique concernant l'oxydation dans l'air de la carbure de tungstène compacte, dans des conditions isothermes-isobares.

Les produits de différents degrès de l'oxydation de la carbure de tungstène ont été analysés par voie chimique, à l'aide des rayons X, par l'absorbtion en IR et par microscopie. Les données obtenues ont permis à identifier le mécanisme cinétique de l'oxydation.

De même on a calculé la vitesse d'oxydation à des différentes températures et l'énergie d'activation du processus.

On a mis en évidence l'influence de la porosité du matériel sur la vitesse de réaction.

BULETINUL INSTITUTULUI POLITEHNIC DIN IAŞI
Tomul XXVI (XXX), fasc. 3—4, 1980
Secţia II
CHIMIE şi INGINERIE CHIMICĂ

C. Z. 547.256.88

COMBINAISONS COMPLEXES DU Tl(III) AVEC DES LIGANDS DU TYPE HÉTÉROCYCLES ORGANIQUES

I. SYNTHÈSE ET QUELQUES PROPRIÉTÉS

PAR

I. BERDAN

1. Introduction

La littérature de spécialité offre nombre de données concernant la capacité des ions métalliques, parmi lesquels le Tl (III), de former des combinaisons complexes avec des ligands du type hétérocycles organiques qui contiennent l'atome d'azote donneur [1]...[4]. Les études effectuées n'offrent cependant pas assez d'informations capables à conduire à une interprétation moderne de la structure des espèces complexes formées. Avec l'ion Tl (III) on a synthétisé et étudié des complexes seulement avec la pyridine, la quinoline [5], la phénanthroline [5], [6], l'éthylènediamine [7], [8] et la pyrrazine [9], [10].

C'est en cet esprit que nous abordons ci-dessous le problème de la synthèse et de la caractérisation d'une nouvelle série de combinaisons complexes du Tl(III) avec les ligands suivants : benzthiazol (BT), 2-amino-benzthiazol (ABT), benzimidazol (BI), N-benzil-benzimidazol (BBI), l'acide-benzimidazolil-2-carboxylique (BIC), les acides pyridin-monocarboxyliques : 1, 2 (PIC), 1, 3 (NIC) et 1, 4 (INIC), nicotinamide (NICA), quinoxaline (QUIN), benzocinoline (BC), 2,7-dimethylbenzocinoline (DMBC) et 2,2'-azodipyridyle (ADIP). En général, les ligands mentionnés ci-dessus contiennent l'azote en état de hybridisation sp^2 dans les circonstances chimiques respectives, ayant des influences directes sur la basicité de l'atome d'azote donneur de la molécule. Leur comportement est celui de base relativement faible, ayant le pK_a inférieur à celui de l'imidazol , $pK_a=7$ [11], [12].

2. Partie expérimentale

2.1. Les réactants

Comme source de Tl(III) nous avons employé le $TlCl_3$ et le $TlBr_3$. On a préparé les halogénures de Tl(III) d'après une recette citée dans la littérature [13]. Dans toutes les synthèses des combinaisons complexes on a utilisé des solutions de TlX_3 (X=Cl, Br) fraichement préparées. On s'est servi de ligands produits p.a. ou bien de produits de synthèse de laboratoire, ultérieurement purifiés, d'après des recettes trouvées dans la littérature, comme pour les ligands : QUIN [14], BC et DMBC [15], BIC [16], BBI [17] et ADIP [18].

2.2. Synthèse des combinaisons complexes

Les synthèses des combinaisons complexes ont été effectuées soit dans des solvants organiques (acétonitryle, acétone), soit dans des solutions aqueuses. Les réactions entre le TlX_3 et les ligands en quantités correspondantes ont été conduites à un pH petit, variant entre 2 et 4, 5, à la température ordinaire. Rares ont été les cas où on a du rechauffer à une température de +70°C tout au plus, pour éviter la réduction du Tl (III) a Tl(I).

Pour les complexes de thiazol et d'imidazol on a employé comme dissolvant l'acétonitryle, tant pour le TlX_3 que pour les quantités stoechiométriques de ligandes. Les complexes qui s'en séparent se présentent sous forme de produits cristallins, qu'après filtrations et lavages avec des solvants adéquats (acétonitryle, éther éthylique) on sèche dans des exiccateurs sous vide. Il est à remarquer que les dérivés de BBI précipitent de la solution instantanément et ont une solubilité très réduite dans la majorité des solvants organiques.

Les complexes qui s'obtiennent dans des réactions en milieu aqueux sont ceux des acides pyridine-monocarboxyliques et ceux de la nicotinamide. Lorsqu'on utilise l'acide isonicotinique on doit rechauffer à 70°C pour que la réaction se produise.

Les réactions entre TlX_3 en acétonitryle et les ligands de la classe des dérivés de pirrazine et de piridazine (QUIN, BC, DMBC) dissous dans l'acétone ou dans l'alcool éthylique on conduit à une nouvelle série de complexes à l'état cristallin.

La séparation des complexes avec ADIP a lieu par le traitement des solutions de TlX_3 dans l'acétonitryle avec la solution du ligand en éther éthylique fraichement préparée, suivie par le refroidissement du mélange à zero degrés.

À l'exception des complexes avec BT les autres sont stables par rapport à l'air et à la lumière ; ceux avec les dérivés de pyridine sont légèrement hydrolisables.

Tableau 1

Quelques propriétés des complexes du Tl(III)

Formule du complexe	Symbole		Couleur		Point de fusion, [°C]	
	X=Cl	X=Br	X=Cl	X = Br	X = Cl	X = Br
$TlX_3.2BT$	I_a	I_b	blanc	vert-faible	164...165	156...157
$TlX_3.2ABT$	II_a	II_b	rouge	rouge	156	150
$TlX_3.2BI$	III_a	III_b	blanc	blanc	200...202	166
$TlX_3.2BBI$	IV_a	IV_b	blanc	jaune	206...207	172...174
$TlX_3.2BIC$	V_a	V_b	blanc	jaune-faible	248	234
$TlX_3.2PIC$	VI_a	VI_b	blanc	blanc	164...165	155...156
$TlX_3.3NIC$	VII_a	VII_b	blanc	blanc	224	204...205
$TlX_3.3NICA$	VIII_a	VIII_b	blanc	blanc	207	186
$TlX_3.3INIC$	IX_a	IX_b	blanc	blanc	241	227
$TlX_3.2QUIN$	X_a	X_b	blanc	blanc	225	195...197
$TlX_3.2BC$	XI_a	XI_b	jaune	vert-faible	166	158
$TlX_3.2DMBC$	XII_a	XII_b	jaune	jaune	201...202	190...192
$TlX_3.ADIP$	XIII_a	XIII_b	jaune	brun-rougeâtre	194	182...184

On a réalisé leur purification par des recristallisations qui reviennent de divers solvants : alcool éthylique, benzène, acétone.

Dans le tableau 1 on présente la série de complexes obtenue avec la mention de quelques propriétés physiques.

3. Résultats et discussions

Les complexes obtenus ont été caractérisés en nous basant sur leur investigation à l'aide des méthodes chimiques et physiques, à savoir : analyse élémentaire, déterminations des masses moléculaires et des conductibilités électriques molaires, spectres électroniques et spectres d'absorption infra-rouge (IR). Dans ce travail on présente une partie des résultats obtenus.

Les données de l'analyse élémentaire sont concentrées dans le tableau 2. En nous basant sur les résultats expérimentaux, trouvés en concordance avec ceux des calculs théoriques, on a atribué aux complexes étudiés les formules brutes correspondantes.

Tableau 2

Analyse élémentaire des complexes thalliques[*])

Formule du complexe	Symbole	C%		H%		N%		Tl%	
		c	t	c	t	c	t	c	t
$TlCl_3.2BT$	I_a	28,92	29,34	1,72	1,83	4,82	5,21	35,19	34,84
$TlBr_3.2BT$	I_b	23,51	22,98	1,39	1,41	3,91	3,78	28,61	28,34
$TlCl_3.2ABT$	II_a	14,09	14,25	1,56	1,48	10,96	11,24	40,01	40,43
$TlBr_3.2ABT$	II_b	11,18	10,88	1,24	1,17	8,69	8,85	31,71	30,98
$TlCl_3.2BI$	III_a	30,72	30,11	2,19	2,30	10,24	10,44	37,38	36,78
$TlBr_3.2BI$	III_b	24,69	25,07	1,76	1,59	8,23	8,79	30,04	29,63
$TlCl_3.2BBI$	IV_a	46,23	45,93	3,30	3,71	7,70	7,28	28,12	28,41
$TlBr_3.2BBI$	IV_b	39,05	39,48	2,79	2,90	6,50	6,79	23,75	24,21
$TlCl_3.2BIC$	V_a	30,34	29,81	1,57	1,48	8,85	9,11	32,30	32,47
$TlBr_3.2BIC$	V_b	25,05	25,83	1,30	1,20	7,30	6,88	26,27	27,12
$TlCl_3.2PIC$	VI_a	25,86	25,12	1,79	2,00	5,03	5,41	36,8	37,25
$TlBr_3.2PIC$	VI_b	20,85	21,30	1,45	1,56	4,05	4,38	29,56	30,21
$TlCl_3.3NIC$	VII_a	31,77	32,25	2,20	1,90	6,18	5,75	30,01	30,28
$TlB_3.3NIC$	VII_b	26,56	26,10	2,21	1,85	5,16	4,78	25,09	24,55
$TlCl_3.3NICA$	VIII_a	31,90	32,45	2,65	2,42	12,41	12,24	30,14	29,74
$TlBr_3.3NICA$	VIII_b	26,66	27,19	2,22	2,64	10,33	9,83	25,19	25,68
$TlCl_3.3INIC$	IX_a	31,77	31,02	2,20	1,89	6,18	5,91	30,01	30,66
$TlBr_3.3INIC$	IX_b	26,56	27,11	2,21	1,71	5,16	4,85	25,09	24,46
$TlCl_3.2QUIN$	X_a	33,64	33,21	2,34	2,70	9,81	10,25	35,81	35,24
$TlBr_3.2QUIN$	X_b	27,25	26,83	1,70	1,85	7,95	8,11	29,01	29,48
$TlCl_3.2BC$	XI_a	42,93	43,28	2,37	2,01	8,34	7,92	30,47	29,85
$TlBr_3.2BC$	XI_b	35,80	36,21	1,98	2,32	6,96	7,31	25,41	25,02
$TlCl_3.2DMBC$	XII_a	46,23	45,78	3,30	3,45	7,70	7,45	28,12	27,45
$TlBr_3.2DMBC$	XII_b	39,05	38,59	2,78	3,08	6,50	6,20	23,75	23,18
$TlCl_3.ADIP$	XIII_a	24,25	23,94	1,63	1,39	11,31	11,74	41,23	40,75
$TlBr_3.ADIP$	XIII_b	19,09	18,48	1,27	1,55	8,91	8,84	32,48	33,12

*) c = calculé ; t = trouvé.

Les déterminations des masses moléculaires ont été effectués par la méthode cryoscopique en utilisant des solvants adéquats, à savoir : dioxane, benzène, sulpholane, camphore. Les résultats expérimentaux sont indiqués dans le tableau 3.

Tableau 3

Données concernant les déterminations des masses moléculaires des complexes thalliques

Formule de complexe	Symbole	$M_{calculé}$	$M_{déterminé}$			
			Dioxane	Benzène	Camphore	Sulpholane
$TlCl_3.2BT$	I_a	580	590	603	—	—
$TlBr_3.2BT$	I_b	714	690	686	—	—
$TlCl_3.2ABT$	II_a	510	528	—	—	—
$TlBr_3.2ABT$	II_b	644	610	—	—	—
$TlCl_3.2BI$	III_a	546	—	—	—	520
$TlBr_3.2BI$	III_b	680	—	—	—	652
$TlCl_3.2BBI$	IV_a	726	—	—	—	712
$TlBr_3.2BBI$	IV_b	860	—	—	—	878
$TlCl_3.2BIC$	V_a	632	—	—	—	610
$TlBr_3.2BIC$	V_b	766	—	—	—	742
$TlCl_3.2PIC$	VI_a	554	—	—	489	—
$TlBr_3.2PIC$	VI_b	688	—	—	645	—
$TlCl_3.3NIC$	VII_a	679	—	—	638	—
$TlBr_3.3NIC$	VII_b	813	—	—	751	—
$TlCl_3.3NICA$	VIII_a	676	—	—	(500)	—
$TlBr_3.3NICA$	VIII_b	810	—	—	(630)	—
$TlCl_3.3INIC$	IX_a	679	—	—	721	—
$TlBr_3.3INIC$	IX_b	813	—	—	842	—
$TlCl_3.2QUIN$	X_a	570	544	—	—	—
$TlBr_3.2QUIN$	X_b	704	685	—	—	—
$TlCl_3.2BC$	XI_a	670	644	—	—	—
$TlBr_3.2BC$	XI_b	804	797	—	—	—
$TlCl_3.2DMBC$	XII_a	726	711	—	—	—
$TlBr_3.2DMBC$	XII_b	860	834	—	—	—
$TlCl_3.ADIP$	XIII_a	494	—	514	—	531
$TlBr_3.ADIP$	XIII_b	628	—	636	—	602

Pour les complexes I, II, X ... XII, de bons résultats ont été obtenus en utilisant le dioxane comme solvant. En outre, la cryoscopie en sulpholane, indiquée aussi dans la littérature [19] , a donné de bons résultats pour les complexes VI ... IX. Dans tous les cas les données expérimentalles prouvent que ces complexes sont mononucléaires.

En vue de l'appréciation du degré de dissociation électrolytique des complexes synthétisés on a effectué des déterminations des conductibilités électriques molaires dans des solvants de polarité différente. Dans ce but on a utilisé un conductomètre de type OK-102. On a effectué les déterminations sur des solutions de la même concentration, $5 \cdot 10^{-3}$ M. Dans le tableau 4 on présente les valeurs expérimentalles de la conductibilité molaire, Λ_M, des complexes thalliques.

Tableau 4

Données concernant les déterminations de conductibilité électrique molaire

Formule du complexe	Symbole	Λ_M, [Ω^{-1} cm^2 mol.$^{-1}$]			
		Dimethyl-formamide	Acétonitryle	Alcool éthylique	Acétone
$TlCl_3$.2BT	I $_a$	—	154,56	—	137,7
$TlBr_3$.2BT	I $_b$	—	124,29	—	128,2
$TlCl_3$.2ABT	II $_a$	—	134,8	—	107,2
$TlBr_3$.2ABT	II $_b$	—	—	—	99,30
$TlCl_3$.2BI	III $_a$	—	—	101,1	107,3
$TlBr_3$.2BI	III $_b$	—	—	98,3	—
$TlCl_3$.2BBI	IV $_a$	—	—	87,4	—
$TlBr_3$.2BBI	IV $_b$	—	—	80,4	—
$TlCl_3$.2BIC	V $_a$	—	—	80,5	—
$TlBr_3$.2BIC	V $_b$	—	—	74,8	—
$TlCl_3$.2PIC	VI $_a$	37,8	—	—	—
$TlBr_3$.2PIC	VI $_b$	32,5	—	—	—
$TlCl_3$.3NIC	VII $_a$	28,5	—	—	—
$TlBr_3$.3NIC	VII $_b$	26,7	—	—	—
$TlCl_3$.3NICA	VIII $_a$	35,4	—	—	—
$TlBr_3$.3NICA	VIII $_b$	28,4	—	—	—
$TlCl_3$.3INIC	IX $_a$	29,4	—	—	—
$TlBr_3$.3INIC	IX $_b$	30,5	—	—	—
$TlCl_3$.2QUIN	X $_a$	—	—	—	108,6
$TlBr_3$.2QUIN	X $_b$	—	—	—	98,4
$TlCl_3$.2BC	XI $_a$	—	—	—	114,4
$TlBr_3$.2BC	XI $_b$	—	—	—	110,3
$TlCl_3$.2DMBC	XII $_a$	—	—	147,5	—
$TlBr_3$.2DMBC	XII $_b$	—	—	141,9	—
$TlCl_3$.ADIP	XIII $_a$	—	105,4	—	113,2
$TlBr_3$ ADIP	XIII $_b$	—	95,4	—	106,4

Pour les complexes avec les ligands BT, ABT, QUIN, BC et DMBC les valeurs Λ_M correspondent à des électrolytes 1 : 1. Dans ces cas on peut admettre l'existence, dans la solution, des équilibres suivants :

$$(1) \qquad TlX_3 . 2L + (S) \rightleftharpoons [TlX_3 . 2L(S)],$$

$$(2) \qquad [TlX_3 . 2L(S)] \rightleftharpoons [TlX_2 . 2L(S)]^+ + X^-,$$

où L—ligand, X=Cl, Br et (S)—solvant.

Selon ce qu'on peut observer, l'action du solvant, en fonction de ses propriétés en tant que donneur, peut se manifester aussi dans le sens de compléter quelques points libres de l'entourage de l'atome central.

Les complexes V_a ... V_b se font remarqués par une solubilité réduite dans la plupart des solvants ce qui s'explique par la formation de chélates. Un comportement semblable on trouve dans le cas des complexes thalliques avec les dérivés de pyridine, (VI) ... (IX), dont les valeurs Λ_M, déterminées dans des solvants fortement polaires (dimethylformamide), sont beaucoup sous la limite admise pour les électrolytes (1 : 1). L'influence de l'atome de halogène est réduite ; les valeurs Λ_M pour les complexes avec le même ligand mais avec X différent ne se modifient pas substantiellement mais suivent l'ordre Cl > Br.

4. Conclusions

Les réactions entre TlX_3 (X=Cl, Br) et les ligands du type des hétérocycles organiques (L) mènent à la formation d'une nouvelle série de combinaisons complexes de rapports molaires différents : $TlX_3 . L$ (L=2,2'-azodipyridyle), $TlX_3 . 2L$ (L=benzthiazol, 2-aminobenzthiazol, benzimidazol, N-benzilbenzimidazol, l'acide benimidazolyle-2-carboxylique, l'acide picolinique, quinoxaline, benziocinoline et 2,7-dimethyl-benzocinoline) et $TlX_3 . 3L$ (L= l'acide nicotinique, l'acide isonicotinique et nicotinamide). Les données de l'analyse élémentaire et les déterminations des masses moléculaires indiquent la formation des complexes mononucléaires. Les complexes obtenus sont stables par rapport à l'air et à la lumière. Leur solutions dans des solvants organiques présentent des valeurs de la conductibilité électrique molaire, Λ_M, qui correspondent à un comportement d'électrolyte 1 : 1.

Reçue le 4 juillet 1978

Institut Polytechnique, Jassy,
Chaire de Chimie Anorganique et Analytique

BIBLIOGRAPHIE

1. **Артеменко М. В., Слинсаренко К. Ф., Ж. Укр. Хим, 38, 3, 227 (1972).**
2. Ouki A., Takenki T., Bull. Chem. Soc. Japan, **43**, *9*, 2840 (1970).
3. Carmichael W. M., Edwards D. A., J. Inorg. Nuclear Chem., 34, *4*, 1181 (1972).
4. **Алявя М. К., Риспаева Р. С., ЖНХ, 17, 4, 957 (1972).**
5. Walton R. A., J. Inorg. Nuclear Chem., 32, 2875 (1970).
6. **Кулба Ф. И., Макашев А. И., ЖНХ, 7, 661 (1962).**
7. Sutton G. I., Austral. J. Chem., **11**, 120 (1958).
8. **Кулба К. И., Баркусов А. В., ЖНХ, 14, 73 (1969).**
9. Walton R. A., Inorg. Chem., **7**, 640 (1968).
10. Lee A. G., J. Chem. Soc., A, **7** (1971).
11. **Захса Е. Р., Жоффе Д. Б.,** *Физические методы в химии гетероциклических соединении.* Изд. Химия, М., 1966.
12. **Катрицкий А. Р., Лаговский М.,** *Химия гетероциклических соединении.* **М., 1963.**
13. Cotton F. A., Johnson B. F., Wing R. M., Inorg. Chem., **4**, 502 (1965).
14. Biltman S., Rendall M., J. Amer. Chem. Soc., **66**, 540 (1944).
15. Badger G. M., Seidler J. H., Thomson B., J. Chem. Soc., 3211 (1951).
16. Reddy K. K., Rao N. V. S., Proc. Indian Acad. Sci., Sect. A, **70**, 81 (1969).
17. Bistrîszycki A., Przeworski G., Chem. Ber., **45**, 3483 (1912).
18. Kipalund A., Reiter E., Ber. dtsch. Chem. Ges., **60**, B, 664 (1927).
19. Burwell, R. L., J. Amer. Chem. Soc., **81**, 3799 (1959).

COMBINAŢII COMPLEXE ALE Tl(III) CU LIGANZI DE TIPUL HETEROCICLURILOR ORGANICE

I. Sinteza şi unele proprietăţi fizice

(Rezumat)

Reacţiile dintre TlX_3 (X = Cl, Br) şi liganzi de tipul heterociclurilor organice conduc la formarea unor combinaţii complexe de raporturi molare diferite : $TlX_3 \cdot L$ (L = 2,2'-azodipiridil), $TlX_3 \cdot 2L$ (L = benztiazol, 2-aminobenztiazol, benzimidazol, N-benzil-benzimidazol, acidul benzimidazolil-2-carboxilic, acidul picolinic, chinoxalină, benzocinolină, 2,7-dimetil-benzocinolină) şi $TlX_3 \cdot 3L$ (L = acidul nicotinic, acidul izonicotinic, nicotinamidă). Datele analizei elementare şi determinările de mase moleculare indică formarea unor complecşi mononucleari. Complecşii obţinuţi sînt stabili faţă de aer, lumină şi umiditate. Soluţiile lor, în solvenţi organici, prezintă valori ale conductibilităţii electrice molare, Λ_M, corespunzătoare unor electroliţi univalenţi 1 : 1.

BULETINUL INSTITUTULUI POLITEHNIC DIN IAŞI
Tomul XXVI (XXX), fasc. 3—4, 1980
Secţia II
CHIMIE şi INGINERIE CHIMICĂ

C. Z. 546.73; 546.74; 576.8

CONCENTRAREA Co(II) ŞI Ni(II) CU COLECTORI MICROBIOLOGICI (LEVURĂ DIN GENUL *CANDIDA*)

DE

VIORICA DULMAN, CONSTANŢA BURCOVEANU şi SIMON FIŞEL

1. Introducere

Este cunoscută influenţa Co(II) şi Ni(II) asupra diferitelor tipuri de microorganisme şi capacitatea lor de a se adapta conţinutului diferit de Co(II) din mediul de viaţă [1]...[6]. De asemenea Co(II) şi Ni(II) au fost concentraţi cu colectori microbiologici din soluţii diluate [7], [8].

În lucrarea de faţă sînt prezentate rezultatele obţinute în problema selectării speciilor de bacterii sau levuri care prezintă capacitatea de a acumula Co(II) sau Ni(II) prin dezvoltare în mediu nutritiv sau prin suspendarea celulelor microorganismelor în tampon fosfat glucozat. În urma încercărilor efectuate s-a izolat o specie de levură din genul *Candida* care, suspendată în tampon fosfat glucozat în prezenţa Co(II) sau Ni(II), poate acumula cantitativ aceste elemente. Pentru aceasta s-au stabilit condiţiile de timp, pH, concentraţia glucozei şi a elementelor din mediu precum şi influenţa unor agenţi complexanţi asupra concentrării Co(II) şi Ni (II) aflaţi în amestec.

2. Partea experimentală

S-a lucrat cu următoarele tulpini bacteriene potenţial patogene: *Escherichia coli*, *Proteus vulgaris*, *Klebsiella pneumoniae* şi trei specii de levuri nepatogene aparţinînd genului *Candida*. Tulpinile au fost întreţinute prin repicări succesive la intervale de trei zile pe mediu optim: bulion simplu pentru bacterii şi mediu S a b o u r a u d pentru levuri. Cultura de 48 de ore obţinută pe mediu solid repartizat în cutii P e t r i a fost recoltată prin spălare cu ser fiziologic, obţinîndu-se o suspensie densă care s-a standardizat prin determinarea greutăţii unei anumite cote uscată la 105°C pînă la greutate constantă.

Suspensia standardizată s-a introdus steril în mediu S a b o u r a u d lichid sau în tampon fosfat glucozat în prezenţa Co(II) sau Ni(II). Probele s-au menţinut în condiţii statice la 37°C pentru bacterii şi la temperatura camerei (20° ± 2°C) pentru levuri.

Soluţiile de Co(II) şi Ni(II) conţin azotaţii corespunzători.

După intervalul de timp necesar probele au fost centrifugate 30 min. la 13 000 rot./min. (Janetzki K 24). Depozitul obținut a fost calcinat, solubilizat cu apă regală, evaporat și reziduul s-a reluat cu apă bidistilată. Co(II) și Ni(II) conținuți în soluție au fost determinați prin spectrofotometrie de absorbție atomică (S.P. - 90, Pay Unicam). Pentru aprecierea capacității de acumulare a Co(II) și Ni(II) s-a calculat coeficientul de distribuție.

$$K_D = \frac{\text{cantitatea, [μg], acumulată de suspensia celulară ce corespunde la 1 g de masă uscată}}{\text{cantitatea, [μg], rămasă în 1 ml mediu}}$$

și procentul de acumulare, $E\%$. Între K_D și $E\%$ există relația :

$$K_D = \frac{E\%\, V}{(100 - E\%)m},$$

unde : V — volumul probei, [ml], m — greutatea masei microorganismului adăugat, [g], exprimată în masă uscată la 105°C.

3. Rezultate și discuții

Pentru testarea capacității de acumulare a unor bacterii sau levuri microorganismele s-au dezvoltat în mediul lor de cultură optim, lichid, în prezența ~ 3μg/ml Co(II) sau Ni(II) timp de 4 zile. Paralel s-au efectuat

Tabelul 1

Acumularea Co (II) și Ni (II) de diferite specii de bacterii si levuri

Bacterii		Cobalt		Nichel	
		Bulion simplu	Tampon fosfat	Bulion simplu	Tampon fosfat
		$E\%$	$E\%$	$E\%$	$E\%$
Klebsiella pneumoniae	*A*	4,3	2,8	1,6	4,7
	B	4,3	2,5	0,5	8,2
	C	2,9	2,9	1,1	2,3
	D	1,8	1,8	1,7	4,4
Escherichia coli	*A*	4,9	3,4	3,5	5,8
	B	10,4	5,2	2,1	1,1
	C	4,3	1,8	1,1	2,2
	D	1,8	1,8	1,7	2,3
Proteus vulgaris	*A*	3,9	4,2	2,1	2,3
	B	3,9	4,2	2,1	2,3
	C	3,8	4,2	1,9	9,6
Levuri		Mediu Sabouraud	Tampon fosfat	Mediu Sabouraud	Tampon fosfat
		$E\%$	$E\%$	$E\%$	$E\%$
Candida	*A*	4,3	26	2,3	29
	B	6,5	49	1	44
	C	4,3	31	2,3	29

determinări prin suspendarea celulelor în tampon fosfat glucozat cu pH= 7,2, avînd aceeași concentrație a elementelor. S-a lucrat pentru bacterii cu $m \sim 0{,}04$ g iar pentru levuri cu $m \sim 0{,}06$ g/50 ml mediu. Rezultatele obținute sînt prezentate în tabelul 1.

Se observă că în condițiile indicate pentru speciile de bacterii, atît în mediu de cultură cît și în tampon fosfat concentrarea ionilor este sub 10%, în timp ce pentru levuri suspendate în tampon fosfat glucozat rezultatele sînt semnificativ mai mari. De aceea atenția noastră s-a îndreptat spre una din cele trei levuri ale genului *Candida*, notată arbitrar cu *B* (tabelul 1).

3.1. Influența cantității de glucoză

Celulele levurice au fost suspendate în tampon fosfat cu pH = 7,2, care conține ~3 μg/ml Co(II) sau Ni(II) și glucoză între 0,5 și 5%. Se obține procentul de acumulare maxim pentru glucoză 2% atît pentru Co(II) cît și pentru Ni(II).

3.2. Influența pH-ului

Suspensia de *Candida* s-a introdus în tampon fosfat cu valori ale pH-ul cuprinse între 3,8 și 8,3, glucoză 2% și aproximativ 3 μg/ml Co(II) sau Ni (II), timp de 3 zile. Se obține procentul de acumulare maxim pentru Co(II), 78% și pentru Ni(II), 71% la pH = 5,2 după care acesta scade în ambele cazuri (fig. 1).

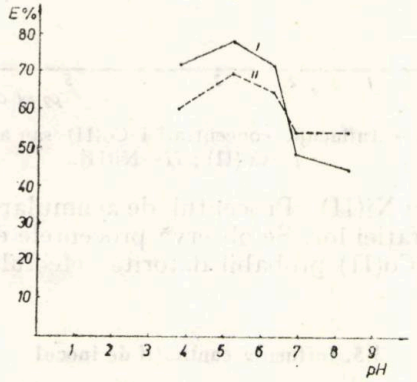

Fig. 1. — Influența pH-ului: *I* — Co(II); *II* — Ni(II).

3.3. Influența timpului

În tampon fosfat cu pH = 5,2, care conține 0,46 μg/ml Co(II) sau 0,48 μg/ml Ni(II), glucoză 2% și o masă levurică $m = 0{,}1033$ g pentru 25 ml mediu, s-a efectuat separarea celulelor levurice de lichid după diferite intervale de timp (4 ... 124 ore). La 69 de ore se obține o acumulare maximă pentru Co(II), de 99% și pentru Ni(II), de 98% (fig. 2). Din primele 4 ore de contact între celule și mediu ionii sînt acumulați în procentaje însemnate (~88% Co(II) și ~ 73% Ni(II)).

3.4. Influența concentrației Co(II) și Ni(II)

Acumularea ionilor de Co(II) sau Ni(II) depinde de concentrația ionilor în mediu după cum reiese din fig. 3. În soluții diluate (0,46 μg/ml, Co(II) sau 0,48 μg/ml Ni(II), pH = 5,2, glucoză 2%, timp de 69 de ore, m = 0,1033 g/25 ml mediu) acumularea este maximă, de 99%, pentru Co

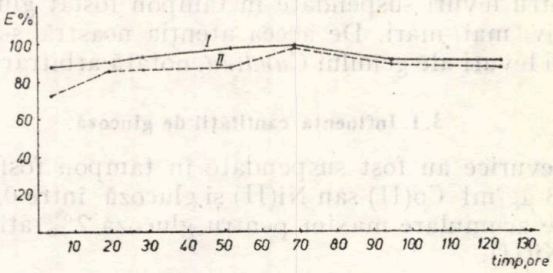

Fig. 2. — Influența timpului: I—Co(II); II—Ni(II).

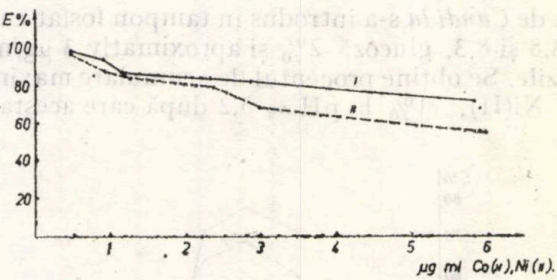

Fig. 3. — Influența concentrației Co(II) sau a Ni(II): I—Co(II); II—Ni(II).

(II) și de 98 % pentru Ni(II). Procentul de acumulare a celor doi ioni scade cu creșterea concentrației lor. Se observă procentele de acumulare mai mici ale Ni(II) față de Co(II) probabil datorită efectului mai toxic al Ni(II) față de Co(II).

3.5. Influența cantității de inocul

În condițiile optime de pH, concentrație a glucozei și concentrație a elementelor s-au suspendat cantități variabile de celule levurice ce corespund la valori pentru m cuprinse între 0,1033 ... 0,3099 g/25 ml mediu și s-au separat de lichid după 24 ore. Creșterea cantității de inocul duce la o mărire a procentului de acumulare de la 91 % la 99,7% pentru Co(II) și de la 86% la 99,6% pentru Ni(II) și la o îmbunătățire a randamentului de acumulare.

3.6. Influența spălării celulelor asupra îndepărtării ionilor acumulați

S-au menținut probele în condițiile optime indicate mai sus, apoi s-au filtrat prin creuzete filtrante G_5 și depozitul s-a spălat de trei ori cu 10 ml ser fiziologic iar în final cu 10 ml apă bidistilată. Apele de spălare au fost anali-

zate și se constată că se îndepărtează în acest mod ~ 5% Co(II) și 7% Ni(II), care reprezintă cantitatea din ionii studiați legată slab la suprafața celulelor, restul presupunîndu-se fie legați puternic de peretele celular, fie pătrunși în interiorul celulelor. Fenomenul de transport intracelular a Co(II) și Ni(II) la levura *Saccharomyces cerevisiae* a fost pus în evidență [5].

3.7. Influența agitării

S-au calculat procentele de acumulare pentru probe agitate magnetic față de probe neagitate, menținute în aceleași condiții și s-au obținut valori superioare (cu ~ 8 %) pentru cele menținute static.

3.8. Influența unor agenți complexanți asupra concentrării Co(II) și Ni(II)

În condițiile optime indicate mai sus o cantitate de levură egală cu 0,0676 g/25 ml mediu concentrează din soluții diluate (~ 0,5 μg/ml Co(II) sau Ni(II)) 96% Co(II) sau 91% Ni(II). Dacă elementele se găsesc în amestec cu aceeași cantitate de levură procentul de acumulare al Co(II) scade la 65% iar cel al Ni(II) crește la 94%.

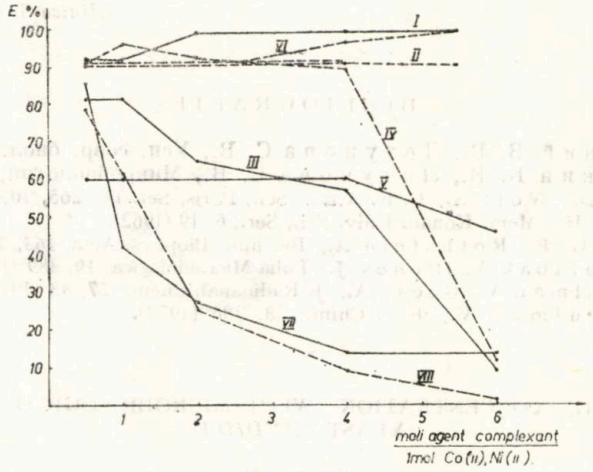

Fig. 4. — Influența agenților complexanți asupra acumulării Co(II) și Ni(II) aflați în amestec; *I* — Co(II); *II* — Ni(II) (în prezența SCN^-); *III* — Co(II); *IV* — Ni(II) (în prezența nitrozo-R); *V* — Co(II); *VI* — Ni(II) (în prezența dimetil glioximei); *VII* — Co(II); *VIII* — Ni(II) (în prezența EDTA).

S-a studiat influența diferitelor concentrații ale unor agenți complexanți ca: SCN^-, dimetilglioxima, EDTA, nitrozo-R asupra concentrării Co(II) și Ni(II) aflați în amestec. Rezultatele sînt prezentate în fig. 4. Se observă că se modifică raportul concentrărilor Co(II) și Ni(II) sub influența agenților complexanți menționați dar nu se poate obține o separare a lor. Procentele de acumulare se micșorează în prezența EDTA și nitrozo-R. La concentrații

de 6...10 ori mai mari ale acestor agenţi complexanţi nu se acumulează nici unul din cei doi ioni, probabil datorită incapacităţii levurii de a extrage ionii metalici din complecşii formaţi în soluţie.

4. Concluzii

1. Din speciile de bacterii şi levuri testate cu privire la capacitatea lor de concentrare a Co(II) sau Ni(II) s-a selectat o specie de levură din genul *Candida*, care suspendată în tampon fosfat glucozat poate concentra cantitativ Co(II) sau Ni(II) din soluţii diluate ($< 0{,}5$ μg/ml).

2. Se poate presupune că Co(II) sau Ni(II) concentrat se află puternic legat la suprafaţa celulelor sau pătruns intracelular deoarece o mică cantitate se îndepărtează prin spălarea repetată a masei levurice.

3. Agenţii complexanţi adăugaţi amestecului de Co(II) şi Ni(II) modifică raportul de concentrare al Co(II) şi Ni(II) dar nu pot duce la o separare a celor două elemente.

Primită la 21 noiembrie 1978

Institutul politehnic, Iaşi,
Catedra de chimie anorganică şi analitică
şi
Institutul de medicină şi farmacie, Iaşi,
Clinica V-a medicală

BIBLIOGRAFIE

1. Ковальский В. В., Летунова С. В., Усп. совр. биол., 71, 57 (1964)
2. Ковальский В. В., Летунова С. В., Микробиология, 32, 859 (1963).
3. Bertrand D., Wolf A., C. R. Acad. Sci., Paris, Ser. D., 265, 1053 (1967).
4. Nakamura H., Mem. Konan. Univ. Sci., Ser., 6, 19 (1962).
5. Fuhrmann G. F., Rothstein A., Biochim. Biophys. Acta, *163*, 325 (1968).
6. Fencl Z., Zalabak V., Benes J., Folia Microbiologica, 19, 489 (1974).
7. Fişel S., Dulman V., Cecal A., J. Radioanal. Chem., 27, 83 (1975).
8. Fişel S., Dulman V., Rev. Chim., 28, 286 (1977).

Co(II) AND Ni(II) CONCENTRATION WITH MICROBIOLOGICAL COLLECTORS (YEAST *CANDIDA*)

(Summary)

Co(II) and Ni(II) can be concentrate quantitatively using as microbiological collector a stain of yeast *Candida* by suspending the culture in glucose-phosphate buffer. There have been studied the optimal conditions (pH, time, concentration of elements) and the influence of some complexing agents on the accumulation of a mixture of Co(II) and Ni(II).

BULETINUL INSTITUTULUI POLITEHNIC DIN IAȘI
Tomul XXVI (XXX), fasc. 3—4, 1980
Secția II
CHIMIE ȘI INGINERIE CHIMICĂ

C. D. 661.8...511, 661.525

CONTRIBUTIONS À L'ÉTUDE PHYSIQUE ET CHIMIQUE DES TRANSFORMATIONS EN PHASE SOLIDE, SOUS L'INFLUENCE DE LA TEMPÉRATURE, DANS UN MÉLANGE BINAIRE DE SULFURE ET D'AZOTATE D'AMMONIUM

II. LA RÉACTION ENTRE MoS_2 et NH_4NO_3

PAR

IANCU HÎNCU, ELENA ȘTEFANCU et DRAGOȘ ȘTEFANCU

1. Introduction

Dans les Notes antérieures [1]...[3] ont été étudiées les réactions chimiques, en phase solide, ayant lieu entre des sulfures de cuivre, zinc, plomb, bismuth et l'azotate d'ammonium seul ou en mélange avec du NaCl. Dans cette Note on propose un mécanisme des transformations thermiques dans le domaine de températures 25°...400°C pour le mélange binaire MoS_2 + + NH_4NO_3. La stabilité thermique et les produits de la décomposition chimique de l'azotate d'ammonium ont été analysés dans la Note [3]. MoS_2 est stable du point de vue thermique dans le domaine de températures étudié.

On admet que la réaction ci-dessous a lieu :

$$MoS_2 + 7NH_4NO_3 \rightleftarrows MoO_3 + 7N_2 + 14H_2O + 2SO_2,$$

compte tenu que MoO_3 est stable en réaction avec l'azotate d'ammonium [4].

Le calcul de l'entalpie et l'énergie libre de réaction et leur variation avec la température ont donné les valeurs suivantes :

$$\Delta_R H^0_{298} = -466{,}96 \text{ Kcal}, \quad \Delta_R G^0_{298} = -657{,}00 \text{ Kcal},$$

$$\Delta_R H^0_T = -419{,}58 - 106{,}24\,T - 0{,}177\,T^2,$$

$$\Delta_R G^0_T = -419{,}58 + 0{,}24\,T \lg T - 1{,}70\,T + 1{,}77.10^{-2}T^2.$$

Le diagramme $\Delta_R G^0_T = f(T)$ (fig. 1) montre que cette réaction est possible dans le domaine de températures 25°...400°C.

Les réactions chimiques ont été étudiées par analyse thermodifférentielle (ATD) et les produits des réactions ont été identifiés à l'aide des spectres en infrarouge (IR) et les rayons X.

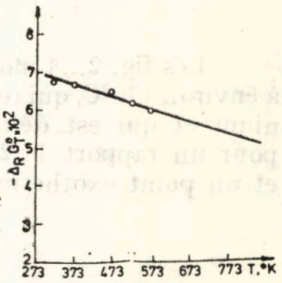

Fig. 1. — La variation de l'energie libre de réaction $\Delta_R G^0_T$, [Kcal], avec la température.

2. Partie expérimentale

2.1. L'étude par ATD

Ont été préparés des mélanges en diverses proportions de MoS_2 et NH_4NO_3, à savoir : 1 : 1 ; 1 : 1,5 ; 1 : 2 ; 1 : 2,5. Les courbes ATD sont représentés dans les fig. 2...5.

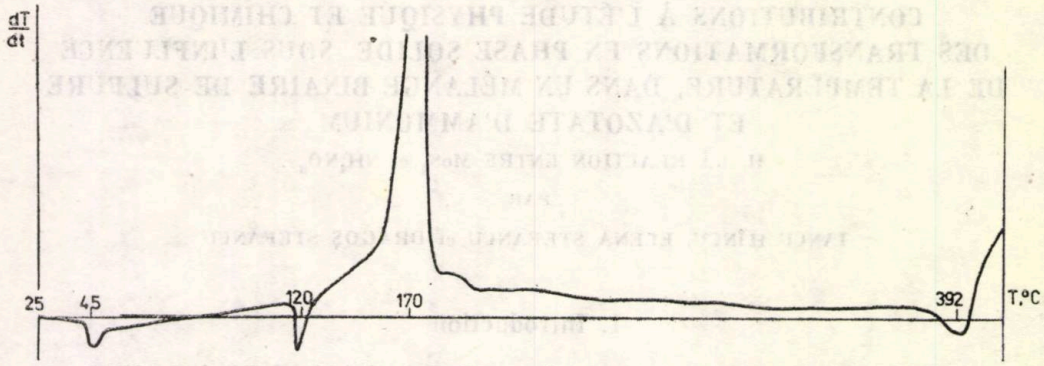

Fig. 2. — La courbe ATD pour le mélange $MoS_2 + NH_4NO_3$ en rapport 1 : 1.

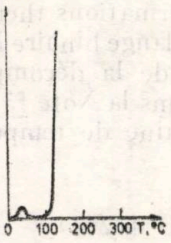

Fig. 3. — La courbe ATD pour le mélange $MoS_2 + NH_4NO_3$ en rapport 1 : 1,5.

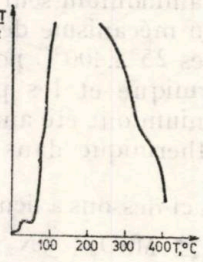

Fig. 4. — La courbe ATD pour le mélange $MoS_2 + NH_4NO_3$ en rapport 1 : 2.

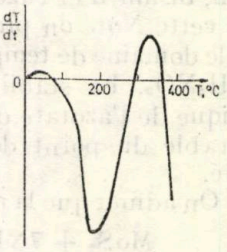

Fig. 5. — La courbe ATD pour le mélange $MoS_2 + NH_4NO_3$ en rapport 1 : 2,5.

Les fig. 2...4 montrent que la réaction chimique a lieu avec explosion à environ 170°C, qui représente la température de fusion de l'azotate d'ammonium et qui est déterminée par la décomposition de celui-ci. La fig. 5, pour un rapport 1 : 2,5 des composants, a un point endotherme à 180°C et un point exotherme à 340°C où a lieu la reaction chimique.

2.2. L'étude par rayons X

Les spectres des rayons X ont été enregistrés à un appareil du type TUR-60 M avec une anticathode de Cu, écran de Ni, en utilisant des rayons K du Cu. Les paramètres de l'appareil sont : 10 mA, 40KV, le temps d'exposition 2 h.

On a préparé des échantillons calcinées à 180°C (*a*) et à 340°C (*b*). Les résultats sont concentrés dans le tableau 1.

Tableau 1

Les résultats de l'analyse par rayons X du mélange $MoS_2 + NH_4NO_3$

Echantillon	*d/n*	*I*	Echantillon	*d/n*	*I*
a	5,98	10	*b*	3,45	8
	2,68	8		2,69	10
	2,31			2,26	1
	2,02	2		1,93	2
	1,57	7		1,83	1
	1,52	7		1,66	2
	1,24	2		1,57	2
	1,09	4		1,38	1
	1,02	1		1,26	1
				1,22	2
				1,03	1
				0,91	3
				0,87	9

Si l'on compare les valeurs obtenues par voie expérimentalle avec celles standards ou de la littérature [5] on constate que pour l'échantillon *a* sont présents des bandes caractéristiques de l'interaction Mo — S en molybdénite naturel ($d/n = 5{,}9$Å), ce qui prouve qu'à la température de 180°C la réaction n'a pas lieu. Pour la température de 340°C (l'echantillon *b*) on met en évidence la bande ayant $d/n = 3{,}45$Å qui correspond à la bande standard, de 3,46 Å, pour le MoO_3.

3. Conclusions

Par les résultats obtenus on peut tirer la conclusion que la réaction étudiée est possible jusqu'à la température de 400°C ayant une double importance. Premièrement, en ce qui concerne les sulfures, on a étudié la possibilité de leur dissolution avec du NH_4NO_3. Deuxièmement, en ce qui concerne le NH_4NO_3, on a étudié la possibilité de son stabilisation. On sait que ce produit est employé sur une large échelle mais son emmagasinage est dangereux parce qu'il explose facilement, la réaction de décomposition en étant catalysée par des acides, des métaux en poudre, le NaCl [6], [7]. On a étudié alors la possibilité d'inhiber cette décomposition en employant de la carbamide [8], la thiourée [9], etc. Les résultats obtenus ont montré que des mélanges en proportions données d'azotate d'ammonium et de sulfures permettent que la décomposition de NH_4NO_3 ne soit pas explosive.

Reçue le 11 décembre 1978

Institut Polytechnique, Jassy,
Chaire de Chimie Anorganique et Analytique

BIBLIOGRAPHIE

1. Hîncu I., Golgoțiu T., Bul. Inst. polit., Iași, **XVII (XXI)**, *3—4*, s. II (1971).
2. Hîncu I., Golgoțiu T., Bul. Inst. polit., Iași, **XIX (XXII)**, *1—2*, s. II, 25 (1973).
3. Hîncu I., Ștefancu E., Ștefancu D., Bul. Inst. polit., Iași, **XXV (XXIX)**, *3—4*, s. **II**, 47 (1979).
4. Pascal P., *Nouveau traité de Chimie Minérale*. T. **XIV**, Masson et C-ie, Paris.
5. Diemann E., Naturwisenschaften, **63**, *8*, 385 (1976).
6. Dimitriades B., Dissert. Abstr., USA, 5, 1508 (1962).
7. Keenan A. G., Dimitriades B., J. Chem. Phys., **37**, *8*, 1583 (1962).
8. Bozman B. J., J. Phys. Chem., 32, 280 (1959).
9. Bobrownicki W., Biskupski A., Kolaczkowski A., Chem. Stosow., 21, *1*, 3 (1977).

CONTRIBUȚIE LA STUDIUL FIZICO-CHIMIC AL TRANSFORMĂRILOR ÎN FAZĂ SOLIDĂ, SUB INFLUENȚA TEMPERATURII, ALE UNOR AMESTECURI BINARE DE SULFURI ȘI AZOTAT DE AMONIU

II. Reacția între MoS_2 și NH_4NO_3

(Rezumat)

S-au studiat reacțiile, în fază solidă, dintre MoS_2 și NH_4NO_3. În acest scop s-au calculat entalpia de reacție, energia liberă de reacție și variația lor cu temperatura. Transformările fizice și chimice au fost urmărite prin metoda ATD. Produșii de reacție s-au identificat prin spectre de raze X.

BULETINUL INSTITUTULUI POLITEHNIC DIN IAŞI
Tomul XXVI (XXX), fasc. 3—4, 1980
Secţia II
CHIMIE şi INGINERIE CHIMICĂ

D.C. 547.259.8

ELECTRONIC SPECTRA OF SOME MIXED CHELATES OF Pd (II) WITH α-AMINO ACIDS (II)

BY

OLGA VICOL and ŞT. RĂPEDE

1. The synthesis and IR spectra of some new chelates of Pd (II) with various α amino acids were described in a previous work [1].

This study lead us the conclusion that in both complexes [PdAnGl] and [PdAnV] the α amino acids are linked to the central metallic ion by the amino and carboxylic groups.

The present paper investigates the UV and visible spectra of these mixed chelates in order to determine their configuration.

2. It is well known from the literature [2]...[4] that the electronic spectra of the complex combinations with d^8 ions in the square-planar configuration show strong bands assigned to a charge transfer mechanism as well as very weak bands generated by d—d transitions.

The most probable order of the energy levels in the plane-tetragonal symmetry was given by H. B. Gray and C. J. Bolhausen using the theory of the molecular orbitals.

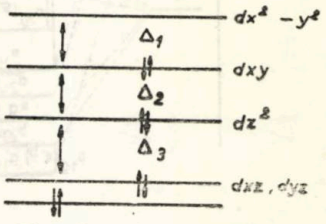

Fig. 1. — The order of the energy levels for the plane tetragonal symmetry for a d^8 ion.

The three parameters Δ_1, Δ_2 and Δ_3 representing the orbitals energies separating the four energy levels are given in Fig. 1.

Three singlet—singlet transitions are foreseen for the $[PdCl_4]^{2-}$ and they appear in the spectrum as in Fig. 1.

It is well known the fact that all square-planar complexes with simple ligands are diamagnetic containing a metallic ion d^8. For such complexes the fundamental state is $^1A_{1g}$.

3. As in the case of $[PdCl_4]^{2-}$ the studied chelates are regarded as complexes containing ligands without π-orbital systems.

In this case one can anticipate that the absorbtion bands of these combinations are a result of three d—d transitions, two bands being assigned to a $L \rightarrow M$ charge transfer transitions. The three $d-d$ transitions are :

$$^1A_{1g} \rightarrow {}^1A_{2g}[b_{2g}(\pi^*) \rightarrow b_{1g}(\sigma^*)],$$
$$^1A_{1g} \rightarrow {}^1B_{1g}[a_{1g}(\sigma^*) \rightarrow b_{1g}(\sigma^*)],$$
$$^1A_{1g} \rightarrow {}^1E_g[e_g(\pi^*) \rightarrow b_{1g}(\sigma^*)].$$

The three d—d transitions are equally forbidden and of a very weak intensity.

Two more charge transfer transitions can also be anticipated, corresponding to the following unielectronic ones :

$$^1A_{1g} \rightarrow {}^1A_{2u}\,[b_{2u}(\pi) \rightarrow b_{1g}(\sigma^*)],$$
$$^1A_{1g} \rightarrow {}^1E_u\,[e_u(\pi^b) \rightarrow b_{1g}(\sigma^*)].$$

They are transitions from the molecular orbitals essentially ligand to those essentially localised on the metallic ion.

The calculations have shown that the last transition, $^1A_{1g} \rightarrow {}^1E_u$, is more intense that the $^1A_{1g} \rightarrow {}^1A_{2u}$ one.

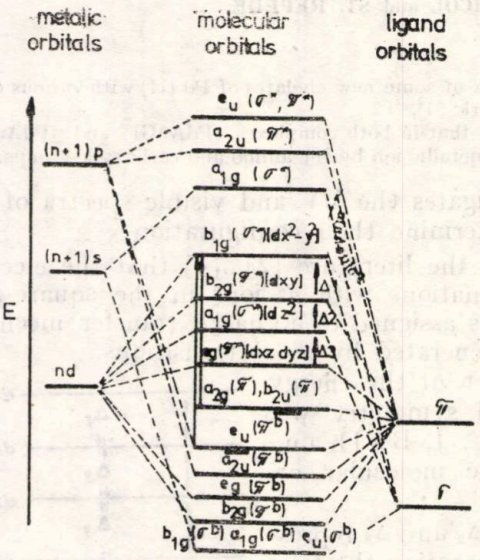

Fig. 2. — The orbital diagram for square-planar complexes with d^8 ions.

The electronic spectra of the mixed chelates we prepared show all the bands mentioned by the literature.

Table 1 shows for each complex the appearence of two intense charge transfer bands and three weak bands, the later resulting from the d—d transitions.

From a comparison with the data in the literature as referred to the electronic spectra of the complex Pt(II) and Pd(II) halides we remarked that in our complexes the bands are shifted as compared to those of $K_2[PdCl_4]$.

This is, of course, a result of substitution of the Cl^- ligand with alanine, glicocole and valine.

4. As we localized the d—d bands we can proceed to the calculations of the crystal field splitting parameters Δ_1, Δ_2 and Δ_3.

The L e v e r's method [5] was applied for this purpose. The calculations take into account the R a c a c h parameters wich refer, as it is well known, to interelectronic repulsions.

Table 1

The Spectral Properties of some Metallic Compounds of Pd(II) with α Amino acids

Compound	ν_{max} cm^{-1}	ε_{max}	Attribution
$K_2[PdCl_4]$	16 700		$^1A_{1g} \rightarrow {}^1A_{2g}$
	21 500		$^1A_{1g} \rightarrow {}^1B_{1g}$
	23 300		$^1A_{1g} \rightarrow {}^1E_{1g}$
	36 000	1.2×10^4	$^1A_{1g} \rightarrow {}^1A_{2u}$
	44 900	3×10^4	$^1A_{1g} \rightarrow {}^1E_u$
[PdAnGl]	17 500	0.2	$^1A_{1g} \rightarrow {}^1A_{2g}$
	21 000	2.7	$^1A_{1g} \rightarrow {}^1B_{1g}$
	23 154	3.6	$^1A_{1g} \rightarrow {}^1E_{1g}$
	31 000	0.025×10^4	$^1A_{1g} \rightarrow {}^1A_{2u}$
	48 300	1×10^4	$^1A_{1g} \rightarrow {}^1E_u$
PdAnV	17 197	1	$^1A_{1g} \rightarrow {}^1A_{2g}$
	20 360	1.5	$^1A_{1g} \rightarrow {}^1B_{1g}$
	22 232	1	$^1A_{1g} \rightarrow {}^1E_{1g}$
	31 000	0.0235×10^4	$^1A_{1g} \rightarrow {}^1A_{2u}$
	47 660	1.34×10^4	$^1A_{1g} \rightarrow {}^1E_u$

Lever, in his work [5], recommends for the calculations of the splitting parameters the use of the following equations:

$$E_{(\nu_1)} = \Delta_1 - C, \quad E_{(\nu_4)} = \Delta_1 + \Delta_2 - 4B - C,$$
$$E_{(\nu_2)} = \Delta_1 + \Delta_2 + \Delta_3 - 3B - C,$$

where $B = 683\ cm^{-1}$ and $C = 2\ 620\ cm^{-1}$. The results of these calculations are tabulated in Table 2.

Table 2

The Crystal Field Splitting Parameters in the Mixed Chelate Compounds of Pd(II) with α-Amino acids

Compound	Δ_1 cm^{-1}	Δ_2 cm^{-1}	Δ_3 cm^{-1}
$K_2[PdCl_4]$*)	19 150	6 200	1 450
[PdAnGl]	20 120	6 232	1 471
[PdAnV]	19 817	5 895	1 189

*) From literature.

Comparing with the results given in the literature for the Pd(II) complex halides a good agreement is obvious.

The results we obtained studying the electronic spectra of the mixed chelates of Pd(II) allowed us to conclude that these compounds have a square-planar configuration.

Conclusions

The electronic spectra of the mixed chelate compounds of Pd(II) with some α-amino acids are determined ; they prove the existence of a square-planar configuration.

The crystal field splitting parameters of these compounds are calculated.

Received, November 11, 1978

Polytechnic Institute, Jassy,
Department of Inorganic and Analytical Chemistry

REFERENCES

1. Vicol O., Repede Şt., Lascăr V., Bul. Inst. polit., Iaşi, **XXV** (**XXIX**), *3—4*, s. II **17** (1979).
2. Gray H. B., Balhausen C. J., J. Am. Chem. Soc., **85**, *3*, 260 (1963).
3. Fenske R. F., Martin D. S., Rendenberg K., Inorg., Chem. 1, *8*, 441 (1962)
4. Carlin R. L., *Transition Metal Chemistry*. 1965.
5. Lever A. B., *Inorganic Electronic Spectroscopy*. Elsevier, Amsterdam, 1968, 164, 351.

SPECTRE ELECTRONICE ALE UNOR CHELAŢI MICŞTI AI Pd(II) CU α-AMINOACIZI

(Rezumat)

Se prezintă spectrele electronice ale unor chelaţi micşti ai Pd(II) cu α-aminoacizi pentru a dovedi configuraţia lor plan-pătrată.

S-au calculat, de asemenea, parametrii de scindare în cîmp cristalin ai acestor compuşi.

BULETINUL INSTITUTULUI POLIŢEHNIC DIN IAŞI
Tomul XXVI (XXX), fasc. 3—4, 1980
Secţia II
CHIMIE şi INGINERIE CHIMICĂ

D. K. 661.868.3

ELEKTRISCHE DIPOLMOMENTEN EINIGER Tl(III)-KOMPLEXVERBINDUNGEN

VON

N. CALU, I. BERDAN und AL. CAŞCAVAL

1. Einführung

In die Reaktionssisteme der Tl(III)-Salze und einige tertiären Amine bilden sich die Komplexverbindungen, die durch Elementaranalyse, elektrische Konduktibilität-Messungen, Molekulargewicht-Messungen auch die Spektralanalyse (UV, VIS, IR) charakterisiert sind [1]...[2].

Da die Bildung diesen Komplexen findet sehr oft durch einen „charge-transfer"-Mechanismus statt, die Dipolmoment-Messungen geben die wichtigste Informationen über den „charge-transfer"-Grad auch über die Bindungspolarität der Tl(III)-Ligand.

Die Messungen haben wir über die folgende Tl(III)-Komplex-Serie gemacht: $TlX_3.2BT$; $TlX_3.2AT$; $TlX_3.2BC$; $TlX_3.2DMBC$; $TlX_3.2QUIN$; $TlX_3.ADIP$, wo: X=Cl, Br; BT=Benzothiazol; AT=2-Amino-thiazol; BC=Benzocinnolin; DMBC=Dimethyl-benzocinnolin; QUIN=Quinoxalin; ADIP=2,2'-Azodipyridil.

Die Fachliteratur zeigt einige ähnliche Versuchen, so z.B. $TlCl_3$ mit Dioxan gibt einen $TlCl_3-2C_4H_8O_2$-Addukt mit $\mu=3{,}5D$ [3] und mit tris-*n*-Buthylphosphorsäure (TBP) bildet einen $TlCl_3.2TBP$-Addukt, der hat $\mu = 3{,}6D$, in Benzol, und eine modifizierte Trigonal-Bipyramidalstruktur in der die Koordination durch den Sauerstoffatom der $>P=O$ Gruppe aus dem tris-*n*-Buthylphosphorsäure-Molekul gemacht hat [4].

2. Ergebnisse. Diskussionen

In der Praxis haben wir die Messungen mit einem W.T.W. Typ DM01-Dipolmeter ausgeführt. Das Gerät wird für die drei Skale mit einer DK-metrische Zelle von Typ DFL-2 und den entsprechenden Standard-Lösungsmitteln vorbereitet.

Die Dipolmoment-Messungen brauchen die Lösungsmitteln mit kleinen Polarität wie Benzol, Cyclohexan, Dioxan u.a. Die Versuchen für die Awendungen des Benzols auch des Cyclohexans waren ohne Erfolg denn die Komplexe sehr unlöslich sind.

Durch die Anwendung des Dioxans auch Diäthyläthers haben wir die gute Ergebnisse dargestellt und einige wichtige Disskusionen können wir bemerken eben die weiche Interaktionen zwischen die Lösungsmittel und die Tl(III)-Komplexverbindungen sind.

Die benutzende Methode ist die H e d e s t r a n d-Methode die von L i p p e r t und M o l e ausgefüllt ist und die dielektrische Konstante (ε) auch die Brechnungindex (n) der Lösungen der Tl(III)-Komplexverbindungen brauchen [5].

Der Dipolmoment berechnet sich nach die allgemeine Gleichung:

$$\mu^2 = \frac{27KT}{4\pi N} \cdot \frac{(a_\varepsilon - a_n)M}{d_1(\varepsilon_1+2)^2},$$

wo: K — B o l t z m a n n s k o n s t a n t e ; T — die absolute Temperatur, [°K] ; d_1 — die Lösungsmittelsdichtung ; ε_1 — dielektrische Konstante der Lösungsmittels ; a_ε — der Abhang der Linie aus der Funktion $\varepsilon_{12} - \varepsilon_1 = f(w)$; a_n — der Abhang der Linie aus der Funktion $n_{12}^2 - n_1^2 = f(w)$; w — die Gewichtsfraktion der jeden Lösung ; M — Molekulargewicht der Komplexes; 1 ist Index für den Lösungsmittel und 12 für die Lösung.

In der Praxis, die Messungen haben wir über die Serie der wenigsten fünf Lösungen gemacht.

In die Tabellen 1....4 sind einige Messungen für die μ-Rechnung angegeben[1]).

Tabelle 1

Die Ergebnisse für die μ-Werte der $TlCl_3 \cdot 2BT$ Komplex

Probe	m_1 g	m_2 g	w	$\varepsilon_{12} - \varepsilon_1$	$n_{12}^2 - n_1^2$	a_ε	a_n
1	0,0112	10,34	$1{,}08.10^{-3}$	$0{,}8.10^{-2}$	$0{,}3.10^{-2}$		
2	0,0231	10,34	$2{,}20.10^{-3}$	$2{,}2.10^{-2}$	$1{,}1.10^{-2}$		
3	0,0342	10,34	$3{,}28.10^{-3}$	$3{,}4.10^{-2}$	$1{,}7.10^{-2}$	11,50	6,26
4	0,0451	10,34	$4{,}94.10^{-3}$	$4{,}7.10^{-2}$	$2{,}4.10^{-2}$		
5	0,0620	10,34	$5{,}90.10^{-3}$	$6{,}5.10^{-2}$	$3{,}4.10^{-2}$		

Tabelle 2

Die Ergebnisse für die μ-Werte der $TlBr_3 \cdot 2BT$ Komplex

Probe	m_1 g	m_2 g	w	$\varepsilon_{12} - \varepsilon_1$	$n_{12}^2 - n_1^2$	a_ε	a_n
1	0,0085	10,34	$8{,}2.10^{-4}$	$0{,}08.10^{-2}$	$1{,}7.10^{-2}$		
2	0,0120	10,34	$11{,}5.10^{-4}$	$0{,}34.10^{-2}$	$2{,}1.10^{-2}$		
3	0,0206	10,34	$19{,}8.10^{-4}$	$1{,}24.10^{-2}$	$2{,}6.10^{-2}$	9,25	6,06
4	0,0252	10,34	$24{,}4.10^{-4}$	$1{,}64.10^{-2}$	$2{,}9.10^{-2}$		
5	0,0342	10,34	$32{,}8.10^{-4}$	$2{,}40.10^{-2}$	$3{,}2.10^{-2}$		

[1]) m_1 — g Verbindung [Tl(III)-Komplex] ; m_2 — g Lösungsmittel. Für Dioxan, als Lösungsmittel, haben wir die folgende physikalische Konstanten : $\varepsilon_1^{20} = 2{,}209$; $n_1^{20} = 1{,}4192$; $d_1^{20} = 1{,}034$ benutzt.

Tabelle 3

Die Ergebnisse für die μ-Werte der $TlCl_3 \cdot ADIP$ Komplex

Probe	m_1 g	m_2 g	w	$\varepsilon_{12}-\varepsilon_1$	$\gamma_{12}^2-\gamma_1^2$	ε	n
1	0,0210	5,17	$4,1.10^{-3}$	$7,03.10^{-2}$	$4,07.10^{-3}$		
2	0,0281	5,17	$5,4.10^{-3}$	$9,27.10^{-2}$	$6,06.10^{-3}$		
3	0,0352	5,17	$6,7.10^{-3}$	$11,51.10^{-2}$	$7,14.10^{-3}$	15,3	0,9
4	0,0432	5,17	$8,3.10^{-3}$	$14,06.10^{-2}$	$8,94.10^{-3}$		
5	0,0628	5,17	$12,0.10^{-3}$	$19,08.10^{-2}$	$10,8.10^{-3}$		

Tabelle 4

Die Ergebnisse für die μ der $TlBr_3 \cdot ADIP$ Komplex

Probe	m_1 g	m_2 g	w	$\varepsilon_{12}-\varepsilon_1$	$\gamma_{12}^2-\gamma_1^2$	ε	n
1	0,0101	10,34	$0,90.10^{-3}$	$0,60.10^{-2}$	$1,95.10^{-3}$		
2	0,0135	10,34	$1,30.10^{-3}$	$1,35.10^{-2}$	$2,50.10^{-3}$		
3	0,0519	20,68	$2,50.10^{-3}$	$2,30.10^{-2}$	$2,90.10^{-3}$	10,2	0,5
4	0,0325	10,34	$3,10.10^{-3}$	$2,70.10^{-2}$	$5,20.10^{-3}$		
5	0,0621	10,34	$5,90.10^{-3}$	$5,40.10^{-2}$	$6,20.10^{-3}$		

In die Tabelle 5 sind die Dipolmoment-Werte in Diäthyläther und Dioxan für die ganze Komplex-Serie gegeben.

Tabelle 5

Elektrische Dipolmomenten der Tl(III)-Komplexverbindungen

Molekularformel der Komplexe	μ(D)		Molekularformel der Komplexe	μ(D)	
	Dioxan	Diäthyl-äther		Dioxan	Diäthyl-äther
$TlCl_3 \cdot 2BT$	5,58	5,02	$TlCl_3 \cdot 2BC$	4,35	—
$TlBr_3 \cdot 2BT$	4,75	4,30	$TlBr_3 \cdot 2BC$	3,70	—
$TlCl_3.2AT$	3,38	—	$TlCl_3 \cdot 2DMBC$	4,85	—
$TlBr_3 \cdot 2AT$	3,25	—	$TlBr_3 \cdot 2DMBC$	4,17	—
$TlCl_3 \cdot 2QUIN$	3,80	—	$TlCl_3.ADIP$	7,43	6,24
$TlBr_3 \cdot 2QUIN$	3,21	—	$TlBr_3 \cdot ADIP$	6,90	6,15

Wie kann man sehen, die große μ-Werte ist für die $TlX_3.ADIP$ auch $TlX_3.2BT$ in den die Tl(III)-Ligand Bindung als die Folge der „charge transfer" Komplex Tl(III)-Ligand genug polare ist. Auf den andere Seite, eine größere Polarität muß mit einer relativ kleine Symmetrie der eine Molekule verbunden.

So $TlX_3.2BT$ auch $TlX_3.ADIP$ kann auch, wie $TlX_3.2DMSO$, als pentakoordinaten Komplexen sein wie in die IR-Spektren zeigen sich [6].

Die kleinere Bazitität der Liganden QUIN, BC und DMBC besteht der hauptsätliche Grund für die niedrige Polarität der Tl(III)-Ligand Bindung aus den Tl(III)-Komplexverbindungen mit diesen Liganden; eine oktaedrische Symmetrie kann für diese Komplexen zuschreiben.

Aus diesen Tabelle 5 kann auch eine kleine Verringerung der Dipolmoment-Werte für denselben Ligand mit $TlBr_3$ wie für der $TlCl_3$ als die Folge der Lewis-Acidität der TlX_3 auch die „charge-transfer" Komplex bemerken.

Eingegangen am 10. Juli 1978

Technische Hochschule, Jassy,
Lehrstuhl für anorganische und analytische Chemie
und
Lehrstuhl für organische und
makromolekulare Chemie

LITERATURVERZEICHNIS

1. Berdan I., Bul. Inst. polit., Iaşi, **XXVI (XXX)**, *3—4*, s. II (1980).
2. Berdan I., Calu N., Rev. Roum. Chim., (unter Druck).
3. Шека И. А., ЖОХ, **26**, 25 (1956).
4. Шухалин Л. К., Пешехевицкий Б. И., Кузин А. И., Ж. Структ. хим., **9**, 158 (1968).
5. Mole F., Lippert E., Ztschr. Elektrochemie, **58**, 553 (1954).
6. Berdan I., unveröffentliche Daten.

DIPOLMOMENTELE ELECTRICE ALE UNOR COMBINAŢII COMPLEXE ALE Tl(III)

(Rezumat)

Se prezintă dipolmomentele electrice ale unor combinaţii complexe ale Tl(III) cu liganzi organici N-donori. Deoarece formarea acestor complexe decurge adesea printr-un mecanism cu transfer de sarcină, măsurătorile de dipolmoment furnizează indicaţii cu privire la gradul transferului de sarcină şi deci a polarităţii legăturii Tl(III)—ligand. Se stabileşte o corelaţie între bazicitatea liganzilor, valorile dipolmomentelor complecşilor şi simetria acestora.

BULETINUL INSTITUTULUI POLITEHNIC DIN IAŞI
Tomul XXVI (XXX), fasc. 3—4, 1980
Secţia II
CHIMIE şi INGINERIE CHIMICĂ

C. Z. 546.881 535.243

DETERMINAREA SPECTROFOTOMETRICĂ A VANADIULUI (V) CU *o*-FENILENDIAMINA

DE

M. FURNICĂ

1. Introducere

După cum se ştie vanadiul (V) are o mare putere de oxidare în mediu acid. Pe baza acestei proprietăţi au fost instituite o serie de metode de determinare fotometrică a **vanadiului (V)** prin oxidarea **unor** substanţe organice în produşi coloraţi. Printre acestea se numără difenilamina şi acidul difenilaminosulfonic [1], benzidina [2], **difen**ilbenzidina [3], stricnina [4], naftilamina [5] ş.a.

Pe de altă parte se cunoaşte proprietatea *o*-fenilendiaminei (*o*-FDA) de a se transforma prin oxidare într-un produs colorat [6], proprietate folosită, în cîteva lucrări anterioare, la determinarea spectrofotometrică a unor ioni cu caracter oxidant [7]...[9].

Toate aceste aspecte sugerează ideea că şi vanadiul (V) ar putea da o reacţie de culoare cu *o*-FDA. Într-adevăr, după cum era de aşteptat, s-a constatat că acesta formează cu *o*-FDA, în mediu acid, o coloraţie orange a cărei intensitate variază proporţional cu concentraţia soluţiei de V(V). De altfel, R o s e n t h a l e r [10] a arătat pentru prima dată că vanadatul de amoniu formează cu clorhidratul de *o*-fenilendiamină, în soluţie apoasă, o coloraţie portocalie pe care o recomandă pentru identificarea V(V).

S-a luat în studiu această reacţie, atît în scopul formulării mecanismului de reacţie, cît, şi mai ales, în scopul stabilirii condiţiilor de determinare spectrofotometrică a V(V) cu *o*-FDA.

La cercetarea reacţiei s-a plecat, ca şi în cazul ionilor studiaţi anterior, de la ideea că la baza formării coloraţiei orange ce se obţine la interacţiunea V(V) cu *o*-FDA în exces, se află procesul de oxidare a *o*-FDA în 2,3-diaminofenazină, întrucît potenţialul sistemului V(V)/V(IV) este suficient de ridicat [11].

2. Partea experimentală

În scopul stabilirii condiţiilor optime pentru desfăşurarea reacţiei dintre V(V) şi *o*-FDA s-a cercetat pe cale spectrofotometrică influenţa cantităţii de reactiv, domeniul de pH şi timpul de reacţie. Determinările au fost efectuate la un spectrofotometru VSU-1, cu o cuvă de 1 cm.

Soluţia iniţială de V(V) s-a preparat prin solvirea unei cantităţi determinate de monometavanadat de sodiu ($NaNO_3.4H_2O$) în apă distilată. Titrul soluţiei s-a determinat potenţiometric.

Soluția de *o*-FDA a fost preparată în concentrație de 1%, prin solvirea în apă distilată a unei cantități corespunzătoare de *o*-FDA recristalizată.

2.1. Stabilirea cantității de reactiv

Pentru stabilirea cantității de *o*-FDA necesară efectuării complete a reacției s-au adăugat volume diferite din soluția de *o*-FDA 1% peste aceeași cantitate de V(V). Valorile absorbanței obținute în cazul unei soluții cu un conținut de 5,094 μg V/ml sînt redate în fig. 1. Din grafic se observă că absorbanța maximă se obține la adăugarea unui ml din soluția de *o*-FDA și că o cantitate de cinci ori mai mare nu exercită nici o influență.

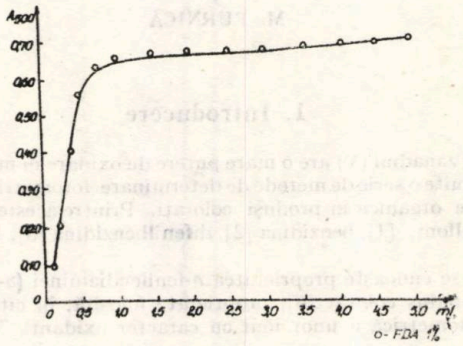

Fig. 1. — Variația absorbanței soluției de V(V) în funcție de cantitatea de *o*-FDA.

2.2. Stabilirea domeniului optim de pH

Studiul reacției dintre V(V) și *o*-FDA în exces efectuat asupra unor soluții cu un conținut constant în V(V) și *o*-FDA, dar de valori diferite ale pH-ului, a arătat că reacția dintre acești componenți decurge cel mai bine în domeniul de pH cuprins între 0,9 și 1,4, după cum rezultă din graficul redat în fig. 2. Ca urmare, determinările ulterioare s-au efectuat la pH= =1,2 realizat cu ajutorul unei soluții de H_2SO_4 1N.

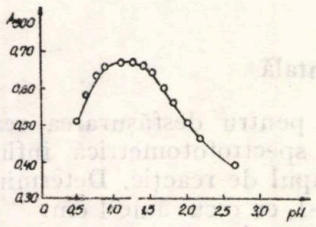

Fig. 2. — Variația absorbanței soluției de V(V), cu exces de *o*-FDA, în funcție de pH.

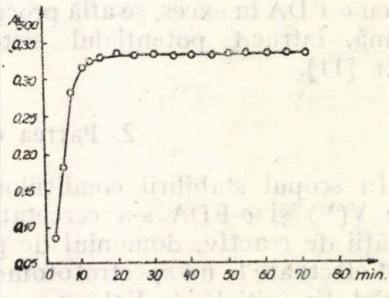

Fig. 3. — Variația absorbanței soluției de V(V) (C_V = 2,50 μg/ml), cu exces de *o*-FDA, în funcție de timp.

2.3. Stabilirea timpului optim de reacție

Urmărindu-se absorbanța unor soluții de V(V) cu exces de *o*-FDA în funcție de timp s-a constatat că aceasta atinge o valoare maximă aproximativ după 30 min. și rămîne apoi constantă, chiar după 60 min. Datele obținute sînt redate în fig. 3.

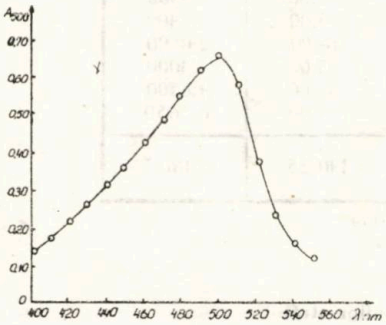

Fig. 4. — Curba de absorbție a soluției de V(V) cu *o*-FDA în exces.

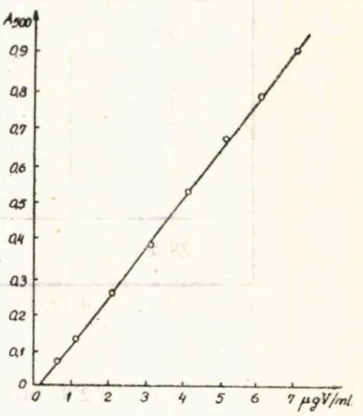

Fig. 5. — Variația absorbanței soluțiilor de V(V), cu exces de *o*-FDA, în funcție de concentrație.

2.4. Curba de absorbție

Studiul absorbanței soluțiilor de V(V) în funcție de lungimea de undă, în condițiile stabilite de timp, pH și cantitate de reactiv, a permis să se constate că maximul de absorbție se situează la 500 nm. Rezultatele sînt redate în graficul din fig. 4.

2.5. Stabilirea domeniului de concentrație în care legea Bouguer-Lambert-Beer este respectată

Urmărind variația absorbanței în funcție de concentrația soluțiilor de V(V), în condițiile de lucru stabilite, s-a constatat că există o dependență liniară între valorile absorbanței și concentrația soluțiilor de V(V) în domeniul 0,5...7,0 μg/ml, după cum rezultă din tabelul 1 și din graficul redat în fig. 5.

Determinările s-au efectuat în raport cu apa, deoarece în condițiile stabilite de pH excesul de *o*-FDA nu este oxidat de oxigenul din aer, în intervalul de timp stabilit.

Pe baza studiului efectuat se propune următorul mod de lucru : un volum determinat din soluția de V(V) se introduce într-un flacon Erlenmeyer de 25 ml, se adaugă 2ml H_2SO_4 1N, 2 ml soluție de *o*-FDA 1%, se completează la 10 ml cu apă distilată și după 30 min. se determină absorbanța față de apă.

Tabelul 1

Variația absorbanței în funcție de concentrația soluțiilor de V(V)

Concentrația V(V) [μg/ml] x	Absorbanța y	x^2	xy
0,5	0,063	0,25	0,0315
1	0,125	1,00	0,1250
2	0,245	4,00	0,4900
3	0,380	9,00	1,1400
4	0,515	16,00	2,0600
5	0,660	25,00	3,3000
6	0,775	36,00	4,6500
7	0,895	49,00	6,2650
28,5	3,658	140,25	18,0615

$y = -0,004 + 0,129x$; $S_y = 0,009$

2.6. Influența ionilor străini

În vederea determinării V(V) alături de alți ioni metalici s-a studiat influența unor ioni, care, de obicei, se găsesc în oțel. Astfel, s-a urmărit influența prezenței Cu(II), Ni(II), Co(II), Cr(III), Mn(II), Mo(VI), W(VI) asupra absorbanței unei soluții cu un conținut determinat în V(V) și cu exces de *o*-FDA. Ionii metalici au fost introduși în soluția de V(V) sub formă de săruri, în cantități variabile și apoi, conform modului de lucru propus, s-a măsurat absorbanța soluțiilor. Din datele obținute s-a constatat că prezența Mn(II) nu influențează determinările, în timp ce restul ionilor exercită o influență mai mică sau mai mare, în funcție de raportul [V]/[Me]. Astfel, W nu influențează pînă la raportul 1/20, Co pînă la 1/15, Cr pînă la 1/2, iar prezența Cu, Ni și Mo influențează chiar la raportul 1/1. În general determinările sînt influențate de prezența ionilor cu caracter oxidant. Influența Fe(III), care produce aceeași reacție de culoare cu *o*-FDA, poate fi eliminată prin complexare cu NaF.

2.7. Identificarea produsului colorat

În scopul identificării produsului colorat rezultat în reacția V(V) cu *o*-FDA în exces, s-a comparat spectrul de absorbție în vizibil al soluției de V(V) cu spectrul unei soluții de 2,3-diaminofenazină, obținute în aceleași condiții de pH. Din compararea acestor spectre s-a constatat că există o asemănare perfectă, ceea ce a permis să se conchidă că are loc o reacție de oxido-reducere între componenții studiați. În sprijinul acestei concluzii s-a ținut seama și de raportul de interacțiune, determinat spectrofotometric, 6V : 2 *o*-FDA. Acest raport, în cazul formării unei molecule de 2,3-diaminofenazină din două molecule de *o*-FDA, presupune un schimb de șase electroni, care se realizează pe seama reducerii V(V) la V(IV). Avînd în vedere că la

pH = 1 V(V) se află în soluție sub formă de VO_2^+]12], [13], reacția dintre V(V) și *o*-FDA s-ar putea considera de forma:

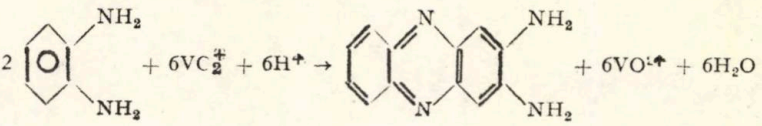

3. Concluzii

Au fost stabilite condițiile în care reacția de culoare dintre V(V) și *o*-FDA poate fi folosită la determinarea spectrofotometrică a V(V), în mediu acid (pH = 1,2). Absorbția maximă a luminii are loc la lungimea de undă de 500 nm, iar legea lui Bouguer-Lamert-Beer este respectată în limitele 0,5...7,0 μg V/ml.

Primită la 30 martie 1978

Institutul politehnic, Iași,
Catedra de chimie fizică

BIBLIOGRAFIE

1. Meaurio V. L., Ann. chim. anal., **23**, **47** (1918).
2. Alimarin I. P., J. Appl. Chem. (USSR), **17**, 83 (1944).
3. Wrightson F. M., Anal. Chem., **21**, 1543 (1949).
4. Gregory A. W., Chem. News, **100**, 222 (1909).
5. Albert F. M., Stoia M., Z. Analyt. Chem., **202**, 420 (1964).
6. Griess P., J., Prakt. Chem., **3**, 142 (1860).
7. Papafil M., Furnică D., An. șt. Univ. „Al. I. Cuza", Iași, s. I, **X**, *2*, 131 (1964).
8. Papafil M., Furnică M., Furnică D., An. șt. Univ. „Al. I. Cuza", Iași, **XI**, *2*, s. I,, 133 (1965).
9. Furnică M., An. șt. Univ. „Al. I. Cuza", Iași, **XIV**, *1*, s. I, 37 (1968).
10. Rosenthaller L., Mikrochem., **23**, 194 (1937).
11. Латимер В. М., *Окислительные состояния элементов и их потенциалы в водных растворах*, (пер. с англ.). Издатинлит, М., 1954, 269.
12. Сырокомский В. И., Клименко Ю. В., *Ванадатометрия. Новый метод объемного химического анализа*. Металлургиздат, М., 1950, 6.
13. Джаваров П. З., Чербачев С.В., ЖНХ, 9, 2 399 (1964).

DÉTERMINATION SPECTROPHOTOMÉTRIQUE DU VANADIUM (V) AVEC L'*o*-PHÉNYLÈNEDIAMINE

(Résumé)

On a étudié les conditions d'un dosage spectrophotométrique du V(V) en milieu acide (pH = 1,2) avec le réactif *o*-phénylènediamine. Le maximum d'absorbtion se produit à une longueur d'onde de 500 nm. La loi de Bouguer-Lambert-Beer est verifiée dans le domaine de concentrations 0,5...7 μg V/ml.

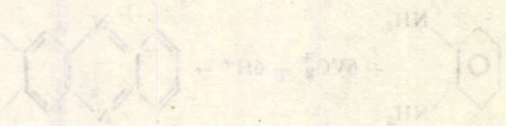

BULETINUL INSTITUTULUI POLITEHNIC DIN IAŞI
Tomul XXVI (XXX), fasc. 3—4, 1980
Secţia II
CHIMIE şi INGINERIE CHIMICĂ

D.C. 661.18

STRUCTURAL ADSORPTIVE CHARACTERIZATION OF THE ACTIVATED VOLCANIC TUFFS

BY

V. ABABI, N. BÎLBĂ, P. ONU, GH. MIHĂILĂ, N. NAUM and C. LUCA

Dedicated to Prof. CRISTOFOR SIMIONESCU of Member of the Academy of the Socialist Republic of Romania on his 60 th aniversary

1. Introduction

The volcanic tuffs have been formed in volcanic ash by an endogene and exogene alteration process during which the minerals have been transformed, from their primary stage, in some zeolites (feldspars, biotite, caolinite, calcite, quartz or colloidal silica). The most abundent zeolites in the volcanic tuffs are those having small pores, such as clinoptilolite, heulandite and phillipsite.

Porous framework of the zeolitic tuffs enables them to act as adsorbents for gas and liquid sorption and separation. The zeolite content of the tuffs is a controlling factor as regard their use in adsorption processes [1], [2]. Mineralogical investigation, performed on some volcanic tuffs occured in our country, has found that they consist of 40...70% clinoptilolite [3].

The present paper deals with the structural-adsorptive properties such as BET specific surface area, pore size distribution as well as adsorption capacity of native and activated volcanic tuffs mined from Pîglişa and Mirşid deposits.

2. Experimental

The experiments have been carried on using volcanic tuffs samples, having granule size less than 0.5 mm and 0.5...1.0 mm. Before the experiments the samples were activated thermically, by ion exchange and by acid treatment [4].

2.1. BET Specific Surface Area Determination

Specific surface area represents a physical characteristic of great importance of a solid, because its value expressed in m^2/g, gives indications as regards the behaviour of solid as adsorbent.

Determination of the specific surface area of the volcanic tuff samples was performed on the basis of nitrogen adsorption isotherms obtained at the liquid nitrogen temperature, i.e. —196°C. For this reason we employed a BET gravimetrical adsorption plant, represented in Fig. 1.

Before adsorption itself, the sample was heated, *in situ*, at 350°C, under a pressure as low as 10^{-3} mm Hg, for three hours, until the length of quartz spring remained constant.

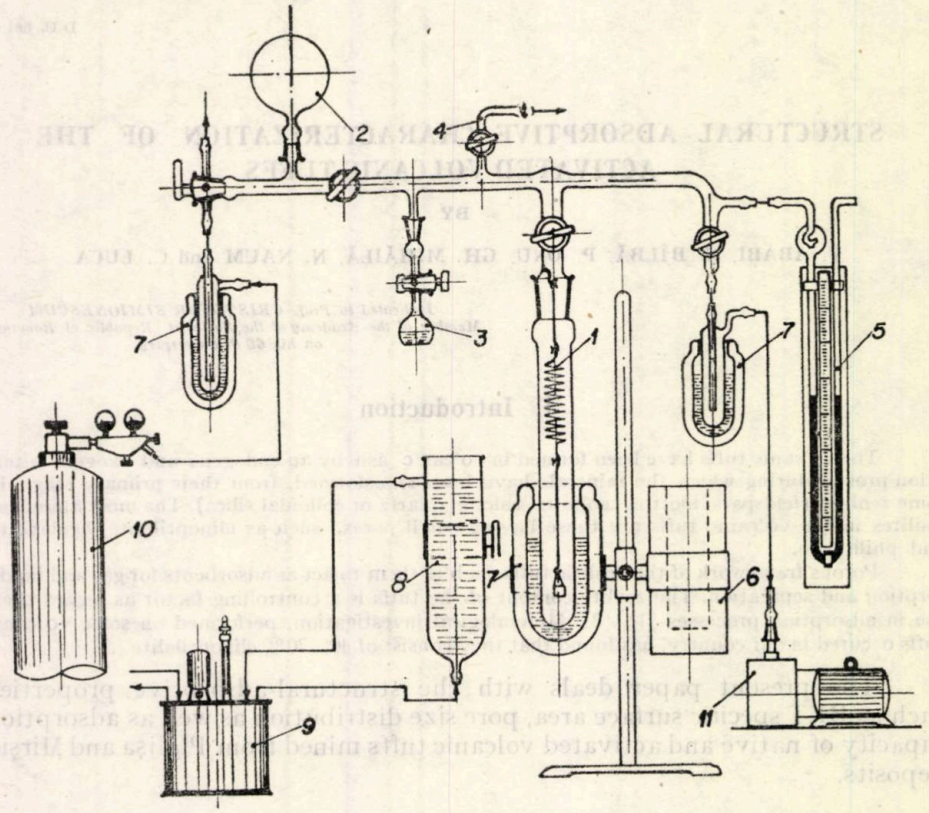

Fig. 1. — BET gravimetrical adsorption plant employed for adsorption study at different temperatures and variable pressure: *1* — quartz spring hanging adsorbent sample; *2* — balloon with purified nitrogen; *3* — vessel with liquid substance employed for adsorption; *4* — outlet to Mac-Leod manometer; *5* — U-shape mercury manometer; *6* — electric furnace; *7* — Dewar vessel for adsorption at —196°C; *8* — thermostating vessel employed in the case of vapour adsorption; *9* — thermostat; *10* — nitrogen cylinder; *11* — vacuum pumpe.

The adsorption isotherms of gaseous nitrogen, at —196°C, are shown in Fig. 2, at which the abscissa represents the relative pressure, P/P_0, and the ordinate, the quantity of adsorbed nitrogen, in mmol/g.

As it comes out from Fig. 2, the nitrogen adsorption isotherms are by the IIth type, what shows the presence of pores having radius larger than 200 Å. At these cases, at certain values of the adsorption pressure tàkes place capillary condensation of the adsorbed substance what makes possible that adsorption to increase again.

Specific surface area calculation was done on the basis of the expression :

(1) $$S_0 = \frac{mA_m}{m},$$

previously reported by S. Brunauer, P. H. Emmet and E. Teller where : A_m — nitrogen molecule area, equal to 16.2 Å^2 ; m — mass of the adsorbent sample, [g] ; n — number of the molecules that cover the surface as monomolecular leyer, determined from single leyer capacity, X_m, expressed by g nitrogen/g tuff. Its value is calculated from the expression:

(2) $$n = \frac{X_m N}{M},$$

where : $N = 6.02.10^{23}$ — Avogadro's number ; M — molecular weight of nitrogen.

Taking $m = 1$ and substituting in (1) the value of n, one obtains

(3) $$S_0 = \frac{X_m N}{M} A_m.10^{-20}, \ [m^2/g].$$

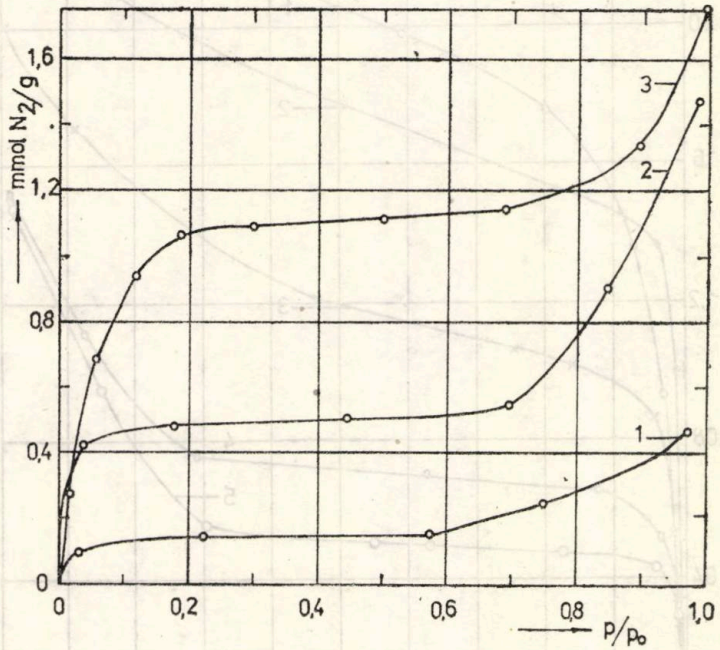

Fig. 2. — Adsorption isotherms of nitrogen at −196°C : *1* — volcanic tuff of Pîglișa deposit ; granule size 0.5...1.0 mm ; *2* — volcanic tuff of Mirșid deposit, granule size 0.5...1.0 mm ; *3* — volcanic tuff of Mirșid deposit, granule size 0.06 mm.

Determination of the single leyer adsorption capacity was approximated by Brunauer-Emmet's method, taking the point B as a characteristic one on isotherm, respectively the first intersection of tangent at isotherm, on its straight part.

The three natural volcanic tuffs, i.e. Pîglișa, Mirșid (0.5...1.0 mm) and Mirșid (0.06 mm), have their specific surface area of 13.65, 46.81 and 106.3 m^2/g respectively.

It has been found that BET specific surface area of the investigated samples has small values, characteristic for the first order solids in which the predominant is, especially, the outer surface.

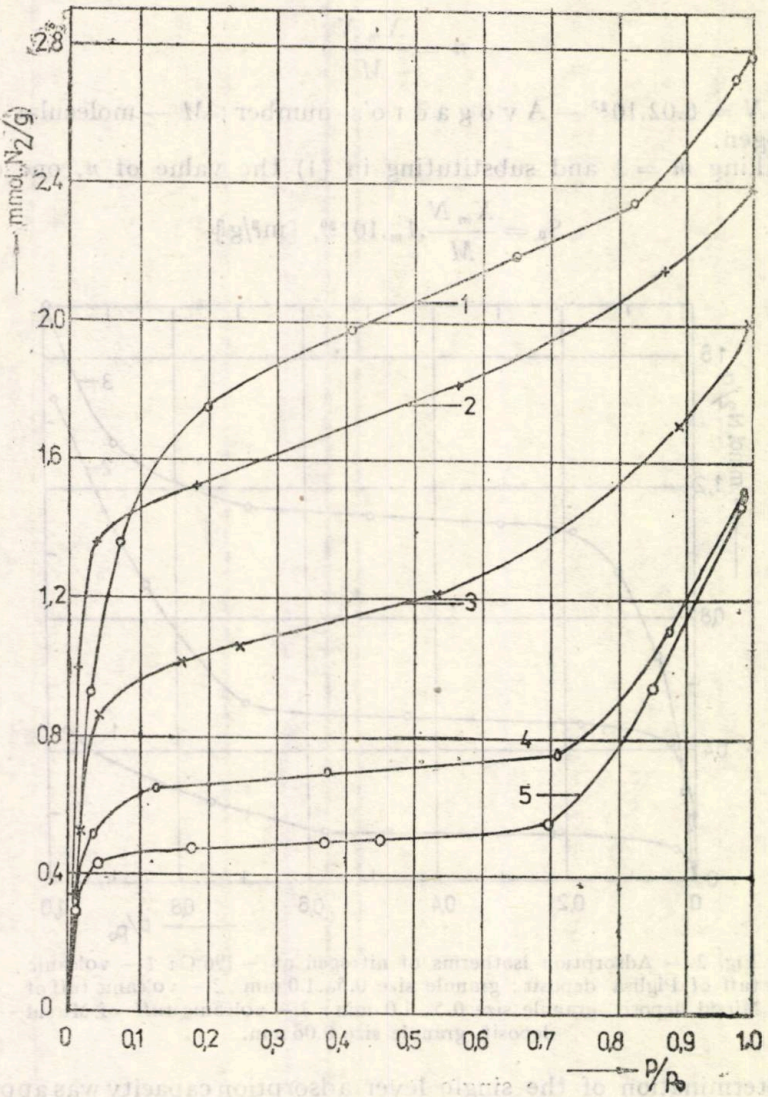

Fig. 3. — Adsorption isotherms of nitrogen at — 196°C, on the acid and thermic activated samples: *1* — 22.8% HCl; *2* — 11.3% HCl; *3* — 4.2% HCl; *4* — 0.8% HCl; *5* — 500°C.

By heating the volcanic tuff samples in air, their specific surface area increases up to a maximum value at 500°C, what corresponds to almost total removal of the water from tuff structure.

In order to increase the specific surface area of the volcanic tuff, their acid treatment was employed too. For this reason, the Mirşid tuff-samples, having granule size of 0.5...1.0 mm, have been treated with hydrochloric acid solutions with increasing concentration from 0.8% up to 22.8%HCl, for two hours, at 80°...90°C, followed by washing and heating up to 500°C. The nitrogen adsorption isotherms at —196°C of the samples activated in such a manner are shown in Fig. 3.

As acid concentration increases, there are taking place the removal of a certain part of cations and dealuminization in the samples, fact reported by the other authors too [7], what leads to free cavities and pores. Consequently, the specific surface area increases as acid concentration increases up to a certain value, over which the crystalline network is destroyed.

The specific surface area of the HCl activated samples is 193.1, 141.4, 103.4 and 66.3 m^2/g for Mirşid tuff, activated with 22.8% HCl solution, Mirşid tuff, activated with 11.3% HCl solution, Mirşid tuff, activated with 4.2% HCl solution and Mirşid tuff, activated with 0.8% HCl solution, respectively.

The data presented above show that the treatment with hydrochloric acid of the samples leads to a significant increase of their specific surface area, fact that improves their adsorption capacity.

2.2. Pore Volume Measurement and Pore Size Distribution

The volcanic tuffs have not only the microporous structure of clinoptilolite, but also the macroporous structure due to their manyminerals composition. The existence of large size pores is shown by the shape of the adsorption isotherms of nitrogen at —196°C. In order to know the pore size distribution of the pores having their radii between 75 and 75 000 Å, a mercury porometer, model AG/65, was employed. The cumulative distribution of macropore volume for the volcanic tuff of Mirşid deposit, granule size of 0.5...1.0 mm, is shown in Fig. 4.

The total volume of macropores is 0.19609 cm^3/g. The predominant macropores are they having the radii of 83.33, 125.00 and 600.00 Å, the sum of their area representing 14.60 m^2/g. The nitrogen adsorption at —196°C points out a specific surface area of 46.80 m^2/g. The difference of 34.0 m^2/g corresponds to the pores having their radii less than 75 Å, including clinoptilolite micropores, that has a specific surface area of approximately 30 m^2/g determined with liquid nitrogen.

Fig. 5 represents the cumulative distribution of macropores in Mirşid volcanic tuff, activated by ion-exchange with $CaCl_2$ solution.

The total volume of the macropores is 0.17578 cm^3/g. The predominant macropores correspond to the radii of 83.33, 100.00, 136.36, 250.00 and 1000.00 Å, their area summing 23.17 m^2/g. It has been found a less increase of the specific surface, but the pores having their size up to 250 Å is better shaped.

The presence of a macroporous structure beside a microporous one, that of clinoptilolite, makes these tuffs to behaviour nonselectively as adsorbants.

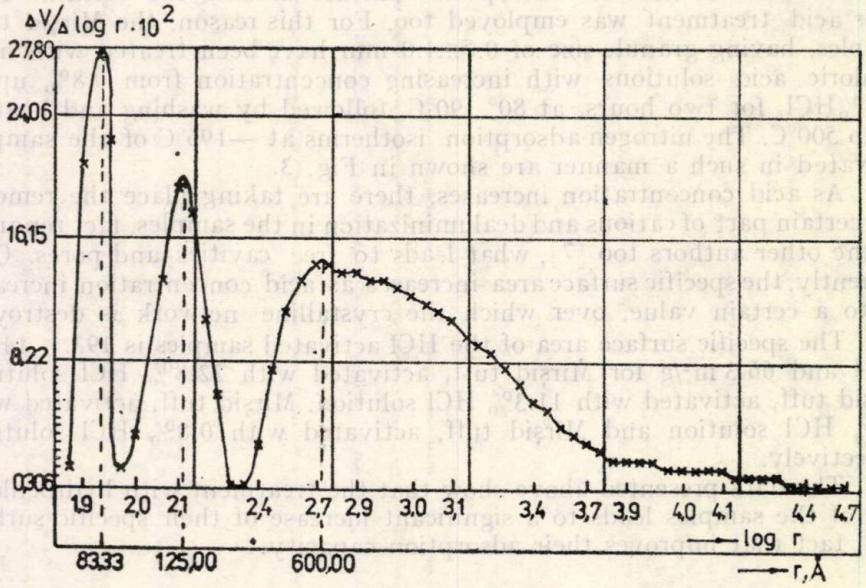

Fig. 4. — The cumulative macropore distribution of the Mirșid volcanic tuff.

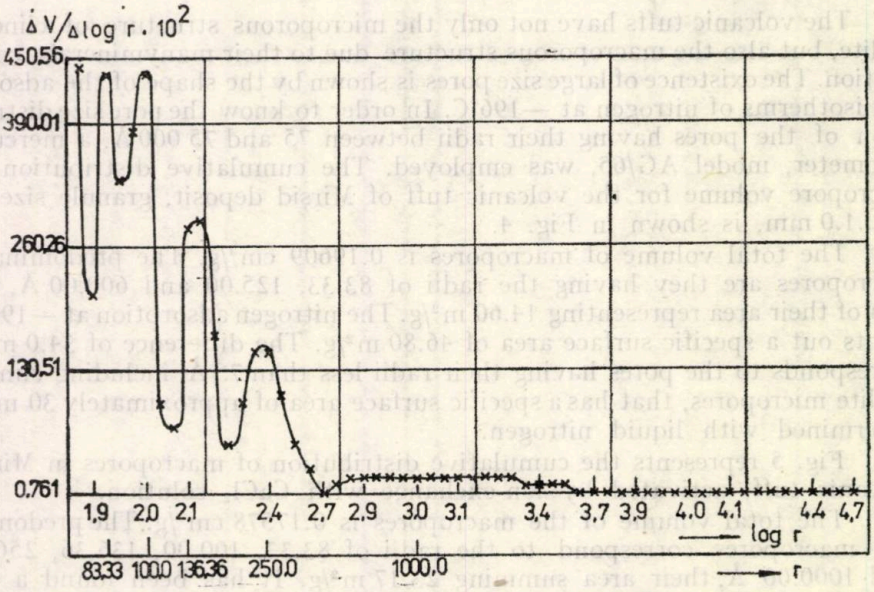

Fig. 5. — Cumulative distribution of the macropores of Mirșid volcanic tuff. activated by ion exchange in $CaCl_2$ solution.

2.3. Adsorption Capacity Determination

The experimental data have been shown that the native volcanic tuff samples do not have adsorption capacity because their porous structure is fulfiled by constitution water and by hydrated water. By thermic way, ion exchange as well as acid treatment activation, the volcanic tuff becomes an adsorbent with medium adsorption capacity.

The optimal activation temperature was determined on the basis of TG curve performed on a Mettler thermoanalyser. The water loss from the native Mirșid volcanic tuff takes place continuously up to 500°C. At a heating rate of 10°C/min. the water loss is 2, 6.5, 9.1, 10.5, 11.5, 12.0, 12.2, 12.6 and 13.0% at 100°, 200°, 300°, 400°, 500°, 600°, 700°, 800° and 900°C, respectively.

Determination of the adsorption capacity of the tuff samples was carried out using the same plant with quartz spring, at 20°C. The water adsorption isotherms on the activated Mirșid volcanic tuff samples are shown in Fig. 6.

The water adsorption on activated volcanic tuff is a reversible one. Adsorption capacity increases as activation temperature increases too and it has greater value for the ion exchange and acid treatment activated samples.

To show the selective behaviour of adsorption is useful to study the adsorption of some substances having their molecules of different size and spatial configuration, especialy, aromatic hydrocarbons.

Because the thermal activated tuff exhibits a small and nonselective adsorption, the adsorption of the aromatic hydrocarbons have been investigated on the samples of Mirșid tuff, activated by acid treatment, having specific surface area of 103.4 m^2/g and 193.1 m^2/g. The benzene adsorption isotherms at 20°C, are plotted on Fig. 7.

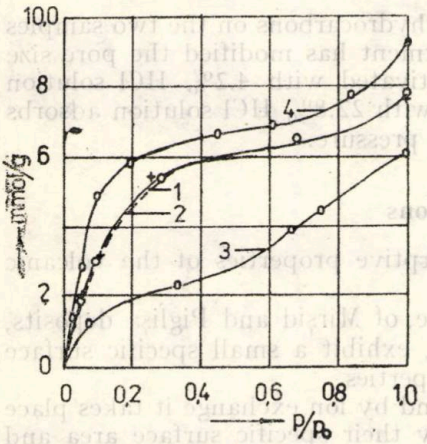

Fig. 6. — Water adsorption isotherms at 20°C, on activated Mirșid volcanic tuff: *1* — 500°C, for 2 h; *2* — 350°C, under vacuum of 10^{-3} mm Hg, for 3 h; *3* — 350°C, for 2 h; *4* — acid treatment.

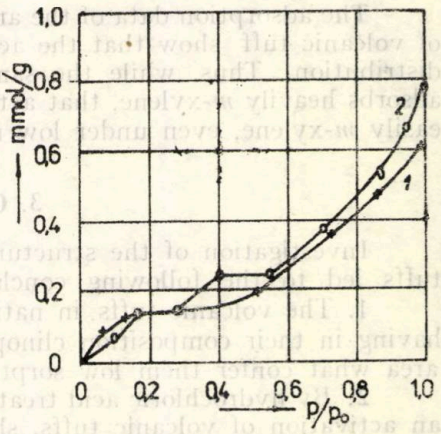

Fig. 7. — Benzene adsorption isotherms at 20°C, on acid activated Mirșid volcanic tuff: *1* — 4.2% HCl; *2* — 22.8% HCl.

The benzene adsorption isotherms are by the IInd type and present the capillary condensation fenomenon under relative presure higher than 0.5. The samples activated with 22.8% HCl solution exhibit a step by step adsorption, what is possible to explain by the presence of the pores with different radius.

On Figs. 8 and 9 are plotted the adsorption isotherms of the principal aromatic hydrocarbons on Mirşid volcanic tuff, activated by acid treatment.

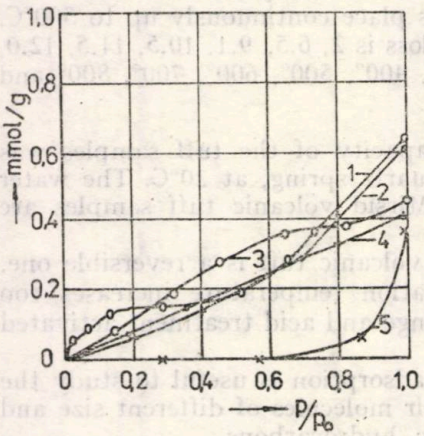

Fig. 8. — Adsorption isotherms of some aromatic hydrocarbons, at 20°C, on Mirşid volcanic tuff, activated with 4.2% HCl solution :
1 — benzene ; *2* — toluene ; *3* — *p*-xylene ; *4* — *o*-xylene ; *5* — *m*-xylene.

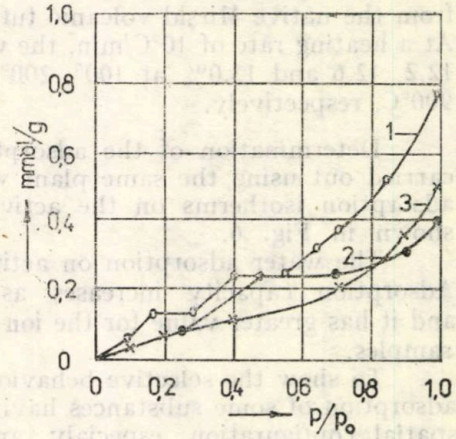

Fig. 9. — Adsorption isotherms of some aromatic hydrocarbons, at 20°C, on Mirşid volcanic tuff, activated with 22.8% HCl solution :
1 — benzene ; *2* — toluene ; *3* — *m*-xylene.

The adsorption data of the aromatic hydrocarbons on the two samples of volcanic tuff show that the acid treatment has modified the pore size distribution. Thus, while the sample activated with 4.2% HCl solution adsorbs heavily *m*-xylene, that activated with 22.8% HCl solution adsorbs easily *m*-xylene, even under low relative pressure.

3. Conclusions

Investigation of the structural-adsorptive properties of the volcanic tuffs led to the following conclusions :

1. The volcanic tuffs, in native state, of Mirşid and Piglişa deposits, having in their composition clinoptilolite, exhibit a small specific surface area what confer them low sorption properties.

2. By hydrochloric acid treatment and by ion exchange it takes place an activation of volcanic tuffs, shown by their specific surface area and adsorption capacity increase.

3. Pore size distribution points out the presence of micropores due to clinoptilolite as well as the existence of macropores having their radii of 83.3, 125.0 and 600.0 Å.

4. In activated state the tuffs adsorb water and aromatic hydrocarbons, but their behaviour is not selective enough because of secondary porosity.

Received, December 21, 1979

Polytechnic Institute, Jassy
Department of General and Technological Chemistry

REFERENCES

1. Peterson D. L., Helfferich F., Blytas G. C., Phys. Chem. Solids, **26**, 835–840 (1965).
2. Цицишвили Г. В., *Клиноптилолит*. Тр. симп. по вопр. иссл. и прим. клиноптилолита, Тбилиси, 1977, 12.
3. Fodor I., Piso P., Bărbat A., Bengeanu M., Felvinczi S., Ciceu S., Todan A., Simp. „Valorificarea substanţelor nemetalifere", Cluj-Napoca, Nov. 26–28, 1979, **3**, Paper Nr. *1*.
4. Ababi V., Onu P., Mihăilă Gh., Bîlbă N., Luca C., Naum N., Simp. „Valorificarea substanţelor nemetalifere", Cluj-Napoca, Nov. 26–28, 1979, **3**, Paper Nr. *12*.
5. Brunauer S., Emmett P. H., Teller E., J. Am. Chem. Soc., **60**, 309 (1938).
6. Gregg S. J., Sing K. S. W., *Adsorption Surface Area and Porosity* Acad. Press, London – N. Y., 1967.
7. Коридзе З. И., Крупеникова А. Ю., Андроникашвили Т. Г., *Клиноптилолит*. Тр. симп. по вопр. иссл. и прим. клиноптилолита, Тбилиси, 1977, 96.

CARACTERIZAREA STRUCTURAL-ADSORPTIVĂ A TUFURILOR VULCANICE ACTIVATE

(Rezumat)

S-au cercetat proprietăţile structural-adsorptive ale tufurilor vulcanice naturale şi activate provenite din zăcămintele de la Mirşid şi Piglişa. Probele de tuf au fost activate termic, chimic şi prin schimb ionic. Folosindu-se o balanţă cu spirală de cuarţ şi un porometru cu mercur s-a determinat suprafaţa specifică, distribuţia porometrică şi capacitatea de adsorbţie. Tufurile vulcanice naturale au o suprafaţă specifică redusă şi nu prezintă bune proprietăţi de sorbţie. Tratamentul acid şi schimbul ionic au condus la probe cu suprafaţă specifică mai mare şi cu bune proprietăţi de sorbţie faţă de apă şi faţă de hidrocarburi. Distribuţia porometrică scoate în evidenţă prezenţa porilor fini ai clinoptilolitului precum şi existenţa unor macropori cu raza de 83,3, 125,0 şi 600,0 Å.

BULETINUL INSTITUTULUI POLITEHNIC DIN IAŞI
Tomul XXVI (XXX), fasc. 3—4, 1980
Secţia II
CHIMIE şi INGINERIE CHIMICĂ

D.C. 66.095.1 ; 547.533 ; 66.097.7

ALKYLATION OF TOLUENE WITH METHANOL OVER SYNTHETIC ZEOLITES

III. INFLUENCE OF PROPERTIES AND STRUCTURAL CHARACTERISTICS OF THE CATALYSTS ON CATALYTIC ACTIVITY

BY

N. NAUM, V. ABABI, GH. MIHĂILĂ and EVELINA POPOVICI

1. Introduction

Due to its many possible transformations, toluene, obtained in large quantities from petrochemical processes, has more and more important uses. Among these uses there are also its alkylation and disproportionation.

For aromatic hydrocarbons alkylation, various reactants as well as different catalysts including the zeolite catalysts, have been employed.

The first investigations on alkylation the aromatic hydrocarbons over acid catalysts, was carried out by Streitwieser et al. [1] in 1959. A little latter, Sidorenko et al. [2] studied alkylation of toluene with methanol on faujasite zeolites, exchanged with alkaline earth metals, obtaining a mixture of xylenes, styrene and ethylbenzene. Recently, many studies as regards the toluene alkylation with methanol and formaldehyde on Y-type zeolites, activated at 350°C [3], [4], as well as toluene alkylation with methanol on X-type zeolites, exchanged with Rb, Ce, Ni and Co, and Y-type zeolites, dicationated at 480°C, have been performed [5].

On the basis of the last investigations there was found that, parallel to alkylation reaction, take place also isomerization and dimethylation reactions.

The zeolite catalysts work, generally, according with an ionic mechanism, by means of carbonium ion and the catalytic activity depends strongly on their acidity which can be transfered to the reactants by their surface [6]. The structural studies, by IR spectroscopy method, of zeolite surface, point out three potential catalytic positions, namely : the superficial hydroxylic groups (Brönsted acid sites), oxigen deficient silicon-aluminium linkages (Lewis acid sites) and cationic acid sites [7]. In the above mentioned literature there are not precised which of the three catalytic active positions are responsible for catalytic activity and selectivity. Some of the authors [3], [4] think that, for catalytic activity in the toluene alkylation with methanol, responsible are the superficial hydroxylic groups.

To establish the conditions for the formation, especially, of one of the three active catalytic position and the correlation between catalytic activity and chemical composition, as well as acid properties of the zeolite catalyst surface, in the present paper has been investigated the toluene alkylation with methanol over X-type and Y-type faujasite zeolites, exchanged with Mg^{2+}, Ce^{3+} and La^{3+}, activated at different temperatures.

Because the mechanism of alkylation process depends on the reactivity of aromatic nucleus positions, susceptible for electrophyl attack, acidity or basicity of the respective catalyst, temperature and the weight ratio reactant/catalyst, earlier, a theoretic study of toluene alkylation with $C_1...C_3$ alcohols was carried out [8]...[11]. This study was performed in order to establish the conditions which favour the selective obtaintion of

monoalkylated products, as well as minimizing the number of the experiments.

2. Experimental

The synthetic faujasite zeolites, like synthetic mordenite, exhibits a very good thermal and chemical stability, as well as a very high selectivity and catalytic activity.

Zeolite catalysts were prepared from the NaX and NaY molecular sieves, obtained on hydrothermal way in solutions of sodium silicate and aluminium silicate, with corresponding molecular ratios SiO_2/Al_2O_3, Na_2O/SiO_2 and H_2O/Na_2O. For comparison, a comercial NaY molecular sieve (D a v i d s o n) was employed too.

The structure and crystallinity of the obtained products was verified by means of X-ray diffraction.

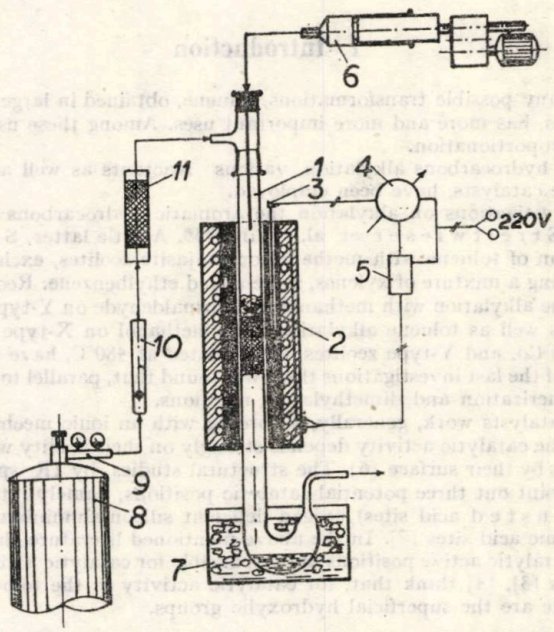

Fig. 1. — Laboratory plant employed for toluene alkylation in gaseous phase : *1* — quartz reactor ; *2* — electric tubular furnace ; *3* — thermocouple ; *4* — thermocontroller ; *5* — relay ; *6* — microfeeder with H a m i l t o n seringe ; *7* — cooling trap ; *8* — nitrogen bottle ; *9* — pressure reduction ; *10* — flowratemeter ; *11* — drying column.

The cationic forms containing bivalent metals (Mg^{2+}) as well as trivalent metals (Ce^{3+}, La^{3+}) were obtained by ion exchange at 85°C, in 0.1 M aqueous solutions of their nitrates. In such a way, by direct ion exchange, in several steps, there were obtained the forms Me^{II} Ze and Me^{III} Ze.

The prepared catalysts, in very fine powder form, having grain size less than 5 μ, were activated by gradual heating up to 500°C and 700°C,

respectively, conditions under which the three forms of acidity can occur. Crystallinity of the prepared catalysts, obtained by ion exchange and thermal activation, was verified by X-ray diffraction method, too. For some cases there were observed small modifications of reflections intensity against those of the original zeolite.

The acid properties as well as chemical and structural analysis of the employed catalysts have been already reported [12].

Finally, the powder catalysts were granulated using a patented procedure [13] by means of a laboratory extruder, having its outlet one milimeter in diameter, using micronized bentonite as binder. The catalyst, prepared in such a manner, was activated *in situ* for 3 hours, in dried nitrogen stream.

Alkylation of toluene with methanol, in gaseous phase, was carried out on a plant whose outline is represented in Fig. 1.

Toluene alkylation was conducted in the temperature range of 180°... 260°C, using toluene excess, with constant feed of the reactants. Nitrogen, as inert gas, entered the reactor with constant flowrate too. The reaction products were collected by an ice cooled trap. Their analysis was done chromatographically, using a gas chromatograph with hot wire detector, having inside a 0.3 cm in diameter and 4.5 m in length, packed with Chromosorb W mixed with 5% benton 34 and 5% dinonylephtalate [15].

3. Results and Discussion

The data concerning the composition of xylenes mixture, obtained by toluene alkylation with methanol, at different temperature, over faujasite catalysts, having various chemical composition, activated *in situ*, are summarized in Tables 1...4.

Table 1

Composition of Xylenes Mixture, [% mol.], *obtained on Faujasite Catalysts, Activated at 500°C.*

Temperature [°C]	MgY*)			CeY**)		
	p-xylene	*m*-xylene	*o*-xylene	*p*-xylene	*m*-xylene	*o*-xylene
180	15.00	5.00	80.00	33.14	11.60	55.26
200	19.85	6.36	73.79	43.96	21.05	34.99
220	22.38	19.96	57.64	46.83	30.92	22.25
240	18.77	28.62	52.61	41.96	37.96	20.08
260	14.04	35.46	50.50	36.54	45.67	17.79
	LaY*)			CeX**)		
180	28.14	9.94	61.92	16.48	5.21	78.31
200	41.05	25.37	33.58	24.09	13.22	62.69
220	44.51	29.66	25.83	25.26	28.89	45.85
240	39.98	35.27	25.75	22.33	37.43	40.24
260	35.09	40.89	24.02	17.60	44.01	38.39

*) NaY molecular sieve (D a v i d s o n) with molar ratio $SiO_2/Al_2O_3 = 5.36$.
**) NaX molecular sieve, synthetized in laboratory.

Table 2

Composition of Xylenes Mixture, [% mol.], obtained on Faujasite Catalysts, Activated at 700°C

Temperature °C	CeY*)			LaY*)		
	p-xylene	*m*-xylene	*o*-xylene	*p*-xylene	*m*-xylene	*o*-xylene
180	30.00	10.00	60.00	24.00	8.00	68.00
200	41.49	31.94	26.57	35.70	34.23	30.07
220	43.78	37.17	19.05	40.26	38.86	20.88
240	39.38	44.23	16.39	34.20	45.90	19.90
260	36.09	48.79	15.12	27.92	52.40	19.68

*) NaY molecular sieve (D a v i d s o n).

Table 3

Composition of Xylenes Mixture, [% mol.], obtained on Faujasite Catalysts, with Molar Ratio $SiO_2/Al_2O_3 = 4.25$, Activated at 500°C

Temperature °C	CeY			LaY		
	p-xylene	*m*-xylene	*o*-xylene	*p*-xylene	*m*-xylene	*o*-xylene
180	20.00	6.50	73.50	18.50	5.80	75.70
200	31.76	29.82	38.42	29.57	27.44	42.99
220	36.27	32.65	31.08	34.37	31.89	30.26
240	31.73	37.15	29.02	28.79	41.71	29.50
260	26.77	43.58	29.65	23.25	48.15	28.60

As it comes out from Tables 1...3, using the investigated catalysts, *orto* isomer is obtained in high amount within temperature range of 180°... 200°C, while *para* isomer, in the temperature range of 200°...240°C. The content of *meta* isomer increases as temperature increases, for all employed catalysts. The presence in the reaction products of *meta* isomer points out that the alkylation reaction is accompanied by isomerization, fact that proves the results of the theoretical study [8], [9]. The *para* isomer was obtained selectively between 200° and 240°C, the optimal temperature being 220°C.

In Table 1 it can be seen that over CeX and MgY catalysts, *orto* isomer was obtained selectively between 180° and 260°C.

As it comes out from Tables 1 and 2, the activated temperature did not have a significant effect on alkylation activity. This fact proves that, by activation at 700°C, the catalytic activity was not affected strongly by superficial hydroxylic groups removal. Therefore, the oxygen deficient silicon—aluminium linkages, created during the activation at 700°C should be equal, as number and activity, to superficial hydroxylic groups. It comes out that the contribution of the two kinds of catalytic active positions is almost the same in the alkylation reaction and the differences observed can be due to the Mg^{2+}, Ce^{3+}, La^{3+} cations. In the case when the oxygen

deficient silicon—aluminium linkages and hydroxylic groups exhibit, in alkylation reaction, the same efficiency, at reaction mechanism discussion must be considered the nature of exchanged ion too. Also, from Tables 1...3 comes out that both catalytic activity and selectivity increase as molar ratio SiO_2/Al_2O_3 increases ; the X-type catalyst are selective for *o*-xylene, while the Y-type catalyst for *p*-xylene. The concentration of *p*-xylene increases on Y-type catalysts as molar ratio SiO_2/Al_2O_3 increases; this depends essentially on the nature of exchanged cation.

In order to see how much the composition of the obtained mixture agrees with the data as regards the thermodynamic equilibrium composition of the investigated system, in Table 4 are presented these data [9].

Table 4

Composition of the Xylenes Mixture, [% mol.], *Possible to be Obtained at Alkylation of Toluene with Methanol, to Thermodynamic Equilibrium.*

Temperature °C	Composition		
	p-xylene	*m*-xylene	*o*-xylene
180	24.59	55.70	19.71
200	24.55	55.28	20.17
220	24.50	54.89	20.61
240	24.45	54.52	21.03
260	24.39	54.17	21.44

Comparing the data from Table 4 with those from Tables 1...3 it comes out that the xylenes mixture, obtained experimentally, has a composition which is far off from that possible to thermodynamic equilibrium. This fact does agree with the experimental data obtained by other authors [3], [4], too.

Kinetics of xylenes isomerization on silicon—aluminium catalysts pointed out that the *orto* and *para* isomers are not transformed directly from one another [15]. Therefore, the *meta* isomer is obtained by isomerization reaction that takes place at the same instant as direct alkylation to the *orto* and *para* isomers. A study about reactivity functions by expended H ü c k e l's method that will follow to be performed, will give more information about the sense of this reaction.

As it comes out from Table 4, from thermodynamic point of view the content of *meta* isomer is highest in the xylenes mixture, but, experimentally, there is observed a significant increase of the *orto* and *para* isomers.This fact should be due to channels geometry in faujasite zeolite structure, which troubles much more the *orto* and *para* xylenes isomerization. This does agree with the fact that in the case of zeolite catalysts the reaction takes place inside of supercavities in their crystalline structure and, consequently, the secondary displacement of methyle group inside of these supercavities, i.e. isomerization, is limited, favouring mainly the formation of the *orto* and *para* isomers [16], [17].

4. Conclusions

The investigation of toluene alkylation with methanol, in gaseous phase, over faujasite zeolites, led to the following conclusions :

1. The Y-type zeolites are more active than X-type zeolites, producing easily the alkylation of aromatic nucleus.

2. Selectivity for formation of the *orto* and *para* alkylated products depends on molar ratio SiO_2/Al_2O_3 and the nature of the cation present in zeolite structure.

3. Geometry of the channels in crystalline structure of faujasites troubles the isomerization, favouring mainly the *orto* and *para* isomers formation.

4. High catalytic activity of zeolites with Ce and La, in studied reaction, can be caused by the existence of strongly acid sites on their surface.

Received, April 6, 1979

Polytechnic Institute, Jassy,
Department of General and Technological Chemistry

REFERENCES

1. Streitwieser A. Jr., Stevenson D. P., Schaeffer W. D., J. Am. Chem. Soc., **81**, 1110 (1959).
2. Сидоренко Я. Н., Галич П. Н., Гутира В. С., Ильин В. Г., Неймарк И. Е., ДАН СССР, **173**, 132 (1967).
3. Yashima T., Ahmad H., Yamazaki K., Katsuta M., Hara N., J. Catalysis, **16**, 273 (1970).
4. Yashima T., Sato K., Hayasaka T., Hara N., J. Catalysis, **26**, 303 (1972).
5. Безоуханова Т. П., Попова З. И., Димитов К., Янков М. Я., Ковашева П. Х., Докл. Былг. АН, **25**, 927 (1972).
6. Ward J. W., J. Catalysis, **11** , 238 (1968).
7. Rabo J. A., *Zeolite Chemistry and Catalysis*, American Chemical Society, Washington D.C., 1976.
8. Naum N., Surpățeanu Gh., Ababi V., Vitan F., Bul. Inst. polit., Iași, **XXIV (XXVIII)**, *1—2*, s. II, 63 (1978).
9. Naum N., Vitan F., Ababi V., Surpățeanu Gh., Bul. Inst. polit., Iași, **XXIV (XXVIII)**, *3—4*, s. II, 57 (1978).
10. Surpățeanu Gh., Naum N., Ababi V., Vitan F., Rev. Chim., **30**, 15 (1979).
11. Vitan F., Naum N., Ababi V., Surpățeanu Gh., Rev. Chim., **30**, 121 (1979).
12. Popovici Ev., Naum N., Ababi V., Bul. Inst. polit., Iași (in print).
13. Russu E., Filloti M. T., Dragomirescu Th., Bîrea M., Brevet RSR, Nr. *52 327* (1970).
14. McNair H. M., Bonelli E. J., *Basic Gas Chromatography*. Varian, Aerograph, Berkeley, California, 197 .
15. Hanson K. L., Engel A., A. I. Ch. E. J., **13**, 260 (1967).
16. Weisz P. B., Frilette V. J., Maatman R. W., Mower E. B., J. Catalysis, **1**, 307 (1962).
17. Venuto P. B., Landis P.S., *Advances in Catalysis*, Vol. **18**, Academic Press, New York, 1968, 259.

ALCHILAREA TOLUENULUI CU METANOL PE ZEOLIȚI SINTETICI

III. Influența proprietăților fizico-structurale ale catalizatorilor asupra activității catalitice

(Rezumat)

S-a cercetat alchilarea toluenului cu metanol, în fază gazoasă, pe zeoliți sintetici de tip faujasitic, într-o instalație cu funcționare continuă. În domeniul de temperatură cuprins între 180° și 240°C, s-a găsit că selectivitatea catalizatorilor utilizați este maximă pentru produșii *orto* și *para* alchilați. Rezultatele experimentale sînt în bună concordanță cu proprietățile fizico-structurale ale catalizatorilor.

BULETINUL INSTITUTULUI POLITEHNIC DIN IAŞI
Tomul XXVI (XXX), fasc. 3—4, 1980
Secţia II
CHIMIE şi INGINERIE CHIMICĂ

D. C. 66.097.3; 661.182.6

ZEOLITIC ADSORBENTS FROM WASTE OXIDIC CATALYSTS

BY

EVELINA POPOVICI, M. CRUCEANU, ANGELA POPA, GH. MIHĂILĂ, ANIŞOARA BOLD and MARIA ALEXANDROAIE

1. Introduction

The industrial catalysts with high contents of aluminium oxide as well as the catalysts with catalytic metal on diatomite or kiselguhr as inert support are widely employed in the modern chemical industry due to their both high catalytic activity and low cost [1]. The poor behaviour against poisoning and koking as well as their poor mechanical resistence have as a result a limited life and, therefore, there are many tens of thausands tones of waste catalysts removed from the industrial reactors, whose storage and capitalization represent very important problems for the exploitation units.

On the basis of the fact that some waste catalysts have their chemical composition rich in silicon and aluminium, being similar to that of the natural kaolin employed in the synthesis of some zeolitic molecular sieves [2], the present paper deals with the results obtained on zeolitization of such catalysts.

2. Experimental

The waste catalyst employed has the following chemical composition : 70...75% Al_2O_3, 9...11% SiO_2, 10...14% Cr_2O_3 and 2...3% K_2O. Before the hydrothermal treatment it was mortared and passed through a 80 μ screen. Its zeolitization was carried out under hydrothermal conditions heating the catalyst, as fine slurry, in a reaction medium. Composition of the reaction medium was established on the basis of both diagram of the K_2O — Al_2O_3 — SiO_2 system and chemical analysis as regard the solubility of each component from waste catalyst in the alkaline medium.

The data concerning analysis of the alkaline extracts under hydrothermal synthesis conditions evidenced the values of chemical composition which is plased in the fields far off from those that generate individual structures homologated in literature [3] (Fig. 1, field *a*). To shift the initial composition of medium near the field generating zeolitic structures (Fig. 1, field *b*) it was necessary the controlled pouring of the sodium silicate alkaline solution.

The reactant mixture was heated up to 98°C under atmospheric pressure on water bath, as well as up to 160°C in a digester under a pressure as high as 6..7 at.

In additional experiments, in order to increase the crystallization rate [2], [4], in the reaction medium was added 5...10% mol triethanolamine (TEA). The reaction products were separated from the reaction medium through filtration. Their analysis was performed after washing and drying.

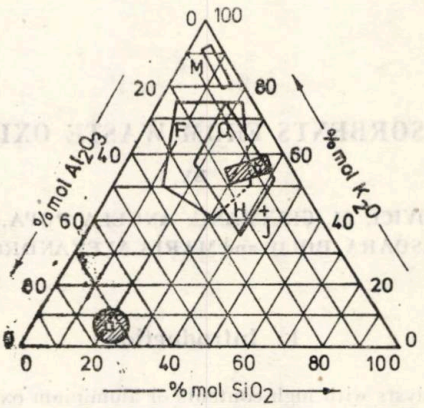

Fig. 1.—The fields of initial chemical composition in the $K_2O - Al_2O_3 - SiO_2$ system.

3. Results and Discussion

The zeoliting experiments in the aqueous medium under both 98°C and 160°C, led to amorphous products with poor adsorptive properties, fact that prove a partial hydrothermal transformation for whose development is necessary to increase both temperature and resident time (Table 1).

Table 1

Zeolitization in the Aqueous Medium

Product	Conditions				Properties		
	Temperature °C	Resident time h	$\frac{SiO_2}{Al_2O_3}$	$\frac{K_2O}{Al_2O_3}$	Water adsorption %	Benzene adsorption %	Crystallinity *)
B-1	98	36	1.23	0.30	3.91	2.14	—
B-2	98	36	2.46	0.61	3.20	2.23	—
B-3	160	16	1.23	0.30	8.21	0.67	+ —
B-4	160	16	2.46	0.61	6.79	0.54	+ —

*) — Amorphous product; + — partial crystalline product.

Since some previous investigations as regard the synthesis of molecular sieves in the organic solvent medium [2], [4]...[6] evidenced the favourable action on hydrothermal crystallization exercised by TEA, a new series of experiments adding this solvent were performed, obtaining the results summarized in Table 2.

Table 2

Zeolitization in the Organic Solvent Medium (TEA)

Product	Conditions					Properties		
	Temperature °C	Resident time h	$\frac{SiO_2}{Al_2O_3}$	$\frac{K_2O}{Al_2O_3}$	$\frac{TEA}{Al_2O_3}$	Water adsorption %	Benzene adsorption %	Crystallinity *)
B-5	98	24	1.23	0.30	1.69	11.69	1.12	+
B-6	142	18	1.23	0.30	1.69	15.07	0.97	+
B-7	160	10	1.23	0.30	1.69	16.28	0.75	++
B-8	160	10	2.46	0.61	1.69	16.18	0.83	++
B-9	160	8	1.23	0.30	2.98	17.61	0.69	+++

*) + Small crystals in compact aggregate; ++ individual small crystals; +++ well shaped individual crystals.

The roentgenographic analysis of the products obtained by hydrothermal transformation of the waste catalyst, in the reaction medium with TEA, points out a mixture of crystalline zeolitic phases by the *F*, *J* and *A* type (Table 3).

Table 3

Roentgenographical Analysis of Some Products

B-8		*B*-10		*B*-16		*J* [11]		*H*[11]		*F*[11]	
d	*I*	*d*	*I*	*d*	*I*	*d*	*I*	*d*	*I*	*d*	*I*
5.27	3	7.28	8	7.28	9	5.862	5.4	13.33	6.4	6.948	10
5.05	2	5.77	3	6.49	7	5.570	1.1	11.65	10.0	6.506	1
4.07	5	4.67	2	5.59	4	4.770	3.2	6.86	6.2	3.347	2
3.84	3	4.02	3	4.77	2	4.725	1.6	6.03	1.1	3.086	5.6
3.75	8	3.71	10	4.16	6	4.271	1.5	5.28	3.8	2.964	7.2
3.48	3	3.48	7	3.89	1	3.995	5.1	4.75	0.8	2.809	4
2.99	5	3.54	2	3.70	7	3.231	4.6	4.46	0.9	2.252	1
2.156	3	3.29	9	3.59	3	3.186	0.4	4.31	1.6	1.738	0.6
1.756	8	2.92	8	3.42	6	3.128	9.3	4.20	2.3	1.685	0.6
1.669	4	2.671	3	3.29	8	3.033	4.0	3.96	4.8	1.637	0.5
1.595	3	2.476	8	3.025	3	3.002	4.1	3.72	1.7		
1.420	6	2.201	7	2.992	10	2.97	3.6	3.37	1.6		
1.314	4	1.888	7	2.671	4	2.89	10.0	3.27	1.8		
1.295	6	1.730	6	2.502	2	2.87	6.1	3.00	3.1		
1.228	5	1.674	1	2.292	2	2.681	1.4	2.92	9.4		
1.141	1	1.585	8	2.263	1	2.662	2.0	2.68	1.7		
1.120	2	1.483	1	2.158	2	2.644	2.5	2.67	2.5		
1.099	4	1.462	2	1.945	8	2.580	2.3	2.63	0.8		
		1.404	5	1.784	6	2.329	1.4	2.59	4.4		
		1.349	8	1.645	3	2.188	1.4	2.55	1.5		
		1.328	1	1.577	4	2.146	6.0	2.33	1.7		
		1.297	2	1.493	2						
		1.215	8	1.438	8						
		1.162	6	1.377	2						
		1.190	5	1.234	6						
		1.095	1	1.201	2						
		1.075	1	1.177	5						
		1.037	4								

The adsorptive properties of the obtained products were investigated by determining the adsorption isotherms for vapour of some substances appreciated as being representative for such a purpose, i.e. water, methanol and benzene (Fig. 2).

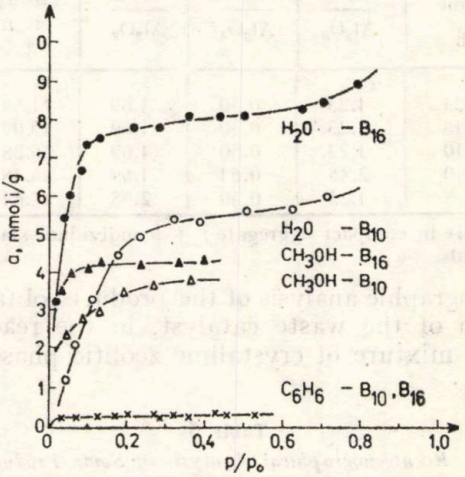

Fig. 2. — Adsorption isotherms under dynamic conditions of some obtained products.

From Fig. 2 it comes out, on one hand, the characteristic shape of adsorption isotherm on the molecular sieves and high value for the adsorption capacity for polar substances and, on the other hand, all products obtained at high temperature exhibit an adsorption capacity higher than those obtained at the lower level of the crystallization temperature.

The structural adsorptive properties of the obtained products required a systematic study to provide a correlation among the principal parameters which influence significantly the structure and adsorption capacity for water vapour (Table 4) and benzene vapour (Table 5). For this study

Table 4

Program of the Factorial Experiments for Water Vapour Adsorption Capacity

$D_1 = 1.69$				$D_2 = 2.98$			
$C_1 = 0.30$		$C_2 = 0.60$		$C_1 = 0.30$		$C_2 = 0.60$	
$B_1 = 1.23$	$B_2 = 2.46$	$B_1 = 1.23$	$B_2 = 2.46$	$B_1 = 1.23$	$B_2 = 1.46$	$B_1 = 1.23$	$B_2 = 1.46$
(1)	*b*	*c*	*bc*	*d*	*bd*	*cd*	*bcd*
$A_1 = 96$ 3.91	3.32	3.16	3.10	11.69	10.40	12.30	12.10
a	*ab*	*ac*	*abc*	*ad*	*abd*	*acd*	*abcd*
$A_2 = 160$ 6.79	4.20	8.21	8.95	16.28	15.90	16.00	16.18

Table 5

Program of the Factorial Experiments for Benzene Vapour Adsorption Capacity

$D_1 = 1.69$				$D_2 = 2.98$			
$C_1 = 0.30$		$C_2 = 0.60$		$C_1 = 0.30$		$C_2 = 0.60$	
$B_1 = 1.23$	$B_2 = 2.46$	$B_1 = 1.23$	$B_2 = 2.46$	$B_1 = 1.23$	$B_2 = 2.46$	$B_1 = 1.23$	$B_2 = 2.46$
(1)	*b*	*c*	*bc*	*d*	*bd*	*cd*	*bcd*
$A_1 = 96$ 1.12	2.23	2.20	2.30	1.12	1.10	0.84	0.80
a	*ab*	*ac*	*abc*	*ad*	*abd*	*acd*	*abcd*
$A_2 = 160$ 1.84	2.20	1.98	1.90	0.75	0.76	0.80	0.83

there was used a program of factorial experiments of the 2^n type, with the following levels of the parameters :

A — Temperature ... 96 and 160°C ; B — SiO_2/Al_2O_3 ... 1.23 and 2.46;
C — K_2O/Al_2O_3 ... 0.30 and 0.60 ; D — TEA/Al_2O_3 ... 1.69 and 2.98.

The study of jump effect from the lower level to upper one of the investigated parameters over the value of water vapour adsorption capacity (Table 6) pointed out that the direct effect of temperature and molar ratio, TEA/Al_2O_3, is very important. Also, the interaction effect temperature— SiO_2/Al_2O_3 and temperature — K_2O/Al_2O_3, over the water adsorption capacity are positive and their values are greater in comparation with other interaction effects.

At the same time, there is found a negative influence of the direct effects of temperature and, especially, TEA concentration, over the benzene vapour adsorption capacity (Table 6). The negative influence exercised by these parameters over the increasing value of benzene vapour adsorption capacity, in fact, points out a favourable effect over the selectivity improvement of these products in the adsorption process.

Verification of the statistical significance of the above experimental data was done on the basis of critical values of the F distribution, at a significance threshold $\alpha = 0.05$ (Table 7).

The results, summarized in Table 7, prove the fact that in the hydrothermal transformation of the waste catalyst in products with adsorptive properties exercises a significant influence both temperature and the molar ratio, TEA/Al_2O_3, in the crystallization medium. As regards the obtention of a porous structure with high adsorption selectivity, proved by the value of benzene vapour adsorption capacity, the significant influence has only the value of the molar ratio, TEA/Al_2O_3.

An entire interpretation over the mechanism of hydrothermal transformation of waste catalyst could be stated as follows. Under temperature action the oxidic mass of waste catalyst is digested releasing progressively in solution aluminium, silicon and sodium ions which cooperate with those

Table 6

Jump Effects of the Parameters

Factors	Water adsorption	Benzene adsorption
	Direct effects	
Temperature	+ 32.65	− 0.65
SiO_2/Al_2O_3	− 4.31	+ 1.47
K_2O/Al_2O_3	+ 7.63	+ 0.53
TEA/Al_2O_3	+ 69.33	− 8.77
	Interaction effects	
Temperature — SiO_2/Al_2O_3	+ 0.21	− 0.83
Temperature — K_2O/Al_2O_3	+ 4.71	− 0.61
Temperature — TEA/Al_2O_3	+ 3.09	− 0.79
TEA/Al_2O_3 — SiO_2/Al_2O_3	+ 0.93	− 1.51
TEA/Al_2O_3 — K_2O/Al_2O_3	− 3.01	− 1.45

Table 7

Dispersional Analysis of the Experimental Data

Dispersion source	Water adsorption	Benzene adsorption	$F_{0.05}$ 1.5
Temperature	46.66	0.265	
SiO_2/A_2O_3	0.822	0.138	
K_2O/Al_2O_3	2.576	0.173	6.61
TEA/Al_2O_3	212.7	49.15	

of the added reagents to generate linear or cycle chain of the silicon and aluminium tetrahedrons and polyhedrons, called soluble species [7], [8]. The stability of such a soluble species as regards the composition, length of chain, tetrahedron succession is influenced by the temperature. After the nucleation and crystallization process these soluble species generate the spatial ediffice of the crystalline zeolitic structure. Their spatial arrangement generates a porous structure whose formation is controlled by the ratio between the number of TEA molecules and the number of aluminium tetrahedrons in their structure.

Quantitative influences are described by the following regression equations:

$$Y_W = -4.674 + 0.078\,x_1 - 0.592\,x_2 + 1.767\,x_3 + 4.995\,x_4,$$
$$Y_B = -0.881 + 0.003\,x_1 + 0.140\,x_2 + 0.123\,x_3 + 1.880\,x_4,$$

where: Y_W represent the adsorption capacity of the product against the water vapour, [% in weight]; Y_B — adsorption capacity of the product against the benzene vapour, [% in weight]; x_1 — crystallization temperature, [°C]; x_2—molar ratio, SiO_2/Al_2O_3; x_3— molar ratio, K_2O/Al_2O_3; x_4 — molar ratio, TEA/Al_2O_3.

The established regression equation come to confirm the observations concerning the influence of the investigated parameters on the hydrothermal transformation process of waste catalyst to zeolitic adsorbents.

4. Conclusions

The experimental investigations, statistical treatment of the results, followed by their theoretical interpretation, led to a controlled hydrothermal transformation process of waste catalysts. The process allows the transformation of some oxidic waste catalysts in zeolitic adsorptive mixtures with high adsorption capacity.

Received, February 1, 1979

Polytechnic Institute, Jassy,
Department of General and
Technological Chemistry

REFERENCES

1. Thomas Ch. L., *Catalytic Processes and Proven Catalysts.* Academic Press, New York and London, 1970.
2. Popovici Ev., Cruceanu M., Brevet R.S.R., *64 451* 1975.
3. Cruceanu M., An. șt. Univ. „Al. I. Cuza" Iași, **XV**, *1*, 105 (1969).
4. Popovici Ev., Ph. D. Diss., Univ. „Al. I. Cuza", Iași, 1973.
5. Popovici Ev., Cruceanu M., Iorga N., Căruntu I., An șt. Univ. „Al. I. Cuza", Iași, **XIX**, *2*, 203 (1973).
6. Cruceanu M., Popovici Ev., Brevet R.S.R., *55 824* 1968.
7. Barrer R. M., Helv. Chim. Acta, **39**, 518 (1956).
8. Breck D. W., J. Chem. Education, 678 (1974).
9. Glück A., *Metode matematice în industria chimică.* Ed. Tehn., Buc., 1971, 241.
10. Dancea I., *Metode de optimizare.* Ed. Dacia, Cluj-Napoca, 1976.
11. Breck D. W., *Zeolite Molecular Sieves.* John Wiley a. Sons, New York, 1973.

ADSORBANȚI ZEOLITICI DIN CATALIZATORI OXIDICI UZAȚI

(Rezumat)

S-a cercetat posibilitatea transformării unor catalizatori oxidici industriali, uzați, cu conținut ridicat de oxid de aluminiu și de siliciu, în adsorbanți zeolitici. S-a procedat la zeolitizarea acestora pe cale hidrotermală, atît în mediu apos cît și în mediu de trietanolamină. Pentru stabilirea influenței parametrilor principali asupra structurii și proprietăților adsorptive ale produselor obținute s-a efectuat un program de experiențe factoriale de tipul 2^4. S-au stabilit două ecuații de regresie care descriu cantitativ influența principalilor parametri asupra capacității de adsorbție a produselor obținute, față de vaporii de apă și față de vaporii de benzen.

BULETINUL INSTITUTULUI POLITEHNIC DIN IAŞI
Tomul XXVI (XXX), fasc. 3—4, 1980
Secţia II
CHIMIE şi INGINERIE CHIMICĂ

C. Z. 669.283

CONTRIBUŢII LA ÎMBUNĂTĂŢIREA PROCESULUI DE CONCENTRARE ŞI CONDIŢIONARE A MOLIBDATULUI DE SODIU

DE

AL. STANCU şi I. IBĂNESCU

1. Molibdatul de sodiu se obţine din minereul de molibdenită conform reacţiei :

$$MoS_2 + Fe_2O_3 + Na_2CO_3 = Na_2MoO_4 + 2FeS + CO_2 .$$

Separarea, din produsul de reacţie, a molibdatului de sodiu, se realizează prin leşiere (dizolvare) cu apă, obţinîndu-se o soluţie cu un conţinut de 120...200 g/l molibdat de sodiu şi mici cantităţi din impurităţile solubile din minereu. În tehnologia elaborată iniţial pentru molibdatul de sodiu, soluţia de la dizolvare era supusă concentrării prin evaporare discontinuă pînă la obţinerea unei mase cristaline cu 30...35% umiditate, care era trecută la uscare. După uscare produsul se prezenta sub forma unei mase compacte care trebuia măcinată înainte de a fi supusă reacţionării cu sulful. Din această ultimă reacţie rezulta bisulfura de molibden utilizată ca lubrifiant solid. Această tehnologie s-a dovedit a fi dezavantajoasă pentru că impurităţile prezente în soluţia iniţială se concentrau şi ajungeau pînă la urmă în bisulfura de molibden afectîndu-i calitatea ; în plus, operaţiile de uscare şi măcinare necesare încărcau preţul de cost al produsului.

2. În vederea perfecţionării tehnologiei de obţinere a molibdatului de sodiu, la Întreprinderea minieră „Bihorul" s-a efectuat, într-o primă etapă, un studiu asupra proprietăţilor soluţiei industriale de molibdat de sodiu, în comparaţie cu acelea ale soluţiei pure. În fig. 1 este reprezentată variaţia densităţii soluţiei industriale de molibdat de sodiu, decantate, în funcţie de concentraţie ; pentru a se putea face o comparaţie cu densitatea soluţiilor pure, densitatea s-a determinat experimental la aceleaşi valori ale concentraţiei ca şi cele date în literatură pentru soluţia pură [1]. Se constată că, în mod practic, densitatea soluţiei industriale nu diferă de aceea a soluţiei pure. Acest fapt demonstrează că în soluţia iniţială impurităţile au o concentraţie mică şi nu-i afectează proprietăţile.

În fig. 2 este redată curba experimentală de fierbere la presiunea atmosferică pentru soluţia pură, iar în fig. 3 este trasată aceeaşi curbă pentru soluţia industrială de molibdat de sodiu. Se poate observa că la ambele soluţii concentraţia de saturaţie este de 54% însă temperatura la care începe separarea fazei solide este diferită, respectiv 109,6°C la soluţia pură şi

111,5°C la soluţia industrială. De asemenea, concentraţia de suprasaturaţie este de 55,5% la soluţia pură şi de 57% la soluţia industrială. Creşterea temperaturii de cristalizare şi a concentraţiei de suprasaturaţie la soluţia industrială se datoreşte impurităţilor a căror concentraţie se măreşte prin evaporare.

3. În continuare s-a cercetat în laborator comportarea la uscare a masei cristaline, compacte, de molibdat de sodiu, obţinut în tehnologia iniţială. S-a constatat că la 100°C se formează o crustă de molibdat de sodiu care frînează procesul de uscare. În paralel s-a cercetat comportarea la uscare a unei mase cristaline umede de molibdat de sodiu pur şi s-a observat că la un conţinut de umiditate iniţială de 5% prin uscare se formează o crustă şi nu se manifestă fenomenul de compactizare a masei de cristale. Se poate afirma, prin urmare, că impurităţile favorizează apariţia de punţi între cristale, ceea ce duce la compactizarea acestora şi la reţinerea, în masa de cristale, a unui conţinut de umiditate mai mare de 5%.

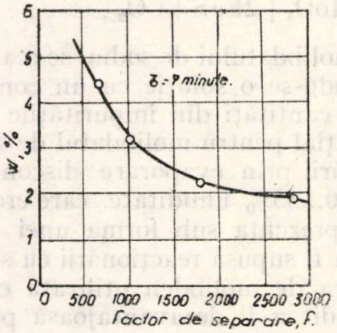

Fig. 4. — Variaţia umidităţii finale a cristalelor de molibdat de sodiu, funcţie de factorul de separare.

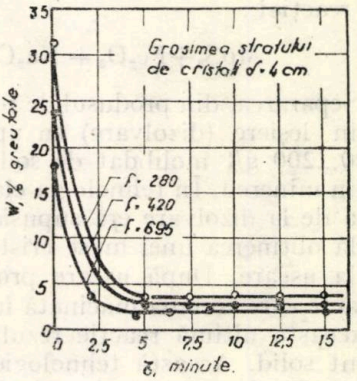

Fig. 5. — Variaţia umidităţii finale a cristalelor de molibdat de sodiu, funcţie de durata de centrifugare.

Deoarece un conţinut de umiditate în jur de 5% este realizabil prin centrifugare şi, totodată, nu afectează reacţia molibdatului de sodiu cu sulful, s-a cercetat posibilitatea uscării prin centrifugare a cristalelor obţinute din soluţia industrială. În fig. 4 este redată variaţia umidităţii finale a cristalelor în funcţie de factorul de separare. Se observă că pentru o durată constantă de centrifugare, (τ=7 min), umiditatea finală scade continuu cu factorul de separare ajungînd pînă la 1,9% pentru un factor de separare de 2 780.

În fig. 5 este reprezentată variaţia umidităţii finale în funcţie de durata centrifugării şi de factorul de separare. Se constată că după o durată de 5 min. de la începutul centrifugării scăderea umidităţii finale este nesemnificativă, indiferent de valoarea factorului de separare; este de menţionat, de asemenea, că pentru toate valorile factorului de separare la care s-a lucrat, după 5 min., umiditatea finală a cristalelor scade sub 5%.

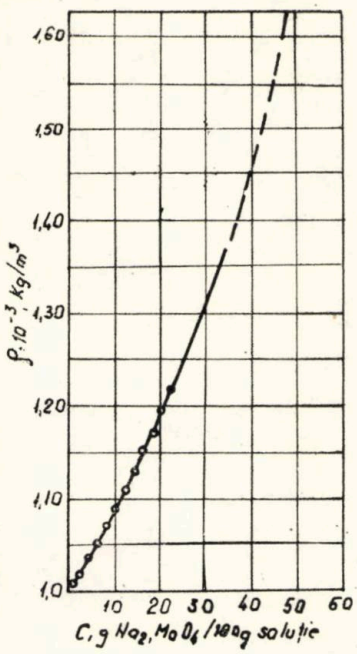

Fig. 1. — Densitatea soluției industriale, decantate, de molibdat de sodiu.

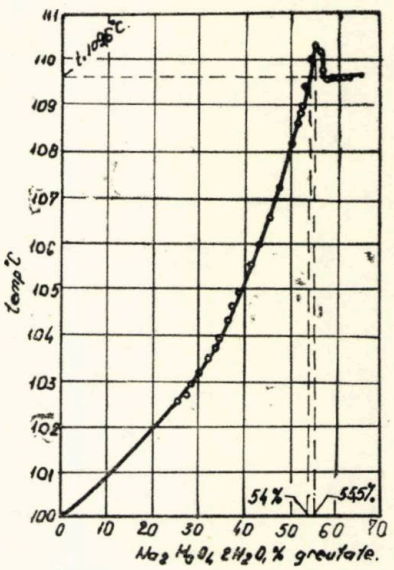

Fig. 2. — Curba de fierbere a soluției pure de molibdat de sodiu.

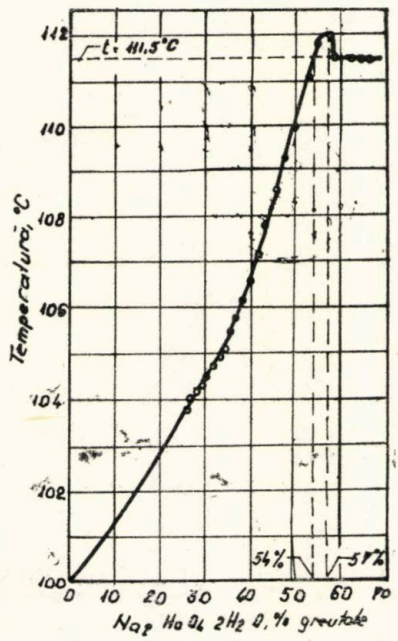

Fig. 3. – Curba de fierbere a soluției industriale de molibdat de sodiu.

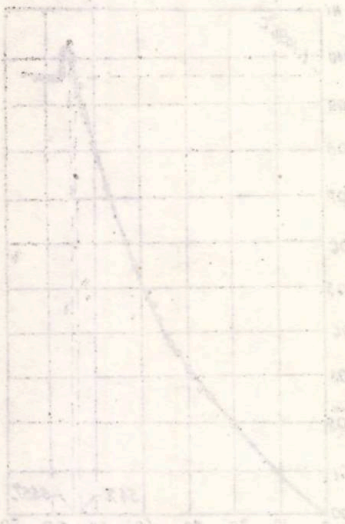

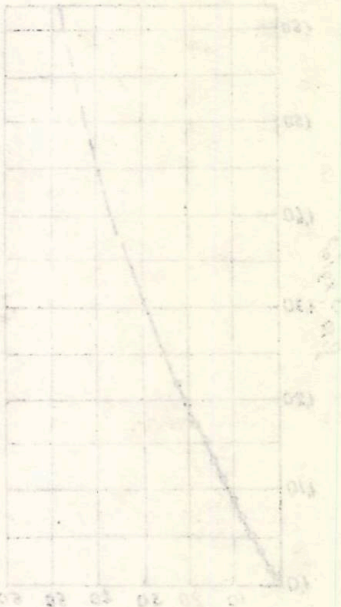

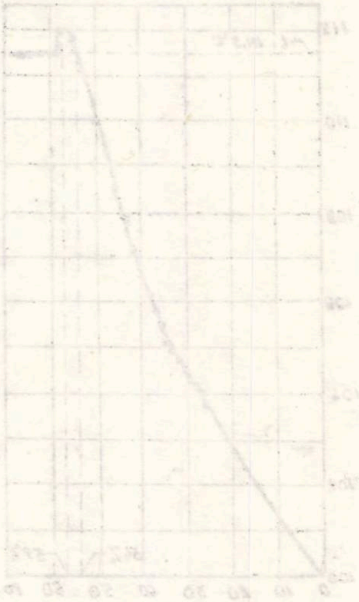

Din cercetările efectuate în prima etapă se desprind următoarele concluzii :

a) procesul de evaporare cu cristalizare a soluției de molibdat de sodiu trebuie condus pînă la concentrații la care impuritățile rămîn în soluția mamă ;

b) prin centrifugarea soluției cu cristale se obțin cristale curate, cu un conținut de umiditate redus și care nu afectează în continuare reacția dintre molibdatul de sodiu și sulf. Produsul de la centrifugare nu mai trebuie supus uscării și măcinării.

4. În a doua etapă s-a conceput și s-a întocmit proiectul tehnologic și de execuție pentru un evaporator — cristalizor care să răspundă cerințelor menționate mai sus. În fig. 6 este redată schița evaporatorului realizat.

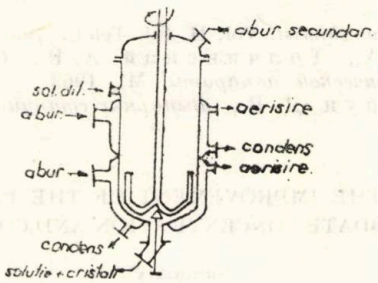

Fig. 6. — Evaporator—cristalizor pentru concentrarea molibdatului de sodiu.

Aparatul constă dintr-un recipient cilindric prevăzut cu o manta în două etaje prin care circulă aburul [2], [3]. La început aparatul se umple cu soluție, al cărei nivel depășește marginea mantalei superioare. După intrarea în regim alimentarea cu soluție se realizează continuu, pînă la atingerea concentrației de 54%. În acest moment se oprește alimentarea cu soluție și se continuă evaporarea pînă cînd nivelul soluției ajunge la înălțimea etajului inferior. Se oprește alimentarea cu abur și se introduce în mantaua inferioară apă de răcire. În condițiile descrise mai sus pentru conducerea evaporării se obțin cristale bine formate, ușor centrifugabile iar impuritățile rămîn în soluție. Soluția cu cristale este eliminată printr-un robinet de construcție adecvată și introdusă la centrifugare ; înainte de deschiderea robinetului soluția cu cristale se agită ușor pentru a înlesni curgerea și a evita rămînerea cristalelor în evaporator. După descărcarea evaporatorului se efectuează alimentarea cu soluție și procesul se reia.

Concluzii

Soluțiile industriale de molibdat de sodiu rezultate după dizolvare sînt destul de pure și au temperatura de cristalizare de 111,5°C ; concentrația de suprasaturație a soluției industriale este de 57%.

Procesul de concentrare și cristalizare poate fi condus într-un evaporator — cristalizor semicontinuu cu manta în două etaje ; în mantaua

inferioară se introduce, spre sfîrşitul procesului, apă de răcire pentru a favoriza creşterea cristalelor. În aparat se obţin cristale curate, impurităţile rămînînd în soluţia mamă.

Prin centrifugarea soluţiei cu cristale din evaporatorul — cristalizor conceput se obţin cristale neaglomerate, cu un conţinut scăzut de umiditate ; cristalele, după centrifugare, pot fi folosite direct în faza următoare de reacţionare cu sulful, fără a mai fi necesare operaţiile de uscare şi măcinare.

Institutul politehnic, Iaşi,
Catedra de inginerie chimică

BIBLIOGRAFIE

1. * * * *Manualul inginerului chimist.* Vol. **II**, Ed. Tehn., Buc., 1952.
2. Лащинский А. А., Толчинский А. Р., *Основы конструирования и расчета химической аппараты.* М., 1963.
3. Колач Т. А., Радун Д. В., *Выпарные станции.* М., 1963.

CONTRIBUTIONS TO THE IMPROVEMENT OF THE PROCESSES OF SODIUM MOLYBDATE CONCENTRATION AND CONDITIONING

(Summary)

An experimental study was carried out regarding the concentration by evaporation with crystallization of the commercial sodium molybdate solutions.

A semi-continuous evaporator—crystalliser was designed where the concentrating process can be so directed as the impurities remain in the solution.

The separation by centrifugation was also investigated, the optimum centrifugation duration being settled when the crystal moisture decreases under the minimum value imposed by the reaction between sodium molybdate and sulphur in the stage of molybden disulphide formation.

BULETINUL INSTITUTULUI POLITEHNIC DIN IAȘI
Tomul XXVI (XXX), fasc. 3—4, 1980
Secția II
CHIMIE și INGINERIE CHIMICĂ

C. Z. 631.859.13

PROPRIETĂȚILE SOLUȚIILOR ÎN SISTEMELE $NH_4H_2PO_4$—H_2O ȘI $(NH_4)_2HPO_4$—H_2O

DE

CAROLINA HAGIU și C. CALISTRU

1. Introducere

Efectuarea calculelor de inginerie chimică pentru procesul de obținere a îngrășămintelor complexe de tip N—P implică cunoașterea datelor necesare pentru caracterizarea soluțiilor de fosfați de amoniu. Datele experimentale referitoare la proprietățile soluțiilor de fosfați de amoniu, existente în literatură, sînt insuficiente pentru o caracterizare completă a soluțiilor ; în literatura de specialitate accesibilă nouă sînt prezentate date referitoare la densitatea, vîscozitatea și conductibilitatea electrică pentru soluții de fosfat monoamoniacal de concentrații 1,91...28,52%, la temperatura de 25°C[1] și pentru soluții de 10, 20, 30 și 40%, la temperaturi de 20°...80°C [2].

În cele ce urmează se prezintă valorile experimentale obținute pentru densitatea și vîscozitatea soluțiilor de fosfat monoamoniacal de concentrații 2...20%, la temperaturi de 25...70°C, astfel încît datele obținute completează valorile existente în literatură. De asemenea s-a determinat densitatea și vîscozitatea soluțiilor de fosfat diamoniacal de concentrații 10...40%, la temperaturi de 25...75°C. Datele experimentale obținute s-au prelucrat grafic și analitic în vederea stabilirii unor ecuații empirice ușor de utilizat, care să pună în evidență variația acestor proprietăți cu temperatura și concentrația soluțiilor.

2. Partea experimentală

Pentru prepararea soluțiilor necesare în determinările experimentale s-au utilizat $(NH_4)H_2PO_4$ și $(NH_4)_2HPO_4$ p.a., cu un conținut de $\pm$ 0,1% impurități. Densitatea soluțiilor s-a determinat prin metoda picnometrică [3], iar vîscozitatea cinematică a soluțiilor s-a determinat prin metoda măsurării timpului de scurgere a lichidului prin capilare calibrate, utilizînd o serie de vîscozimetre Ubelhode — Holde [4], [5]. Reproductibilitatea datelor experimentale s-a asigurat și verificat prin stabilirea valorilor medii a patru determinări experimentale pentru densitate și a șapte determinări experimentale pentru vîscozitate.

Rezultatele experimentale sînt prezentate în fig. 1...4.

3. Prelucrarea datelor experimentale

Rezultatele experimentale s-au prelucrat în scopul stabilirii unor ecuații empirice care să reflecte variația densității și vîscozității cu temperatura și concentrația soluțiilor.

Se remarcă din fig. 1 că densitatea soluțiilor de fosfat monoamoniacal variază liniar cu temperatura și concentrația soluțiilor, deci se poate stabili o relație de forma $\rho = A + Bc + CT$, care să reflecte acest mod de vari-

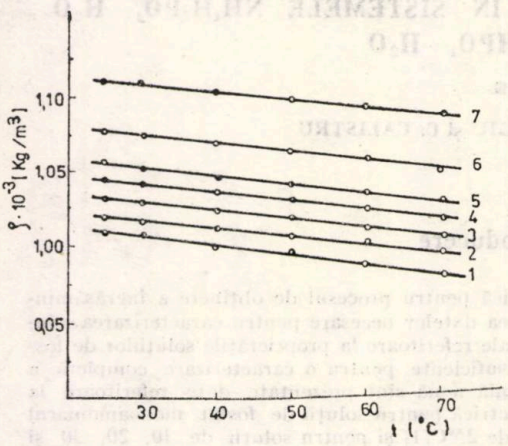

Fig. 1. — Densitatea soluțiilor de $NH_4H_2PO_4$ la temperaturi de 25...70°C: *1*—$c = 2\%$ $NH_4H_2PO_4$, *2*—$c = 4\%$, *3*—$c = 6\%$, *4*—$c = 8\%$, *5*—$c = 10\%$, *6*—$c = 14\%$, *7*—$c = 20\%$.

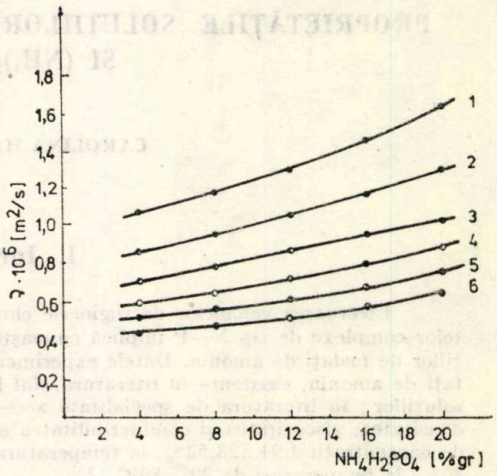

Fig. 2. — Vîscozitatea cinematică a soluțiilor de $NH_4H_2PO_4$ de concentrații 4...20%: *1*—$t = 20°C$, *2*—$t = 30°C$, *3*—$t = 40°C$, *4*—$t = 50°C$, *5*—$t = 60°C$; *6*—$t = 70°C$.

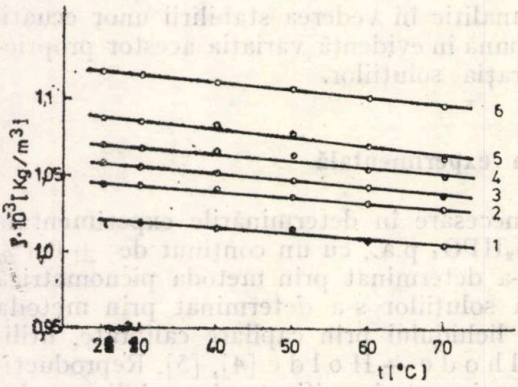

Fig. 3. — Densitatea soluțiilor de $(NH_4)_2HPO_4$ la temperaturi de 25...70°C: *1*—$c = 4\%$, *2*—$c = 8\%$, *3*—$c = 10\%$, *4*—$c = 12\%$, *5*—$c = 15\%$, *6*—$c = 20\%$.

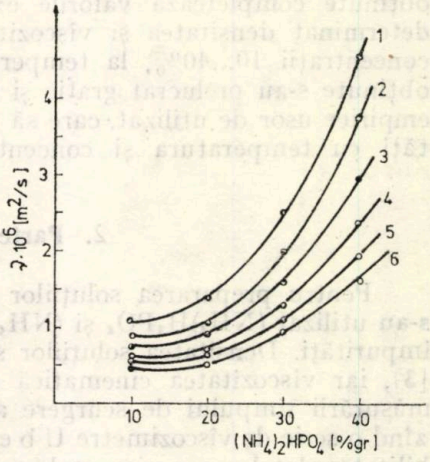

Fig. 4. — Vîscozitate cinematică a soluțiilor de $(NH_4)_2HPO_4$ de concentrații 10...40%: *1*—$t = 25°C$, *2*—$t = 35°C$, *3*—$t = 45°C$, *4*—$t = 55°C$, *5*—$t = 65°C$, *6*—$t = 75°C$.

ație. Ecuația stabilită de noi, valabilă pentru soluții de fosfat monoamoniacal cu concentrații cuprinse între 2...20% și la temperaturi de 298°... 343°K, are forma:

$$(1) \qquad \rho = 1{,}12453 + 0{,}005711c - 0{,}4307.10^{-3}T,$$

în care: c reprezintă concentrația soluției de fosfat monoamoniacal, [% de masă]; T—temperatura, [°K].

Pentru verificarea valabilității acestei ecuații s-au comparat valorile experimentale referitoare la densitate cu cele obținute prin calcul cu ecuația (1). Cîteva din aceste rezultate sînt prezentate în tabelul 1.

Tabelul 1

Densitatea soluțiilor de fosfat monoamoniacal, [g/cm³]

Nr. crt.	t °C	Concentrația soluției %	Valori experimentale	Valori calculate cu ecuația (1)	Valori calculate cu ecuația Sarbaev [2
1	30	2	1,00625	1,00544	1,00666
		4	1,01650	1,01687	1,01762
		6	1,02870	1,02829	1,02869
		8	1,04120	1,03971	1,39860
		10	1,05180	1,05113	1,05113
		14	1,07500	1,07398	1,07397
		20	1,10980	1,10824	1,10900
2	50	2	0,99680	0,99683	0,99850
		4	1,00800	1,00825	1,00947
		6	1,01980	1,01968	1,02050
		8	1,03125	1,03110	1,03171
		10	1,04250	1,04252	1,04297
		14	1,06510	1,06536	1,06582
		20	1,10000	1,09963	1,10084
3	70	2	0,98620	0,98822	0,98828
		4	0,99875	0,99964	0,99924
		6	1,01020	1,01106	1,01031
		8	1,02180	1,02248	1,02147
		10	1,03290	1,03390	1,03274
		14	1,05625	1,05675	1,05559
		20	1,09125	1,09101	1,09061

Pentru calculul densității soluțiilor de fosfat monoamoniacal, cu concentrația de 10...40% și pentru t=20°...80°C, A. N. Sarbaev [2] propune o ecuație de forma:

$$\rho = A + BT + CT^2 + Dc + Ec^2.$$

În conformitate cu tabelul 1 se observă că datele obținute pe cale experimentală sînt verificate, suficient de exact, de ecuația Sarbaev, deci domeniul de valabilitate al acestei ecuații poate fi extins și pentru soluții cu concentrații de 2...10%.

Densitatea soluțiilor de fosfat diamoniacal de 4...20% variază liniar cu temperatura și concentrația soluției (fig. 3); pentru calculul densității acestor soluții se propune ecuația

$$\rho = 1{,}110403 + 0{,}0058208\, c - 0{,}0003733\, T, \quad (3)$$

în care: c reprezintă concentrația soluției, [% fosfat diamoniacal]; T—temperatura absolută, [°K], valabilă pentru $T = 293° \ldots 343°$ K și $c = 4 \ldots 20\%$.

În tabelul 2 sînt prezentate datele privind compararea valorilor experimentale privitoare la densitatea soluțiilor de $(NH_4)_2HPO_4$ cu cele calculate cu ajutorul ecuației (2). Se observă că ecuația propusă verifică suficient de exact datele experimentale pentru soluții cu concentrația cuprinsă în intervalul 4...20%.

Tabelul 2

Densitatea soluțiilor de fosfat diamoniacal, [g/cm³]

t °C	Concentrația soluției %	Valori experimentale	Valori calculate cu ecuația (2)
30	4	1,0200	1,02057
	8	1,0449	1,04385
	10	1,0568	1,05550
	12	1,0679	1,06710
	15	1,0862	1,08460
	20	1,1152	1,11370
50	4	1,0131	1,01310
	8	1,0373	1,03630
	10	1,0487	1,04800
	12	1,0604	1,05960
	15	1,0789	1,07710
	20	1,1073	1,10624
70	4	1,0051	1,00564
	8	1,0292	1,02892
	10	1,0414	1,04056
	12	1,0512	1,05221
	15	1,0648	1,06967
	20	1,0988	1,09877

Datele experimentale referitoare la vîscozitatea soluțiilor de fosfat monoamoniacal și fosfat diamoniacal sînt prezentate în fig. 2 și 4 și tabelele 3 și 4.

Vîscozitatea soluțiilor de fosfat monoamoniacal și diamoniacal variază neliniar cu concentrația și temperatura. Pentru soluțiile de fosfat monoamoniacal, la o temperatură constantă, s-au stabilit ecuații pentru calculul vîscozității funcție de concentrația soluției. Cîteva din aceste ecuații sînt prezentate în tabelul 5.

Tabelul 3

Viscozitatea cinematică a soluțiilor de fosfat monoamoniacal ($\nu \cdot 10^6$, [m^2/s])

Temp. °C	Concentrația soluției, [% $NH_4H_2PO_4$]				
	4	8	12	16	20
20	1,0681	1,1747	1,2980	1,4605	1,6352
30	0,8571	0,9528	1,0546	1,1699	1,3029
40	0,7114	0,7826	0,8644	0,9519	1,0588
50	0,5958	0,6498	0,7109	0,7881	0,8818
60	0,5234	0,5649	0,6148	0,6756	0,7481
70	0,4500	0,4794	0,5169	0,5763	0,6513

Tabelul 4

Viscozitatea cinematică a soluțiilor de fosfat diamoniacal ($\nu \cdot 10^6$, [m^2/s])

Temp. °C	Concentrația soluției, [% $(NH_4)_2HPO_4$]			
	10	20	30	40
25	1,15879	1,39945	2,53235	—
35	0,94154	0,11114	1,99560	3,79359
45	0,76782	0,92031	1,61528	2,95846
55	0,64738	0,75483	1,31719	2,37780
65	0,54826	0,64222	1,11593	1,96386
75	0,48035	0,53991	0,95951	1,63415

Tabelul 5

Ecuații pentru calculul vîscozității cinematice a soluțiilor de fosfat monoamoniacal

Ecuația de calcul a vîscozității $\nu \cdot 10^6$, [m^2/s])	Domeniul de valabilitate	
	t, [°C]	c, [% g]
$\nu = 0{,}9933875 + 1{,}5325 \cdot 10^{-2}\, c + 8{,}3828 \cdot 10^{-4}\, c^2$	20	4...20
$\nu = 0{,}6504325 + 1{,}39475 \cdot 10^{-2}\, c + 3{,}2359 \cdot 10^{-3}\, c^2$	40	4...20
$\nu = 0{,}4934125 + 0{,}61875 \cdot 10^{-2}\, c + 3{,}2734 \cdot 10^{-3}\, c^2$	60	4...20

Vîscozitatea soluțiilor de fosfat diamoniacal se reprezintă în coordonatele lg ν—$1/T$ sub forma unor drepte (fig. 5).

Prin prelucrarea datelor prezentate în fig. 5 s-au stabilit ecuații aproximative pentru calculul vîscozității soluțiilor de fosfat diamoniacal, prezentate în tabelul 6. Eroarea introdusă prin calculul vîscozității cu aceste ecuații, în raport cu valorile experimentale, este cuprinsă între 0,001...1%.

Tabelul 6

Ecuații pentru calculul vîscozității soluțiilor de fosfat diamoniacal

Ecuația pentru calculul vîscozității soluțiilor, $\nu \cdot 10^6$, [m²/s])	Domeniul de valabilitate	
	c, [% g]	T, [°K]
$\lg \nu = -2{,}5688864 + \frac{783{,}17256}{T}$	10	298...348
$\lg \nu = -2{,}7112379 + \frac{851{,}7828}{T}$	20	298...348
$\lg \nu = -2{,}543778 + \frac{875{,}9195}{T}$	30	298...348
$\lg \nu = -2{,}642195 + \frac{992{,}1582}{T}$	40	298...348

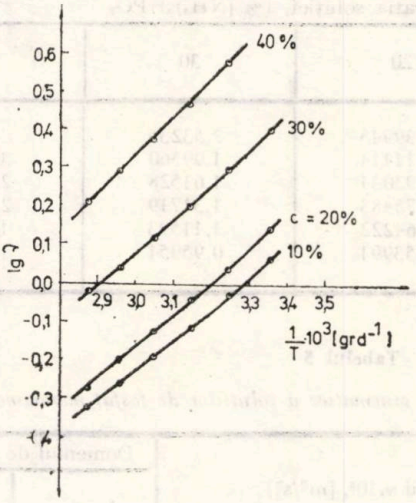

Fig. 5. — Diagrama $\lg \nu - 1/T$, pentru soluții de fostat diamoniacal 10...40 %.

4. Concluzii

1. S-au determinat densitățile și vîscozitățile soluțiilor de $NH_4H_2PO_4$ pentru $c = 4...20$ % și $t = 20°...70°C$, astfel încît datele obținute completează valorile existente în literatură pentru aceste proprietăți.

2. S-au determinat densitățile și vîscozitățile soluțiilor de $(NH_4)_2HPO_4$ pentru $c = 10...40$ % și $t = 25°...75°C$.

Datele experimentale s-au prelucrat grafic și analitic, pentru stabilirea unor ecuații ușor de utilizat, care să reflecte variația acestor mărimi cu temperatura și concentrația soluțiilor.

Primită la 4 decembrie 1978

Institutul politehnic, Iași,
Catedra de tehnologia substanțelor anorganice și a materialelor de construcții

BIBLIOGRAFIE

1. Linfesty F. A., Broshev T. C., Jurnal Chem. Eng. Data, 5, 152 (1960).
2. Сарбаев А. Н. и сотр., ЖПХ, 12, 2749 (1972).
3. Guillemiu C., *Technique de l'ingénieur. Densimetrie au laboratoire.* Paris, 1965, 520.
4. Solomon M., *Viscozimetrie și elemente de teorie a viscozității.* Ed. Tehn., Buc., 1958.
5. * * * STAS 117/1966.

SOLUTION PROPERTIES IN $NH_4H_2PO_4-H_2O$ AND $(NH_4)_2HPO_4-H_2O$ SYSTEMS

(Summary)

The chemical engineering calculations for the processes of obtaining complex fertilizers of the N—P type involve knowledge of the properties of ammonium phosphate solutions.

The densities and viscosities of monoammonium phosphate solutions (conc. 2...20%) and diammonium phosphate solutions (conc. 10...40%) have been determined experimentally over temperature ranges of 20°...70°C and 25°...75°C, respectively. To obtain easily utilisable equations, able to describe accurately the variation of these properties with temperature and concentration the experimentally obtained data were worked graphically and analytically.

BULETINUL INSTITUTULUI POLITEHNIC DIN IAŞI
Tomul XXVI (XXX), fasc. 3—4, 1980
Secţia II
CHIMIE şi INGINERIE CHIMICĂ

C.Z. 66.074.34

METODĂ PENTRU EVIDENŢA ŞI REDUCEREA CONTINUĂ A COEFICIENŢILOR DE CONSUM ÎN INDUSTRIA AMONIACULUI*)

DE

C. CALISTRU, CORNELIA LEONTE şi ILIE SIMINICEANU

1. Introducere

Sarcina fundamentală a industriei chimice din ţara noastră, în etapa actuală, o constituie creşterea puternică a eficienţei economice în toate sectoarele acesteia. În acest sens în documentele de partid se arată că în cincinalul viitor gradul de valorificare a materiilor prime şi materialelor urmează să sporească cu 20...30%, una din căile de realizare a acestei prevederi fiind utilizarea cu maximum de eficienţă a capacităţilor de producţie [1]. Aceasta creează implicit şi necesitatea de stabilire a condiţiilor de fabricare a produselor chimice cu coeficienţi minimi de consum de materiale şi energie.

La nivelul actual de dezvoltare al ingineriei chimice există mai multe metode de stabilire a coeficienţilor de consum. Important este, însă, faptul că odată cu stabilirea coeficienţilor de consum este necesar să se pună în evidenţă factorii care au determinat obţinerea anumitor valori, deci şi măsurile care trebuie luate pentru modificarea regimului tehnologic al utilajelor în vederea reducerii continue a coeficienţilor de consum.

Una din metodele cunoscute şi descrisă în literatură este metoda EVOP [2].

În cele de mai jos se prezintă o altă metodă, care poate fi aplicată în fiecare linie industrială şi care permite, mai ales în condiţiile utilizării calculatoarelor, stabilirea continuă atît a coeficienţilor de consum reali, cît şi a coeficienţilor de consum teoretici. Compararea acestora permite aprecierea condiţiilor de funcţionare a unei instalaţii şi indică imediat măsurile care se pot lua şi eficienţa acestor măsuri. Metoda, aşa cum se arată în această lucrare, se referă numai la consumul de materii prime şi auxiliare.

Evident, este necesar să se ţină seama de faptul că realizarea conducerii automate a procesului impune, în mod corespunzător, stabilirea metodelor în forme capabile să permită prelucrarea automată a datelor.

2. Metoda propusă

Metoda constă în a întocmi, în primul rînd, lista proceselor fizice şi chimice, în ordinea în care acestea sînt folosite în linia industrială analizată. Pe această bază procesele componente se grupează în procese tehnologice componente, fiecare proces tehnologic component reprezentînd un ansamblu unitar, cu o independenţă relativă faţă de celelalte procese. În urma acestei operaţii se reprezintă schema bloc a liniei industriale, alcătuită din procesele tehnologice componente şi schema bloc a fiecărui proces

*) Prezentată la sesiunea ştiinţifică jubiliară dedicată celei de a XXXV-a aniversări a Eliberării României de sub dominaţia fascistă şi Congresului al XII-lea al Partidului Comunist Român, din 13—14 iulie 1979.

tehnologic component, constituită din procesele fizice și chimice care-l compun. În fig. 1 este reprezentată această schemă bloc pentru linia industrială de obținere a amoniacului.

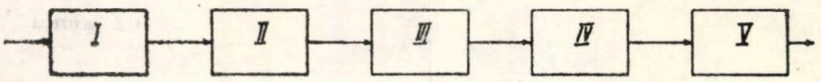

Fig. 1. — Schema bloc a procesului tehnologic de obținere a amoniacului.

În a doua etapă este necesar să se elaboreze modelele matematice de bilanț. În acest scop a apărut necesitatea de a se face distincție între reacția chimică și procesul chimic și, în același timp, necesitatea de a defini prin analogie cu reacția chimică toate procesele macroscopice elementare de transformare și transfer [4].

În continuare, pentru fiecare proces fizic sau chimic component se elaborează modelele matematice de bilanț sub forma unui sistem de ecuații algebrice primare sau secundare.

Tabelul 1

Faza	Component	Ecuația de bilanț
$[\,]_g$	H_2S	$n_{H_2S} = n^0_{H_2S}(1 - \eta_{H_2S})$
	H_2O	$n_{H_2O} = n^0_{H_2S}\ \eta_{H_2S}$
	CH_4	$n_{CH_4} = n^0_{CH_4}$
	Total	$n_g = n^0_g$
$[\,]_s$	ZnO	$n_{ZnO} = n^0_{ZnO} - n^0_{H_2S}\ \eta_{H_2S}$
	ZnS	$n_{ZnS} = n^0_{H_2S}\ \eta_{H_2S}$
	Total	$n_s = n^0_{ZnO} = n^0_s$
Parametrii care trebuie determinați: η_{H_2S}		

Pentru elaborarea unui astfel de sistem de ecuații s-a plecat de la metoda cunoscută a întocmirii bilanțurilor pentru reacții omogene [3]. Așa cum rezultă din tabelele 1 și 1′, în cazul sistemului de ecuații primare evoluția procesului pînă la un moment oarecare este exprimată prin mărimi inițiale cunoscute și grade de transformare. Sistemul ecuațiilor secundare, așa după cum se constată din tabelul 1′, caracterizează nivelul desfășurării procesului prin mărimi inițiale cunoscute și concentrațiile componenților la un moment dat.

Prin analogie cu reacția chimică se definesc mărimile caracteristice și apoi se stabilesc ecuații de bilanț pentru toate procesele macroscopice elementare [5].

Tabelul 1'

Faza	Component	Ecuația de bilanț
$[\,]_g$	H_2S	$n_{H_2S} = n_g^0 X_{H_2S}$
	H_2O	$n_{H_2O} = n_g^0 (X_{H_2S}^0 - X_{H_2S})$
	CH_4	$n_{CH_4} = n_g^0 X_{CH_4}^0$
	Total	$n_g = n_g^0$
$[\,]_s$	ZnO	$n_{ZnO} = n_{ZnO}^0 - n_g^0 (X_{H_2S}^0 - X_{H_2S})$
	ZnS	$n_{ZnS} = n_g^0 (X_{H_2S}^0 - X_{H_2S})$
	Total	$n_s = n_{ZnO}^0 = n_s^0$
Parametrii care trebuie determinați: X_{H_2S}		

Problema cea mai complexă, mai dificil de rezolvat, este aceea a determinării ecuațiilor proceselor componente independente sau a ecuațiilor stoichiometrice independente [5]. Odată rezolvată această problemă se scriu ecuațiile independente și, în continuare, se definește pentru fiecare din aceste ecuații, indiferent dacă aceasta se referă la o reacție sau la alt proces macroscopic elementar, gradul de transformare. După ce se stabilesc „relațiile de concretizare" se obțin ecuațiile algebrice primare de bilanț. Este util ca prin stabilirea „relațiilor de transformare" să se elaboreze și ecuațiile algebrice secundare de bilanț. În acest fel se pot stabili, fără erori, ceea ce se numesc „parametrii care trebuie determinați" și relațiile de calcul ale gradelor de transformare în funcție de acești parametri.

Parametrii care trebuie determinați sînt concentrațiile sau temperaturile componentelor și fazelor la ieșirea din aparat sau reactor și care, odată cunoscute, permit calculul debitelor tuturor componentelor și fazelor, respectiv a tuturor concentrațiilor la ieșire. Valoarea numerică a unui parametru care trebuie determinat poate fi aflată pe două căi: prin măsurarea directă a concentrației sau temperaturii din masa de reacție la ieșirea din aparat sau reactor și prin determinarea cu ajutorul modelului matematic folosit în studiul procesului considerat la echilibru.

Trebuie remarcat că valoarea numerică a unui astfel de parametru determinat experimental trebuie să reprezinte o medie statistică.

Ecuațiile algebrice de bilanț cuprind două tipuri de mărimi: parametrii care trebuie determinați sau gradele de transformare care pot fi calculate cu ajutorul acestora și mărimile de ieșire și de intrare. Mărimile de intrare într-un aparat sau reactor sînt mărimile de ieșire din aparat sau reactorul precedent și, ca urmare, valorile lor numerice sînt cunoscute. În ultimă instanță aceste mărimi reprezintă debitul și compoziția materiilor prime, care trebuie cunoscute prin analize chimice și respectiv prin capacitatea de producție a liniei.

După ce se stabilesc ecuațiile algebrice de bilanț pentru fiecare din procesele fizice și chimice care aparțin procesului tehnologic component considerat, se elaborează ecuațiile algebrice de bilanț pentru întregul proces tehnologic component. În fine, după constituirea ecuațiilor algebrice de bilanț pentru fiecare proces tehnologic component se trece la elaborarea ecuațiilor algebrice de bilanț pe întreaga linie.

Pentru rezolvarea, cu ajutorul calculatorului, a modelelor matematice stabilite este necesar să se determine debitul și compoziția materiilor prime cît și valoarea numerică a parametrilor care trebuie determinați în fiecare aparat sau reactor din linia analizată.

3. Exemplu

În continuare se exemplifică aplicarea metodei la instalația de fabricare a amoniacului.

Procesul tehnologic de obținere a amoniacului prin procedeele moderne se împarte în cinci procese tehnologice componente (P.T.C.) (I...V) prezentate în fig. 1. Fiecare P.T.C. poartă denumirea procesului chimic fundamental pe care-l include:

I. Procesul tehnologic de reformare.
II. Procesul tehnologic de conversie a oxidului de carbon.
III. Procesul tehnologic de eliminare a dioxidului de carbon.
IV. Procesul tehnologic de metanizare.
V. Procesul tehnologic de sinteză.

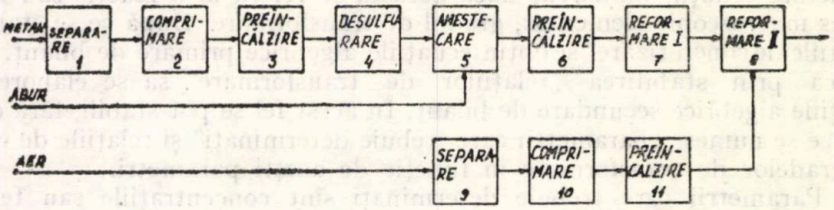

Fig. 2. — Schema bloc a procesului tehnologic de reformare.

Fiecare din procesele I...V se poate scinda în procese fizice și chimice componente. În fig. 2 este prezentată schema bloc a procesului tehnologic de reformare.

Pentru elaborarea bilanțului de materiale și calculul coeficienților de consum de materii prime se iau în considerație toate procesele chimice precum și procesele fizice care duc la modificarea compoziției fluxului de materiale. Pentru P.T.C. de reformare din fig. 2 aceste procese sînt:

a) Procesul chimic de desulfurare a gazului natural, reprezentat prin ecuația caracteristică:

$$(1) \qquad [CH_4+H_2S+A'']_g+[ZnO]_s \rightarrow [CH_4+H_2O+A'']_g+[ZnS]_s$$

și ecuația stoichiometrică:

$$(2) \qquad H_2S+ZnO=ZnS+H_2O.$$

b) Procesul fizic de amestecare :

$$[CH_4+H_2O+A'']_g+[H_2O]_g \rightarrow [CH_4+H_2O+A'']_g. \quad (3)$$

c) Procesul chimic de reformare treapta I :

$$[CH_4+H_2O+A'']_g+[K]_s \rightarrow [H_2+CO+CO_2+CH_4+H_2O+A'']_g+[K]_s; \quad (4)$$

$$CH_4+H_2O=CO+3H_2, \quad (5) \qquad CO+H_2O=CO_2+H_2. \quad (6)$$

d) Procesul chimic de reformare treapta II :

$$[H_2+CO+CO_2+CH_4+H_2O+A'']_g+[O_2+N_2]_g+[K]_s \rightarrow \rightarrow [H_2+N_2+CO+CO_2+CH_4+H_2O+A'']_g+[K]_s, \quad (7)$$

$$2H_2+O_2=2H_2O, \quad (8) \qquad CH_4+H_2O=CO+3H_2, \quad (9)$$

$$CO+H_2O=CO_2+H_2. \quad (10)$$

Ecuațiile algebrice primare de bilanț de masă pentru procesele chimice componente de mai sus sînt prezentate în tabelele 1...3. În aceleași tabele sînt precizați și parametrii care trebuie determinați pentru fiecare proces, respectiv : X_{H_2S}, pentru desulfurare, X_{CH_4}, X_{CO_2} pentru reformare I, X_{CH_4}, X_{CO} pentru reformare II.

Tabelul 2

Component	Ecuația de bilanț
CH_4	$n_{CH_4} = n^0_{CH_4}(1-\alpha)$
CO	$n_{CO} = n^0_{CH_4}(\alpha-\beta)$
CO_2	$n_{CO_2} = n^0_{CH_4}\beta$
H_2	$n_{H_2} = n^0_{CH_4}(3\alpha+\beta)$
A''	$n_{A''} = n^0_{A''}$
H_2O	$n_{H_2O} = n^0_{H_2O} - n^0_{CH_4}(\alpha+\beta)$
Total	$n_T = n^0_T(1+2x^0_{CH_4}\alpha)$
Parametrii care trebuie determinați : X_{CH_4}, X_{CO_2}	

Pentru procesele de reformare se pot alege două concentrații oarecare la ieșire, dar după cum se observă din tabelele 2 și 3, X_{CH_4} și X_{CO_2} au expresiile cele mai simple. Relațiile dintre gradele de transformare α și β și fracțiile molare X_{CH_4} și X_{CO_2} raportate la gazul uscat, așa cum se determină în instalație, sînt :

a) pentru reformare I :

$$X_{CH_4}=\frac{1-\alpha'}{1+3\alpha'+\beta'}, \quad (11) \qquad X_{CO_2}=\frac{\beta'}{1+3\alpha'+\beta'}; \quad (12)$$

Tabelul 3

Component	Ecuaţia de bilanţ
CH_4	$n_{CH_4} = n^0_{CH_4}(1-\alpha)$
CO	$n_{CO_2} = n^0_{CO} + n^0_{CH_4}\alpha - n^0_{CH_4}\beta - n^0_{CO}\beta/\alpha$
CO_2	$n_{CO_2} = n^0_{CO_2} + n^0_{CO}\beta/\alpha + n^0_{CH_4}\beta$
H_2	$n_{H_2} = n^0_{H_2} + 3n^0_{CH_4}\alpha + n^0_{CO}\beta/\alpha + n^0_{CH_4}\beta - 2n^0_{O_2}$
A''	$n_{A''} = n^0_{A''}$
N_2	$n_{N_2} = n^0_{N_2}$
H_2O	$n_{H_2O} = n^0_{H_2O} + 2n^0_{O_2} - n^0_{CH_4}\alpha - n^0_{CO}\beta/\alpha - n^0_{CH_4}\beta$
Total	$n_T = n^0_T(1+2x^0_{CH_4}\alpha)$
Parametrii care trebuie determinaţi: X_{CH_4}, X_{CO_2}	

b) pentru reformare II :

$$X_{CH_4} = \frac{1-\alpha''}{A+3\alpha''+\beta''+\dot{X}^0_{CO}\beta''/\alpha''}, \tag{13}$$

$$X_{CO_2} = \frac{\dot{X}^0_{CO_2}+\dot{X}^0_{CO}\beta''/\alpha''+\beta''}{A+3\alpha''+\beta''+\dot{X}^0_{CO}\beta''/\alpha''}, \tag{14}$$

unde

$$A = 1+\dot{X}^0_{CO}+\dot{X}^0_{CO_2}+\dot{X}^0_{H_2}+\dot{X}^0_{N_2}+2\dot{X}^0_{O_2}.$$

În procesul de desulfurare, în general $X_{H_2S}=0$ şi deci $\eta_{H_2S}=1$, atît cel real cît şi la echilibru.

În tabelul 4 sînt prezentate valorile parametrilor care trebuie determinaţi precum şi gradele de transformare reale corespunzătoare proceselor chimice componente ale P.T.C. reformare.

Pentru determinarea gradelor de transformare teoretice (la echilibru) în procesele componente de mai sus se utilizează modelele matematice ale desfăşurării lor la echilibru. Pentru procesul de reformare primară acesta cuprinde ecuaţiile [6]:

$$K_{p5} = \frac{(\alpha-\beta)(3\alpha+\beta)^3P^2}{(1-\alpha)(\dot{X}^0_{H_2O}-\alpha-\beta)(1+\dot{X}^0_{H_2O}+2\alpha)^2}, \tag{15}$$

$$K_{p6} = \frac{\beta(3\alpha+\beta)}{(\alpha-\beta)(\dot{X}^0_{H_2O}-\alpha-\beta)}, \tag{16}$$

$$\lg K_{p5} = -\frac{11\,650}{T}+13{,}076, \tag{17}$$

$$\lg K_{p6} = \frac{1910}{T}-1{,}764. \tag{18}$$

Tabelul 4

Gradele de transformare reale în procesele chimice componente

Nr.	Procesul	Valorile parametrilor măsurați	Gradele de transformare
1	Reformare I	$X_{CH_4} = 0,103$ $X_{CO_2} = 0,1208$	$\alpha' = 0,6664$ $\beta' = 0,391$
2	Reformare II	$X_{CH_4} = 0,0024$ $X_{CO_2} = 0,0886$	$\alpha'' = 0,9657$ $\beta'' = 0,0312$
3	Desulfurare	$X_{H_2S} = 0$	$\eta_{H_2S} = 1$

Sistemul de ecuații (15)...(18) exprimă dependența:

$$(\alpha', \beta')_{echil.} = F(P, T, \dot{X}^0_{H_2O}). \tag{19}$$

Pentru procesul de reformare secundară modelul matematic al desfășurării sale la echilibru este [7]:

$$K_{p9} = \frac{P^2(\dot{X}^0_{CO} - \dot{X}^0_{CO}\beta/\alpha + \alpha - \beta)(\dot{X}^0_{H_2} + \dot{X}^0_{CO}\beta/\alpha - 2\dot{X}^0_{O_2} + 3\alpha + \beta)^3}{(1-\alpha)(\dot{X}^0_{H_2O} - \dot{X}^0_{CO}\beta/\alpha + 2\dot{X}^0_{O_2} - \alpha - \beta)(A + 2\alpha)^2}, \tag{20}$$

$$K_{p10} = \frac{(\dot{X}^0_{CO_2} + \dot{X}^0_{CO}\beta/\alpha + \beta)(\dot{X}^0_{H_2} + \dot{X}^0_{CO}\beta/\alpha - 2\dot{X}^0_{O_2} + 3\alpha + \beta)}{(\dot{X}^0_{CO_2} + \alpha - \beta - \dot{X}^0_{CO}\beta/\alpha)(\dot{X}^0_{H_2O} - \dot{X}^0_{CO}\beta/\alpha + 2\dot{X}^0_{O_2} - \alpha - \beta)}. \tag{21}$$

Pentru constantele K_{p9} și K_{p10} se utilizează relațiile (17) și (18). Sistemul (20), (21) exprimă dependența:

$$(\alpha'', \beta'')_{echil.} = F(P, T, \dot{X}^0_{CO}, \dot{X}^0_{CO_2}, \dot{X}^0_{H_2}, \dot{X}^0_{H_2O}, \dot{X}^0_{O_2}).$$

În procesul de desulfurare, modelul desfășurării la echilibru are forma:

$$\eta^e_{H_2S} = \frac{K_{p2}}{1 + K_{p2}}, \tag{22}$$

$$\lg K_{p2} = \frac{4000}{T} - 0,39. \tag{23}$$

În tabelul 5 sînt prezentate gradele de transformare teoretice obținute prin rezolvarea, cu ajutorul calculatorului numeric, a sistemelor (15)...(18), (20), (21) și (22), (23), în aceleași condiții (presiune, temperatură, compoziție inițială) în care s-au obținut valorile reale din tabelul 4.

Se remarcă faptul că în ambele trepte de reformare gradul de transformare al metanului α', α'' (tabelul 4) este foarte apropiat de cel teoretic (tabelul 5) pentru instalația analizată iar desulfurarea este totală.

Tabelul 5

Gradele de transformare teoretice în procesele chimice componente

Procesul	Parametrii tehnologici	Gradele de transformare
Reformare I	$P = 30$ at, $T = 1\,050°K$, $\dot{X}^0_{H_2O} = 4$	$\alpha' = 0{,}678$ $\beta' = 0{,}401$
Reformare II	$P = 28$ at, $T = 1\,235°K$, $\dot{X}^0_{CO} = 0{,}825$, $\dot{X}^0_{CO_2} = 1{,}175$, $\dot{X}^0_{H_2} = 0{,}710$, $\dot{X}^0_{N_2} = 3{,}16$, $\dot{X}^0_{H_2O} = 8{,}650$, $\dot{X}^0_{O_2} = 0{,}845$	$\alpha'' = 0{,}9667$ $\beta'' = 0{,}04012$
Desulfurare	$T = 673°K$	$\eta^e_{H_2S} = 1$ $(K_{p_2} > 10^4)$

Pe baza ecuațiilor de bilanț ale proceselor fizice și chimice componente se stabilesc ecuațiile de bilanț ale procesului component (PTS). Ecuațiile PTS de reformare astfel stabilite sînt prezentate în tabelul 6, în forma primară. Ele includ gradele de transformare α', β' și α'', β'' în cele două trepte de reformare precum și mărimi inițiale: $n^0_{CH_4}$, $n^0_{H_2O}$, $n^0_{A''}$, n^0_{aer}. În mod analog se stabilesc ecuațiile pentru celelalte PTS iar în final pentru întreaga linie [9].

Tabelul 6

Nr.	Component	Ecuația de bilanț
1	CH_4	$n_{CH_4} = n^0_{CH_4}(1-\alpha')(1-\alpha'')$
2	CO	$n_{CO} = n^0_{CH_4}(\alpha''-\beta'')\left(\frac{\alpha'-\beta'}{\alpha''}+1-\alpha'\right)$
3	CO_2	$n_{CO_2} = n^0_{CH_4}\left[\beta'+(\alpha'-\beta')\frac{\beta''}{\alpha''}+(1-\alpha')\beta''\right]$
4	H_2	$n_{H_2} = n^0_{CH_4}\left[3\alpha'+\beta'+(1-\alpha')(3\alpha''+\beta'')+(\alpha'-\beta')\frac{\beta''}{\alpha''}-2\dot{X}^0_{O_2}\right]$
5	A''	$n_{A''} = n^0_{A''}$
6	N_2	$n_{N_2} = 0{,}79\, n^0_{aer}$
7	H_2O	$n_{H_2O} = n^0_{H_2O} + 0{,}42\, n^0_{aer} - n^0_{CH_4}(\alpha''+\beta'')\left(1-\alpha'+\frac{\alpha'+\beta'}{\alpha''}\right)$
8	Total	$n_T = n^0_T + 2n^0_{CH_4}\left[\alpha'+\alpha''-\beta'\left(\frac{\beta''}{\alpha''}\right)\right]$

4. Concluzii

Se prezintă o metodă de elaborare a bilanțurilor pe întreaga linie care permite stabilirea și controlul coeficienților de consum reali și teoretici în instalațiile de amoniac. Pentru aplicarea metodei fiecare instalație industrială trebuie să posede :

a) modelul matematic de bilanț (ecuații algebrice primare și secundare) ;

b) modele matematice pentru desfășurarea fiecărui proces component la echilibru ;

c) modele matematice pentru desfășurarea reală a proceselor ;

d) programe de rezolvare a modelelor la calculator ;

e) lista parametrilor care trebuie determinați și metodele de interpretare statistică.

Notații și indici

A'' — inerte ;
K_{pi} — constanta de echilibru a reacției i ;
α — gradul de transformare în reacția (5) sau (9) ;
β — produsul dintre gradul de transformare α și gradul de transformare al CO în reacția (6) sau (10) ;
X_{A_i} — fracția molară a componentului A_i ;
$\dot{X}^0_{A_i}$ — raportul molar al componentului A_i, dat de n^0A_i/n^0CH_4 ;
P — presiunea totală, [at] ;
T — temperatura, [°K] ;
η_{H_2S} — gradul de transformare al hidrogenului sulfurat ;
α', β' — gradele de transformare în procesul de reformare, treapta I ;
α'', β'' — gradele de transformare în procesul de reformare, treapta II.

Primită la 24 iulie 1979

Institutul politehnic, Iași,
Catedra de tehnologia substanțelor
anorganice și materialelor de construcții

BIBLIOGRAFIE

1. Ceaușescu N., *Cuvîntarea la Consfătuirea de lucru de la C. C. al P.C.R. din 28 septembrie 1978*. Ed. polit., Buc., 1978.
2. Box G., Draper N., *EVOP—operarea evolutivă*, (trad. din l. engl.). Ed. tehn., Buc., 1975.
3. Brotz N., *Grundiss der Chemischen Reaktionstechnick*. Verlag Chemie, Weinheim, 1958, 15.
4. Calistru C., Leonte C., Ind. Chimique belge, **32**, 409 (1967).
5. Calistru C., Leonte C., *Tehnologia substanțelor anorganice*. EDP, Buc., 1972.
6. Calistru C., Siminiceanu I., Hagiu C., Petrilă C., Rev. chim., **24**, *11*, 880 (1973).
7. Calistru C., Siminiceanu I., Hagiu C., Petrilă C., Rev. chim., **26**, *12*, 1003 (1975).
8. Siminiceanu I., Calistru C., Rev. chim., **30**, *1*, 45 (1979).
9. Siminiceanu I., Calistru C., Hagiu C., Belaşcu F., Al II-lea Simpozion de ingineria proceselor chimice. Piatra Neamț, octombrie 1978.

A METHOD FOR THE CONTINUOUS DECREASING OF THE SPECIFIC CONSUMPTIONS IN THE AMMONIA INDUSTRY

(Summary)

A general method to compute the real and theoretical specific consumptions in any industrial chemical process is presented. The method is based on the mathematical balance models which finally correlate the specific consumption as a function of the operation parameters. The specific consumptions are decreased by moving these parameters to their optimum values. The method is illustrated by an example from ammonia technology.

BULETINUL INSTITUTULUI POLITEHNIC DIN IAȘI
Tomul XXVI (XXX), fasc. 3—4, 1980
Secția II
CHIMIE și INGINERIE CHIMICĂ

D. C. 547.84

TRIAZOLIUM-YLIDE

IV. ON THE REGIOSELECTIVITY OF THE CYCLOADDITION REACTIONS OF THE TRIAZOLIUM-PHENACYLIDE TO ACRYLONITRILE AND METHYL ACRYLATE

BY

GH. SURPĂȚEANU, CRISTINA LUCHIAN, MIRCEA CONSTANTINESCU, VIRGIL BĂRBOIU and MAGDA PETROVANU

1. Introduction

Early the regioselectivity of 3 + 2 cycloadditions are well studied. Experimentally, in many reactions of the type :

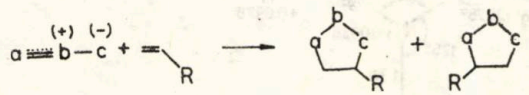

two regioisomers are obtained by the two posible additions between above reaction components [1], [2]. In these conditions the regioselectivity of these cycloadditions must be determined. There are three factors which control the regioselectivity : sterical, electronic and orbital factors. The frontier orbitals can be used to explain the regioselectivity. In brief, the regioselectivity of a cycloaddition could be predicted by the following sequence : a) estimate the energies of the HOMO (the highest occupied molecular orbital) and the LUMO (the lowest unoccupied molecular orbital) of both components ; b) identify which HOMO/LUMO pair is closer in energy ; c) using this HOMO/LUMO pair, estimate the relative size of the coefficients of the atomic orbitals on the atoms at which bonding is to take place ; d) match up the larger coefficient on one component with the larger on the other [3]...[6].

2. Results and Discussions

In this paper we proposed a theoretical study using the frontier molecular orbital theory on the regioselectivity of 3+2 cycloaddition reactions of 4-phenyl-1, 2, 4-triazolium-phenacylide to methyl acrylate and acrylonitrile.

In order to calculate the atomic charge values, the coefficients of atomic orbitals and the energy values of frontier molecular orbitals we used the CNDO/2 method [7]. The calculus was performed by means of a C-256 Felix computer. The geometry of 4-phenyl-1, 2, 4-triazolium-phenacylide (ylide (I)) molecule considered in calculus was presented in a previous paper [8] (Fig. 1).

The geometry of acrylonitrile molecule is already described [9] (Fig. 2).

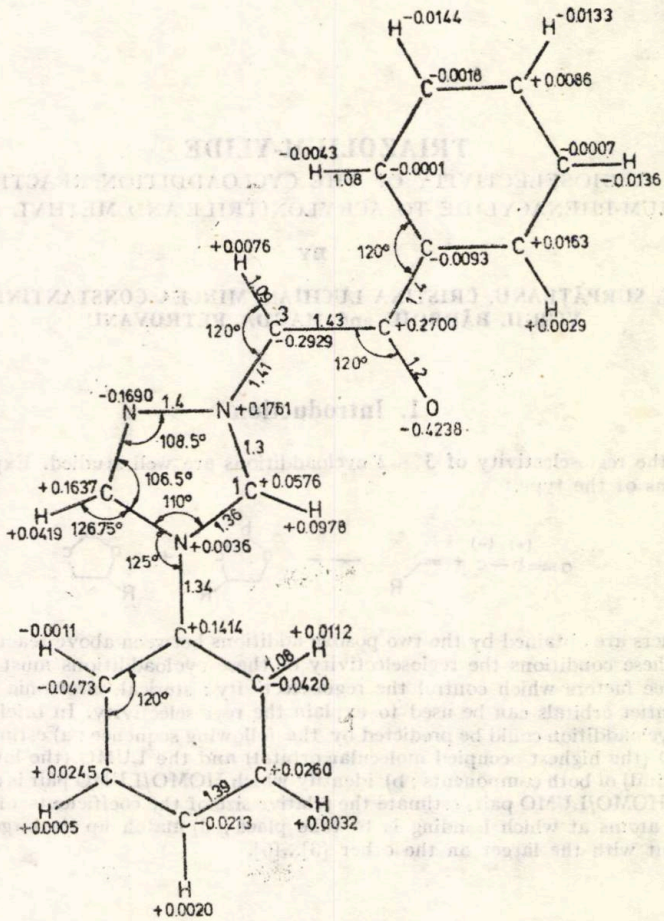

Fig. 1. — The geometry and total atomic charges of the ylide (I) molecule.

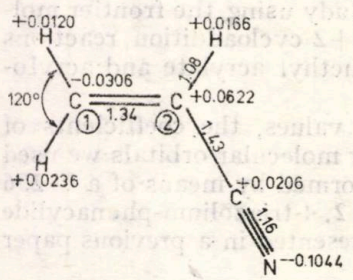

Fig. 2. The geometry and total atomic charges of the acrylonitrile molecule.

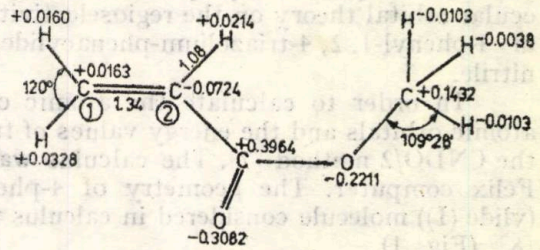

Fig. 3. — The geometry and total atomic charges of the methyl acrylate molecule.

The geometry of methyl acrylate molecule was approximated taking into account the standard interatomic angles and distances for hybridization states of all atoms which compose this molecule [10] (Fig. 3).

In the Figs. 1...3 are presented the calculated atomic charges for the 4-phenyl-1, 2, 4-triazolium-phenacylide, methyl acrylate and acrylonitrile, respectively. A survey of the atomic charges on the arbitrary noted 1 and 3 carbon atoms in the ylide and 1 and 2 carbon atoms in the dipolarophile, shows that all these values are small. In a 3 + 2 cycloaddition reaction between these compounds the electrostatic interaction is not so important [11].

Taking into account the atomic charge signs of atoms 1 and 3 in ylide and 1 and 2 in dipolarophiles, in the cycloaddition reaction between ylide and methyl acrylate the C_1 (ylide)—C_2 (methyl acrylate) and C_3 (ylide)—C_1 (methyl acrylate) bonds are formed. In the cycloaddition reaction between ylide and acrylonitrile the C_1 (ylide)—C_1 (acrylonitrile) and C_3 (ylide)—C_2 (acrylonitrile) bonds are formed. It is well known that these two dipolarophiles are of the same type (double bond C = C activated by the *Z* substituents [5]). In these conditions it is difficult to accept the above ways of cycloaddition reactions. The signs of the charges of the atoms which participate in cycloadditions appear in these reactions as insignificant.

Using the frontier molecular orbital theory we studied the same cycloaddition reactions supposing that the reaction occurs between the p_z orbitals of 1 and 3 carbon atoms in ylide and p_z orbitals of 1 and 2 carbon atoms in dipolarophiles.

In the Tables 1...3 are presented the frontier molecular orbital energies and the p_z atomic orbital coefficients of all atoms participating in cycloaddition reactions.

Table 1

The HOMO, LUMO Orbital Energies and the p_z Atomic Orbital Coefficients of the C_1 and C_3 Carbon Atoms in 4-Phenyl-1, 2, 4-triazolium-phenacylide

Orbital	Energy eV	C_1	C_3
HOMO	−8.28	−0.3583	0.7019
LUMO	2.22	0.4411	0.1008

Table 2

The HOMO, LUMO, NHOMO, NLUMO Orbital Energies and the p_z Atomic Orbital Coefficients of the C_1 and C_2 Carbon Atoms in Methyl Acrylate

Orbital	Energy eV	C_1	C_2
HOMO	−13.55	0	0
NHOMO	−13.81	0.3708	0.2859
LUMO	2.77	−0.6194	0.4286
NLUMO	6.87	0	0

Table 3

The HOMO, NHOMO, LUMO, NLUMO Orbital Energies and the p_z Atomic Orbital Coefficients of the C_1 and C_2 Carbon Atoms in Acrylonitrile

Orbital	Energy eV	C_1	C_2
HOMO	−14.11	0	0
NHOMO	−14.33	+0.6046	−0.4934
LUMO	3.50	−0.6531	0.5241
NLUMO	4.03	0	0

In the Tables 2 and 3 are also presented the same quantities for the NHOMO (the next HOMO) and NLUMO (the next LUMO) orbitals because the HOMO orbitals in dipolarophiles are null and they could not be taken into account in the determinations of the regioselectivity.

Taking into account the data presented in the Tables 1...3, the diagrams shown in the Figs. 4...7 could be constructed. In the Figs. 4 and 5 are presented the two theoretical ways of the cycloaddition reaction between 4-phenyl-1, 2, 4-triazolium-phenacylide and methyl acrylate. In both cases the C_3 ylide carbon atom is bonded to the C_2 carbon atom in methyl acrylate. The energy differences between frontier interacting orbitals, ΔE, indicate that the interaction presented in Fig. 4 is more probable.

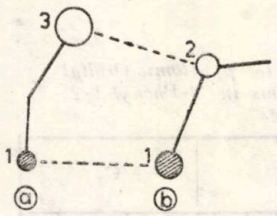

Fig. 4. — The atomic orbital coefficients on the 1 and 3 carbon atoms of HOMO orbital in ylide I (*a*) and on the 1 and 2 carbon atoms of LUMO orbital in methyl acrylate (*b*) ; $\Delta E = 11{,}05$ eV ; ● — negative sign, ○ — positive sign.

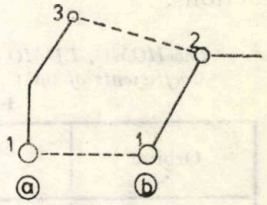

Fig. 5. — The atomic orbital coefficients on the 1 and 3 carbon atoms of LUMO orbital in ylide I (*a*) and on the 1 and 2 carbon atoms of NHOMO orbital in methyl acrylate (*b*) ; $\Delta E = 16{,}03$ eV ; ● — negative sign, ○ — positive sign.

In the cycloaddition reaction between 4-phenil-1, 2, 4-triazolium-phenacylide and acrylonitrile only the interaction of the ylide by its HOMO orbital with acrylonitrile by its LUMO orbital is theoretically possible (Fig. 6). The other interaction by ylide LUMO orbital and acrylonitrile NHOMO orbital is theoretically forbidden (Fig. 7). Thus, in this cycloaddition reaction too, the C_3 ylide carbon atom is bonded to the C_2 substituted carbon atom in acrylonitrile.

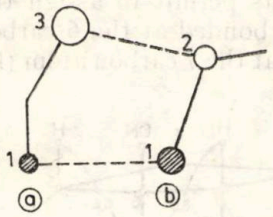

Fig. 6. — The atomic orbital coefficients on the 1 and 3 carbon atoms of HOMO orbital in ylide I(*a*) and on the 1 and 2 carbon atoms of LUMO orbital in acrylonitrile (*b*) ; $\Delta E = 11{,}78$ eV; ● — negative sign, ○ — positive sign.

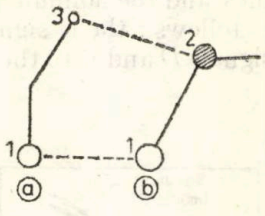

Fig. 7. — The atomic orbital coefficients on the 1 and 3 carbon atoms of LUMO orbital in ylide I (*a*) and on the 1 and 2 carbon atoms of NHOMO orbital in acrylonitrile (*b*); $\Delta E = 16{,}55$ eV; ● — negative sign, ○ — positive sign.

As a theoretical conclusion, these cycloaddition reactions are HOMO controlated [5] in respect to the ylide and take place contrary to the classical accepted electronic displacement in these dipolarophiles :

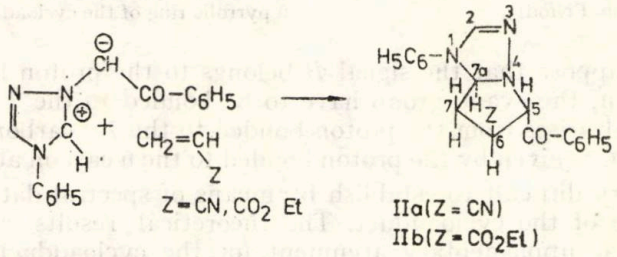

Experimentally, the products (II) are obtained by the cycloaddition reaction between ylide (I) generated *in situ* from corresponding cycloimmonium salt in the presence of triethylamine and dipolarophiles, in chloroformic solution [12]. We tryed to establish the structure of the cycloadducts (II), using the ^{1}H—NMR spectra. Next, we present the spectral data for the compound (II a), with Z=CN.The spectra show the following chemical shifts: $\tau_A = 5.73$ (doublet), $\delta_B = 5.63$ (multiplet), $\delta_C = 3.58$ (multiplet), $\delta_D = 2.75$ (multiplet), $\delta_E = 2.32$ ppm (multiplet) with the following coupling constants : $J_{AC} = 6.4$, $J_{BE} = 7.5$, $J_{BD} = 3.4$, $J_{CD} = 8.6$, $J_{CE} = 8.6$ and $J_{DE} = 13.5$ Hz. The chemical shifts and the nonnull coupling constants could be justified if the five protons belong to a saturated pyrrolic ring. The difficulty is to assign these spectral data and to determine where is bonded the cyano group. Thus, we used the induced chemical shifts by $Pr(fod)_3$. The results were presented in Fig. 8.

The more shifted protons are the protons B and H_2 (the triazolium ring proton). If we supposed that the complex with praseodymium is formed at the triazolium ring level and that the multiplet B belong to the proton bonded at the 7*a* carbon atom, it results that cyano group is bonded to the 6 carbon atom. Thus, the doublet A belongs to the proton bonded to the 5 carbon atom. The localisation of signals A and B, the chemical

shift values and the nonnull coupling constants permit to assign the other signals as follows : the *C* signal to the proton bonded at the 6 carbon atom and the signals *D* and *E* to the protons bonded at the 7 carbon atom (Fig. 9 *a*).

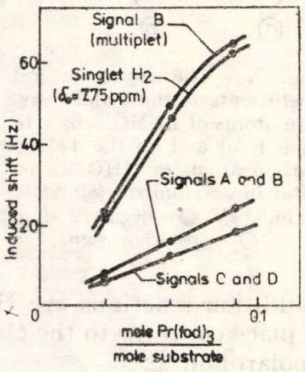

Fig. 8. — The induced shifts by the $Pr(fod)_3$.

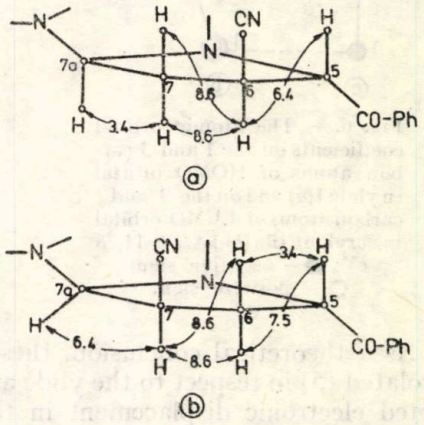

Fig. 9. — The proton spatial distributions in pyrrolic ring of the cycloadduct II (*a*).

If we suppose that the signal *B* belongs to the proton bonded at the 5 carbon atom, the cyano group have to be bonded to the 7 carbon atom. The doublet *A* arises from the proton bonded to the 7*a* carbon atom. Next, the multiplet *C* is given by the proton bonded to the 6 carbon atom (Fig. 9 *b*).

It is very difficult to establish by means of spectral data what is the real structure of the cycloadduct. The theoretical results could be considerated as a supplementary argument for the cycloadducts (II).

Received, October 22, 1979

Polytechnic Institute, Jassy,
Department of Organic and Macromolecular Chemistry,
Department of Physical Chemistry
and
Institute of Macromolecular Chemistry „P. Poni", Jassy

REFERENCES

1. Christl M., Huisgen R., Chem. Ber., **106**, 3345 (1973).
2. Huisgen R., Christl M., Chem. Ber., **106**, 3291 (1973).
3. Houk K. H., Sims J., Duke R. E. Jr., Storzier R. W., George J. K., J. Amer. Chem. Soc., **95**, 7287 (1973).
4. Houk K. H., Sims J., Watts C. R., Luskus L. J., J. Amer. Chem. Soc., **95**, 7301 (1973).
5. Fleming J., *Frontier Orbitals and Organic Chemical Reactions.* J. Wiley, London, 1974.
6. Klopman G., *Chemical Reactivity and Reaction Paths.* J. Wiley, London, 1974.
7. Pople J. A., Beveridge D. L., *Approximate Molecular Orbital Theory.* McGraw-Hill, London, 1970.
8. Surpățeanu G., Luchian C., Constantinescu M., Bărboiu V., Petrovanu M., Rev. Roumaine Chim. (in press).
9. Wilcox W. S., Goldstein J. H., Simmons J. W., J. Chem. Phys., **22**, 516 (1954).

10. Ukaji T., Bull. Chem. Soc. Japan, **32**, 1275 (1959).
11. Fukui K., *Theory of Orientation and Stereoselection*. Springer-Verlag, Berlin, 1975.
12. Petrovanu M., Luchian C., Surpăţeanu G., Bărboiu V., Rev. Roumaine Chim., **24**, 1053 (1979).

TRIAZOLIU-ILIDE

IV. Asupra reacţiilor de cicloadiţie ale triazoliu-fenacilidei cu acrilonitril şi acrilat de metil

(Rezumat)

Continuînd studiul regioselectivităţii reacţiilor de cicloadiţie se propune o interpretare teoretică a rezultatelor privind reacţiile între triazoliu-fenacilida (I) cu acrilonitril şi acrilat de metil. Această interpretare se bazează pe utilizarea teoriei orbitalilor moleculari de frontieră din cadrul metodei perturbaţiilor de ordinul doi. Rezultatele teoretice obţinute arată că sensul cicloadiţiei dipolului ilidic la dipolarofili este contrar celui indicat de factorii electronici (schema (II)).

BULETINUL INSTITUTULUI POLITEHNIC DIN IAŞI
Tomul XXVI (XXX), fasc. 3—4, 1980
Secţia II
CHIMIE şi INGINERIE CHIMICĂ

D. K. 547.425

ORGANISCHE SCHWEFELVERBINDUNGEN

XII. KONDENSATION DES 2,5-BIS (HIDRAZINOCARBONYL-METHYLMERCAPTO)-1,3,4-THIADIAZOL MIT EINIGE KETONE

VON

AL. CAŞCAVAL

1. Einführung

Aryloxyalkansäuren und ihre Derivaten wie z.B. Ester, Amide, Ureide usw. sind pflanzenphysiologisch wirksam und werden als Herbicide angewandt [1]. In neurer Zeit wurden auch pharmakologische Untersuchungen durchgeführt, wobei besonders die tuberkulostatische Wirkung einiger Hydrazide und ihrer Kondensationsprodukte mit Ketone zu erwähnen ist [2].

H. Gehlen und K.-H.Uteg [3] haben gezeigt daß die Aryloxy(thio)-1, 3, 4-Oxadiazole auch physiologisch wirksam sind. In Fortführung unserer Arbeiten an die Erweiterung des wirksames organischen Schwefelverbindungen haben wir gezeigt [4] daß 2,5-Bis(Hydrazinocarbonyl-methylmercapto)-1, 3, 4-Thiadiazol (I) mit einige aromatische Aldehyde reagiert.

Nun stellen wir die erhaltene Ergebniße in die Reaktion zwischen (I) und einige Ketone vor auf die Hoffnung daß diese Verbindungen ebenfalls wirksam sind.

2. Ergebnisse

Wir fanden, daß Dihydrazidone (III *a*...*i*) in sehr einfacher Weise erhält man wenn läßt man die Dihydrazide (I) mit Ketone (II *a*...*i*) einwirken :

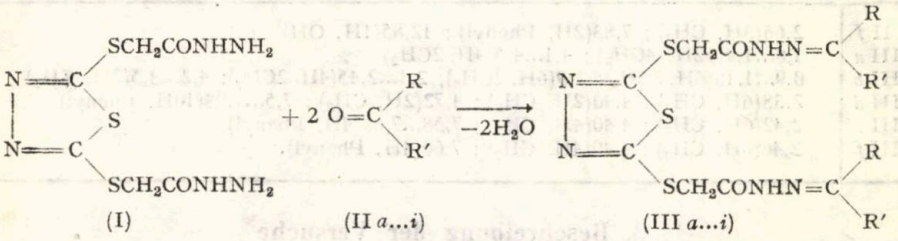

(I) (II *a*...*i*) (III *a*...*i*)

a : R=R′=CH_3 *d* : R=CH_3 ; R′=C_6H_5, *g* : R=CH_3 ; R′=$CH_2COOC_2H_5$,
b : R=CH_3 ; R′=C_2H_5, *e* : R=CH_3 ; R′=2(HO) 3,5$Cl_2C_6H_2$, *h* : R=CH_3 ; R′=2(HO)C_6H_4,
c : R+R′=$(CH_2)_5$, *f* : R=CH_3 ; R′=2(HO) 3,5$Br_2C_6H_2$, *i* : R=CH_3 ; R′=4(HO)C_6H_4.

Die erhaltene Ergebnisse u.zw.: Ausbeute, Schmelzpunkte, Elementaranalyse-Daten sind in Tabelle 1 angegeben; in die Tabelle 2 sind IR-Daten und in Tabelle 3 die ^{1}H-NMR-Daten einiger Verbindungen angegeben.

Tabelle 1

Verb.	Ausbeute, [%] Reaktionszeit, [Stunde]	Schmelzpunkt °C	C%		H%		N%	
			Ber.	Gef.	Ber.	Gef.	Ber.	Gef.
II *f*	60	110	32,65	33,05	2,04	2,48		
III *a*	91(0,5)	203...204	38,50	38,60	4,81	4,89	22,46	22,17
III *b*	76(0,5)	178...179	41,79	41,39	5,47	5,17	20,89	21,13
III *c*	77(2)	181	47,57	47,85	5,72	5,92	18,27	18,37
III *d*	58(1,5)	229...230	53,01	52,71	4,41	4,90	16,86	17,02
III *e*	95(2)	162(Zer.)	39,50	39,32	2,73	2,83	12,57	13,00
III *f*	69 (2)	179...180	31,20	31,02	2,12	2,59	9,92	10,36
III *g*	83(0,5)	160	41,69	41,01	5,02	5,17	16,21	16,01
III *h*	52(1)	223	49,81	49,40	4,15	3,78	15,84	15,44
III *i*	74(1)	219...220	49,81	50,05	4,15	4,27	15,84	15,20

Tabelle 2

Verb.	ν_{CO} cm^{-1}	weitere Maxima cm^{-1}									
II *f*	1 645	3 100	1 420	1 350	1 300	1 220	1 160	980	875	800	
III *a*	1 680	3 200	1 396	1 260	1 200	1 120	1 050	900	880	800	730
III *b*	1 680	3 200	3 000	1 400	1 200	1 120	1 040	890	860	730	
III *c*	1 670	3 200	2 950	1 450	1 380	1 200	1 130	1 040	890	710	
III *d*	1 680	3 200	3 060	1 380	1 300	1 200	1 020	1 000	900	760	
III *e*	1 680	3 250	3 000	1 530	1 440	1 360	1 250	1 200	950	860	745
III *f*	1 680	3 250	1 560	1 510	1 440	1 320	1 250	1 190	1 050	860	700

Tabelle 3

Verb.	Chemische Verschiebung, δ ppm
II *f*	2,66(3H, CH_3); 7,83(2H, Phenyl); 12,85(1H, OH)
III *a*	1,8...1,9(12H, $4CH_3$); 4,1...4,5(4H, $2CH_2$)
III *b*	0,9...1,18(6H, $2CH_3$); 1,9(6H, $2CH_3$); 2,1...2,45(4H, $2CH_2$); 4,2...4,5(2H, CH_2)
III *d*	2,38(6H, CH_3); 4,40(2H, CH_2); 4,72(2H, CH_2); 7,5...7,98(10H, Phenyl)
III *e*	2,42(6H, CH_3); 4,40(4H, CH_2); 7,58...7,88(4H, Phenyl)
III *f*	2,46(6H, CH_3); 4,40(4H, CH_2); 7,60(4H, Phenyl).

3. Beschreibung der Versuche

Die IR-Spektren wurden mit einem Spekord-71 IR-Spektrophotometer, die NMR-Spektren mit einem JEOL 60 Mhz-Gerät (in DMSO-D_6 und HMDS als Standard) aufgenommen.

a) *2-Oxy-3,5-dibrom-acetophenon (IIf)*

10,4 g 2,4-Dibromphenil-acetat mit 12,5 g $AlCl_3$ ergeben 10 g (II f) durch Erhitzen bei 140°C (II j); Schmp. 110°C (Lit. [5], 110°C).

b) *Allgemeine Vorschrift zur Darstellung von (IIIa...i)*

Berechnete Mengen Dihydrazid (I) und Ketone (II *a...i*) in Äthanol einige Zeit (s. Tabelle 1) unter Rückfluß gekocht. Man läßt den Ansatz abkühlen zur Kristallisation stehen, saugt die Kristalle ab und kristallisiert aus Äthanol um.

Der Verfasser verdankt der „Alexander von Humboldt Stiftung" für eine Stipendium (1975—1976, Freiburg i. Br.) wann diese Forschung begonnen hat.

Eingegangen am 29. Juli 1978

Technische Hochschule, Jassy
Lehrstuhl für organische und makromolekulare Chemie

LITERATURVERZEICHNIS

1. Sherman W. R., in Elderfield R. C., *Heterocyclic Compounds*. Vol. 7, 541, 1961.
2. Manishi M. B., Yer B. M., Sirsi M., J. Ind. Chem. Soc., 42, 67 (1965).
3. Gehlen H., Uteg K.-H., Arch. Pharm., *301*, 911 (1968).
4. Caşcaval Al., Cantow H.-J., Wegner G., Bul., Inst. polit., Iaşi, **XXV(XXIX)**, *3—4*, s. II, 77 (1979).
5. Donnelly J. A., Murphy J. J., J. Chem. Soc. (C), 2596 (1970).

COMBINAŢII ORGANICE ALE SULFULUI

XII. Condensarea 2,5-bis(hidrazinocarbonil-metilmercapto)-1, 3, 4-tiodiazolului cu unele cetone

(Rezumat)

În continuarea cercetărilor efectuate în vederea lărgirii gamei de substanţe organice cu sulf în moleculă se studiază obţinerea unor noi hidrazidone derivate de la 2,5-bis(hidrazinocarbonil-metilmercapto)-1, 3, 4-tiadiazol prin condensarea acesteia cu cetone alifatice sau alifatico-aromatice. Se caracterizează compuşii obţinuţi prin analize elementare şi spectral (IR, RMN).

BULETINUL INSTITUTULUI POLITEHNIC DIN IAŞI
Tomul XXVI (XXX), fasc. 3—4, 1980
Secţia II
CHIMIE şi INGINERIE CHIMICĂ

C. Z. 547.574.3 ; 547.789.6

COMPLECŞI METALICI AI UNOR ANILI CU NUCLEU BENZTIAZOLIC

DE

IOANA CIOCOIU, VIORICA DULMAN şi SIMON FIŞEL

1. Introducere

Anilii aldehidei salicilice şi derivaţilor ei ocupă o poziţie specială printre liganzii de chelatare deoarece prezintă o gamă foarte variată de posibilităţi de coordinare la un atom central. Această comportare este determinată, în primul rînd, de caracterul potenţial polidentat al salicilidenanililor iar în al doilea rînd de faptul că particularităţile lor structurale şi electronice determină stereochimii foarte variate în combinaţiile pe care le formează cu diferite metale. Complecşii salicilidenanililor cu metalele tranziţionale prezintă o mare varietate de structuri de coordinaţie a căror stereochimie este uneori atît de labilă încît conduce la configuraţii moleculare diferite în soluţie faţă de cele în stare solidă.

Aceste constatări generale, mult discutate în literatura de specialitate [1]...[7], ne-au determinat să alegem pentru studiu o serie de salicilidenanili a căror complexare a fost încercată cu cloruri şi acetaţi de nichel, cobalt şi cupru, metale trenziţionale ce formează complecşi cu importante şi variate utilizări industriale, analitice sau biocatalitice.

Salicilidenanilii aleşi de noi [8] au legat de azotul aldiminic un nucleu benztiazolic divers substituit. Prin aceasta ligandul capătă capacitatea de a deveni — în condiţii adecvate — tridentat, putînd forma la metal şi o legătură coordinativă prin intermediul electronilor neparticipanţi ai azotului sau, poate chiar, ai sulfului din molecula heterociclului.

Comportarea unui asemenea rest aminic nu a fost încă studiată la complexarea salicilidenanililor.

Pentru început, din seria salicilidenanililor benztiazolici luaţi în cercetare, în Nota de faţă se prezintă complecşii obţinuţi la tratarea 2-salicilidenamino,6-metoxi-benztiazolului de structura (I) cu acetaţi şi cloruri de cupru, nichel şi cobalt.

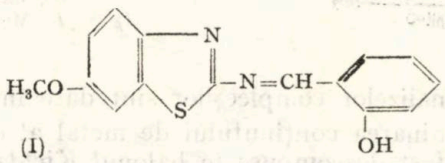

(I)

În aceste procese de complexare au rezultat şase produşi noi.

În vederea determinării structurii lor s-au efectuat analize cantitative de azot şi metal, precum şi spectrele electronice în UV şi vizibil, spectrele de reflexie ca şi cele de vibraţie (IR).

2. Partea experimentală

Complecșii ($I_{A...D}$) au fost obținuți prin solvirea a 2 moli anil I, 1 mol de sare anorganică în 25 ml metanol și 25 ml benzen. Precipită imediat un produs colorat intens, care se purifică prin spălare cu benzen, apă. Complecșii ($I_{E,F}$) s-au obținut din 2 moli anil I, 1 mol sare anorganică, care se solvă într-un amestec de 25 ml metanol și 25 ml benzen. La adăugare de amoniac precipită complexul care este apoi spălat cu benzen, apă.

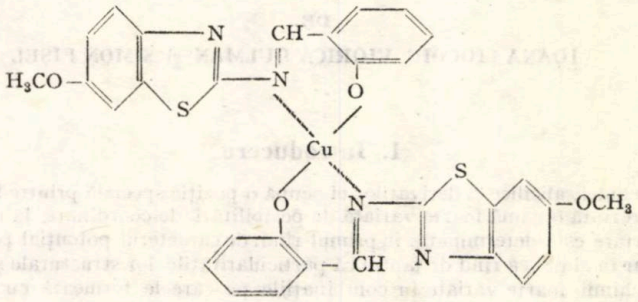

(I_A)

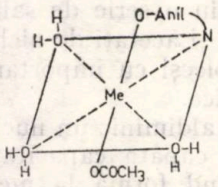

($I_{B;C}$) B : Me=Co
C : Me=Ni

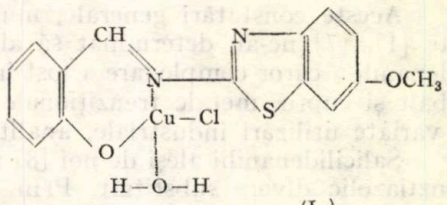

(I_D)

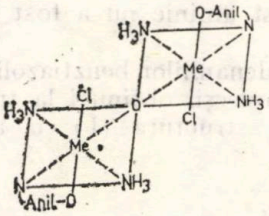

E : Me=Co
($I_{E,F}$) F Me=Ni

Rezultatele analizelor complecșilor sînt date în tabelul 1.

Pentru determinarea conținutului de metal al complecșilor analizați probe cîntărite au fost descompuse în balonul Kjeldahl utilizînd acid sulfuric concentrat și apă oxigenată 30%. În soluțiile obținute s-au determinat elementele gravimetric: nichelul sub forma complexului cu dimetil-glioximă, cobaltul cu pirofosfat iar cuprul prin precipitare din soluții omogene cu sulfură de cupru [10], [11].

Tabelul 1

Rezultatele analitice ale complecșilor studiați

Nr.	Anil	Sarea	Formula brută	Greutate moleculară	N %		Metal %		p.t. °C	Culoare
					calc.	găsit	calc.	găsit		
I_A	I	$(CH_3COO)_2Cu.H_2O$	$C_{30}H_{22}O_4N_4S_2Cu$	629	8,89	8,68	10,08	10,01	206	brun-verzui
I_B	I	$(CH_3COO)_2Co.4H_2O$	$C_{17}H_{20}O_7N_2SCo$	404	6,15	6,02	12,97	12,38	280	brun-cărămiziu
I_C	I	$(CH_8COO)_2Ni.4H_2O$	$C_{17}H_{20}O_7N_2SNi$	404	6,15	6,89	12,97	12,20	300	cărămiziu
I_D	I	$CuCl_2.2H_2O$	$C_{15}H_{13}O_3N_2SCuCl$	400	7,00	6,98	15,75	15,50	115	negru
I_E	I	$CoCl_2.6H_2O$	$C_{30}H_{34}O_5N_8S_2Cl_2Co_2$	429	13,36	12,85	14,08	13,91	250	verde
I_F	I	$NiCl_2.6H_2O$	$C_{30}H_{34}O_5N_8S_2Cl_2Ni_2$	429	13,36	12,75	14,08	13,80	192	brun

3. Rezultate şi discuţii

Spectrele electronice ale complecşilor cercetaţi au fost obţinute la un spectrofotometru UNICAM SP 800B, folosind cuve de 1 cm grosime. S-a lucrat la temperatura camerei. Benzile găsite sînt trecute în tabelul 2.

Tabelul 2

Maximele de absorbţie în UV-vizibil ale complecşilor obţinuţi

Compus	Solvent	λ nm					
Anil I	benzen	—	—	393	—	286+281	—
	etanol	—	—	390	—	278	219
Complex I_A	benzen	—	490	388	313	278,5	—
Complex I_B	benzen	446	435	382	—	282	—
Complex I_C	benzen	—	434	—	334	283	—
Complex I_D	metanol	500	457	376	304	266,5	221,5
Complex I_E	metanol	—	—	380	—	268	220,5
Complex I_F	metanol	—	—	360	339	252	237,5

Întrucît unii dintre complecşii studiaţi sînt solubili în benzen iar alţii în alcool, pentru comparaţie, spectrul electronic al anilului de plecare a fost determinat atît în solventul nepolar (benzen) cît şi în solventul polar utilizat (etanol) [9].

În etanol 2-aminosaliciliden-6-metoxi-benztiazolul prezintă două benzi puternice la 219 şi 278 nm, precum şi una la 390 nm în vizibilul apropiat. În benzen banda de la 219 nm nu poate fi identificată deoarece în acest domeniu începe absorbţia solventului. În schimb în jur de 280 nm apare o bandă puternică cu două maxime la 281 şi 286 nm, iar banda de absorbţie din vizibilul apropiat se situează la 393 nm.

Dintre complecşi, spectrele electronice ale celor obţinuţi plecînd de la acetaţi au fost determinate în benzen, în timp ce complecşii separaţi plecînd de la cloruri au fost studiaţi în etanol.

Trebuie să se remarce că în spectrele tuturor complecşilor apar o serie de benzi noi datorate procesului de complexare. Benzile de absorbţie existente la anil apar şi în complecşi dar, în toate cazurile, deplasate spre lungimi de undă mai mici.

Din literatura de specialitate rezultă că benzile de absorbţie din domeniul lungimilor de undă mari sînt determinate de procese ce au loc în învelişul electronic *d* incomplet al ionului metalic central, iar cele ce apar la lungimi de undă mai mici sînt datorate tranziţiilor electronilor neparticipanţi ai ligandului, ce iau parte la legătura coordinativă. În spectrele tuturor complecşilor apar în domeniul vizibil una pînă la două benzi noi situate între 434 şi 500 nm. În ceea ce priveşte banda nouă din domeniul 300...

340 nm ea poate fi atribuită implicării dubletului de electroni a azotului azometinic într-o legătură donor—acceptor.

Spectrele de vibrație în IR ale complecșilor cercetați au fost înregistrate la un spectrofotometru SP 1 000, în pastile de bromură de potasiu. Aceste spectre se caracterizează printr-un număr foarte mare de benzi. În tabelul 3 sînt trecute numai benzile caracteristice necesare în discutarea structurii. Tabelul mai conține și benzile anilului de plecare pentru a putea urmări schimbările survenite în urma complexării.

Tabelul 3

Maximele de absorbție în IR ale complecșilor obținuți

Anil I	—OH	$\nu_{C=N\ anilic}$	$\nu_{C=N\ tiazolic}$	Nucleu benztiazolic	—O—CH_3	Nucleu aromatic substituit
Anil I	3 490 s	1 630 s	1 605 i	1 470 m 1 450 m 1 370 i	1 290 m 1 270 m	760 u 750 i 740 s
Complex (I_A)	3 600... 3 300 m	1 645 s	1 615 fi 1 589 i 1 545 i	1 480 s 1 460 s 1 455 s 1 445 s 1 390 i	1 330 i 1 270 m	760 m 735 m
Complex (I_B)	3 600... 3 300 m	1 650 m	1 615 m 1 589 m 1 540 m	1 475 m 1 455 s 1 435 s 1 420 u	1 340 u 1 330 s 1 275 m	760 i 740 u
Complex (I_C)	3 600... 3 300 m	1 650 u	1 615 i 1 589 s 1 570 m 1 538 i	1 465 m 1 440 fi 1 390 s 1 373 i	1 330 i 1 270 i	740 u
Complex (I_D)	3 400... 3 020 m	1 650 u	1 612 fi 1 545 m	1 445 m 1 390 s	1 350 m 1 320 m 1 280 i	765 m
Complex (I_E)	3 440... 3 370 m	1 650 fi	1 590 u 1 535 u 1 525 u	1 445 fi	1 355 fi 1 320 m 1 275 i	725 s
Complex (I_F)	3 400 m	1 655 m	1 615 u 1 560 i 1 343 u	1 475 i	1 355 u 1 340 i 1 310 s	755 m

În spectrul ligandului se observă $\nu_{C=N\ anilic}$ la 1 630 cm^{-1}, $\nu_{C=N\ tiazolic}$ la 1 605 cm^{-1}, ν_{Ph-O} la 1 290 și 1 270 cm^{-1} (suprapus peste ν_{-OCH_3}), ν_{-OH} slab asociat intramolecular la 3 490 cm^{-1}, vibrațiile nucleului benzenic disubstituit între 730...760 cm^{-1} ca și cele caracteristice nucleului benztiazolic, care apar sub forma a trei benzi situate între 1 370...1 470 cm^{-1}.

Trebuie să se observe, în primul rînd, că ν_{-OH} apare, în toți complecșii, lărgită, intensificată și deplasată. În complecșii cu acetați această deplasare are loc spre lungimi de undă mai mari, banda situîndu-se între 3 300... 3 650 cm^{-1}, în timp ce în complecșii cu cloruri deplasarea are loc spre lungimi de undă mai mici, banda este mai intensă, situîndu-se între 3 000...3 450 cm^{-1}. Unii autori consideră că —OH chelatat apare în domeniul 2 700...3 100 cm^{-1} sub forma unei benzi imprecis conturate. Acesta ar fi cazul complecșilor cu cloruri. Alte studii spectroscopice consideră că în cazul în care se produce o slăbire a legăturii intramoleculare de hidrogen, vibrațiile de valență ale grupei —OH apar la lungimi de undă mai mari, ceea ce este cazul complecșilor studiați cu acetați.

Frecvența de vibrație $\nu_{C=O}$ de la 1 290 cm^{-1} apare la complecși deplasată față de ligand cu 40...60 cm^{-1} spre valori mai mari, ceea ce pare să indice formarea unei legături C—O—Me. Cealaltă vibrație, ce ar putea fi atribuită legăturii Ph—O de la 1 270 cm^{-1}, se deplasează foarte puțin în jurul acestei valori, ceea ce permite să se presupună că ea poate fi atribuită mai curînd vibrației ν_{-OCH_3}, situată în același domeniu.

În complecși frecvența de vibrație $\nu_{C=N\ anilic}$ apare deplasată spre lungimi de undă mai mari cu 15...25 cm^{-1}. Acest lucru indică faptul că legătura anilică este afectată datorită formării unei legături coordinative prin electronii p ai azotului și apariției unui ciclu cvasiaromatic care include și metalul. Prin complexare apare la azotul azometinic o sarcină parțial pozitivă care îngreunează conjugarea π—π din întreaga moleculă a ligandului. Eliberarea grupării azometinice din conjugare duce la creșterea frecvenței acestei grupe în spectrul de vibrație.

Formarea legăturii coordinative —HC=N→Me afectează repartiția electronilor din întreaga moleculă a ligandului. Astfel, în domeniul în care sînt situate vibrațiile caracteristice nucleului benztiazolic și legăturii C=N tiazolice apar un număr mai mare de maxime, în timp ce în domeniul în care sînt situate vibrațiile caracteristice nucleului benzenic disubstituit, numărul benzilor scade și slăbește în intensitate. Toate aceste aspecte indică o slăbire a conjugării în molecula ligandului datorită chelatării și antrenării electronilor neparticipanți în procesul de fixare a metalului.

4. Concluzii

Plecînd de la datele obținute în studiul efectuat se poate trage concluzia că în complecșii formați există atît legături covalente O—Me cît și legături coordinative N—Me.

La aceste rezultate se dau ca probabile structurile ($I_{A...F}$).

Primit la 24 mai 1978

Institutul politehnic, Iași,
Catedra de chimie organică și macromoleculară
și
Catedra de chimie analitică și anorganică

BIBLIOGRAFIE

1. Henrici-Olivé V. G., Olivé S., Angew. Chem., 1,1 (1974).
2. Vogt L. H., Chem. Rew., 63, 299 (1963).
3. Fallab V., Chimia, 23, 177 (1969).

4. Fallab V., Chimia, **19**, 463 (1965).
5. Miller B. E., J. Am. Chem. Soc., **92**, 2687 (1970).
6. Miller B. E., J. Am. Chem. Soc., **91**, 1962 (1969).
7. Zuberbühler B., Helv. Chim. Acta, **54**, 1502 (1971).
8. Avramovici S., Ciocoiu I., Airinei A., Soifer S., An. șt. Univ., „Al. I. Cuza", Iași, **XVIII**, 61 (1972).
9. Avramovici S., Airinei A., Ciocoiu I., Rev. Roum. Chim., **18**, 1881 (1973).
10. Macarovici Gh., *Manual de chimie analitică cantitativă*. Ed. Tehn., Buc., 1956.
11. Fișel S., Bold A., Mocanu R., Sîrghie I., *Chimie analitică cantitativă*. EDP Buc., 1973.

COMPLEXES MÉTALLIQUES DE CERTAINS SALICYLIDÈNE-ANILS À NOYAU BENZOTHIAZOLIQUE

(Résumé)

On a synthétisé six complexes métalliques du salicylidène, amino-2 méthoxy-6, benzothiazole avec des acétates et des chlorures de Cu, Ni et Co. La structure des produits a été prouvée par des analyses quantitatives, par des spectres électroniques (UV-visible), de réflexion ainsi que par des spectres IR.

BULETINUL INSTITUTULUI POLITEHNIC DIN IAŞI
Tomul XXVI (XXX), fasc. 3—4, 1980
Secţia II
CHIMIE şi INGINERIE CHIMICĂ

D.C. 547.564.4

REACTION BETWEEN *o*-AMINOTHIOPHENOL AND ISOTHIOCYANIC ACID

BY

BORIS ARVENTIEV and TATIANA NICOLAESCU

1. Introduction

E. Vinkler and F. Klivenyi [1] have recently carried out the reaction between 2,2'-diaminodiphenyldisulfide (I) and isothiocyanic acid starting from (I) and ammonium thiocyanate in diluted hydrogen chloride solution by heating on the water bath for an hour.

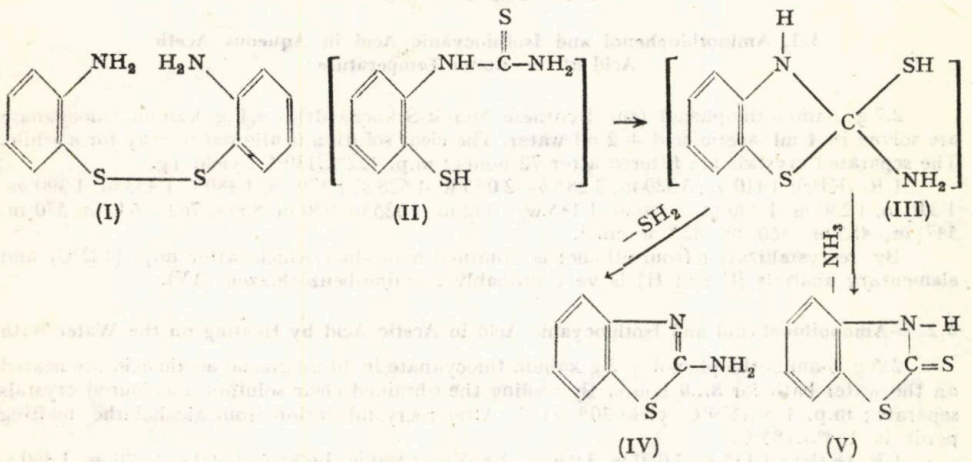

The above mentioned authors obtained a mixture of 2-amino-benzothiazole (IV) and 2-benzothiazolinthiole (V) which were separated chromatographically on silicagele column with petroleum ether, benzene and finally methanol as eluents. The authors suppose the compound (I) to be reduced to *o*-aminothiophenol which reacts then with isothiocyanic acid to give the unseparable addition product (II) which by ring closure (III) followed by SH_2 elimination gives (IV) and by NH_3 elimination gives (V).

2. Results and Discussion

In the present paper the reaction between *o*-aminothiophenol and isothiocyanic acid is carried out starting from *o*-aminothiophenol and kalium thiocyanate in acetic acid solution at the room temperature and by heating on the water bath for a longer period.

When the reaction is carried out at the room temperature the reaction product separates which is filtered after 72 hours and submitted to the elemental analysis. The carbon and hydrogen contents indicate this product to

be either (II) or (VI). When the reaction is carried out on the water bath for 8...9 hours the 2-benzthiazolinthiole (V) is separated with a yield of 30%. Other compounds were also separated from these two reactions, which are now under study. In the aqueous alcoholic solution the reaction between *o*-aminothiophenol and kalium thiocyanate does not take place, the *o*-amino-thiophenol being instead oxydized to the disulphide (I), probably by the air oxygen.

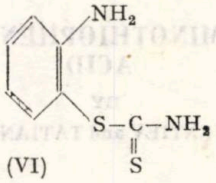

(VI)

The *o*-aminothiophenol oxidation was also noticed to take place after the same period in the kalium thiocyanate absence.

3. Experimental

3.1. Aminothiophenol and Isothiocyanic Acid in Aqueous Acetic Acid at the Room Temperature

2.7 g *o*-aminothiophenol (zur Synthese Merck-Schuchardt) + 4.1 g kalium thiocyanate are solved in 4 ml acetic acid + 2 ml water. The clear solution is allowed to stay for a while. The separated crystals are filtered after 72 hours; m.p. 122°...130°C; yield 1 g.

I.R. (KBr): 3 410 vs, 3 320 m, 3 285 vs, 2 055 w, 1 628 s, 1 570 vs, 1 480 s, 1 453 m, 1 390 vs, 1 310 m, 1 250 m, 1 200 m, 1 160 m, 1 145 w, 1 112 m, 1 025 m, 950 m, 850 s, 762 s, 650 m, 570 m, 547 m, 485 m, 460 m, 425 w cm^{-1}.

By recrystallization from ethanol is obtained a product which, after m.p. (132°C) and elementary analysis (C and H) is very probably 2-amino-benzothiazole (IV).

3.2. *o*-Amonothiophenol and Isothiocyanic Acid in Acetic Acid by Heating on the Water Bath

2.5 g *o*-aminothiophenol + 2 g kalium thiocyanate in 10 ml glacial acetic acid are heated on the water bath for 8...9 hours. By cooling the obtained clear solution uncoloured crystals separate; m.p. 178...179°C, yield 30% (1 g). After recrystallization from alcohol the melting point is 184°...185°C.

I.R. (KBr): 3 115 w, 3 080 w, 3 040 w, 2 895 w, 2 840 w, 1 650 w, 1 600 s, 1 500 vs, 1 460 s, 1 430 vs, 1 320 vs, 1 285 s, 1 250 vs, 1 155 m, 1 140 w, 1 130 m, 1 080 s, 1 035 vs, 1 015 s, 1 000 s, 940 w, 885 w, 875 m, 853 w, 753 vs, 720 w, 705 w, 670 s, 605 s, 570 m, 525 w, 502 w, 425 m cm^{-1}. vs — very strong, s — strong, m — medium, w — weak.

Received, November 11, 1978

Polytechnic Institute, Jassy,
Department of Organic and Macromolecular Chemistry

REFERENCES

1. Vinkler E., Klivenyi F., Acta chim. Acad. Sci. hung., **94** (4), 357 (1977).

REACŢIA DINTRE *o*-AMINOTIOFENOL ŞI ACID IZOTIOCIANIC

(Rezumat)

S-a efectuat reacţia dintre *o*-aminotiofenol şi acidul izotiocianic. În cazul cînd reacţia are loc la temperatura camerei se formează produsul de adiţie (II) sau (VI). La încălzire pe baie de apă timp de 8...9 ore se formează produsul (V). În soluţie alcoolico-apoasă nu are loc reacţia dintre *o*-aminotiofenol şi tiocianat de potasiu, primul oxidîndu-se la (I).

BULETINUL INSTITUTULUI POLITEHNIC DIN IAŞI
Tomul XXVI (XXX), fasc. 3—4, 1980
Secţia II
CHIMIE şi INGINERIE CHIMICĂ

D.C. 547.785.5

CONTRIBUTION TO THE SYNTHESIS AND STUDY OF SOME BENZIMIDAZOLE DERIVATIVES

BY

CRISTOFOR SIMIONESCU
Member of the Academy of the Socialist Republic of Romania
and
MARIA DUMITRU

1. Introduction

Since the benzimidazole ring is resistent to halogenation [1] one commonly uses the halogenated derivatives of 1,2-phenylenediamine for introducing the halogene into molecule. Benzimidazole derivatives containing chlorine or bromine atoms in position 5 are obtained when reacting 4-chloro- or 4-bromo-phenylenediamine 1,2 with formic [2], [3] or acetic [3] acide while the iodine substitution în position 2 takes place when treating with sodium hypoiodide solution [4].

Starting from 4-chloro-phenylenediamine-1,2 and lactic acid we obtained 5-chloro-2-(α-hydroxyethyl)-benzimidazole which was converted by oxydation into 5-chloro-2-acetyl-benzimidazole [5]:

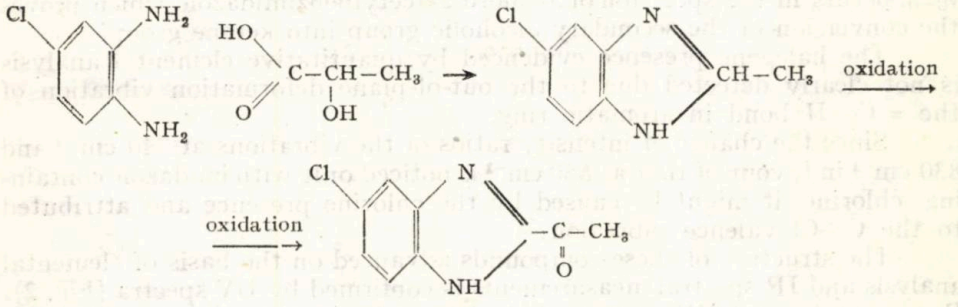

The structure of these compound has been elucidated by means of both quantitative elemental analysis as well as IR, UV and NMR spectral measurements.

2. Results and Discussion

Characteristics of some benzimidazole derivatives containing chlorine in molecule are summarized in Table 1.

Table 1

Characteristics of some Benzimidazole Derivatives containing Chlorine in Molecule

Compound	m.p. °C	Analyses							
		Calculated				Found			
		C %	H %	N %	Cl %	C %	H %	N %	Cl %
5-Chloro-2-(α-hydroxyethyl)-benzimidazole	190	54.96	4.61	14.24	18.03	54.78 54.85	4.67 4.70	14.26 14.28	17.90 17.80
5-Chloro-2-acetylbenzimidazole	180	55.53	3.62	14.39	18.21	55.47 55.51	3.70 3.72	14.22 14.40	18.10 18.30

The IR spectra of the two derivatives containing chlorine in the benzimidazole ring show the characteristic bands of the heterocyclic nucleus. In spectra of two compounds the vibrations 1 620 and 1 590 cm^{-1}, characteristic of the heterocyclic ring, are to be found. In the spectrum of 5-chloro-2-(α-hydroxyethyl)-benzimidazole a broad bands occurs within the 2 400... 3 300 cm^{-1} range characteristic of benzimidazole derivatives containing a α-hydroxyethyl residue in position 2.

The conversion of 5-chloro-2-(α-hydroxyethyl)-benzimidazole into 5-chloro-2-acetylbenzimidazole modifies the appearance in this region of a strong absorption being noticed in the spectrum of the latter characteristic of the N—H valence vibration in benzimidazole ring at 3 300 cm^{-1} (Fig. 1).

The absorption at 1 685 cm^{-1}, attributed to the valence vibration $\nu_{C=O}$, occurs in the spectrum of 5-chloro-2-acetylbenzimidazole which proves the conversion of the secondary alcoholic group into ketone group.

The halogene presence evidenced by quantitative elemental analysis is not clearly detected due to the out-of-plane deformation vibration of the =C—H bond in aromatic ring.

Since the change of intensity ratios of the vibrations at 740 cm^{-1} and 830 cm^{-1} in favour of that at 830 cm^{-1} is noticed only with imidazole containing chlorine it might be caused by the chlorine presence and attributed to the C—Cl valence vibration.

The structure of these compounds advanced on the basis of elemental analysis and IR spectral measurements is confirmed by UV spectra (Fig. 2). By comparing the UV spectra of the 2-acetylbenzimidazole (λ = 210, 242, 305 nm) with that of 5-chloro-2-acetylbenzimidazole (λ = 220, 247, 310 nm) a weak bathochromic shift is noticed for the $\pi \rightarrow \pi^*$ and $n \rightarrow \pi^*$ transitions due to the halogene introduction into the heterocyclic ring.

The conversion of the secondary alcoholic group into 5-chloro-2-(α-hydroxyethyl)-benzimidazole, by oxydation, causes a bathochromic shift of the absorption bands due to the substituent with effect $-E$ which impose the attraction of electrons of the aromatic system and thus the chromophore system extending.

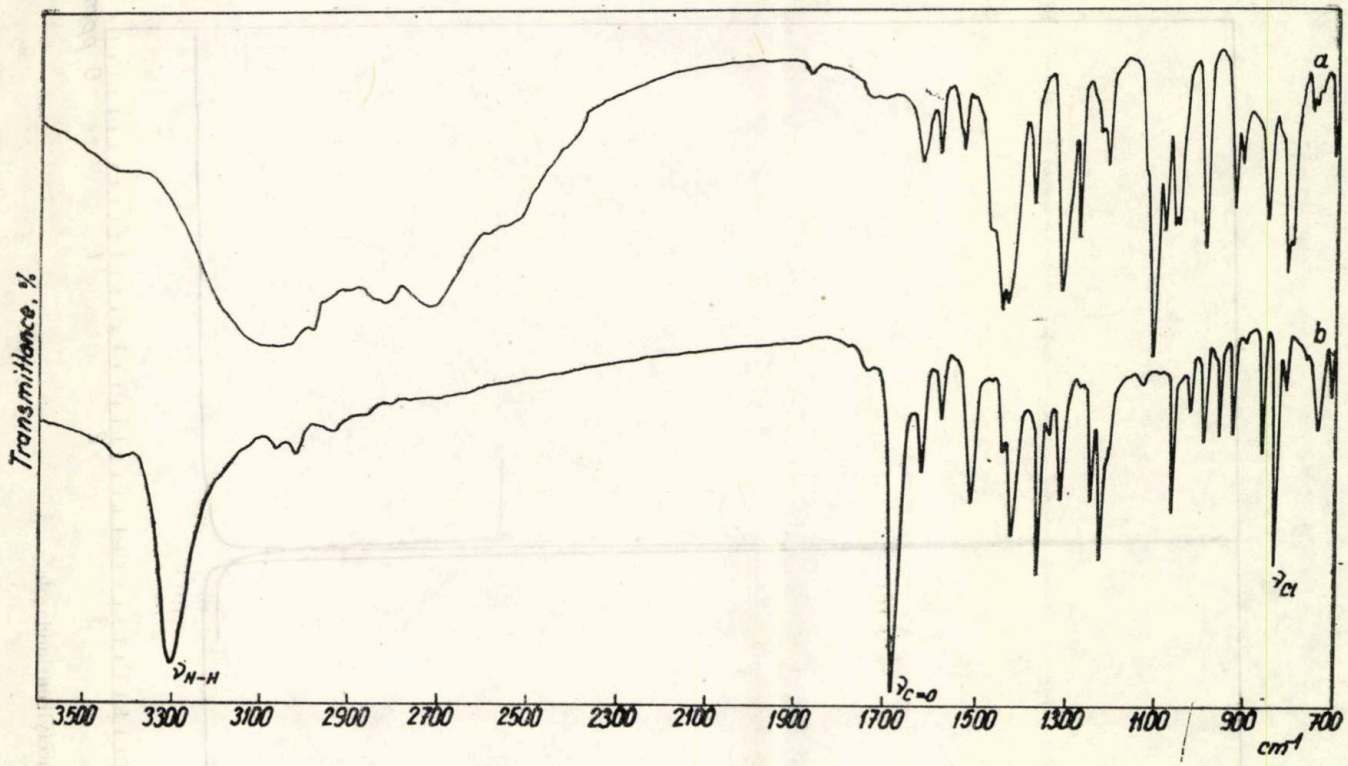

Fig. 1. — IR spectra of the 5-chloro-substituted benzimidazole derivatives: *a* — 5-Chloro-2-(α-hydroxyethyl)-benzimidazole; *b* — 5-Chloro-2-acetylbenzimidazole.

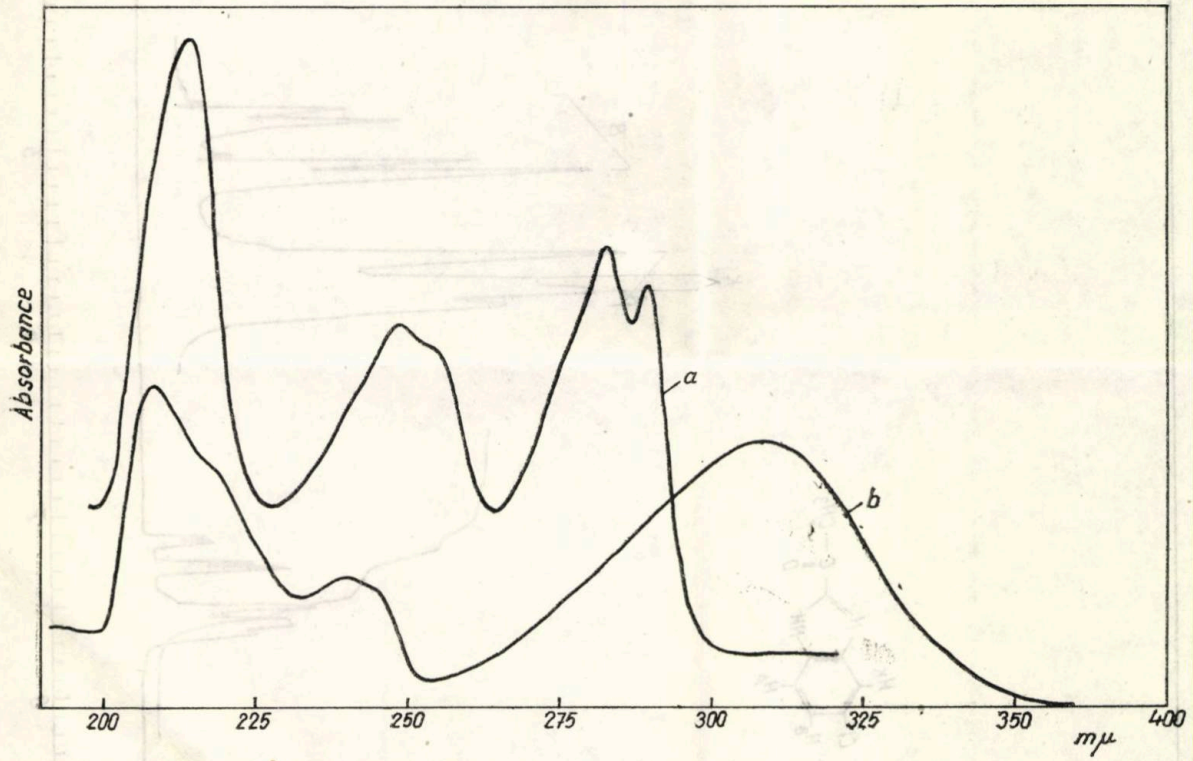

Fig. 2. — UV spectra of the benzimidazole containing chlorine in molecule: *a* — 5-Chloro-2-(α-hydroxyethyl)-benzimidazole; *b* — 5-Chloro-2-acetylbenzimidazole.

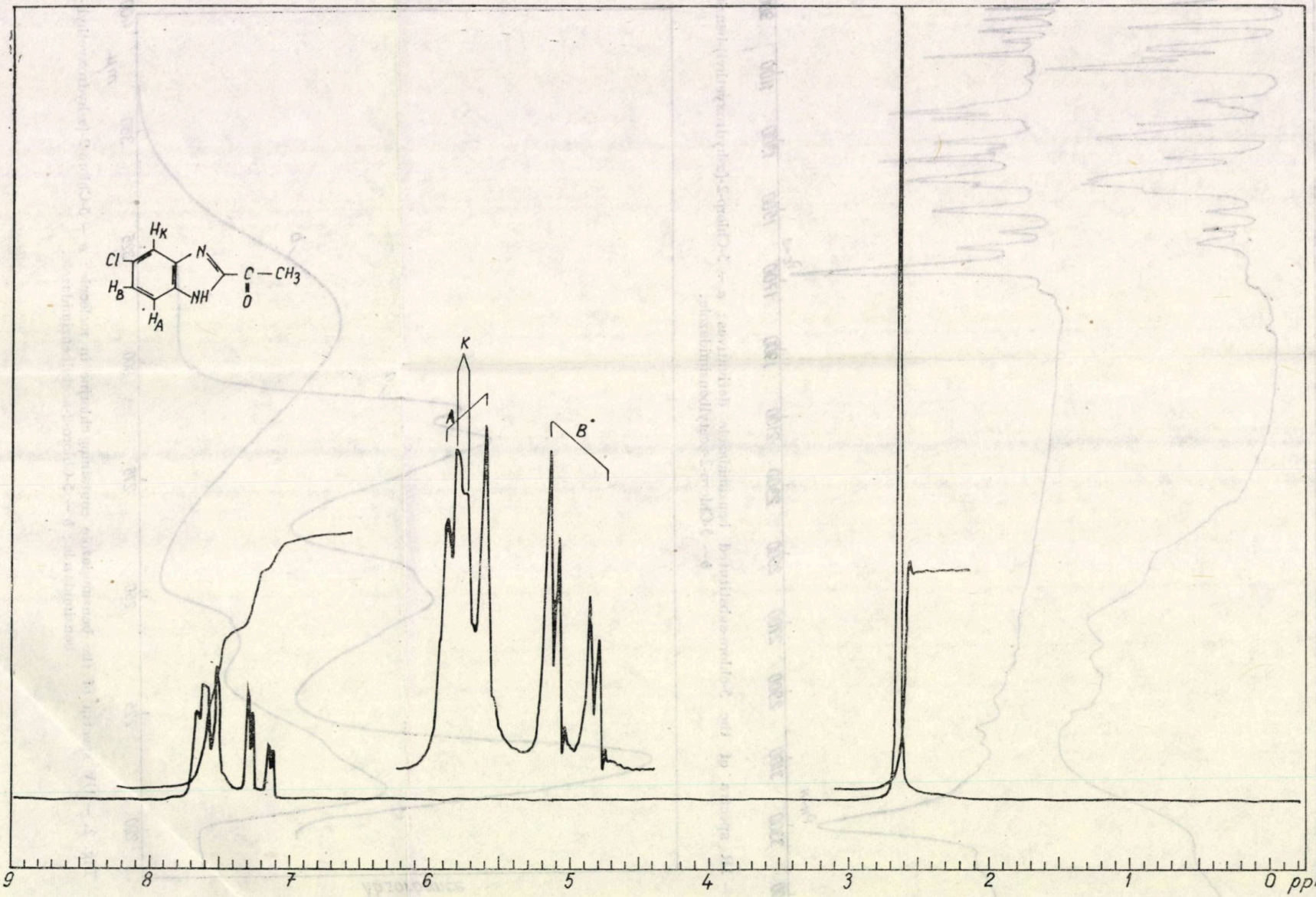

Fig. 3. — NMR spectrum of 5-chloro-2-acetylbenzimidazole.

Thus the $\pi—\pi^*$ transitions are shifted towards longer wavelengths occuring at $\lambda = 220$ nm, 247 nm in 5-chloro-2-acetylbenzimidazole compared to $\lambda = 214$ nm, 255 nm in 5-chloro-2-(α-hydroxyethyl)-benzimidazole and are converted into the weaker band with fine structure at 315 nm. This bathochromic shifting is due to participation of the unpaired electrons at the carboxylic group to the $n — \pi^*$ transition.

The NMR spectral data confirm the structure of the carboxylic product containing chlorine.

In the NMR spectrum of 5-chloro-2-acetylbenzimidazole (Fig. 3) the ratio of relative intensities of the signals indicating the equivalent proton number checks the proportion within the molecule of the hydrogen atom in the acetyl residue with respect to those in aromatic ring.

To establish the number of different proton sorts the following calculations have been made taking into account the signal intensities :

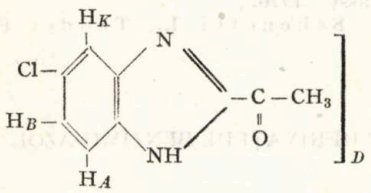

$D = 6.6$; $A+K = 4.5$; $B = 1.2$;

$D + A + K + B = 13.2$;

$6/13.2 = 0.455$ H/unit.

For D $6.6 \times 0.455 = 3$ 3H

$A + K4 \times 0.455 = 2.02$ 2H

$B\,2.1 \times 0.455 = 0.96$ 1H

The low field multiplet lies in the region characteristic of aromatic protons ; the signal at $\delta = 7.66$ ppm is attributed to the K proton. The positions occupied by the other absorptions indicate presence of A and B proton ($\delta_A = 7.6$ ppm ; $\delta_B = 7.21$ ppm). The curve alure within this region is characteristic for the substituted phenyl ring in which the unsubstituted hydrogens are located in A, B and K positions.

With this compound the chemical shift of the protons neighbouring the chlorine atom occurs at higher fields compared to the compound in which the same position is substituted by a nitro group [6].

The intensity and the chemical shift of the singlet, $\delta = 2.65$ ppm, indicate the presence of methyl proton in the acetyl residue.

The values of the proton chemical shifts in the heteroatomic ring are identically with those reported in literature by other authors [7] for benzimidazole derivatives containing chlorine.

Analyses: C% 55.51; H% 3.72% ; N% 14.40 ; Cl% 18.30.

IR Spectra ($\nu_{N-H} = 3\,300$ cm^{-1} ; $\nu_{C=O} = 1\,680$ cm^{-1} ; $\nu_{Cl} = 830$ cm^{-1}. Other absorptions : at 740 cm^{-1} characteristic of the substituent in position 2 and at 1 625 cm^{-1} characteristic of the substitution in position 5).

UV Spectra : $\lambda_{max} = 310$, 247, 220 nm.

NMR Spectra : multiplets in the aromatic region : $\delta_K = 7.66$ ppm ; $\delta_A = 7.60$ ppm ; $\delta_B = 7.21$ ppm and the singlet $\delta = 2.65$ ppm, indicating the presence of methylic protons in the residue.

3. Conclusions

The results of IR, UV and NMR spectroscopical measurements confirm the structure of 5-chloro-2-acetylbenzimidazole obtained by oxydation of 5-chloro-2-(α-hydroxyethyl)-benzimidazole with chromic anhydride in acetic acid.

Received, April 2, 1979

Polytehnic Institute, Jassy, Department of Organic and Macromolecular Chemistry

REFERENCES

1. Elderfield R. C., *Heterocyclic Compounds*. Vol.5, John Wiley and Sons, New-York, 267.
2. Fischer O., Ber., **37**, 556 (1904).
3. Fischer O., Mouson G., Ber., **38**, 325 (1905).
4. Pauly H., Gumdermann K., Ber., **41**, 3999 (1908).
5. Simionescu C., Dumitriu M., Patent R.S. Romania, nr. *65 724* (1975).
6. Dumitriu M., *Cercetări în domeniul poliacetilenelor heterociclice. Polibenzimidazolil-acetilene*. Ph. D. Diss., Polyt. Inst., Jassy, 1976.
7. Dembech P., Seconi G., Vivareli P., Schenetti L., Taddei F., J. Chem. Soc. (B), 1670 (1971).

CONTRIBUŢII LA SINTEZA ŞI STUDIUL UNOR DERIVAŢI DE BENZIMIDAZOL

(Rezumat)

Se prezintă rezultatele studiului spectral IR, UV şi RMN pentru derivaţi de benzimidazol avînd clor în moleculă — 5-clor-2-acetil-benzimidazol — obţinut prin oxidarea 5-clor-2-(α-hidroxietil)-benzimidazolului cu anhidridă cromică în acid acetic glacial.

BULETINUL INSTITUTULUI POLITEHNIC DIN IAŞI
Tomul XXVI (XXX), fasc. 3—4, 1980
Secţia II
CHIMIE şi INGINERIE CHIMICĂ

D.C. 661.857 : 615.7

SYNTHESIS AND ELECTRICAL PROPERTIES OF SOME NEW SILVER SALTS DERIVATIVES OF N-(*p*-AMINOBENZOYL)-L-ASPARAGINE

BY

VALERIU ŞUNEL, M. RUSU, G. I. RUSU and I. MAZILU

1. Introduction

In recent times numerous studies have been performed for elucidating the mechanism of electrical conductivity in the organic compounds showing semiconducting properties [1]...[3].

In previous papers [4]...[7] the electrical properties of some L-asparagic acid and L-asparagine derivatives have been studied and a correlation settled between the chemical structure and the values of the parameters determining their semiconducting properties. To explain the electroconductivity mechanism for these substances the zonal model was advanced.

In view of the connection between the electrical properties and the structure of the organic compounds, we found interesting to extend our studies on other L-asparagic acid and L-asparagine derivatives with silver ion in their structure.

2. Results and Discussion

2.1. Preparation of the Silver Salts of β-Amido-N-[*p*-(acyl-amino)-benzoyl]-*L*-asparagic Acids

In order to study the correlation between the chemical structure and the electrical conductivity the silver salts of the β-amido-N-[*p*-(acyl-amino)-benzoyl]-L-asparagic acids with the silver ion supported by the N-[*p*-(acylamino)-benzoyl]-L-asparagine residual were synthesized. The silver salts (IV)...(VI) were obtained by solving the β-amido-N-[*p*-(acylamino)-benzoyl]-L-asparagic acids (I)...(III) [8], [9] in a natrium bicarbonate solution followed by precipitation with a silver nitrate solution.

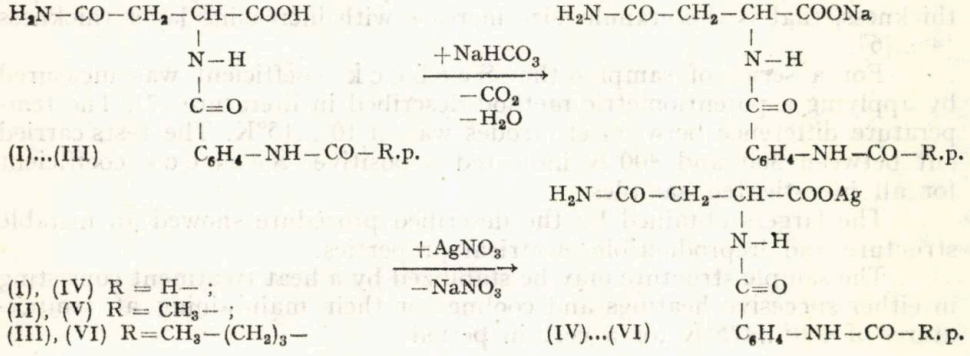

The three silver salts which are not described in literature are solid, crystalline compounds and do not melt till 280°C.

The silver salts described in the present paper were prepared as follows: 1,5 g β-amido-N-[*p*-(acylamino)-benzoyl]-L-asparagic acid are solved in 17 ml of N/5 natrium bicarbonate solution and 17 ml N/5 silver nitrate solution added gradually under good strirring. A bulky precipitate separates which is filtered and washed with a great amount of water. The obtained product is dried in a oven under low pressure and temperature of 70°...90°C. In Table 1 the formula of the obtained products, their yields and analytical data are listed.

Table 1

Structure Formula and Analytical Data of some New Silver Salts Derivatives of N-(p-aminobenzoyl)-L-asparagine

No.	Molecular structure	C, [%]		H, [%]		N, [%]		Ag, [%]		Yield %
		calcd.	found	calcd.	found	calcd.	found	calcd.	found	
IV	$C_{12}H_{12}N_3O_5Ag$	37.30	37.55	3.10	3.42	10.83	11.20	28.00	27.76	80.50
V	$C_{13}H_{14}N_3O_5Ag$	39.00	39.35	3.50	3.67	10.50	10.71	27.00	26.84	77.25
VI	$C_{16}H_{20}N_3O_5Ag$	43.44	43.63	4.52	4.79	9.50	9.80	24.43	24.17	70.22

2.2. Study of the Electrical Properties

In order to study the electrical properties of the obtained substances the samples were used as thin layers laid from their dimethylformamide solutions on glass supports.

The electrical conductivity variation was recorded by means of a device specially designed [4].

For electrical resistivity measurements the surface type cells and silver electrodes (their interval being of 5...15 mm) were used. The temperature measurements were made by means of an iron-constantan thermocouple. The thickness values of the layers under study, measured by an interferometric method, were found to be 0.15...1.75 μm.

The metallographic studies showed that all the layers have a granular structure. The crystal dimensions depend essentially on the layer thickness, that is the granule size increase with increasing layer thickness [4]...[6].

For a series of samples the S e e b e c k coefficient was measured by applying a potentiometric method described in literature [7]. The temperature difference between electrodes was of 10°...15°K. The tests carried out between 300° and 400°K indicated a positive S e e b e c k coefficient for all investigated samples.

The largers obtained by the described procedure showed an instable structure and ireproductible electrical properties.

The sample structure may be stabilized by a heat treatment consisting in either succesive heatings and coolings or their maintaining at temperatures of 400°...475°K for a certain period.

In order to obtain some information on layer structure modification the electrical conductivity σ dependence on the temperature during this treatment was studied. In Figs. 1...3 the curves $\ln \sigma = f(10^3/T)$ are plotted for three samples.

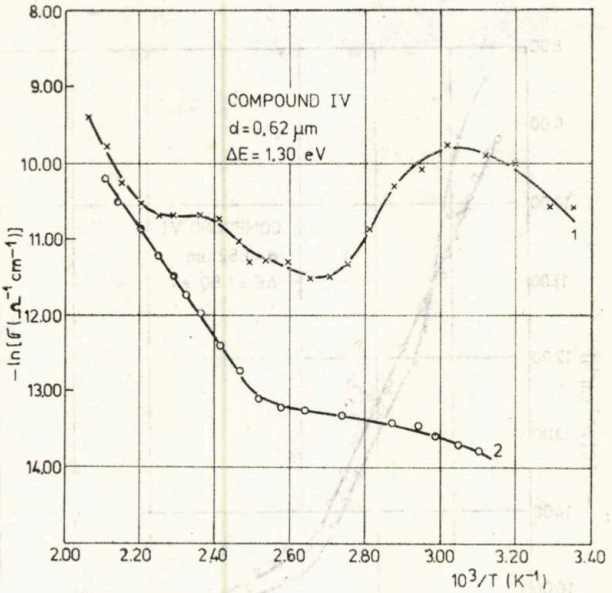

Fig. 1

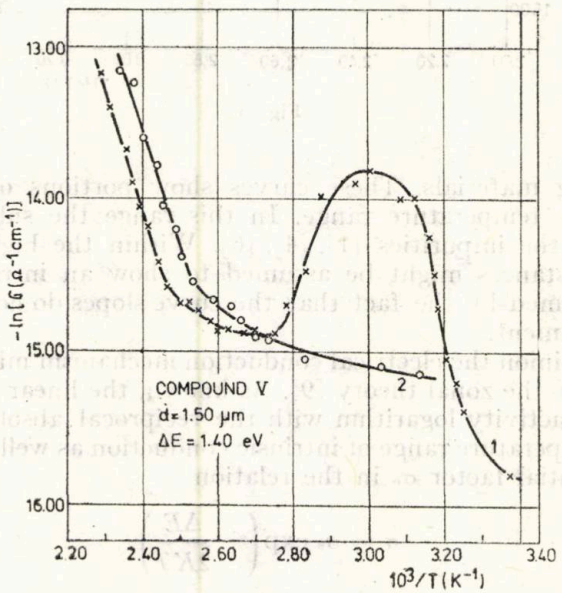

Fig. 2

During the first heating (curves *1*, Figs. 1...3) the curve shape is strongly influenced by the layer structure modification. After the thermal treatment the dependence $\ln\sigma = f(10^3/T)$ become reversible due to the layer structure stabilization. As can be seen in Figs. 1...3 (curves *2*) the electrical conductivity dependence on the temperature is typical for the

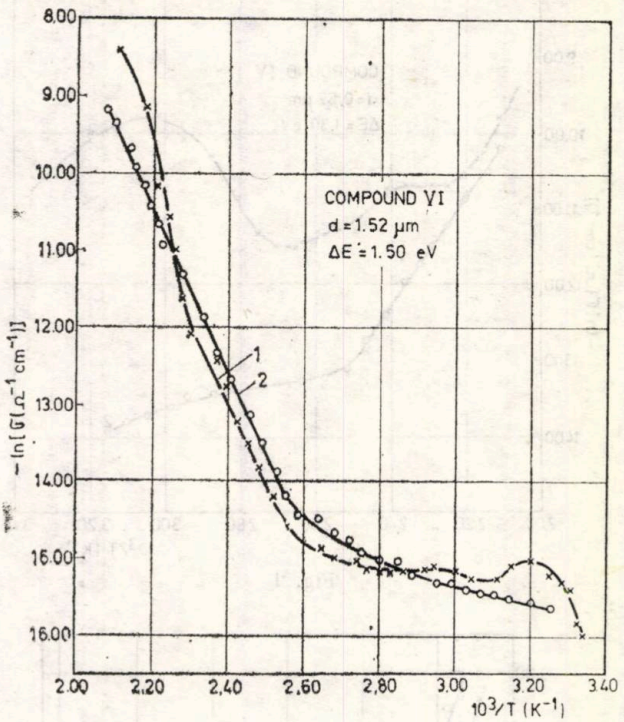

Fig. 3

semiconducting materials. These curves show portions of smaller slopes within the low temperature range. In this range the substances show a conduction of the impurities [1], [4], [6]. Within the higher temperature range the substances might be assumed to show an intrinsic conduction which is confirmed by the fact that the curve slopes do not modify during the heat treatment.

In our opinion the electrical conduction mechanism might be explained on the basis of the zonal theory [9]. As known, the linear variation of the electrical conductivity logarithm with the reciprocal absolute temperature within the temperature range of intrinsic conduction as well as the fact that the preexponential factor σ_0 in the relation

$$\sigma = \sigma_0 \exp\left(-\frac{\Delta E}{2KT}\right) \tag{1}$$

does not depend on temperature are consequences of this model.

In the expression (1) K denotes the B o l t z m a n n's constant and ΔE — the width of the ferbidden energy zone between the valence and the conduction zone.

The heat-treated layers are also possible to show a hopping conduction within the lower temperature range. This would impey the presence of some electron donating and with drawing impurities in close concentrations. In this case, a part of the electrons on the donating levels are with drawe by the withdrawing levels and the presence of an electrical field the electrod pass from the neutral donors to the positively charged ones which results in an electric current [1], [11].

During the heat treatment a great amount of impurities are eliminated from the layer.

On the other hand the shape of the electrical conductivity dependence on the temperature for the samples untreated thermally is strongly influenced by the layer structure modification.

The values of the thermal activation energy of the electrical conductivity as calculated from the dependence $\ln \sigma = f(10^3/T)$ within the intrinsic conduction domain are given in Figs. 1...3. These values are noticed to depend on the chemical structure of the corresponding compounds. The substitution of the CH_3— and CH_3—$(CH_2)_3$ — groups for the aminic hydrogen in the compound (I) resulted in the activation energy decrease.

3. Conclusions

The silver salts (IV)...(VI) of the β-amido-N-[*p*-(acyl-amino)-benzoyl]-L-asparagic acids were prepared by solving the corresponding acids in a natrium bicarbonate solution followed by the precipitation with a silver nitrate solution.

The electrical properties of the salts (IV)...(VI) were studied. Their electrical conductivity dependence on the temperature indicates semiconducting properties.

The electrical conductivity σ and the thermal energy of activating the electrical conductivity, ΔE, show lower values compared to other organic semiconductors.

Received, December 18, 1978

Polytechnic Institute, Jassy,
Department of Organic and Macromolecular Chemistry
and
University „Al. I. Cuza", Jassy,
Department of Physics

REFERENCES

1. G u t m a n F., L y o n s L. E., *Organic Semiconductors.* John Wiley, New-York, 1967.
2. R o s e n b e r g B., B h o w i k B. B., H a r d e r H. C., P o s t o v E., J. Chem. Phys., 49, 4108 (1968).
3. J o n s t o n G. R., L y o n s L. E., Phys. Stat. Sol., 37, K-43 (1970).
4. Р у с у Г. И., Канд. дисс., Ленинград, 1969.
5. R u s u G. I., Ş u n e l V., B u d e a n u C. H., An. Şt. Univ. „Al. I. Cuza", Iaşi, s. I b, 20, 189 (1974).

6. Rusu G. I., Șunel V., Gheorghiu M., An. șt. Univ. „Al. I. Cuza", Iași, s. I b, 23, 61 (1977).
7. Глазов В. М., Охотин А. С., Боровикова Р. П., *Методы исследования термоэлектрических свойств полупроводников*. Атомиздат, М., 1969.
8. Druță I. D., Budeanu C., An șt. Univ. „Al. I. Cuza", Iași, s. I c, 19, 71 (1973).
9. Budeanu C., Șunel V., Bul. Inst. polit., Iași, XXIV(XXVIII), s. II, 95 (1978).
10. Eley D. D., J. Polymer Sci., Part C, 17, 73 (1967).
11. Saha K., Abbi S. C., Pohl H. A., J. Nov. Cryst. Solids, 21, 17 (1976).

SINTEZA ȘI STUDIUL PROPRIETĂȚILOR ELECTRICE A UNOR NOI SĂRURI DE ARGINT DERIVATE DE LA N-(*p*-AMINOBENZOIL)-L-ASPARAGINĂ

(Rezumat)

În scopul obținerii de noi substanțe care să prezinte caracteristicile structurale ale materialelor semiconductoare s-au sintetizat sărurile de argint (IV)...(VI) ale acizilor β-amido-N-[*p*-(acilamino)-benzoil]-L-asparagici prin solvirea mai întîi a acizilor respectivi (I)...(III) într-o soluție de bicarbonat și apoi precipitarea cu o soluție de azotat de argint. Conductibilitatea electrică σ și energia termică de activare, ΔE, a compușilor sintetizați, au valori mici în comparație cu alți semiconductori organici.

1982 FEB 16

40822